■■■■■■ **CHAPTER 5**

Fourier Transforms of Analog Signals

This chapter furnishes a detailed introduction to the theory and application of the Fourier transform—the first of several transforms we shall encounter in this book. Many readers, including engineers, scientists, and mathematicians, may already be familiar with this widely used transform. The Fourier transform analyzes the frequency content of a signal, and it has four variations, according to whether the time-domain signal is analog or discrete, periodic or aperiodic. The present chapter covers the two analog transforms: the Fourier series, for periodic signals, and the Fourier transform proper, for aperiodic signals.

Technology involving filtering, modulation, and wave propagation all rely heavily upon frequency analysis accomplished by the Fourier transform operation. But biological systems execute spectral analysis as well. Our senses, especially hearing and sight, are living examples of signal processors based on signal frequency spectra. The color response of the human eye is nothing more than the end result of optical signal processing designed to convert solar electromagnetic waves into the various hues of the visible electromagnetic spectrum. On a daily basis, we are exposed to sounds which are easily classified according to high and low pitch as well as purity—we are all too aware of a tenor or soprano who wobbles into a note. All instances of frequency-domain analysis, these life experiences beg the question of how engineered systems might achieve like results.

This chapter develops the first of several practical frequency-domain analysis tools. Indeed we already have practical motivations:

- Experiments in finding the period of apparently periodic phenomena, such as example of sunspot counts in the first chapter
- Attempts to characterize texture patterns in the previous chapter

Our actual theoretical development relies heavily upon the general notions of Hilbert space and orthogonal functions developed in Chapter 3. For the mathematician, who may already have a thorough understanding of the Fourier series as a complete orthonormal expansion, Chapters 5 and 6 present an opportunity to get

down to the business of calculating the coefficients and functions which shed so much information about the physical world.

The transform consists of two complementary operations. The first is the *analysis*—that is, the breaking down of the signal into constituent parts. In the case of Fourier analysis, this involves generation and interpretation of coefficients whose magnitude and phase contain vital information pertaining to the frequency content of a signal. In the case of the continuous Fourier transform studied in this chapter, these coefficients are a continuous function of frequency as represented by the Fourier transform $F(\omega)$. The Fourier series, which is applicable to periodic waveforms, is actually a special case of this continuous Fourier transform, and it represents spectral data as a discrete set of coefficients at selected frequencies.

The second operation involves *synthesis*, a mathematical picking up of pieces, to reconstruct the original signal from $F(\omega)$ (or from the set of discrete Fourier coefficients, if appropriate), as faithfully as possible. Not all waveforms readily submit to Fourier operations, but a large set of practical signals lends itself quite readily to Fourier analysis and synthesis. Information obtained via Fourier analysis and synthesis remains by far the most popular vehicle for storing, transmitting, and analyzing signals. In some cases the analysis itself cannot be performed, leaving synthesis out of the question, while in others the physically valid analysis is available, but a reconstruction via Fourier synthesis may not converge. We will consider these issues in some detail as Chapter 5 develops. Some waveforms amenable to Fourier analysis may be better suited to more advanced transform methods such as time-frequency (windowed) Fourier transforms or time-scale (wavelet) transforms considered in later chapters. However, the basic notion of 'frequency content' derived from Fourier analysis remains an important foundation for each of these more advanced transforms.

Communication and data storage systems have a finite capacity, so the storage of an entire spectrum represented by a continuous function $F(\omega)$ is impractical. To accommodate the combined requirements of efficiency, flexibility, and economy, a discrete form of the Fourier transform is almost always used in practice. This discrete Fourier transform (DFT) is best known in the widely used fast Fourier transform (FFT) algorithm, whose development revolutionized data storage and communication. These algorithms are discussed in Chapter 7, but their foundations lie in the concepts developed in Chapters 5 and 6.

Introductory signal processing [1–5] and specialized mathematics texts [6–9] cover continuous domain Fourier analysis. Advanced texts include Refs. [10–12]. Indeed, the topic is almost ubiquitous in applied mathematics. Fourier himself developed the Fourier series, for analog periodic signals, in connection with his study of heat conduction.[1] This chapter presupposes some knowledge of Riemann integrals, ideas of continuity, and limit operations [13]. Familiarity with Lebesgue integration, covered briefly in Chapter 3, remains handy, but definitely not essential [14].

---

[1]Jean-Baptiste Joseph Fourier (1768–1830). The French mathematical physicist developed the idea without rigorous justification and amid harsh criticism, to solve the equation for the flow of heat along a wire [J. Fourier, *The Analytical Theory of Heat*, New York: Dover, 1955].

Essential indeed are the fundamentals of analog L^p and abstract function spaces [15, 16]. We use a few unrigorous arguments with the Dirac delta. Chapter 6 covers the generalized Fourier transform and distribution theory [17, 18]. Hopefully this addresses any misgivings the reader might harbor about informally applying Diracs in this chapter.

5.1 FOURIER SERIES

Consider the problem of constructing a synthesis operation for periodic signals based on complete orthonormal expansions considered in Chapter 3. More precisely, we seek a series

$$x_n(t) = \sum_{k=1}^{n} c_k \phi_k(t) \tag{5.1}$$

which converges to $x(t)$, a function with period T, as n approaches infinity. Equation (5.1) is a statement of the synthesis problem: Given a set of coefficients c_k and an appropriate set of orthonormal basis functions $\{\phi_1(t), \phi_2((t), ..., \phi_n(t))\}$, we expect a good facsimile of $x(t)$ to emerge when we include a sufficient number of terms in the series. Since the linear superposition (5.1) will represent a periodic function, it is not unreasonable to stipulate that the $\phi_k(t)$ exhibit periodicity; we will use simple sinusoids of various frequencies, whose relative contributions to $x(t)$ are determined by the phase and amplitude of the c_k. We will stipulate that the basis functions be orthonormal over some fundamental interval $[a, b]$; intuitively one might consider the period T of the original waveform $x(t)$ to be sufficiently "fundamental," and thus one might think that the length of this fundamental interval is $b - a = T$. At this point, it is not obvious where the interval should lie relative to the origin $t = 0$ (or whether it really matters). But let us designate an arbitrary point $a = t_0$, requiring that the set of $\{\phi_k(t)\}$ is a complete orthonormal basis in $L^2[t_0, t_0 + T]$:

$$\langle \phi_i, \phi_l \rangle = \int_{t_0}^{t_0 + T} \phi_i(t)\phi_j(t)^* dt = \delta_{ij}, \tag{5.2}$$

where δ_{ij} is the Kronecker[2] delta.

We need to be more specific about the form of the basis functions. Since periodicity requires $x(t) = x(t + T)$, an examination of (5.1) suggests that it is desirable to select a basis with similar qualities: $\phi_k(t) = \phi_k(t + T)$. This affords us the prospect of a basis set which involves harmonics of the fundamental frequency $1/T$. Consider

$$\phi_k(t) = A_0 e^{jk2\pi Ft} = A_0 e^{jk\Omega t}, \tag{5.3}$$

[2]This simple δ function takes its name from Leopold Kronecker (1823–1891), mathematics professor at the University of Berlin. The German algebraist was an intransigent foe of infinitary mathematics—such as developed by his pupil, Georg Cantor—and is thus a precursor of the later *intuitionists* in mathematical philosophy.

where $F = 1/T$ cycles per second (the frequency common unit is the hertz, abbreviated Hz; one hertz is a single signal cycle per second). We select the constant A_0 so as to normalize the inner product as follows. Since

$$\langle \phi_l, \phi_m \rangle = A_0^2 \int_{t_0}^{(t_0 + T)} e^{jl\Omega t} e^{-jm\Omega t} p dt = \delta_{lm}, \tag{5.4a}$$

if $m = l$, then

$$\langle \phi_m, \phi_m \rangle = A_0^2 \int_{t_0}^{t_0 + T} dt = A_0^2 T. \tag{5.4b}$$

Setting $A_0 = 1/\sqrt{T}$ then establishes normalization. Orthogonality is easily verified for $m \neq l$, since

$$\langle \phi_l | \phi_m \rangle = \frac{1}{T} \int_{t_0}^{t_0 + T} e^{j(l-m)\Omega t} dt$$

$$= \frac{1}{T} \int_{t_0}^{t_0 + T} (\cos[(l-m)\Omega t] + j \sin[(l-(m))\Omega t]) dt = 0. \tag{5.5a}$$

This establishes orthonormality of the set

$$\left\{ \frac{1}{\sqrt{T}} e^{jk\Omega t} \right\} \tag{5.5b}$$

for integer k.

When the set of complex exponentials is used as a basis, all negative and positive integer k must be included in the orthonormal expansion to ensure completeness and convergence to $x(t)$. (We can readily see that restricting ourselves to just positive or negative integers in the basis, for example, would leave a countably infinite set of functions which are orthogonal to each function in the basis, in gross violation of the notion of completeness.)

Relabeling of the basis functions provides the desired partial series expansion for both negative and positive integers k:

$$x_{2N+1}(t) = \sum_{k=-N}^{N} c_k \frac{1}{\sqrt{T}} e^{jk\Omega t}. \tag{5.6}$$

Completeness will be assured in the limit as $N \to \infty$:

$$\lim_{N \to \infty} x_{2N+1}(t) = \sum_{k=-\infty}^{\infty} c_k \frac{1}{\sqrt{T}} e^{jk\Omega t} = x(t), \tag{5.7}$$

where the expansion coefficients are determined by the inner product,

$$c_k = \langle x(t), \phi_k(t) \rangle = \int_{t_0}^{t_0 + T} x(t) \frac{1}{\sqrt{T}} e^{-jk\Omega t} dt. \tag{5.8}$$

Remark. The c_k in (5.8) are in fact independent of t_0, which can be shown by the following heuristic argument. Note that all the constituent functions in (5.8)—namely $x(t)$, as well as $\cos(k\Omega t)$ and $\sin(k\Omega t)$, which make up the complex exponential—are (at least) T-periodic. As an exercise, we suggest the reader draw an arbitrary function which has period T: $f(t + T) = f(t)$. First, assume that $t_0 = 0$ and note the area under $f(t)$ in the interval $t \in [0, T]$; this is, of course, the integral of $f(t)$. Next, do the same for some nonzero t_0, noting that the area under $f(t)$ in the interval $t \in [t_0, t_0 + T]$ is unchanged from the previous result; the area over $[0, t_0]$ which was lost in the limit shift is compensated for by an equivalent gain between $[t_0, t_0 + T]$. This holds true for any finite t_0, either positive or negative, but is clearly a direct consequence of the periodicity of $x(t)$ and the orthogonal harmonics constituting the integral (5.8). Unless otherwise noted, we will set $t_0 = 0$, although there are some instances where another choice is more appropriate.

5.1.1 Exponential Fourier Series

We can now formalize these concepts. There are two forms of the Fourier series:

- For exponential basis functions of the form $Ae^{jk\Omega t}$
- For sinusoidal basis functions of the form $A\cos(k\Omega t)$ or $A\sin(k\Omega t)$

The exponential expansion is easiest to use in signal theory, so with it we begin our treatment.

5.1.1.1 *Definition and Examples.* The Fourier series attempts to analyze a signal in terms of exponentials. In the sequel we shall show that broad classes of signals can be expanded in such a series. We have the following definition.

Definition (Exponential Fourier Series). The *exponential Fourier series* for $x(t)$ is the expansion

$$x(t) = \sum_{k = -\infty}^{\infty} c_k \phi_k(t), \tag{5.9}$$

whose basis functions are the complete orthonormal set,

$$\phi_k(t) = \frac{1}{\sqrt{T}} e^{jk\Omega t}, \tag{5.10}$$

and whose expansion coefficients take the form (5.8).

According to the principles governing complete orthonormal expansions, (5.9) predicts that the right-hand side converges to $x(t)$, provided that the infinite summation is performed. In practice, of course, an infinite expansion is a theoretical ideal, and a cutoff must be imposed after a selected number of terms. This results in a partial series defined thusly:

Definition (Partial Series Expansion). A *partial Fourier series* for $x(t)$ is the expansion

$$x(t) = \sum_{k=-N}^{N} c_k \phi_k(t) \tag{5.11}$$

for some integer $0 < N < \infty$.

The quality of a synthesis always boils down to how many terms (5.11) should include. Typically, this judgment is based upon how much error can be tolerated in a particular application. In practice, every synthesis is a partial series expansion, since it is impossible to implement (in a finite time) an infinite summation.

Example (Sine Wave). Consider the pure sine wave $x(t) = \sin(\omega t)$. The analysis calculates the coefficients

$$c_k = \int_0^T \left(\sin \Omega t \frac{1}{\sqrt{T}} [\cos k\Omega t - j\sin k\Omega t] \right) dt. \tag{5.12}$$

Orthogonality of the sine and cosine functions dictates that all c_k vanish except for $k = \pm 1$:

$$c_{\pm 1} = \frac{\mp j}{\sqrt{T}} \left\{ \int_0^T [\sin(\Omega t)]^2 dt \right\} = (\mp j)\frac{\sqrt{T}}{2}. \tag{5.13}$$

Synthesis follows straightforwardly:

$$x(t) = (-j)\frac{\sqrt{T}}{2}\left(\frac{e^{j\Omega t}}{\sqrt{T}} \right) + j\frac{\sqrt{T}}{2}\left(\frac{e^{(-j)\Omega t}}{\sqrt{T}} \right) = \sin(\Omega t). \tag{5.14}$$

Example (Cosine Wave). For $x(t) = \cos(\omega t)$ there are two equal nonzero Fourier coefficients:

$$c_{\pm 1} = \frac{1}{\sqrt{T}}\int_0^T [\cos(\Omega t)]^2 dt = \frac{\sqrt{T}}{2}. \tag{5.15}$$

Remark. Fourier analysis predicts that each simple sinusoid is composed of frequencies of magnitude $|\Omega|$, which corresponds to the intuitive notion of a pure oscillation. In these examples, the analysis and synthesis were almost trivial, which stems from the fact that $x(t)$ was projected along the real (in the case of a cosine) or imaginary (in the case of a sine) part of the complex exponentials comprising the orthonormal basis. This property—namely a tendency toward large coefficients when the signal $x(t)$ and the analyzing basis match—is a general property of orthonormal expansions. When data pertaining to a given signal is stored or transmitted, it is often in the form of these coefficients, so both disk space and bandwidth can be reduced by a judicious choice of analyzing basis. In this simple example of Fourier analysis applied to sines and cosines, only two coefficients are required to

perform an exact synthesis of $x(\ddot{t})$. But Fourier methods do not always yield such economies, particularly in the neighborhood of transients (spikes) or jump discontinuities. We will demonstrate this shortly. Finally, note that the two Fourier coefficients are equal (and real) in the case of the cosine, but of opposite sign (and purely imaginary) in the case of the sine wave. This results directly from symmetries present in the sinusoids, a point we now address in more detail.

5.1.1.2 *Symmetry Properties.* The Fourier coefficients acquire special properties if $x(t)$ exhibits even or odd symmetry. Recall that if $x(t)$ is odd, $x(-t) = -x(t)$ for all t, and by extension it follows that the integral of an odd periodic function, over any time interval equal to the period T, is identically zero. The sine and cosine harmonics constituting the Fourier series are odd and even, respectively. If we expand the complex exponential in the integral for c_k,

$$c_k = \int_0^T \frac{x(t))}{\sqrt{T}} [\cos(k\Omega t) - j\sin(k\Omega t)] \ dt, \tag{5.16}$$

then some special properties are apparent:

- If $x(t)$ is real and even, then the c_k are also real and even, respectively, in k-space; that is, $c_k = c_{-k}$.
- If $x(t)$ is real and odd, then the coefficients are purely imaginary and odd in k-space: $c_{-k} = -c_k$.

The first property above follows since the second term in (5.16) vanishes identically and since $\cos(k\Omega t)$ is an even function of the discrete index k. If even–odd symmetries are present in the signal, they can be exploited in numerically intensive applications, since the number of independent calculations is effectively halved. Most practical $x(t)$ are real-valued functions, but certain filtering operations may transform a real-valued input into a complex function. In the exercises, we explore the implications of symmetry involving complex waveforms.

Example (Rectangular Pulse Train). Consider a series of rectangular pulses, each of width t and amplitude A_0, spaced at intervals T, as shown in Figure 5.1. This waveform is piecewise continuous according to the definition of Chapter 3, and in due course it will become clear this has enormous implications for synthesis. The inner product of this waveform with the discrete set of basis functions leads to a straightforward integral for the expansion coefficients:

$$c_k = \langle x(t), \phi_k(t) \rangle = \frac{A_0}{\sqrt{T}} \int_0^{\frac{\tau}{2}} (\cos k\Omega t - j\sin k\Omega t) \ dt + \frac{A_0}{\sqrt{T}} \int_{T-\frac{\tau}{2}}^{T} (\cos k\Omega t - j\sin k\Omega t) \ dt$$
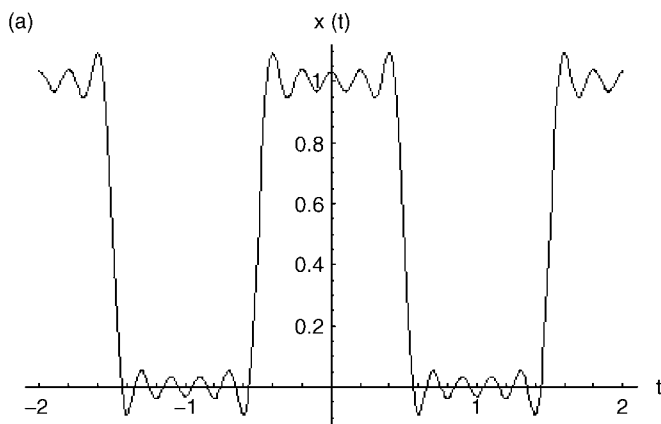
$$\tag{5.17}$$
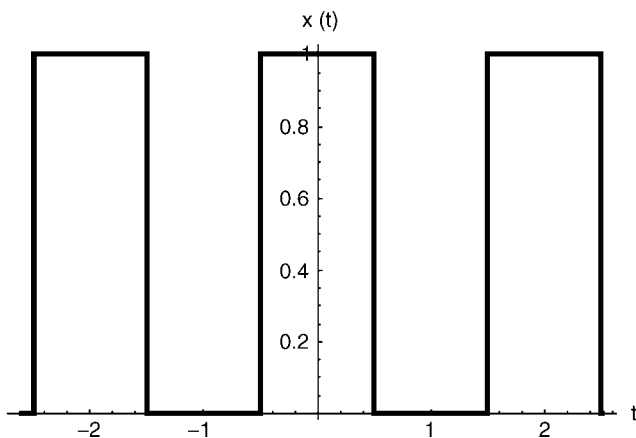
Fig. 5.1. A train of rectangular pulses. Shown for pulse width $\tau = 1$, amplitude $A_0 = 1$, and period $T = 2$.

Some algebra reduces this to the succinct expression

$$c_k = \frac{A_0}{\sqrt{T}} \cdot \tau \cdot \frac{\sin\left(\frac{k\Omega\tau}{2}\right)}{\left(\frac{k\Omega\tau}{2}\right)}. \tag{5.18}$$

Example (Synthesis of Rectangular Pulse). In Figure 5.2 we illustrate the synthesis of periodic rectangular pulses for several partial series, using (5.10) and (5.16).

Fig. 5.2. Synthesis of the rectangular pulse train. (a) Partial series $N = 10$, (b) $N = 50$, (c) $N = 100$. The number of terms in the series is $2N + 1$.
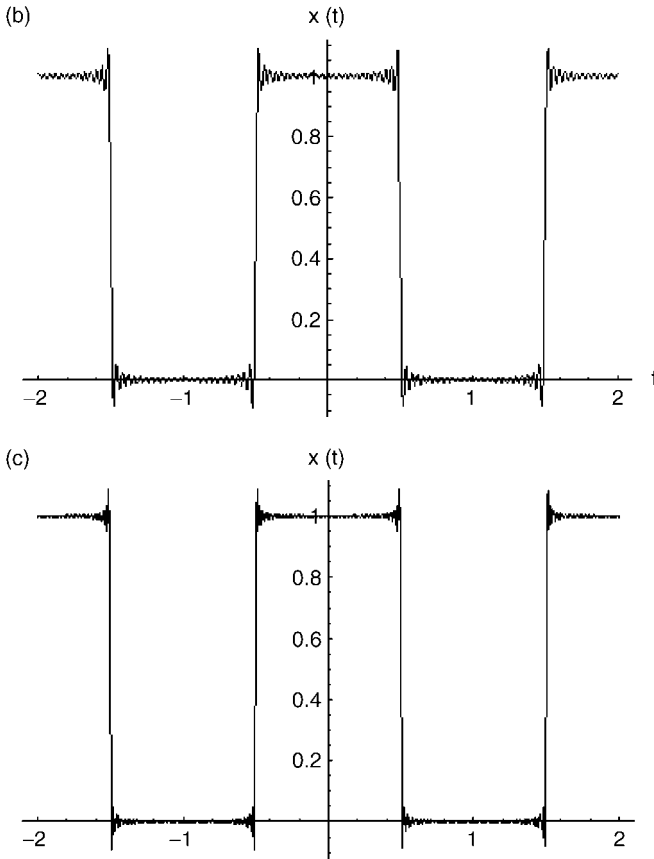
(b)

(c)

Fig. 5.2 (*Continued*)

5.1.2 Fourier Series Convergence

We are now in a position to prove the convergence of the exponential Fourier series for a signal $x(t)$. We shall consider two cases separately:

- At points where $x(t)$ is continuous;
- At points where $x(t)$ has a jump discontinuity.

5.1.2.1 *Convergence at Points of Continuity.* It turns out that the Fourier series does converge to the original signal at points of continuity. We have the following theorem.

Theorem (Fourier Series Convergence). Suppose $S_N(s)$ is a partial series summation of the form

$$S_N(s) \; = \; \sum_{k=-N}^{N} c_k \frac{1}{\sqrt{T}} e^{jk\Omega t}, \tag{5.19a}$$

where N is a positive integer. If $x(t)$ is continuous at s (including points of continuity within piecewise continuous functions), then

$$\lim_{N \to \infty} S_N(s) = x(s). \tag{5.19b}$$

Proof: Consider the partial series summation:

$$S_N(s) = \sum_{k=-N}^{N} \left\langle x(t), \frac{e^{jk\Omega t}}{\sqrt{T}} \right\rangle \frac{1}{\sqrt{T}} e^{jk\Omega t}. \tag{5.20}$$

Writing the inner product term (in brackets) as an explicit integral, we have

$$S_N(s) = \frac{1}{T} \sum_{k=-N}^{N} \int_0^T x(t) e^{jk\Omega(s-t)} dt = \frac{2}{T} \int_0^T x(t) \cdot K(s-t) \, dt, \tag{5.21}$$

where

$$K(s-t) = \frac{1}{2} + \sum_{k=1}^{N} \cos(k\Omega(s-t)). \tag{5.22}$$

The function $K(s-t)$ reduces—if we continue to exploit the algebraic properties of the exponential function for all they are worth—to the following:

$$K(s-t) = \mathrm{Re}\left[\left(1 - \frac{1}{2}\right) + \sum_{k=1}^{N} e^{jk\Omega(s-t)} \right]. \tag{5.23a}$$

This reduces to the more suggestive form,

$$K(s-t) = \frac{\sin\left[\left(N + \frac{1}{2}\right)(s-t)\right]}{2\sin\left[\frac{1}{2}(s-t)\right]}. \tag{5.23b}$$

Returning to the partial series expansion (5.21), the change of integration variable $u = s - t$ gives

$$S_N(s) = -\int_s^{s-T} x(s-u) \left[\frac{\sin\left(N + \frac{1}{2}\right)u}{T\sin\left(\frac{T}{2}\right)} \right] du. \tag{5.24}$$

The quantity in brackets is the *Dirichlet kernel*[3],

$$D_N(u) = \frac{\sin\left(N + \frac{1}{2}\right)u}{T\sin\left(\frac{u}{2}\right)}, \tag{5.25}$$

---

[3]P. G. Legeune Dirichlet (1805–1859) was Kronecker's professor at the University of Berlin and the first to rigorously justify the Fourier series expansion. His name is more properly pronounced "Dear-ah-klet."

whose integral exhibits the convenient property

$$- \int_s^{s-T} D_N(u)\, du = 1. \tag{5.26}$$

Equation (5.26) is easily demonstrated with a substitution of variables, $2v = u$, which brings the integral into a common tabular form:

$$- \int_s^{s-T} D_N(u)\, du = -\frac{1}{T}\int_0^{-\frac{T}{2}} 2 \cdot \frac{\sin\,2N+1)v}{\sin\,v}\, dv = \frac{-2}{T}\left[2\sum_{m=1}^{N}\frac{\sin(mv)}{2m}+v\right]\Bigg|_0^{-\frac{T}{2}} = 1. \tag{5.27}$$

The beauty of this result lies in the fact that we can construct the identity

$$x(s) = -\int_s^{s-T} x(s)D_N(u)\, du \tag{5.28}$$

so that the difference between the partial summation $S_N(s)$ and the original signal $x(s)$ is an integral of the form

$$S_N(s) - x(s) = \frac{-1}{T}\int_s^{s-T} g(s,u)\cdot\sin\left[\left(N+\frac{1}{2}\right)u\right]du, \tag{5.29}$$

where

$$g(s,u) = \frac{x(s-u)-x(s)}{\sin\left(\frac{u}{s}\right)}. \tag{5.30}$$

In the limit of large N, (5.29) predicts that the partial series summation converges pointwise to $x(s)$ by simple application of the Riemann–Lebesgue lemma (Chapter 3):

$$\lim_{N\to\infty}[S_N(s)-x(s)] = \lim_{N\to\infty}\int_s^{s-T}\frac{-g(s,u)}{T}\sin\left[\left(N+\frac{1}{2}\right)u\right]du = 0, \tag{5.31}$$

thus concluding the proof.   ■

The pointwise convergence of the Fourier series demonstrated in (5.31) is conceptually reassuring, but does not address the issue of how rapidly the partial series expansion actually approaches the original waveform. In practice, the Fourier series is slower to convergence in the vicinity of sharp peaks or spikes in $x(t)$. This aspect of the Fourier series summation is vividly illustrated in the vicinity of a step discontinuity—of the type exhibited by rectangular pulse trains and the family of sawtooth waves, for example. We now consider this problem in detail.

5.1.2.2 *Convergence at a Step Discontinuity.*

It is possible to describe and quantify the quality of convergence at a jump discontinuity such as those exhibited by the class of piecewise continuous waveforms described in Chapter 3. We represent such an $x(t)$ as the sum of a continuous part $x_c(t)$ and a series of unit steps, each term of which represents a step discontinuity with amplitude $A_k = x(t_k^+) - x(t_k^-)$ located at $t = t_k$:

$$x(t) = x_c(t) + \sum_{k=1}^{M} A_k u(t - t_k). \tag{5.32}$$

In the previous section, convergence of the Fourier series was established for continuous waveforms and that result applies to the $x_c(t)$ constituting part of the piecewise continuous function in (5.32). Here we turn to the issue of convergence in the vicinity of the step discontinuities represented by the second term in that equation. We will demonstrate that

- The Fourier series converges pointwise at each t_k.
- The discontinuity imposes oscillations or ripples in the synthesis, which are most pronounced in the vicinity of each step. This artifact, known as the *Gibbs phenomenon*,[4] is present in all partial series syntheses of piecewise continuous $x(t)$; however, its effects can be minimized by taking a sufficiently large number of terms in the synthesis.

The issue of Gibbs oscillations might well be dismissed as a mere mathematical curiosity were it not for the fact that so many practical periodic waveforms are piecewise continuous. Furthermore, similar oscillations occur in other transforms as well as in filter design, where ripple or overshoot (which are typically detrimental) arise from similar mathematics.

Theorem (Fourier Series Convergence: Step Discontinuity). Suppose $x(t)$ exhibits a step discontinuity at some time t about which $x(t)$ and its derivative have well-behaved limits from the left and right, $t_{(l)}$ and $t_{(r)}$, respectively. Then $x(t)$ converges pointwise to the value

$$x(t) = \frac{[x(t_{(r)}) + x(t_{(l)})]}{2}. \tag{5.33}$$

Proof: For simplicity, we will consider a single-step discontinuity and examine the synthesis

$$x(t) = x_c(t) + A_s u(t - t_s), \tag{5.34}$$

---

[4]The Yale University chemist, Josiah Willard Gibbs (1839–1903), was the first American scientist of international renown.

where the step height is $A_s = x(t_s+) - x(t_s-)$. We begin by reconsidering (5.24):

$$S_N(s) = \int_0^T x(t) \left(\frac{\sin\left[\left(N+\frac{1}{2}\right)(s-t)\right]}{T\sin\left[\frac{1}{2}(s-t)\right]} \right) dt = \int_{-\frac{T}{2}}^{\frac{T}{2}} x(s-t)D_N(\Omega t) \, dt. \qquad (5.35)$$

For convenience, we have elected to shift the limits of integration to a symmetric interval $[-T/2, T/2]$. Furthermore, let us assume that the discontinuity occurs at the point $t = t_s = 0$. (These assumptions simplify the calculations enormously and do not affect the final result. The general proof adds complexity which does not lead to any further insights into Fourier series convergence.) It is convenient to break up the integral into two segments along the t axis:

$$S_N(s) = \int_{-T/2}^{T/2} x_c(s-t)D_N(\Omega t)\Omega \, dt + A_0 \cdot \int_{-T/2}^{T/2} u(s-t)D_N(\Omega t)\Omega \, dt, \qquad (5.36)$$

where $A_0 = x(0_{(r)}) - x(0_{(1)})$ is the magnitude of the jump at the origin. In the limit $N \to \infty$, the first term in (5.36) converges to $x_c(t)$, relegating the discontinuity's effect to the second integral, which we denote $e_N(s)$:

$$\varepsilon_N(s) = A_0 \cdot \int_{-\frac{T}{2}}^{\frac{T}{2}} u(t)D_N(\Omega(s-t))t\Omega \, dt = A_0 \cdot \int_0^{\frac{T}{2}} D_N(\Omega(s-t))\Omega \, dt. \qquad (5.37)$$

The task at hand is to evaluate this integral. This can be done through several changes of variable. Substituting for the Dirichlet kernel provides

$$\varepsilon_N(s) = A_0 \cdot \int_0^{\frac{T}{2}} \left[\frac{\sin\left[\left(N+\frac{1}{2}\right)\Omega(s-t)\right]}{T\sin\left[\frac{\Omega(s-t)}{2}\right]} \right] \Omega \, dt. \qquad (5.38)$$

Defining a new variable $u = \Omega(t-s)$ and expanding the sines brings the dependence on variable s into the upper limit of the integral:

$$\varepsilon_N(s) = A_0 \cdot \int_0^{-\Omega\left(s+\frac{T}{2}\right)} \left[\frac{\sin(nu) \cdot \cos\left(\frac{u}{2}\right)}{2\pi\sin\left[\frac{u}{2}\right]} + \cos(nu) \right] du. \qquad (5.39)$$

Finally, we define a variable $2v = u$ which brings (5.39) into a more streamlined form

$$\varepsilon_N(s) = A_0 \cdot \int_0^{-\frac{\Omega}{2}\left(s+\frac{T}{2}\right)} \left[\frac{\sin(2nv) \cdot \cos(v)}{2\pi \sin(v)} + \cos(2nv) \right] dv. \tag{5.40}$$

This is as close as we can bring $e_N(s)$ to an analytic solution, but it contains a wealth of information. We emphasize that s appears explicitly as an upper limit in each integral. Tabulation of (5.40) produces an oscillatory function of s in the neighborhood of $s = 0$; this accounts for the ripple—Gibbs oscillations—in the partial series synthesis near the step discontinuity. As we approach the point of discontinuity at the origin, (5.40) can be evaluated analytically:

$$\varepsilon_N(s) = A_0 \cdot \int_0^{\frac{\pi}{2}} \left[\frac{\sin(2nv) \cdot \cos(v)}{2\pi \sin(v)} + \cos(2nv) \right] dv = A_0 \cdot \left[\left(\frac{1}{\pi} \cdot \frac{\pi}{2} \right) + 0 \right] = \frac{1}{2}A_0. \tag{5.41}$$

(Note that in going from (5.40) to (5.41), a sign change can be made in the upper limit, since the integrand is an even function of the variable v.) Accounting for both the continuous portion $x_c(t)$ —which approaches $x(0_{(l)})$ as $N \to \infty$ and as $t \to 0$— and the discontinuity's effects described in (5.41), we find

$$x(0) = x_c(0) + \frac{1}{2}[x(0_{(r)}) - x(0_{(l)})] = \frac{1}{2}[x(0_{(r)}) + x(0_{(l)})]. \tag{5.42}$$

A similar argument works for a step located at an arbitrary t; this provides the general result

$$x(0) = \frac{1}{2}[x(t_{(r)}) + x(t_{(l)})], \tag{5.43}$$

and the proof is complete.   ∎

Figure 5.3 illustrates the convergence of $e_N(s)$ near a step discontinuity in a rectangular pulse train. Note the smoothing of the Gibbs oscillations with increasing N.

As N approaches infinity and at points t where $x(t)$ is continuous, the Gibbs oscillations get infinitesimally small. At the point of discontinuity, they contribute an amount equal to one-half the difference between the left and right limits of $x(t)$, as dictated by (5.42).

When approaching this subject for the first time, it is easy to form misconceptions about the nature of the convergence of the Fourier series at step discontinuities, due to the manner in which the Gibbs oscillations (almost) literally cloud the issue. We complete this section by emphasizing the following points:

- The Gibbs oscillations do *not* imply a failure of the Fourier synthesis to converge. Rather, they describe how the convergence behaves.
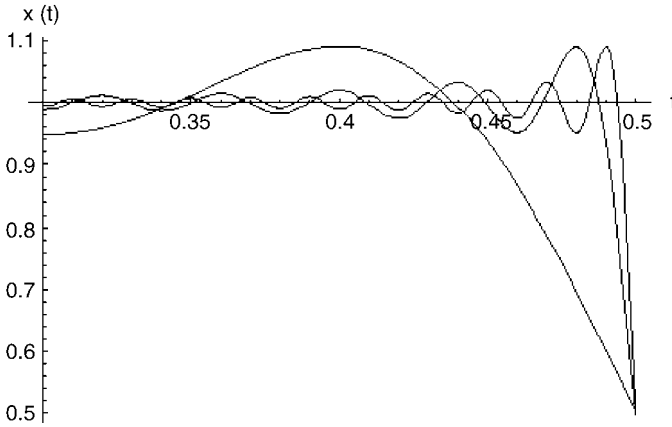
Fig. 5.3. Convergence of the Fourier series near a step, showing Gibbs oscillations for N = 10, 50, 100. For all N, the partial series expansion converges to 1/2 at the discontinuity.

- The Fourier series synthesis converges to an exact, predictable value at the point of discontinuity, namely the arithmetic mean of the left and right limits of $x(t)$, as dictated by (5.43).
- In the vicinity of the discontinuity, at points for which $x(t)$ is indeed continuous, the Gibbs oscillations disappear in the limit as N becomes infinite. That is, the synthesis converges to $x(t)$ with no residual error. It is exact.

5.1.3   Trigonometric Fourier Series

Calculations with the exponential basis functions make such liberal use of the orthogonality properties of the constituent sine and cosine waves that one is tempted to reformulate the entire Fourier series in a set of sine and cosine functions. Such a development results in the trigonometric Fourier series, an alternative to the exponential form considered in the previous section.

Expanding the complex exponential basis functions leads to a synthesis of the form

$$x(t) = \sum_{k=-\infty}^{\infty} c_k \phi_k(t) = \frac{1}{\sqrt{T}} \sum_{k=-\infty}^{\infty} c_k [\cos(k\Omega t) + j\sin(k\Omega t)] . \qquad (5.44)$$

Since $\cos(k\Omega t)$ and $\sin(k\Omega t)$ are even and odd, respectively, in the variable k, and since for $k = 0$ there is no contribution from the sine wave, we can rearrange the summation and regroup the coefficients. Note that the summations now involve only the positive integers:

$$x(t) = \frac{1}{\sqrt{T}} \left\{ c_0 + \sum_{k=1}^{\infty} (c_k + c_{-k})\cos(k\Omega t) \right\} + \sum_{k=1}^{\infty} (c_k - c_{-k})\sin(k\Omega t) . \qquad (5.45)$$

The zeroth coefficient has the particularly simple form:

$$c_0 = \langle x(t), 1 \rangle = \int_0^T x(t)\ dt,\tag{5.46}$$

where 1 is the unit constant signal on $[0, T]$. Regrouping terms gives an expansion in sine and cosine:

$$x(t) = a_0 + \sum_{k=1}^{\infty} a_k \cos(k\Omega t) + \sum_{k=1}^{\infty} b_k \sin(k\Omega t),\tag{5.47}$$

where

$$a_k = \frac{c_k + c_{-k}}{\sqrt{T}},\tag{5.48a}$$

$$b_k = j \cdot \frac{c_k - c_{-k}}{\sqrt{T}},\tag{5.48b}$$

and

$$a_0 = \frac{1}{\sqrt{T}} \int_0^T x(t)\ dt.\tag{5.48c}$$

Under circumstances where we have a set of exponential Fourier series coefficients c_k at our disposal, (5.47) is a valid definition of the trigonometric Fourier series. In general, this luxury will not be available. Then a more general definition gives explicit intergrals for the expansion coefficients, a_k and b_k, based on the inner products $\langle x(t), f_m(t) \rangle$, where $f_m(t) = C_m \cos(m\Omega t)$ or $S_m \sin(m\Omega t)$ and C_m and S_m are normalization constants.

The C_m are determined by expanding the cosine inner product:

$$\langle x(t), C_m \cos(m\Omega t) \rangle = \langle a_0, C_m \cos(m\Omega t) \rangle + \sum_{k=1}^{\infty} a_k \langle C_k \cos(k\Omega t), C_m \cos(m\Omega t) \rangle$$

$$+ \sum_{k=1}^{\infty} a_k \langle S_k \sin(k\Omega t), C_m \cos(m\Omega t) \rangle\tag{5.49}$$

Consider each term above. The first one vanishes for all m, since integrating cosine over one period $[0, T]$ gives zero. The third term also vanishes for all k, due to the orthogonality of sine and cosine. The summands of the second term are zero, except for the bracket

$$\langle C_m \cos(m\Omega t), C_m \cos(m\Omega t) \rangle = \frac{T}{2} C_m{}^2.\tag{5.50}$$

To normalize this inner product, we set

$$C_m = \sqrt{\frac{2}{T}} \qquad (5.51)$$

for all m. Consequently, the inner product defining the cosine Fourier expansion coefficients a_k is

$$a_k = \left\langle x(t), \sqrt{\frac{2}{T}} \cos(k\Omega t) \right\rangle. \qquad (5.52)$$

The sine-related coefficients are derived from a similar chain of reasoning:

$$b_k = \left\langle x(t), \sqrt{\frac{2}{T}} \sin(k\Omega t) \right\rangle. \qquad (5.53)$$

Taking stock of the above leads us to define a Fourier series based on sinusoids:

Definition (Trigonometric Fourier Series). The *trigonometric Fourier series* for $x(t)$ is the orthonormal expansion

$$x(t) = a_0 + \sum_{k=1}^{\infty} a_k \phi_k(t) + \sum_{k=1}^{\infty} b_k \Psi_k(t), \qquad (5.54)$$

where

$$\phi_k(t) = \sqrt{\frac{2}{T}} \cos(k\Omega t) \qquad (5.55a)$$

and

$$\Psi_k(t) = \sqrt{\frac{2}{T}} \sin(k\Omega t). \qquad (5.55b)$$

Remark. Having established both the exponential and trigonometric forms of the Fourier series, note that it is a simple matter to transform from one coefficient space to the other. Beginning in (5.48a), we derived expressions for the trigonometric series coefficients in terms of their exponential series counterparts. But these relations are easy to invert. For $k > 0$, we have

$$c_k = \frac{\sqrt{T}}{2}(a_k - jb_k) \qquad (5.56a)$$

and

$$c_{-k} = \frac{\sqrt{T}}{2}(a_k + jb_k). \qquad (5.56b)$$

Finally, for $k = 0$, we see

$$c_0 = a_0 \sqrt{T}. \tag{5.57}$$

5.1.3.1 *Symmetry and the Fourier Coefficients.*
As in the case of the exponential Fourier coefficients, the a_k and b_k acquire special properties if $x(t)$ exhibits even or odd symmetry in the time variable. These follow directly from (5.52) and (5.53), or by the application of the previously derived c_k symmetries to (5.45). Indeed, we see that

- If $x(t)$ is real and odd, then the a_k vanish identically, and the b_k are purely imaginary.
- On the other hand, if $x(t)$ is real and even, the b_k vanish and the a_k are real quantities.

The even/odd coefficient symmetry with respect to k is not an issue with the trigonometric Fourier series, since the index k is restricted to the positive integers.

5.1.3.2 *Example: Sawtooth Wave.*
We conclude with a study of the trigonometric Fourier series for the case of a sawtooth signal. Consider the piecewise continuous function shown in Figure 5.4a. In the fundamental interval $[0, T]$, $x(t)$ consists of two segments, each of slope μ. For $t \in [0, T/2]$:

$$x(t) = \mu t, \tag{5.58a}$$

and for $t \in [T/2, T]$:

$$x(t) = \mu(t - T). \tag{5.58b}$$

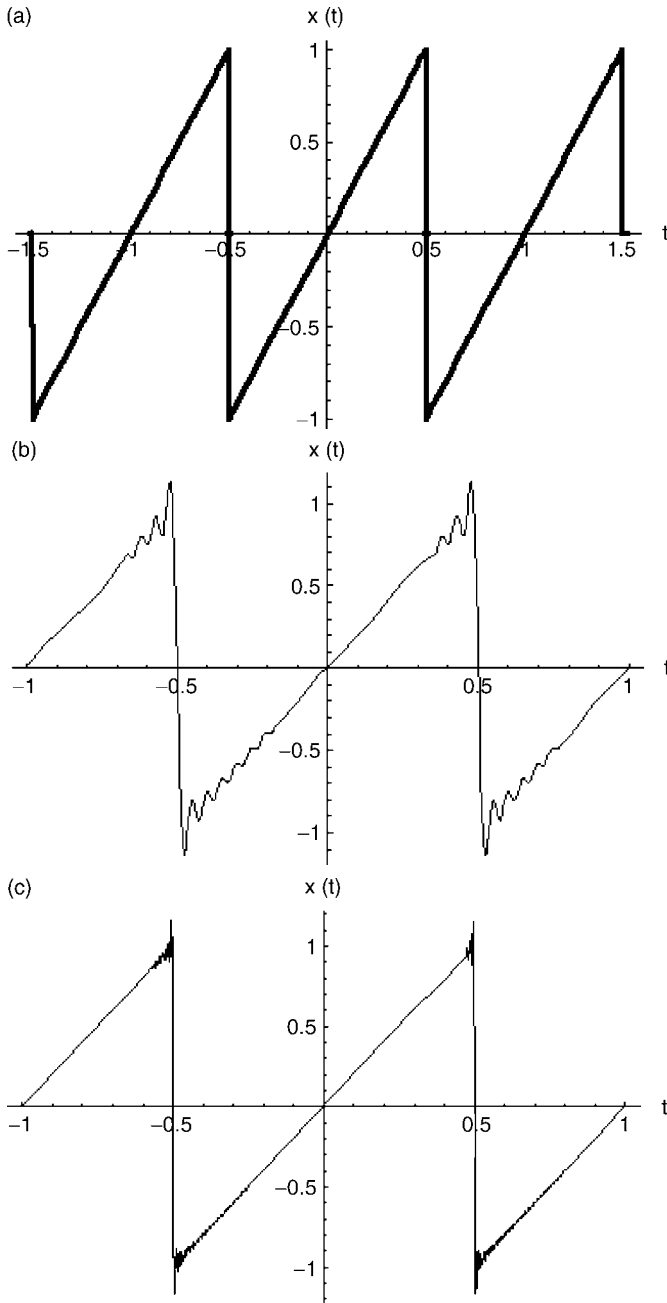The coefficients follow straightforwardly. We have

$$b_n = \frac{T}{2} \langle x(t), \sin(n\Omega t) \rangle = \frac{2\mu}{T} \int_0^T t \sin(n\Omega t) \, dt + \left(-\frac{4h}{T} \right) \int_{T/2}^T \sin(n\Omega t) \, dt. \tag{5.59}$$

The first integral on the right in (5.59) is evaluated through integration by parts:

$$\frac{2\mu}{T} \int_0^T t \sin(n\Omega t) \, dt = \frac{-2h}{\pi n}. \tag{5.60}$$

The second integral is nonzero only for $n = 1, 3, 5, \ldots$,

$$\frac{-4h}{T} \int_{T/2}^T \sin(n\Omega t) \, dt = \frac{4h}{\pi n}. \tag{5.61}$$

Fig. 5.4. Synthesis of the sawtooth wave using the trigonometric Fourier series. (a) The original waveform. (b) Partial series, $N = 20$. (c) For $N = 100$. (d) For $N = 200$. There are $N + 1$ terms in the partial series. (e) Details illustrating Gibbs oscillation near a discontinuity, for $N = 20$, 100, and 200. Note that all partial series converge to $x_N(t) = 0$ at the discontinuity.
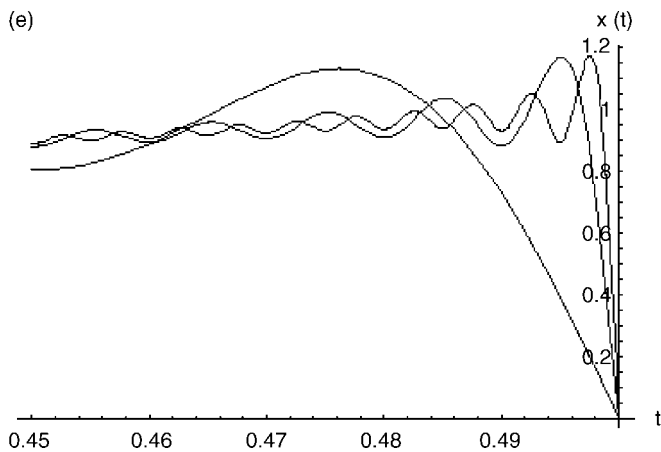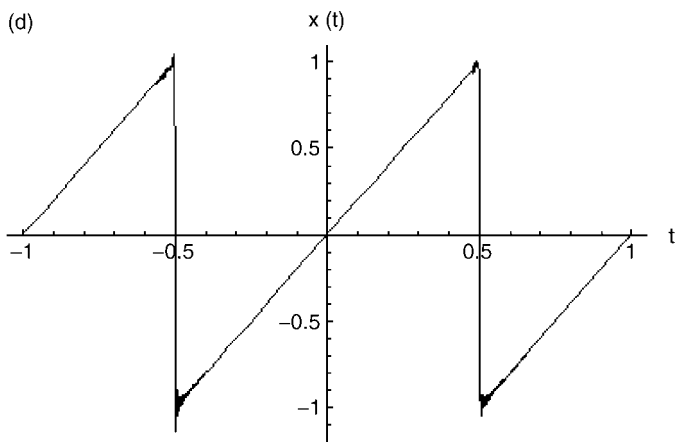
(d)

(e)

Fig. 5.4   (*Continued*)

Therefore, for $n = 1, 3, 5, ...$,

$$b_n = \frac{2h}{\pi n},$$ (5.62a)

while for $n = 2, 4, 6, ...$,

$$b_n = \frac{-2h}{\pi n}.$$ (5.62b)

Since $x(t)$ exhibits odd symmetry in t, the coefficients for the cosine basis are identically zero for all n:

$$a_n = 0.$$ (5.63)

Example (Sawtooth Wave Synthesis). Figure 5.4 illustrates several partial series syntheses of this signal using the coefficients (5.62a). The Gibbs oscillations are clearly in evidence. The convergence properties follow the principles outlined earlier and illustrated in connection with the rectangular pulse train.

Remark. From the standpoint of physical correctness, the exponential and trigonometric series are equally valid. Even and odd symmetries—if they exist—are more easily visualized for the trigonometric series, but mathematically inclined analysts find appeal in the exponential Fourier series. The latter's formalism more closely relates to the Fourier transform operation considered in the next section, and it forms the basis for common numerical algorithms such as the fast Fourier transform (FFT) discussed in Chapter 7.

5.2 FOURIER TRANSFORM

In the case of periodic waveforms considered in the previous section, the notion of "frequency content" is relatively intuitive. However, many signals of practical importance exhibit no periodicity whatsoever. An isolated pulse or disturbance, or an exponentially damped sinusoid, such as that produced by a resistor–capacitor (RC) circuit, would defy analysis using the Fourier series expansion. In many practical systems, the waveform consists of a periodic sinusoidal carrier wave whose envelope is modulated in some manner; the result is a composite signal having an underlying sinusoidal structure, but without overall periodicity. Since the information content or the "message," which could range from a simple analog sound signal to a stream of digital pulses, is represented by the modulation, an effective means of signal analysis for such waves is of enormous practical value. Furthermore, all communications systems are subject to random fluctuations in the form of noise, which is rarely obliging enough to be periodic.

5.2.1 Motivation and Definition

In this section, we develop a form of Fourier analysis applicable to many practical aperiodic signals. In fact, we will eventually demonstrate that the Fourier series is a special case of the theory we are about to develop; we will need to equip ourselves, however, with a mathematical arsenal appropriate to the task. Many notions will carry over from the Fourier series. The transformation to frequency space—resulting in an analysis of the waveform in terms of its frequency content—will remain intact. Similarly, the synthesis, whereby the original signal is reconstructed based on the frequency spectrum, will be examined in detail. We will develop the criteria by which a given waveform will admit a transform to frequency space and by which the resulting spectra will admit a viable *synthesis*, or *inverse transform*.

Since our nascent Fourier transform involves integrals, analysis and synthesis relations lean heavily on the notion of absolute integrability. Not surprisingly, the analog L^p signal spaces—in particular, $L^1(\mathbb{R})$ and $L^2(\mathbb{R})$—will figure prominently.

We recall these abstract function spaces from Chapter 3: $L^p(\mathbb{K}) = \{x(t) \mid \|x\|_p < \infty\}$. Here

$$\|x\|_p = \left[\int\limits_{-\infty}^{\infty} |x(t)|^p dt \right]^{\frac{1}{p}} \tag{5.64}$$

is the L^p norm of $x(t)$ and $\mathbb{K}$ is either the real numbers $\mathbb{R}$ or the complex numbers $\mathbb{C}$. We define the set of bounded signals to be L^∞. These signal classes turn out to be Banach spaces, since Cauchy sequences of signals in L^p converge to a limit signal also in L^p. L^1 is also called the space of *absolutely integrable* signals, and L^2 is called the space of *square-integrable* signals. The case of $p = 2$ is special: L^2 is a Hilbert space. That is, there is an inner product relation on square-integrable signals $\langle x, y \rangle \in \mathbb{K}$, which extends the idea of the vector space dot product to analog signals.

In the case of the Fourier series, the frequency content was represented by a set of discrete coefficients, culled from the signal by means of an inner product involving the signal and a discrete orthonormal basis:

$$c_k = \langle x(t), \phi_k(t) \rangle = \int\limits_{t_0}^{t_0 + T} x(t) \frac{1}{\sqrt{T}} e^{-jk\Omega t} dt . \tag{5.65}$$

One might well ask whether a similar integral can be constructed to handle nonperiodic signals $f(t)$. A few required modifications are readily apparent. Without the convenience of a fundamental frequency or period, let us replace the discrete harmonics $k\omega$ with a continuous angular frequency variable ω, in radians per second. Furthermore, all values of the time variable t potentially contain information regarding the frequency content; this suggests integrating over the entire time axis, $t \in [-\infty, \infty]$. The issue of multiplicative constants, such as the normalization constant $1/\sqrt{T}$, appears in a different guise as well. Taking all of these issues into account, we propose the following definition of the Fourier transform:

Definition (Radial Fourier Transform). The radial Fourier transform of a signal $f(t)$ is defined by the integral,

$$F(\omega) = \int\limits_{-\infty}^{\infty} f(t) e^{-j\omega t} dt. \tag{5.66a}$$

It is common to write a signal with a lowercase letter and its Fourier transform with the corresponding uppercase letter. Where there may be confusion, we also write $F(\omega) = \mathcal{F}[f(t)](\omega)$, with a "fancy F" notation.

Remark. Note that the Fourier transform operation $\mathcal{F}$ is an analog system that accepts time domain signals $f(t)$ as inputs and produces frequency-domain signals

$F(\omega)$ as outputs. One must be cautious while reading the signal processing litera-
ture, because two other definitions for $\mathcal{F}$ frequently appear:

- The *normalized* radial Fourier transform;
- The *Hertz* Fourier transform.

Each one has its convenient aspects. Some authors express a strong preference for
one form. Other signal analysts slip casually among them. We will mainly use the
radial Fourier transform, but we want to provide clear definitions and introduce spe-
cial names that distinguish the alternatives, even if our terminology is not standard.
When we change definitional forms to suit some particular analytical endeavor,
example, or application, we can then alert the reader to the switch.

Definition (Normalized Radial Fourier Transform). The *normalized radial Fou-
rier transform* of a signal $f(t)$ is defined by the integral,

$$F(\omega) = \frac{1}{\sqrt{2\pi}} \int_{-\infty}^{\infty} f(t) e^{-j\omega t} dt. \qquad (5.66b)$$

The $(2\pi)^{-1}$ factor plays the role of a normalization constant for the Fourier trans-
form much as the factor $1/\sqrt{T}$ did for the Fourier series development. Finally, we
have the Hertz Fourier transform:

Definition (Hertz Fourier Transform). The *Hertz Fourier transform* of a signal
$x(t)$ is defined by the integral

$$x(f) = \int_{-\infty}^{\infty} x(t) e^{-j2\pi ft} dt. \qquad (5.66c)$$

Remark. The units of ω in both the radial and normalized Fourier transforms are in
radians per second, assuming that the time variable t is counted in seconds. The
units of the Hertz Fourier transform are in hertz (units of inverse seconds or cycles
per second). A laboratory spectrum analyzer displays the Hertz Fourier transform—
or, at least, it shows a reasonably close approximation. So this form is most conve-
nient when dealing with signal processing equipment. The other two forms are more
convenient for analytical work. It is common practice to use ω (or Ω) as a radians
per second frequency variable and use f (or F) for a Hertz frequency variable. But
we dare to emphasize once again that Greek or Latin letters do no more than hint of
the frequency measurement units; it is rather the particular form of the Fourier
transform definition in use that tells us what the frequency units must be.

The value of the Fourier transform at $\omega = 0$, $F(0)$, is often called, in accord with
electrical engineering parlance, the *direct current* or *DC* term. It represents that
portion of the signal which contains no oscillatory, or *alternating current* (*AC*),
component.

Now if we inspect the radial Fourier transform's definition (5.66a), it is tempting to write it as the inner product $\langle x(t), e^{j\omega t} \rangle$. Indeed, the Fourier integral has precisely this form. However, we have not indicated the signal space to which $x(t)$ may belong. Suppose we were to assume that $x(t) \in L^2(\mathbb{R})$. This space supports an inner product, but that will not guarantee the existence of the inner product, because, quite plainly, the exponential signal, $e^{j\omega t}$ is not square-integrable. Thus, we immediately confront a theoretical question of the Fourier transform's existence. Assuming that we can justify this integration for a wide class of analog signals, the Fourier transform does appear to provide a measure of the amount of radial frequency ω in signal $x(t)$. According to this definition, the frequency content of $x(t)$ is represented by a function $X(\omega)$ which is clearly analogous to the discrete set of Fourier series coefficients, but is—as we will show— a continuous function of angular frequency ω.

Example (Rectangular Pulse). We illustrate the radial Fourier transform with a rectangular pulse of width $2a > 0$, where

$$f(t) = 1 \tag{5.67}$$

for $-a \le t < a$, and vanishes elsewhere. This function has compact support on this interval and its properties under integration are straightforward when the Fourier transform is applied:

$$F(\omega) = \int_{-\infty}^{\infty} f(t) e^{-j\omega t} dt = \int_{-a}^{a} e^{-j\omega t} dt = 2a \left[\frac{\sin(\omega a)}{\omega a} \right]. \tag{5.68}$$

The most noteworthy feature of the illustrated frequency spectrum, Figure 5.5, is that the pulse width depends upon the parameter a.

Note that most of the spectrum concentrates in the region $\omega \in [-\pi/a, \pi/a]$. For small values of a, this region is relatively broad, and the maximum at $\omega = 0$ (i.e.,
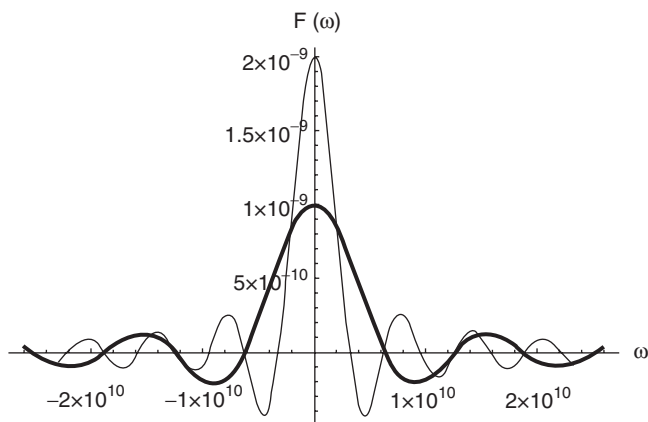
Fig. 5.5. The spectrum for a 1-ns rectangular pulse (solid line), and a 2-ns pulse. Note the inverse relationship between pulse width in time and the spread of the frequency spectrum.

the DC contribution) is, relatively speaking, low. This is an indication that a larger proportion of higher frequencies are needed to account for the relatively rapid jumps in the rectangular pulse. Conversely, as the pulse width increases, a larger proportion of the spectrum resides near the DC frequency. In fact, as the width of the pulse approaches infinity, its spectrum approaches the Dirac delta function $\delta(\omega)$, the generalized function introduced in Chapter 3. This scaling feature generalizes to all Fourier spectra, and the inverse relationship between the spread in time and the spread in frequency can be formalized in one of several uncertainty relations, the most famous of which is attributed to Heisenberg. This topic is covered in Chapter 10.

Example (Decaying Exponential). By their very nature, transient phenomena are short-lived and often associated with exponential decay. Let $\alpha > 0$ and consider

$$f(t) = e^{-\alpha t} u(t), \tag{5.69}$$

which represents a damped exponential for all $t > 0$. This signal is integrable, and the spectrum is easily calculated:

$$F(\omega) = \int_0^\infty e^{-\alpha t} e^{-j\omega t} dt = \frac{-1}{\alpha + j\omega} e^{-(\alpha - j\omega)t} \Big|_0^\infty = \frac{1}{\alpha + j\omega}. \tag{5.70}$$

Remark. $F(\omega)$ is characterized by a singularity at $\omega = j\alpha$. This pole is purely imaginary—which is typical of an exponentially decaying (but nonoscillatory) response $f(t)$. In the event of decaying oscillations, the pole has both real and imaginary parts. This situation is discussed in Chapter 6 in connection with the modulation theorem. In the limit $\alpha \to 0$, note that $f(t) \to u(t)$, but (it turns out) $\mathcal{F}[u(t)](\omega)$ does *not* approach $1/j\omega$. In this limit, $f(t)$ is no longer integrable, and the Fourier transform as developed so far does not apply. We will rectify this situation with a generalized Fourier transform developed in Chapter 6.

TABLE 5.1. Radial Fourier Transforms of Elementary Signals

Signal Expression	Radial Fourier Transform
$f(t)$	$F(\omega) = \int_{-\infty}^{\infty} f(t) e^{-j\omega t} dt$
Square pulse: $u(t + a) - u(t - a)$	$2a \left[\dfrac{\sin(\omega a)}{\omega a} \right] = 2a\,\mathrm{sinc}(\omega a)$
Decaying exponential: $e^{-\alpha t} u(t),\ \ \alpha > 0$	$\dfrac{1}{\alpha + j\omega}$
Gaussian: $e^{-\alpha t^2},\ \ \alpha > 0$	$\sqrt{\dfrac{\pi}{\alpha}} e^{\frac{-\omega^2}{4\alpha}}$

5.2.2   Inverse Fourier Transform

The integral Fourier transform admits an inversion formula, analogous to the synthesis for Fourier series. One might propose a Fourier synthesis analogous to the discrete series (5.9):

$$f(t) \approx \int_{-\infty}^{\infty} F(\omega) e^{j\omega t} d\omega. \qquad (5.71)$$

In fact, this is complete up to a factor, encapsulated in the following definition:

Definition (Inverse Radial Fourier Transform). The *inverse radial Fourier transform* of $F(\omega)$ is defined by the integral

$$f(t) = \frac{1}{2\pi} \int_{-\infty}^{\infty} F(\omega) e^{j\omega t} d\omega. \qquad (5.72)$$

The Fourier transform and its inverse are referred to as a *Fourier transform pair.*

The inverses for the normalized and Hertz variants take slightly different forms.

Definition (Inverse Normalized Fourier Transform). If $F(\omega)$ is the normalized Fourier transform of $f(t)$, then the *inverse normalized Fourier transform* of $F(\omega)$ is the integral

$$f(t) = \frac{1}{\sqrt{2\pi}} \int_{-\infty}^{\infty} F(\omega) e^{j\omega t} d\omega. \qquad (5.73a)$$

Definition (Inverse Hertz Fourier Transform). If $X(f)$ is the Hertz Fourier transform of $x(t)$, then the *inverse Hertz Fourier transform* of $X(f)$ is

$$x(t) = \int_{-\infty}^{\infty} X(f) e^{j2\pi ft} df. \qquad (5.73b)$$

Naturally, the utility of this pair is constrained by our ability to carry out the integrals defining the forward and inverse transforms. At this point in the development one might consider the following:

- Does the radial Fourier transform $F(\omega)$ exist for all continuous or piecewise continuous functions?
- If $F(\omega)$ exists for some $f(t)$, is it always possible to invert the resulting spectrum to synthesize $f(t)$?

The answer to both these questions is *no*, but the set of functions which are suitable is vast enough to have made the Fourier transform the stock and trade of signal analysis. It should come as no surprise that the integrability of $f(t)$, and of its spectrum,

can be a deciding factor. On the other hand, a small but very important set of common signals do not meet the integrability criteria we are about to develop, and for these we will have to extend the definition of the Fourier transform to include a class of generalized Fourier transform, treated in Chapter 6.

We state and prove the following theorem for the radial Fourier transforms; proofs for the normalized and Hertz cases are similar.

Theorem (Existence). If $f(t)$ is absolutely integrable—that is, if $f(t) \in L^1(\mathbb{R})$— then the Fourier transform $F(\omega)$ exists.

Proof: This follows directly from the transform's definition. Note that

$$|F(\omega)| = \left| \int_{-\infty}^{\infty} f(t)e^{-j\omega t} dt \right| \le \int_{-\infty}^{\infty} |f(t)| \left| e^{-j\omega t} \right| dt = \int_{-\infty}^{\infty} |f(t)| \, dt. \qquad (5.74)$$

So $F(\omega)$ exists if

$$\int_{-\infty}^{\infty} |f(t)| dt < \infty; \qquad (5.75)$$

that is, $f(t) \in L^1(\mathbb{R})$. ∎

Theorem (Existence of Inverse). If $F(\omega)$ is absolutely integrable, then the inverse Fourier transform $\mathcal{F}^{-1}[F(\omega)](t)$ exists.

Proof: The proof is similar and is left as an exercise. ∎

Taken together, these existence theorems imply that if $f(t)$ and its Fourier spectrum $F(\omega)$ belong to $L^1(\mathbb{R})$, then both the analysis and synthesis of $f(t)$ can be performed. Unfortunately, if $f(t)$ is integrable, there is no guarantee that $F(\omega)$ follows suit. Of course, it *can* and often *does*. In those cases where synthesis (inversion) is impossible because $F(\omega)$ not integrable, the spectrum is still a physically valid representation of frequency content and can be subjected to many of the common operations (filtering, band-limiting, and frequency translation) employed in practical systems. In order to guarantee both analysis and synthesis, we need a stronger condition on $f(t)$, which we will explore in due course. For the time being, we will further investigate the convergence of the Fourier transform and its inverse, as applied to continuous and piecewise continuous functions.

Theorem (Convergence of Inverse). Suppose $f(t)$ and $F(\omega)$ are absolutely integrable and continuous. Then the inverse Fourier transform exists and converges to $f(t)$.

Proof: Define a band-limited inverse Fourier transform as follows:

$$f_\Omega(t) = \frac{1}{2\pi} \int_{-\Omega}^{\Omega} F(\omega)e^{j\omega t} \, d\omega. \qquad (5.76)$$

In the limit $\Omega \to \infty$, (5.76) should approximate $f(t)$. (There is an obvious analogy between the band-limited Fourier transform and the partial Fourier series expansion.) Replacing $F(\omega)$ with its Fourier integral representation (5.66a) and interchanging the limits of integration, (5.76) becomes

$$f_\Omega(t) = \frac{1}{2\pi} \int_{-\Omega}^{\Omega} \left[\int_{-\infty}^{\infty} f(\tau) e^{-j\omega t} d\tau \right] e^{j\omega t} d\omega = \int_{-\infty}^{\infty} f(\tau) K_\Omega(t - \tau) \, d\tau, \qquad (5.77a)$$

where

$$K_\Omega(t - \tau) = \frac{\sin \Omega(t - \tau)}{\pi(t - \tau)} \equiv \int_{-\Omega}^{\Omega} e^{j\omega(t - \tau)} d\omega. \qquad (5.77b)$$

There are subtle aspects involved in the interchange of integration limits carried out in the preceding equations. We apply Fubini's theorem [13, 14] and the assumption that both $f(t)$ and $F(\omega)$ are in $L^1(\mathbb{R})$. This theorem, which we reviewed in Chapter 3, states that if a function of two variables is absolutely integrable over a region, then its iterated integrals and its double integral over the region are all equal. In other words, if $\|x(t, \omega)\|_1 < \infty$, then:

- For all $t \in \mathbb{R}$, the function $x_t(\omega) = x(t, \omega)$ is absolutely integrable (except— if we are stepping up to Lebesgue integration—on a set of measure zero).
- For all $\omega \in \mathbb{R}$, the function $x_\omega(t) = x(t, \omega) \in L^1(\mathbb{R})$ (again, except perhaps on a measure zero set).
- And we may freely interchange the order of integration:

$$\int_{-\infty}^{\infty} \left[\int_{-\infty}^{\infty} x(t, \omega) dt \right] d\omega = \int_{-\infty}^{\infty} \left[\int_{-\infty}^{\infty} x(t, \omega) d\omega \right] dt. \qquad (5.78)$$

So we apply Fubini here to the function of two variables, $x(\tau, \omega) = f(\tau) e^{-j\omega\tau} e^{j\omega t}$, with t fixed, which appears in the first iterated integral in (5.77a). Now, the function

$$K_\Omega(x) = \frac{\sin \Omega x}{\pi x} \qquad (5.79)$$

is the Fourier kernel. In Chapter 3 we showed that it is one of a class of generalized functions which approximates a Dirac delta function in the limit of large Ω. Thus,

$$\lim_{\Omega \to \infty} f_\Omega(t) = \lim_{\Omega \to \infty} \int_{-\Omega}^{\Omega} f(\tau) \frac{\sin \Omega(t - \tau)}{\pi(t - \tau)} d\tau = \int_{-\infty}^{\infty} f(\tau) \delta(t - \tau) \, d\tau = f(t). \quad (5.80)$$

completing the proof.   ■

5.2.3 Properties

In this section we consider the convergence and algebraic properties of the Fourier transform. Many of these results correspond closely to those we developed for the Fourier series. We will apply these properties often—for instance, in developing analog *filters*, or frequency-selective convolutional systems, in Chapter 9.

5.2.3.1 Convergence and Discontinuities. Let us first investigate how well the Fourier transform's synthesis relation reproduces the original time-domain signal. Our first result concerns time-domain discontinuities, and the result is quite reminiscent of the case of the Fourier series.

Theorem (Convergence at Step Discontinuities). Suppose $f(t) \in L^1(\mathbb{R})$ has a step discontinuity at some time t. Let $F(\omega) = \mathcal{F}[f(t)](\omega)$ be the radial Fourier transform of $f(t)$ with $F(\omega) \in L^1(\mathbb{R})$. Assume that, in some neighborhood of $t, f(t)$ and its derivative have well-defined limits from the left and from the right: $f(t_{(l)})$ and $f(t_{(r)})$, respectively. Then the inverse Fourier transform, $\mathcal{F}^{-1}[F(\omega)](t)$, converges pointwise to the value,

$$\mathcal{F}^{-1}[F(\omega)](t) = \frac{[f(t_{(r)}) + f(t_{(l)})]}{2}. \tag{5.81}$$

Proof: The situation is clearly analogous to Fourier series convergence at a step discontinuity. We leave it as an exercise to show that the step discontinuity (assumed to lie at $t = 0$ for simplicity) gives a residual Gibbs oscillation described by

$$\varepsilon_N(t) = A_0 \left[\int_{-\infty}^{0} \frac{\sin v}{\pi v} \, dv + \int_{0}^{\Omega t} \frac{\sin v}{\pi v} \, dv \right] = \frac{1}{2}A_0 + A_0 \int_{0}^{\Omega t} \frac{\sin v}{\pi v} \, dv, \tag{5.82a}$$

where the amplitude of the step is

$$A_0 = [f(0_{(r)}) - f(0_{(l)})]. \tag{5.82b}$$

Therefore in the limit as $\Omega \to \infty$,

$$\varepsilon_N(0) = \frac{1}{2}A_0. \tag{5.83}$$

Hence the inverse Fourier transform converges to the average of the left- and right-hand limits at the origin,

$$f(0) = f_c(0) + \frac{1}{2}[f(0_{(r)}) - f(0_{(l)})] = \frac{1}{2}[f(0_{(r)}) + f(0_{(l)})]. \tag{5.84}$$

For a step located at an arbitrary $t = t_s$ the result generalizes so that

$$f(0) = f_c(t_s) + \frac{1}{2}[f(t_{s(r)}) - f(t_{s(l)})] = \frac{1}{2}[f(t_{s(r)}) + f(t_{s(l)})], \tag{5.85}$$

and the proof is complete.   ∎

The Gibbs oscillations are an important consideration when evaluating Fourier transforms numerically, since numerical integration over an infinite interval always involves approximating infinity with a suitably large number. Effectively, they are band-limited Fourier transforms; and in analogy to the Fourier series, the Gibbs oscillations are an artifact of truncating the integration.

5.2.3.2   Continuity and High- and Low-Frequency Behavior of Fourier Spectra. The continuity of the Fourier spectrum is one of its most remarkable properties. While Fourier analysis can be applied to both uniform and piecewise continuous signals, the resulting spectrum is *always* uniformly continuous, as we now demonstrate.

Theorem (Continuity). Let $f(t) \in L^1(\mathbb{R})$. Then $F(\omega)$ is a uniformly continuous function of ω.

Proof: We need to show that for any $\varepsilon > 0$, there is a $\delta > 0$, such that $|\omega - \theta| < \delta|$ implies that $|F(\omega) - F(\theta)| < \varepsilon|$. This follows by noting

$$|F(\omega + \delta) - F(\omega)| = \int_{-\infty}^{\infty} f(t)(e^{-j\delta t} - 1)e^{-j\omega t} dt \leq 2\|f\|_1. \tag{5.86}$$

Since $|F(\omega + \delta) - F(\omega)|$ is bounded above by $2\|f\|_1$, we may apply the Lebesgu-dominated convergence theorem (Chapter 3). We take the limit, as $\delta \to 0$, of $|F(\omega + \delta) - F(\omega)|$ and the last integral in (5.86). But since $e^{-j\delta t} \to 1$ as $\delta \to 0$, this limit is zero:

$$\lim_{\delta \to 0} |F(\omega + \delta) - F(\omega)| = 0 \tag{5.87}$$

and $F(\omega)$ is continuous. Inspecting this argument carefully, we see that the limit of the last integrand of (5.86) does not depend on ω, establishing uniform continuity as well.   ∎

Remark. This theorem shows that absolutely integrable signals—which includes every practical signal available to a real-world processing and analysis system—can have no sudden jumps in their frequency content. That is, we cannot have $|F(\omega)|$ very near one value as ω increases toward ω_0, and $|F(\omega)|$ approaches a different value as ω decreases toward ω_0. If a signal is in $L^1(\mathbb{R})$, then its spectra are smooth. This

is an interesting situation, given the abundance of piecewise continuous waveforms (such as the rectangular pulse) which are clearly in $L^1(\mathbb{R})$ and, according to this theorem, exhibit continuous (note, not piecewise continuous) spectra. Moreover, the uniform continuity assures us that we should find no cusps in our plots of $|F(\omega)|$ versus ω.

Now let us consider the high-frequency behavior of the Fourier spectrum. In the limit of infinite frequency, we shall show $F(\omega) \to 0$. This general result is easily demonstrated by the Riemann–Lebesgue lemma, a form of which was examined in Chapter 3 in connection with the high-frequency behavior of simple sinusoids (as distributions generated by the space of testing functions with compact support). Here the lemma assumes a form that suits the Fourier transform.

Proposition (Riemann–Lebesgue Lemma, Revisited). If $f(t)$ is integrable, then

$$\lim_{|\omega| \to \infty} |F(\omega)| = 0. \tag{5.88}$$

Proof: The proof follows easily from a convenient trick. Note that

$$e^{-j\omega t} = -e^{-j\omega t - j\pi} = -e^{-j\omega\left(t + \frac{\pi}{\omega}\right)}. \tag{5.89}$$

Thus, the Fourier integral can be written

$$F(\omega) = -\int_{-\infty}^{\infty} f(t)e^{-j\omega\left(t + \frac{\pi}{\omega}\right)} dt = -\int_{-\infty}^{\infty} f\left(t - \frac{\pi}{\omega}\right)e^{-j\omega t} dt. \tag{5.90}$$

Expressing the fact that $F(\omega) \equiv \frac{1}{2}[F(\omega) + F(\omega)]$ by utilizing the standard and revised representations (as given in (5.90)) of $F(\omega)$, we have

$$F(\omega) = \frac{1}{2}\int_{-\infty}^{\infty}\left[f(t) - f\left(t - \frac{\pi}{\omega}\right)\right]e^{-j\omega t} d\omega, \tag{5.91}$$

so that

$$|F(\omega)| \leq \int_{-\infty}^{\infty}\left|\left[f(t) - f\left(t - \frac{\pi}{\omega}\right)\right]\right| d\omega. \tag{5.92}$$

Taking the high-frequency limit, we have

$$\lim_{\omega \to \infty} |F(\omega)| \leq \lim_{\omega \to \infty}\int_{-\infty}^{\infty}\left|\left[f(t) - f\left(t - \frac{\pi}{\omega}\right)\right]\right| d\omega = 0, \tag{5.93}$$

and the lemma is proven.   ∎

Taken in conjunction with continuity, the Riemann–Lebesgue lemma indicates that the spectra associated with integrable functions are well-behaved across all frequencies. But we emphasize that despite the decay to zero indicated by (5.93), this does not guarantee that the spectra decay rapidly enough to be integrable. Note that the Fourier transform $F(\omega)$ of $f(t) \in L^1(\mathbb{R})$ is bounded. In fact, we can easily estimate that $\|F\|_\infty \le \|f\|_1$ (exercise).

5.2.3.3 *Algebraic Properties.*

These properties concern the behavior of the Fourier transform integral under certain algebraic operations on the transformed signals. The Fourier transform is an analog system, mapping (some) time-domain signals to frequency-domain signals. Thus, these algebraic properties include such operations that we are familiar with from Chapter 3: scaling (amplification and attenuation), summation, time shifting, and time dilation.

Proposition (Linearity). The integral Fourier transform is linear; that is,

$$\mathcal{F}\left[\sum_{k=1}^{N} a_k f_k(t)\right](\omega) \;=\; \sum_{k=1}^{N} a_k F_k(\omega). \tag{5.94}$$

Proof: This follows from the linearity of the integral. ∎

From a practical standpoint, the result is of enormous value in analyzing composite signals and signals plus noise, indicating that the spectra of the individual components can be analyzed and (very often) processed separately.

Proposition (Time Shift). $\mathcal{F}[f(t - t_0)](\omega) \;=\; e^{-j\omega t_0} F(\omega).$

Proof: A simple substitution of variables, $v = t - t_0$, applied to the definition of the Fourier transform leads to

$$\mathcal{F}[f(t - t_0)](\omega) \;=\; \int_{-\infty}^{\infty} f(t - t_0) e^{-j\omega t}\, dt \;=\; e^{-j\omega t_0} \int_{-\infty}^{\infty} f(v) e^{-j\omega v}\, dv \;=\; e^{-j\omega t_0} F(\omega)$$

$$\tag{5.95}$$

completing the proof. ∎

Remark. Linear systems often impose a time shift of this type. Implicit in this property is the physically reasonable notion that a change in the time origin of a signal $f(t)$ does not affect the magnitude spectrum $|F(\omega)|$. If the same signal arises earlier or later, then the relative strengths of its frequency components remain the same since the energy $\|F(\omega)\|_2$ is invariant.

Proposition (Frequency Shift). $\mathcal{F}[f(t)e^{j\omega_0 t}](\omega) = F(\omega - \omega_0)$.

Proof: Writing out the Fourier transform explicitly, we find

$$\mathcal{F}[f(t)e^{j\omega t_0}](\omega) = \int_{-\infty}^{\infty} f(t)e^{-j(\omega - \omega_0)t}\, dt = F(\omega - \omega_0) \tag{5.96}$$

completing the proof. ∎

Remark. This is another result which is central to spectral analysis and linear systems. Note the ease with which spectra can be translated throughout the frequency domain by simple multiplication with a complex sinusoidal phase factor in the time domain. Indeed, (5.96) illustrates exactly how radio communication and broadcast frequency bands can be established [19–21]. Note that the Fourier transform itself is not translation invariant. The effect of a frequency shift is shown in Figure 5.6. Note that ω_0 can be positive or negative.

The simplicity of the proof belies the enormous practical value of this result. Fundamentally, it implies that by multiplying a waveform $f(t)$ by a sinusoid of known frequency, the spectrum can be shifted to another frequency range. This idea makes multichannel communication and broadcasting possible and will be explored more fully in Chapter 6.

Proposition (Scaling). Suppose $a \neq 0$. Then

$$F[f(at)](\omega) = \frac{1}{|a|}F\left(\frac{\omega}{a}\right). \tag{5.97}$$
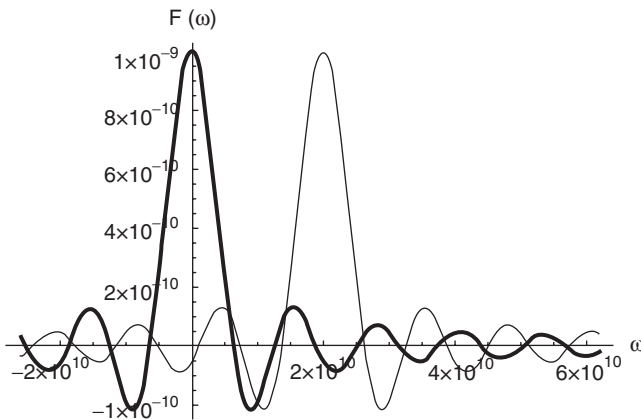
Fig. 5.6. Frequency translation. A "sinc" spectrum (solid line) and same spectrum shifted in frequency space by an increment $\omega_0 = 2 \times 10^{10}$.

Proof: Consider the cases of the scale parameter, $a > 0$ and $a < 0$, separately. First, suppose $a > 0$. With the substitution, $v = at$, it follows that

$$\mathcal{F}[f(at)](\omega) = \frac{1}{a} \int_{-\infty}^{\infty} f(v) e^{-j(\omega/a)v} dv = \frac{1}{a} F\left(\frac{\omega}{a}\right).$$

(5.98)

Following a similar argument for $a < 0$, carefully noting the signs on variables and the limits of integration, we find

$$\mathcal{F}[f(at)](\omega) = \frac{-1}{a} \int_{\infty}^{-\infty} f(v) e^{-j(\omega/a)v} dv = \frac{-1}{a} F\left(\frac{\omega}{a}\right).$$

(5.99)

In either case, the desired result (5.97) follows.   ∎

Scaling in the time domain is a central feature of the wavelet transform, which we develop in Chapter 11. For example, (5.97) can be used to describe the spectral properties of the crucial 'mother' wavelet, affording the proper normalization and calculation of wavelet coefficients (analogous to Fourier coefficients).

The qualitative properties previously observed in connection with the rectangular pulse and its spectrum are made manifest by these relations: The multiplicative scale a in the time-domain scales as a^{-1} in the spectrum. A Gaussian pulse serves as an excellent illustration of scaling.

Example (Gaussian). The Gaussian function

$$f(t) = e^{-\alpha t^2}$$

(5.100)

and its Fourier transform are shown in Figure 5.7. Of course, we assume $\alpha > 0$. Panel (a) shows Gaussian pulses in the time domain for $\alpha = 10^{11}$ and $\alpha = 11^{11}$. Panel (b) shows the corresponding Fourier transforms.

We will turn to the Gaussian quite frequently when the effects of noise on signal transmission are considered. Although noise is a nondeterministic process, its statistics—the spread of noise amplitude—often take the form of a Gaussian. Noise is considered a corruption whose effects are deleterious, so an understanding of its spectrum, and how to process noise so as to minimize its effects, plays an important role in signal analysis. Let us work out the calculations. In this example, we have built in a time scale, $a = \sqrt{\alpha}$, and we will trace its effects in frequency space:

$$F(\omega) = \int_{-\infty}^{\infty} e^{-\alpha t^2} [\cos(\omega t) - j\sin(\omega t)] \, dt.$$

(5.101)
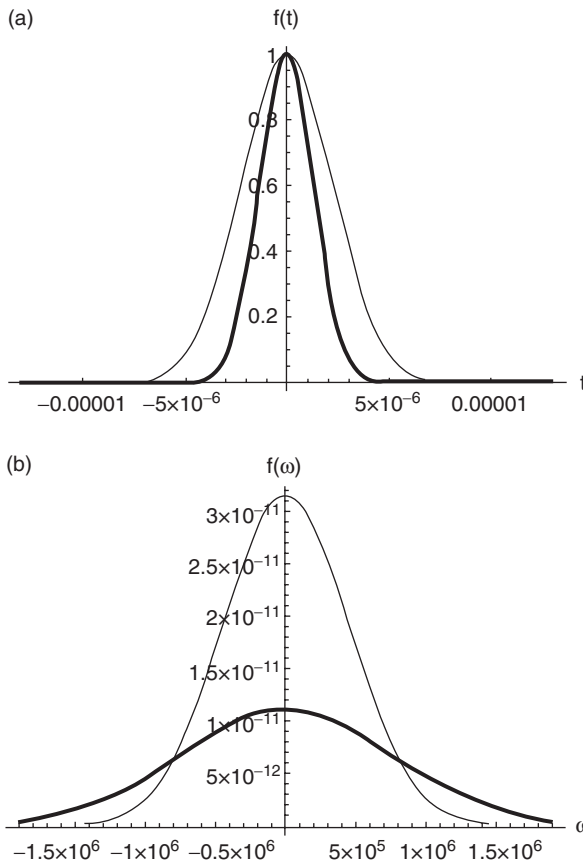
Fig. 5.7. (a) Gaussian pulses in the time domain, for $\alpha = 10^{11}$ and $\alpha = 11^{11}$ (solid lines). (b) Corresponding Fourier transforms.

If we informally assume that the integration limits in (5.101) approach infinity in perfect symmetry, then—since sine is an odd signal—we can argue that the contribution from $\sin(\omega t)$ vanishes identically. This leaves a common tabulated integral,

$$F(\omega) = \int_{-\infty}^{\infty} e^{-\alpha t^2} \cos(\omega t)\, dt = \sqrt{\frac{\pi}{\alpha}}\, e^{\frac{-\omega^2}{4\alpha}}. \qquad (5.102)$$

Note several features:

- The Fourier transform of a Gaussian is again a Gaussian.
- Furthermore, the general effects of scaling, quantified in (5.97), are clearly in evidence in Figure 5.7 where the Gaussian spectra are illustrated.

Corollary (Time Reversal)

$$\mathcal{F}[f(-t)](\omega) = F(-\omega).\qquad(5.103)$$

Proof: This is an instance of the scaling property.   ∎

Proposition (Symmetry)

$$\mathcal{F}[F(t)](\omega) = 2\pi f(-\omega).\qquad(5.104)$$

Proof: A relationship of this sort is hardly surprising, given the symmetric nature of the Fourier transform pair. Since

$$\mathcal{F}^{-1}[F(\omega)](t) = \frac{1}{2\pi}\int_{-\infty}^{\infty} F(\omega)e^{j\omega t}d\omega,\qquad(5.105a)$$

it follows that

$$f(-t) = \frac{1}{2\pi}\int_{-\infty}^{\infty} F(\omega)e^{-j\omega t}d\omega.\qquad(5.105b)$$

With a simple change of variables, we obtain

$$f(-\omega) = \frac{1}{2\pi}\int_{-\infty}^{\infty} F(t)e^{-j\omega t}d\omega,\qquad(5.106)$$

concluding the proof.   ∎

From a practical standpoint, this symmetry property is a convenient trick, allowing a list of Fourier transform pairs to be doubled in size without evaluating a single integral.

5.2.3.4   Calculus Properties. Several straightforward but useful properties are exhibited by the Fourier transform pair under differentiation. These are easily proven.

Proposition (Time Differentiation). Let $f(t)$ and $\frac{d^k f}{dt^k}$ be integrable functions, and suppose $\lim_{|t| \to \infty} \frac{d^k f}{dt^k} = 0$ for all $k = 0, 1, \ldots, n$. Then

$$\mathcal{F}\left[\frac{d^n f}{dt^n}\right](\omega) = (j\omega)^n F(\omega).\qquad(5.107)$$

Proof: We establish this result for the first derivative; higher orders follow by induction. Representing the Fourier integral by parts gives

$$\int_{-\infty}^{\infty} \frac{d}{dt} f(t) e^{-j\omega t} dt = f(t) e^{-j\omega t} \Big|_{-\infty}^{\infty} - \int_{-\infty}^{\infty} f(t)(-j\omega) e^{-j\omega t} dt. \tag{5.108}$$

Under the expressed conditions, the result for the first derivative follows immediately:

$$\mathcal{F}\left[\frac{df}{dt}\right](\omega) = j\omega F(\omega). \tag{5.109}$$

Repeated application of this process lead to (5.107). ∎

Proposition (Frequency Differentiation)

$$\mathcal{F}[(-jt)^n f(t)](\omega) = \frac{d^n}{d\omega^n} F(\omega). \tag{5.110}$$

Proof: The proof is similar to time differentiation. Note that the derivatives of the spectrum must exist in order to make sense of this propostion. ∎

The differentiation theorems are useful when established $f(t)$ or spectra are multiplied by polynomials in their respective domains. For example, consider the case of a Gaussian time signal as in (5.100), multiplied by an arbitrary time-dependent polynomial. According to the frequency differentiation property,

$$\mathcal{F}\left[(a_0 + a_1 t + \cdots + a_k t^k) e^{-\alpha t^2}\right](\omega) = \left[a_0 + \frac{-a_1}{j} \frac{d}{d\omega} + \cdots + \frac{a_k}{(-j)^k} \frac{d^k}{d\omega^k}\right] \sqrt{\frac{\pi}{\alpha}} e^{-\omega^2/(4\alpha)} \tag{5.111}$$

so that the act of taking a Fourier transform has been reduced to the application of a simple differential operator. The treatment of spectra corresponding to pure polynomials defined over all time or activated at some time t_0 will be deferred until Chapter 6, where the generalized Fourier transform of unity and $u(t - t_0)$ are developed.

Now let us study the low-frequency behavior of Fourier spectra. The Riemann–Lebesgue lemma made some specific predictions about Fourier spectra in the limit of infinite frequency. At low frequencies, in the limit as $\omega \to 0$, we can formally expand $F(\omega)$ in a Maclaurin series,

$$F(\omega) = \sum_{k=0}^{\infty} \frac{\omega^k}{k!} \frac{d^k F(0)}{d\omega^k}. \tag{5.112}$$

The Fourier integral representation of $F(\omega)$ can be subjected to a Maclaurin series for the frequency-dependent exponential:

$$F(\omega) = \int_{-\infty}^{\infty} f(t) \left[\sum_{k=0}^{\infty} \frac{(-j\omega t)^k}{k!} \right] dt = \sum_{k=0}^{\infty} (-j)^k \frac{\omega^k}{k!} \int_{-\infty}^{\infty} t^k f(t) \, dt. \qquad (5.113)$$

The last integral on the right is the kth moment of $f(t)$, defined as

$$m_k = \int_{-\infty}^{\infty} t^k f(t) \, dt \qquad (5.114)$$

If the moments of a function are finite, we then have the following proposition.

Proposition (Moments)

$$\frac{d^k F(0)}{d\omega^k} = (-j)^k m_k, \qquad (5.115)$$

which follows directly on comparing (5.112) and (5.113).

The moment theorem allows one to predict the low-frequency behavior of $f(t)$ from an integrability condition in time. This is often useful, particularly in the case of the wavelet transform. In order to qualify as a wavelet, there are necessary conditions on certain moments of a signal. This matter is taken up in Chapter 11.

Table 5.2 lists radial Fourier transformation properties. Some of these will be shown in the sequel.

5.2.4 Symmetry Properties

The even and odd symmetry of a signal $f(t)$ can have a profound effect on the nature of its frequency spectrum. Naturally, the impact of even–odd symmetry in transform analysis comes about through its effect on integrals. If $f(t)$ is odd, then its integral over symmetric limits $t \in [-L, L]$ vanishes identically; if $f(t)$ is even, this integral may be nonzero. In fact, this property was already put to use when discussing the Gaussian and its spectrum.

Not all functions $f(t)$ exhibit even or odd symmetry. But an arbitrary $f(t)$ may be expressed as the sum of even and odd parts: $f(t) = f_e(t) + f_o(t)$, where

$$f_e(t) = \frac{1}{2}[f(t) + f(-t))] \qquad (5.116a)$$

and

$$f_o(t) = \frac{1}{2}[f(t) - f(-t)]. \qquad (5.116b)$$

For example, in the case of the unit step,

$$f_e(t) = \frac{1}{2}[u(t) + u(-t))] = \frac{1}{2} \qquad (5.117a)$$

and

$$f_o(t) = \frac{1}{2}[u(t) - u(-t)] = \frac{1}{2}\operatorname{sgn} t.$$ (5.117b)

where sgn t is the signum function. These are illustrated in Figure 5.8 using the unit step as an example.

TABLE 5.2. Summary of Radial Fourier Transform Properties

Signal Expression	Radial Fourier Transform or Property
$f(t)$	$F(\omega) = \int_{-\infty}^{\infty} f(t)e^{-j\omega t}dt$ (Analysis equation)
$f(t) = \frac{1}{2\pi}\int_{-\infty}^{\infty} F(\omega)e^{j\omega t}d\omega$	$F(\omega)$ (Inverse, synthesis equation)
$af(t) + bg(t)$	$aF(\omega) + bG(\omega)$ (Linearity)
$f(t-a)$	$e^{-j\omega a}F(\omega)$ (Time shift)
$f(t)\exp(j\theta t)$	$F(\omega - \theta)$ (Frequency shift, modulation)
$f(at), a \neq 0$	$\frac{1}{|a|}F\left(\frac{\omega}{a}\right)$ (Scaling, dilation)
$f(-t)$	$F(-\omega)$ (Time reversal)
$\left[\dfrac{d^n f(t)}{dt^n}\right]$	$(j\omega)^n F(\omega)$ (Time differentiation)
$(-jt)^n f(t)$	$\dfrac{d^n}{d\omega^n}F(\omega)$ (Frequency differentiation)
$\|x\|_2 = \dfrac{\|X(\omega)\|_2}{\sqrt{2\pi}}$	Plancherel's theorem
$\langle f, g \rangle = \frac{1}{2\pi}\langle F, G \rangle \; f, g \in L^2(\mathbb{R})$	Parseval's theorem
$f * h,$ where $f, h \in L^2(\mathbb{R})$	$F(\omega)H(\omega)$
$f(t)h(t)$	$(2\pi)^{-1}F(\omega) * H(\omega)$

(a)

(b)

(c)
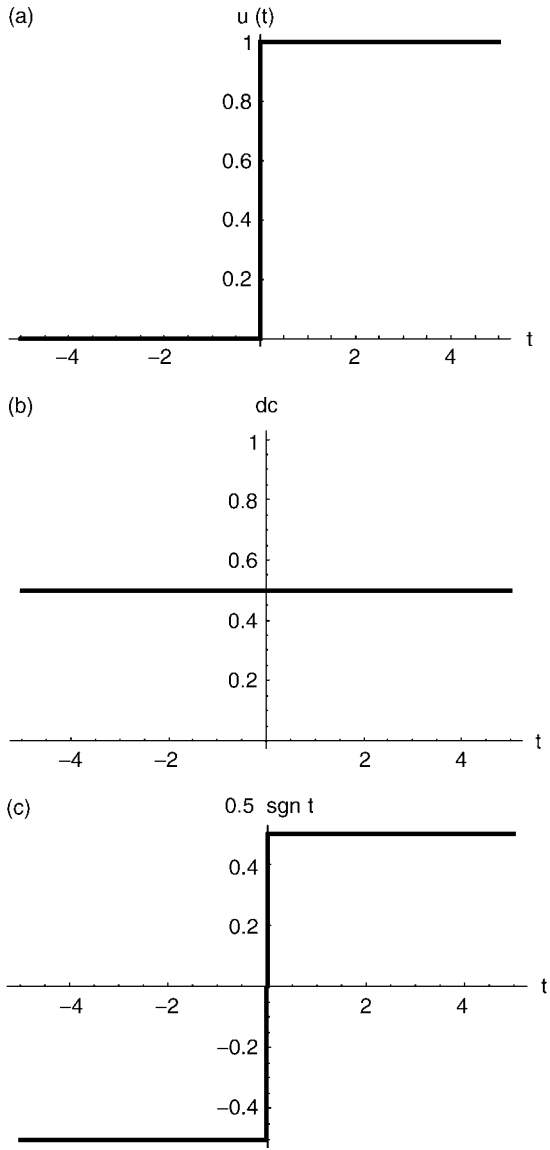
Fig. 5.8. (a) The unit step. (b) Its even-symmetry portion, a DC level of amplitude 1/2. (c) Its odd-symmetry portion, a signum of amplitude 1/2.

Whether the symmetry is endemic to the $f(t)$ at hand, or imposed by breaking it into even and odd parts, an awareness of its effects on the Fourier transform can often simplify calculations or serve as a check. Consider the spectrum of an arbitrary $f(t)$ written as the sum of even and odd constituents, $f(t) = f_e(t) + f_o(t)$:

$$F(\omega) = \int_{-\infty}^{\infty} [f_e(t) + f_o(t)]e^{-j\omega t}\,dt$$

$$= \int_{-\infty}^{\infty} [f_e(t) + f_o(t)]\cos(\omega t)\,dt - j\int_{-\infty}^{\infty} [f_e(t) + f_o(t)]\sin(\omega t)\,dt. \quad (5.118)$$

Elimination of the integrals with odd integrands reduces (5.110) to the elegant form

$$F(\omega) = \int_{-\infty}^{\infty} f_e(t)\cos(\omega t)\,dt - j\int_{-\infty}^{\infty} f_o(t)\sin(\omega t)\,dt. \quad (5.119)$$

This is a general result, applicable to an arbitrary $f(t)$ which may be real, complex, or purely imaginary. We consider these in turn.

5.2.4.1   Real f(t). A Fourier spectrum will, in general, have real and imaginary parts:

$$\mathrm{Re}[F(\omega)] = \int_{-\infty}^{\infty} f_e(t)\cos(\omega t)\,dt, \quad (5.120a)$$

which is an even function of ω (since $\cos(\omega t)$ is even in this variable) and

$$\mathrm{Im}[F(\omega)] = \int_{-\infty}^{\infty} f_o(t)\sin(\omega t)\,dt, \quad (5.120b)$$

which inherits the odd ω symmetry of $\sin(\omega t)$.

According to (5.120a), if $f(t)$ is even in addition to being real, then $F(\omega)$ is also real and even in ω. The Gaussian is a prime example, and many "mother wavelets" considered in Chapter 11 are real-valued, even functions of time. On the other hand, (5.120b) implies that if $f(t)$ is real but of odd symmetry, its spectrum is real and odd in ω.

5.2.4.2   Complex f(t). An arbitrary complex $f(t)$ can be broken into complex even and odd constituents $f_e(t)$ and $f_o(t)$ in a manner similar to the real case. When an expansion similar to (5.118) is carried out, it becomes apparent that $F(\omega)$ is, in general, complex, and it will consist of even and odd parts, which we denote $F_e(\omega)$ and $F_o(\omega)$. It is straightforward to show that the transforms break down as follows:

$$\mathrm{Re}[F_e(\omega)] = \int_{-\infty}^{\infty} \mathrm{Re}[f_e(t)]\cos(\omega t)\,dt, \quad (5.121a)$$

$$\mathrm{Re}[F_o(\omega)] = \int_{-\infty}^{\infty} \mathrm{Im}[f_o(t)]\sin(\omega t)\,dt, \quad (5.121b)$$

$$\text{Im}[F_e(\omega)] = \int_{-\infty}^{\infty} \text{Im}[f_e(t)]\cos(\omega t)\ dt, \tag{5.121c}$$

and

$$\text{Im}[F_o(\omega)] = -\int_{-\infty}^{\infty} \text{Re}[f_o(t)]\sin(\omega t)\ dt. \tag{5.121d}$$

The reader may easily verify that the earlier results for real $f(t)$ can be derived as special cases of (5.121a)–(5.121d).

5.2.4.3 *Imaginary f(t).*

This is also a special case of the above, derived by setting $\text{Re}[f_e(t)] = \text{Re}[f_o(t)] = 0$. In particular, note that if $f(t)$ is imaginary and odd, then $F(\omega)$ is odd but real. If $f(t)$ is imaginary and even, then the spectrum is also even but imaginary.

Most signals $f(t)$ are real-valued, but there are notable cases where a signal may be modified, intentionally or as a by-product of transmission and processing, to become complex or even purely imaginary. Examples include exponential carrier modulation and filtering. Either operation may impose a phase shift that is not present in the original signal.

5.2.4.4 *Summary.*

Familiarity with the symmetry properties of the Fourier transform can reduce unnecessary calculations and serve as a check of the final results. In the event that a waveform is not intrinsically odd or even, it is not always necessary, or even advisable, to break it into even and odd constituents, but doing so may be helpful when one is calculating transforms by hand and has access to a limited set of tabulated integrals. In most practical situations, numerical implementation of the Fourier transform, such as the fast Fourier transform (FFT) considered in Chapter 7, will handle the symmetries automatically.

5.3 EXTENSION TO L²(ℝ)

This section extends the Fourier transform to square-integrable signals. The formal definition of the Fourier transform resembles an inner-product integral of a signal $f(t)$ with the exponential $\exp(j\omega t)$. The inner product in $L^2(\mathbb{R})$ works as a measure of similarity between two signals, so $F(\omega)$, when it exists, indicates how much of radial frequency ω we find in $f(t)$. This is intuitive, simple, and attractive.

There are some fundamental difficulties, however, with this quite informal reasoning. We have shown that the Fourier transform of a signal $f(t)$ exists when $f(t)$ is absolutely integrable, but $L^1(\mathbb{R})$ signals are not the best realm for signal theorizing. In Chapter 3, for example, we found that they do not comprise an inner product space; that alone immediately breaks our intuitive concept of the Fourier integral as an inner product. Moreover, the Fourier transform of an $L^1(\mathbb{R})$ signal is not necessarily integrable, so we cannot assume to take its inverse transform. An example is the

square pulse, $x(t) = u(t + 1) - u(t - 1)$ whose radial Fourier transform is a sinc function, $X(\omega) = 2a\,\text{sinc}(\omega a)$.

Several approaches exist for developing a Fourier transform for $f(t) \in L^2(\mathbb{R})$. These methods include:

(i) Defining $F(\omega)$ as an infinite series expansion using special Hermite functions [22];

(ii) Writing square-integrable signals as limits of elements of the Schwarz class S of infinitely differentiable, rapidly decreasing signals (Chapter 3) [10];

(iii) Using the familiar L^p spaces, in particular the intersection of L^1 and L^2, which is dense in L^2, as the seed for a general Fourier transform for square-integrable signals [23, 24].

We follow the last approach above.

5.3.1   Fourier Transforms in $L^1(\mathbb{R}) \cap L^2(\mathbb{R})$

Toward defining a Fourier transform for finite-energy signals, the main ideas are to:

- Show the validity of the forward transforms for a narrow signal class: $L^1 \cap L^2$
- Argue that this is a dense set within L^2, so we can write any general square-integrable $f(t)$ as a limit of integrable, finite-energy signals: $f(t) = \lim_{n\to\infty} f_n(t)$ where $\{f_n(t) \in L^1 \cap L^2 \mid n \in \mathbb{N}\}$;
- Then extend the transform to square-integrable by defining the transform as a limit $F(\omega) = \lim_{n\to\infty} F_n(\omega)$, where $F_n(\omega) = \mathcal{F}[f_n(t)]$.

Theorem. If $f(t) \in L^1 \cap L^2$, then its Fourier transform $F(\omega)$ is square-integrable.

Proof: Consider a rectangular pulse of width 2α in the frequency domain. For $-\alpha < \omega < \alpha$

$$P_\alpha(\omega) = 1 \tag{5.122}$$

and vanishes outside this interval. Our strategy is to incorporate one such pulse inside the spectral energy integral and consider the limit as the pulse width becomes infinite. We claim

$$\lim_{\alpha \to \infty} \int_{-\infty}^{\infty} P_\alpha(\omega)|F(\omega)|^2 d\omega = \int_{-\infty}^{\infty} |F(\omega)|^2 d\omega = \|F(\omega)\|_2. \tag{5.123}$$

Let us verify that this integral is finite: $F \in L^2(\mathbb{R})$. Inserting the explicit integrals for $F(\omega)$ and its complex conjugate into (5.123) gives

$$\int_{-\infty}^{\infty} P_\alpha(\omega)F(\omega)F^*(\omega)\, d\omega = \int_{-\infty}^{\infty} f(t) \int_{-\infty}^{\infty} f^*(\tau)\left\{ \int_{-\infty}^{\infty} e^{j\omega(\tau - t)} P_\alpha(\omega)d\omega \right\} d\tau\, dt.$$

$$\tag{5.124}$$

The integral in curly brackets is proportional to the Fourier kernel,

$$\int_{-\infty}^{\infty} e^{j\omega(\tau - t)} P_\alpha(\omega)d\omega = 2\pi K_\alpha(\tau - t)= 2\pi \frac{\sin\alpha(\tau - t)}{\pi(\tau - t)}, \qquad (5.125)$$

so thereby takes the streamlined form,

$$\int_{-\infty}^{\infty} P_\alpha(\omega)|F(\omega)|^2 d\omega = \int_{-\infty}^{\infty} f(t) \int_{-\infty}^{\infty} f^*(\tau)K_\alpha(\tau - t) \, d\tau \, dt . \qquad (5.126)$$

A substitution of variables, $v = t - \tau$, provides

$$\int_{-\infty}^{\infty} P_\alpha(\omega)|F(\omega)|^2 d\omega = 2\pi \int_{-\infty}^{\infty} C_f(v)K_\alpha(v) \, dv, \qquad (5.127)$$

where

$$C_f(v) = \int_{-\infty}^{\infty} f(v + \tau)f(\tau) \, d\tau . \qquad (5.128)$$

Taking the limit as $\alpha \to \infty$, the kernel behaves like a Dirac:

$$\lim_{\alpha \to \infty} \int_{-\infty}^{\infty} P_\alpha(\omega)|F(\omega)|^2 d\omega = \int_{-\infty}^{\infty} |F(\omega)|^2 d\omega = 2\pi \int_{-\infty}^{\infty} C_f(v)\delta(v) \, dv$$

$$= 2\pi C_f(0)= 2\pi \int_{-\infty}^{\infty} |f(t)|^2 dt \qquad (5.129)$$

Since $\|f\|_2 < \infty$, so too is $\|F\|_2 < \infty$.   ∎

An interesting and valuable corollary from the above proof is the following result showing the proportionality of the energy of a signal and its Fourier transform.

Corollary (Plancherel's Theorem). If $f(t) \in L^1(\mathbb{R}) \cap L^2(\mathbb{R})$, then $\|F\|_2 = (2\pi)^{1/2} \|f\|_2$.

Proof: Evident from the theorem's proof (5.129).   ∎

Corollary. The radial Fourier transform $\mathcal{F}: L^1 \cap L^2 \to L^2$ is a bounded linear operator with $\|\mathcal{F}\| = (2\pi)^{1/2}$.

Proof: Recall from Chapter 3 that a bounded linear operator T is a linear map $T: N \to K$ of normed spaces when there is a constant $0 \le M$ such that $\|x\|_N \le M\|Tx\|_K$ for all $x \in N$. The Fourier transform is linear, which follows from the linearity of

the integral. Also, the norm of T is $\|T\| = \sup\{\|x\|_N \,/\, \|Tx\|_K \mid x \in N, x \neq 0\}$; as long as T is bounded, this set is nonempty, and so it must have a least upper bound. From Plancherel's theorem, the ratio between the norms in N and K is always $(2\pi)^{1/2}$, giving the bound condition. ∎

Corollary. If $\{f_n(t) \mid n \in \mathbb{N}\}$ is a Cauchy sequence in $L^1 \cap L^2$, then the sequence of Fourier transforms $\{F_n(\omega) \mid n \in \mathbb{N}\}$ is also Cauchy in L^2.

Proof: The Fourier transform is linear, so Plancherel's theorem implies $\|F_m - F_n\|_2 = (2\pi)^{1/2}\|f_m - f_n\|_2$. ∎

5.3.2 Definition

Now we are in a position to define the Fourier transform for $L^2(\mathbb{R})$. We can write any general square-integrable f(t) as a limit of integrable, finite-energy signals: $f(t) = \lim_{n\to\infty} f_n(t)$. It is easy to find the requisite sequence by setting $f_n(t) \in L^1 \cap L^2$ to be $f(t)$ restricted to $[-n, n]$ and zero otherwise. In Chapter 3, we noted that $L^1 \cap L^2$ is dense in L^2, and by the last corollary the Fourier transforms $\{F_n(\omega) \mid n \in \mathbb{N}\}$ also comprise a Cauchy sequence in L^2.

Definition (Fourier Transform for $L^2(\mathbf{R})$). If $f(t) \in L^2(\mathbb{R})$, then we define the *Fourier transform* of $f(t)$ by $F(\omega) = \lim_{n\to\infty} F_n(\omega) = \mathcal{F} + [f(t)](\omega)$, where $\{f_n(t) \mid n \in \mathbb{N}\}$ is any Cauchy sequence in $L^1 \cap L^2$ that converges to $f(t)$, and $F_n(\omega) = \mathcal{F}[f_n(t)](\omega)$.

Remark. $F(\omega)$ must exist because $L^2(\mathbb{R})$ is complete and $\{F_n(\omega) \mid n \in \mathbb{N}\}$ is Cauchy. In order for the definition to make sense, we need to show the following:

- The designation of $\lim_{n\to\infty} F_n(\omega)$ to be the Fourier transform of $f(t)$ must be shown independent of what particular sequence $\{f_n(t) \mid n \in \mathbb{N}\}$ is taken as having $f(t)$ as its limit.
- The definition of $F(\omega)$ should match the conventional definition in terms of the Fourier transform analysis equation when $f(t) \in L^1(\mathbb{R})$ too.

We introduce a very temporary notation $\mathcal{F}+$ for the extension. Once we show that the extension of the Fourier transform from $L^1 \cap L^2$ to all of L^2 makes mathematical sense, then we can forget the superscript "+" sign. This next proposition shows that the Fourier transform on $L^2(\mathbb{R})$ is in fact well-defined and agrees with our previous definition for absolutely integrable signals.

Proposition (Well-Defined). The Fourier transform of $f(t) \in L^2(\mathbb{R})$, $F(\omega) = \lim_{n\to\infty} F_n(\omega)$, where $F_n(\omega) = \mathcal{F}[f_n(t)](\omega)$ and $\lim_{n\to\infty} f_n(t) = f(t)$. Then:

  (i) $F(\omega)$ is well-defined; that is, it does not depend on the choise of limit sequence.

(ii) If $f(t) \in L^1(\mathbb{R})$, and $F(\omega)$ is given by the radial Fourier transform analysis equation (5.66a), then $F(\omega) = \lim_{n\to\infty} F_n(\omega)$.

(iii) $\mathcal{F}+: L^2 \to L^2$ is a norm-preserving extension of the map $\mathcal{F}: L^1 \cap L^2 \to L^2$ defined in Section 5.3.1.

Proof: That the limit $F(\omega)$ does not depend on the particular sequence whose limit is $f(t)$ follows from Plancherel's theorem. For the second claim, let $f_n(t)$ be $f(t)$ restricted to $[-n, n]$. Note that the $F_n(\omega) = \mathcal{F}[f_n(t)](\omega)$ in fact converge pointwise to $F(\omega)$ given by (5.66a), and any other Cauchy sequence $\{g_n(t) \mid n \in \mathbb{N}\}$ in $L^1 \cap L^2$ which converges to $f(t)$ must converge to $F(\omega)$ almost everywhere as well [24]. The third point follows immediately. ∎

The next result shows inner products are preserved by $\mathcal{F}+$.

Corollary (Parseval's Theorem). If $f(t)$, $g(t) \in L^2(\mathbb{R})$ with radial Fourier transforms $F(\omega)$ and $G(\omega)$, respectively, then $\langle f, g \rangle = (2\pi)^{-1} \langle F, G \rangle$.

Proof: This follows because we can define the inner product in terms of the norm by the polarization identity (Chapter 2) for inner product spaces [15]:

$$4 \langle f, g \rangle = \|f + g\|_2^2 - \|f - g\|_2^2 + \frac{\|f - jg\|_2^2}{j} - \frac{\|f + jg\|_2^2}{j}. \tag{5.130}$$

∎

Corollary (Plancherel's Theorem). If $f(t) \in L^2(\mathbb{R})$ with radial Fourier transform $F(\omega)$, then $\|f\|_2 = (2\pi)^{-1/2}\|F\|_2$.

Proof: By Parseval's relation for $L^2(\mathbb{R})$ signals above. ∎

Now that we have successfully extended the Fourier transform to all finite-energy signals, let us agree to drop the special notation $\mathcal{F}+$ for the extension and consider $\text{Domain}(\mathcal{F}) = L^2(\mathbb{R})$. Now that we have enough machinery, we can build a theory of analog signal frequency quite rapidly. For example, signals with almost everywhere identical spectra must themselves be identical almost everywhere.

Corollary (Uniqueness). Let $f(t)$, $g(t) \in L^2(\mathbb{R})$ with radial Fourier transforms $F(\omega)$ and $G(\omega)$, respectively. Suppose $F(\omega) = G(\omega)$ for almost all $\omega \in \mathbb{R}$. Then $f(t) = g(t)$ for almost all $t \in \mathbb{R}$.

Proof: If $F(\omega) = G(\omega)$ for almost all $\omega \in \mathbb{R}$, then $\|F - G\|_2 = 0$. But by Plancherel's theorem for $L^2(\mathbb{R})$, we then know $\|f - g\|_2 = 0$, whence $f(t) = g(t)$ for almost all $t \in \mathbb{R}$ by the properties of the Lebesgue integral (Chapter 3). ∎

Theorem (Convolution). Let $f(t)$, $h(t) \in L^2(\mathbb{R})$ with radial Fourier transforms $F(\omega)$ and $H(\omega)$, respectively, and let $g(t) = (f * h)(t)$ be the convolution of f and h. Then $G(\omega) = F(\omega)H(\omega)$.

Proof: By the Schwarz inequality, $g = (f * h) \in L^1(\mathbb{R})$, and it has a Fourier transform $G(\omega)$. Let us expand the convolution integral inside the Fourier transform analysis equation for $g(t)$:

$$\int_{-\infty}^{\infty} (f*h)(t)e^{-j\omega t}dt = \int_{-\infty}^{\infty}\int_{-\infty}^{\infty} f(s)h(t-s)ds\,e^{-j\omega t}dt. \tag{5.131}$$

Since $g \in L^1(\mathbb{R})$, we can apply Fubini's theorem (Section 3.4.2.4) to the integrand of the Fourier analysis equation for $g(t)$. Interchanging the order of integration gives

$$\int_{-\infty}^{\infty}\int_{-\infty}^{\infty} f(s)h(t-s)ds\,e^{-j\omega t}dt = \int_{-\infty}^{\infty} f(s)e^{-j\omega s}ds \int_{-\infty}^{\infty} h(t-s)e^{-j\omega(t-s)}dt. \tag{5.132}$$

The iterated integrals on the right we recognize as $F(\omega)H(\omega)$.   ∎

The convolution theorem lies at the heart of analog filter design, which we cover in Chapter 9.

Finally, we observe that the normalized and Hertz Fourier transforms, which are a scaling and a dilation of the radial transform, respectively, can also be extended precisely as above.

5.3.3 Isometry

The normalized radial Fourier transform, extended as above to finite enery signals, in fact constitutes an isometry of $L^2(\mathbb{R})$ with itself. We recall that an isometry T between Hilbert spaces, H and K, is a linear map that is one-to-one and onto and preserves inner products. Since $\langle x, y\rangle_H = \langle Tx, Ty\rangle_J$, T also preserves norms, and so it must be bounded; in fact, $\|T\| = 1$. Conceptually, if two Hilbert spaces are isometric, then they are essentially identical. We continue working out the special properties of the radial Fourier transform $\mathcal{F}$ and, as the last step, scale it to $(2\pi)^{-1/2}\mathcal{F}$, and thereby get the isometry.

The following result is a variant of our previous Plancherel and Parseval formulas.

Theorem. Let $f(t)$, $g(t) \in L^2(\mathbb{R})$ with radial Fourier transforms $F(\omega)$ and $G(\omega)$, respectively. Then,

$$\int_{-\infty}^{\infty} F(\omega)g(\omega)d\omega = \int_{-\infty}^{\infty} f(t)G(t)\,dt. \tag{5.133}$$

Proof: We prove the result in two steps:

   (i) First for $f(t)$, $g(t) \in (L^1 \cap L^2)(\mathbb{R})$;
   (ii) For all of $L^2(\mathbb{R})$, again using the density of $L^1 \cap L^2$ within L^2.

Let us make the assumption (i) and note that this stronger condition implies that $F(\omega)$ and $G(\omega)$ are bounded (exercises). Then, since $F(\omega) \in L^\infty(\mathbb{R})$, the Hölder inequality gives $\|Fg\|_1 \leq \|F\|_\infty \|g\|_1$. Because the integrand $F(\omega)g(\omega)$ is absolutely integrable, Fubini's theorem allows us to interchange the order of integration:

$$\int_{-\infty}^{\infty} F(\omega)g(\omega) \, d\omega = \int_{-\infty}^{\infty} \left(\int_{-\infty}^{\infty} f(t)e^{-j\omega t} dt \right) g(\omega) \, d\omega = \int_{-\infty}^{\infty} \left(\int_{-\infty}^{\infty} g(\omega)e^{-j\omega t} d\omega \right) f(t) \, dt.$$

(5.134)

Notice that the integral in parentheses on the right-hand side of (5.134) is precisely $G(t)$, from which the result for the special case of $L^1 \cap L^2$ follows.

For (ii), let us assume that $\lim_{n\to\infty} f_n(t) = f(t)$ and $\lim_{n\to\infty} g_n(t) = g(t)$, where f_n, $g_n \in (L^1 \cap L^2)(\mathbb{R})$. Then $F(\omega) = \lim_{n\to\infty} F_n(\omega)$, where $F_n(\omega) = \mathcal{F}[f_n(t)](\omega)$ and $G(\omega) = \lim_{n\to\infty} G_n(\omega)$, where $G_n(\omega) = \mathcal{F}[g_n(t)](\omega)$. Then, f_n, g_n, F_n, and $G_n \in L^2(\mathbb{R})$, so that by the Schwarz inequality, $F_n g_n$ and $f_n G_n \in L^1(\mathbb{R})$. The Lebesgue Dominated Convergence theorem applies (Section 3.4.2.3). By part (i) of the proof, for all $n \in \mathbb{N}$, $\int F_n g_n = \int f_n G_n$. Taking limits of both sides gives

$$\lim_{n\to\infty} \int F_n g_n = \int \lim_{n\to\infty} F_n g_n = \int Fg = \lim_{n\to\infty} \int G_n f_n = \int \lim_{n\to\infty} G_n f_n = \int Gf. \quad (5.135)$$

as required. ∎

We know that every $f \in L^2(\mathbb{R})$ has a radial Fourier transform $F \in L^2(\mathbb{R})$ and that signals with (almost everywhere) equal Fourier transforms are themselves (almost everywhere) equal. Now we can show another result—an essential condition for the isometry, in fact—that the Fourier transform is onto.

Theorem. If $G \in L^2(\mathbb{R})$, then there is a $g \in L^2(\mathbb{R})$ such that $F(g)(\omega) = G(\omega)$ for almost all $\omega \in \mathbb{R}$.

Proof: If $G(\omega) \in L^2(\mathbb{R})$, we might well guess that the synthesis formula for the case $G(\omega) \in (L^1 \cap L^2)(\mathbb{R})$ will give us a definition of $g(t)$:

$$g(t) = \frac{1}{2\pi} \int_{-\infty}^{\infty} G(\omega)e^{j\omega t} d\omega. \quad (5.136)$$

We need to show that the above integral is defined for a general $G(\omega)$, however. If we let $H(\omega) = G(-\omega)$ be the reflection of $G(\omega)$, then $H \in L^2(\mathbb{R})$. We can take its radial Fourier transform, $\mathcal{F}[H]$:

$$p\frac{1}{2\pi} \mathcal{F}[H](t) = \frac{1}{2\pi} \int_{-\infty}^{\infty} H(\omega)e^{-j\omega t} d\omega. \quad (5.137)$$

A change of integration variable in (5.137) shows that $(2\pi)^{-1}\mathcal{F}[H](t)$ has precisely the form of the radial Fourier synthesis equation (5.136). We therefore propose $g(t) = (2\pi)^{-1}\mathcal{F}[H](t) \in L^2(\mathbb{R})$. Now we need to show that the Fourier transform of $g(t)$ is equal to $G(\omega)$ almost everywhere. We calculate

$$\|\mathcal{F}g - G\|_2^2 = \langle \mathcal{F}g, \mathcal{F}g \rangle - 2\mathrm{Real}\langle \mathcal{F}g, G \rangle + \langle G, G \rangle . \tag{5.138}$$

We manipulate the middle inner product in (5.138),

$$\mathrm{Real}\langle \mathcal{F}g, G \rangle = \mathrm{Real}\langle G, \mathcal{F}g \rangle = \mathrm{Real}\int G(\overline{\mathcal{F}g}) = \mathrm{Real}\int \mathcal{F}G(\overline{g(-t)}) , \tag{5.139a}$$

applying the previous Parseval result to obtain the last equality above. Using the definition of $g(t)$, we find

$$\mathrm{Real}\langle \mathcal{F}G, \frac{1}{2\pi}[\mathcal{F}H](-t) \rangle = \mathrm{Real}\langle \mathcal{F}G, \frac{1}{2\pi}[\mathcal{F}H](-t) \rangle = \frac{1}{2\pi} \mathrm{Real}\langle \mathcal{F}G, \mathcal{F}G \rangle . \tag{5.139b}$$

By Parseval's theorem, $\langle \mathcal{F}g, \mathcal{F}g \rangle = 2\pi\langle g, g \rangle$ and $\langle \mathcal{F}G, \mathcal{F}G \rangle = 2\pi\langle G, G \rangle$, which is real. Thus, putting (5.138), (5.139a), and together implies

$$\|\mathcal{F}g - G\|_2^2 = 2\pi\langle g, g \rangle - \frac{2}{2\pi}\langle \mathcal{F}G, \mathcal{F}G \rangle + \frac{1}{2\pi}\langle \mathcal{F}G, \mathcal{F}G \rangle = 2\pi\langle g, g \rangle - \frac{1}{2\pi}\langle \mathcal{F}G, \mathcal{F}G \rangle$$

$$= \frac{2\pi}{(2\pi)^2}\langle \mathcal{F}[G(-\omega)], \mathcal{F}[G(-\omega)] \rangle - \frac{1}{2\pi}\langle \mathcal{F}G, \mathcal{F}G \rangle . \tag{5.140}$$

But $\|\mathcal{F}G\|_2 = \|\mathcal{F}[G(-\omega)]\|_2$, so the last term in (5.140) is zero: $\|Fg - G\|_2^2 = 0$ almost everywhere, and the theorem is proven. ∎

Corollary (Isometry of Time and Frequency Domains). The normalized radial Fourier transform $(2\pi)^{-1/2}\mathcal{F}$, where $\mathcal{F}$ is the radial Fourier transform on $L^2(\mathbb{R})$, is an isometry from $L^2(\mathbb{R})$ onto $L^2(\mathbb{R})$.

Proof: Linearity follows from the properties of the integral. We have shown that $\mathcal{F}$ on $L^2(\mathbb{R})$ is one-to-one; this is a consequence of the Parseval relation. The map $\mathcal{F}$ is also onto, as shown in the previous theorem. Since $\langle Fx, Fy \rangle = 2\pi\langle x, y \rangle$, we now see clearly that $(2\pi)^{-1/2}\mathcal{F}$ preserves inner products and constitutes an isometry. ∎

Remark. The uniqueness implied by this relationship assures that a given Fourier spectrum is a true signature of a given time-domain signal $f(t)$. This property is a valuable asset, but we emphasize that two signals are equivalent if their spectra are identical across the *entire* frequency spectrum. Deviations between spectra, even if they are small in magnitude or restricted to a small range of frequencies, can result in large discrepancies between the respective $f(t)$. This is a legacy of the complex

exponentials which form a basis of the Fourier transform. They are defined across the entire line (both in frequency and time), so small perturbations run the risk of infecting the entire Fourier synthesis. In practical situations, where spectral information is stored and transmitted in the form of discrete Fourier coefficients, errors or glitches can wreak havoc on the reconstruction of $f(t)$. This inherent sensitivity to error is one of the least appealing attributes of Fourier analysis.

The time-domain and frequency-domain representations of a square-integrable signal are equivalent. Neither provides more information. And Fourier transformation, for all its complexities, serves only to reveal some aspects of a signal at the possible risk of concealing others.

5.4 SUMMARY

The Fourier series and transform apply to analog periodic and aperiodic signals, respectively.

The Fourier series finds a set of discrete coefficients associated with a periodic analog signal. These coefficients represent the expansion of the signal on the exponential or sinusoidal basis sets for the Hilbert space $L^2[0, T]$. We shall have more to say about the Fourier series in Chapter 7, which is on discrete Fourier transforms.

For absolutely integrable or square-integrable aperiodic signals, we can find a frequency-domain representation, but it is an analog, not discrete, signal. We have had to consider three different Banach spaces in our quest for a frequency-domain description of a such a signal: $L^1(\mathbb{R})$, $(L^1 \cap L^2)(\mathbb{R})$, and $L^2(\mathbb{R})$. We began by defining the Fourier transform over the space of absolutely integrable signals. Then we considered the restricted transform on $L^1 \cap L^2$, but noted that this transform's range is in L^2. Applying the limit theorems available with the modern (Lebesgue) integral to this restricted signal class, we were able to extend the transform to the full space of square-integrable signals. Ultimately, we found an isometry between the time and frequency domain representations of a finite energy signal.

5.4.1 Historical Notes

Prior to Fourier, there were a number of attempts by other mathematicians to formulate a decomposition of general waves into trigonometric functions. D'Alembert, Euler, Lagrange, and Daniel Bernoulli used sinusoidal expansions to account for the vibrations of a string [4]. Evidently, ancient Babylonian astronomers based their predictions on a rudimetary Fourier series [10]. Fourier applied trigonometric series to the heat equation, presented his results to the French Academy of Sciences, and published his result in a book [25]. Criticism was severe, however, and the method was regarded with suspicion until Poisson, Cauchy, and especially Dirichlet (1829) provided theoretical substantiation of the Fourier series.

Plancherel proved that L^2 signals have L^2 Fourier transforms in 1910. The basis for so doing, as we have seen in Section 5.3, is the modern Lebesgue integral and the powerful limit properties which it supports. The L^2 theory of the Fourier integral is often called the Plancherel theory.

5.4.2 Looking Forward

The next chapter generalizes the Fourier transform to include even signals that are neither absolutely integrable nor square-integrable. This so-called generalized Fourier transform encompasses the theory of the Dirac delta, which we introduced in Chapter 3. Chapters 7 and 8 consider the frequency-domain representation for discrete signals. Chapter 9 covers applications of analog and discrete Fourier transforms.

REFERENCES

1. H. Baher, *Analog and Digital Signal Processing*, New York: Wiley, 1990.
2. J. A. Cadzow and H. F. van Landingham, *Signals, Systems, and Transforms*, Englewood Cliffs, NJ: Prentice-Hall, 1989.
3. L. B. Jackson, *Signals, Systems, and Transforms*, Reading, MA: Addison-Wesley, 1991.
4. A. V. Oppenheim, A. S. Willsky, and S. H. Nawab, *Signals and Systems*, Englewood Cliffs, NJ: Prentice-Hall, 1989.
5. R. E. Ziemer, W. H. Tranter, and D. R. Fannin, *Signals and Systems: Continuous and Discrete*, New York: Macmillan, 1989.
6. J. S. Walker, *Fourier Analysis*, New York: Oxford University Press, 1988.
7. D. C. Champeney, *A Handbook of Fourier Theorems*, Cambridge: Cambridge University Press, 1987.
8. G. B. Folland, *Fourier Analysis and its Applications*, Pacific Grove, CA: Wadsworth and Brooks/Cole, 1992.
9. R. E. Edwards, *Fourier Series: A Modern Introduction*, vol. I, New York: Hold, Rinehart and Winston, 1967.
10. H. Dym and H. P. McKean, *Fourier Series and Integrals*, New York: Academic, 1972.
11. E. M. Stein and G. Weiss, *Introduction to Fourier Analysis on Euclidean Spaces*, Princeton, NJ: Princeton University Press, 1971.
12. A. Zygmund, *Trigonometic Series*, vols. I & II, 2nd ed., Cambridge: Cambridge University Press, 1977.
13. M. Rosenlicht, *Introduction to Analysis*, New York: Dover, 1978.
14. H. L. Royden, *Real Analysis*, 2nd. ed., Toronto: Macmillan, 1968.
15. E. Kreysig, *Introductory Functional Analysis with Applications*, New York: Wiley, 1989.
16. A. W. Naylor and G. R. Sell, *Linear Operator Theory in Engineering and Science*, New York: Springer-Verlag, 1982.
17. A. H. Zemanian, *Distribution Theory and Transform Analysis*, New York: Dover, 1987.
18. M. J. Lighthill, *Fourier Analysis and Generalized Functions*, New York: Cambridge University Press, 1958.
19. A. B. Carlson, *Communication Systems*, 3rd ed., New York: McGraw-Hill, 1986.
20. L. W. Couch III, *Digital and Analog Communication Systems*, 4th ed., Upper Saddle River, NJ: Prentice-Hall, 1993.
21. S. Haykin, *Communication Systems*, 3rd ed., New York: Wiley, 1994.
22. N. Wiener, *The Fourier Integral and Certain of Its Applications*, London: Cambridge University Press, 1933.
23. C. K. Chui, *An Introduction to Wavelets*, San Diego, CA: Academic, 1992.

24. W. Rudin, *Real and Complex Analysis*, 2nd ed., New York: McGraw-Hill, 1974.

25. I. Gratton-Guiness, *Joseph Fourier 1768–1830*, Cambridge, MA: MIT Press, 1972.

PROBLEMS

1. Find the exponential Fourier series coefficients (5.9) for the following signals.
   (a) $x(t) = \cos(2\pi t)$.
   (b) $y(t) = \sin(2\pi t)$.
   (c) $s(t) = \cos(2\pi t) + \sin(2\pi t)$.
   (d) $z(t) = x(t - \pi/4)$.
   (e) $w(t) = 5y(-2t)$.

2. Find the exponential Fourier series coefficients for the following signals:
   (a) Signal $b(t)$ has period $T = 4$ and for $0 \le t < 4$, $b(t) = u(t) - u(t - 2)$, where $u(t)$ is the analog unit step signal.
   (b) $r(t) = tb(t)$, where $b(t)$ is given in (a).

3. Let $x(t) = 7\sin(1600t - 300)$, where t is a (real) time value in seconds. Give:
   (a) The amplitude of x.
   (b) The phase of x.
   (c) The frequency of x in radians/second.
   (d) The frequency of x in Hz (cycles/second).
   (e) The period of x.
   (f) Find the exponential Fourier series coefficients for $x(t)$.

4. Suppose $x(t)$ has period $T = 1$ and $x(t) = t^2$ for $0 \le t < 1$.
   (a) Find the exponential Fourier series coefficients for $x(t)$.
   (b) Sketch and label the signal $y(t)$ to which x's Fourier series synthesis equation converges.

5. Find the exponential Fourier series coefficients for the periodic sawtooth signal $x(t)$ (Figure 5.9).
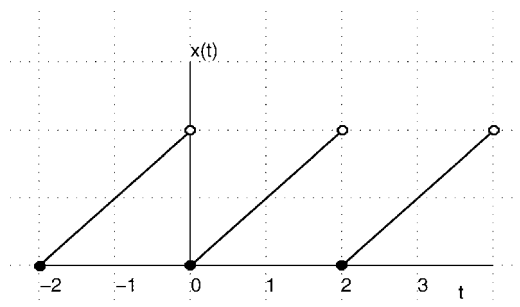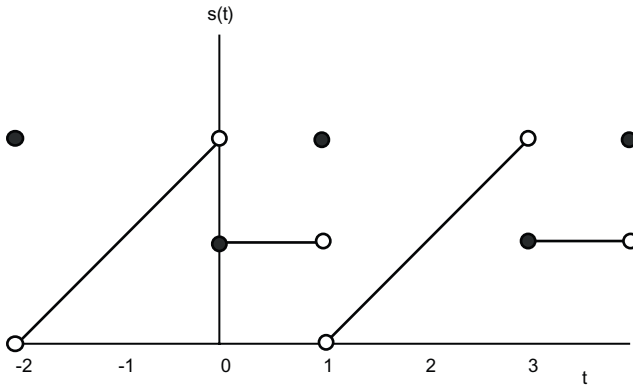

Fig. 5.9. Sawtooth signal $x(t)$.

s(t)

Fig. 5.10. Another sawtooth signal s(t).

6. Consider the signal $s(t)$ shown in Figure 5.10.

  (a) Find the exponential Fourier series for the signal $s(t)$.

  (b) Consider the signal $y(t)$ to which the Fourier series synthesis equation for $s(t)$ converges. Sketch $y(t)$ and label the graph to show the exact values of $y(t)$ at places where it is the same and where it differs from $s(t)$.

7. The impulse response of an analog linear time invariant (LTI) system H is $h(t) = u(t + 50) - u(t)$, where $u(t)$ is the unit step signal.

  (a) What is the response of the system to the signal $x(t) = u(t)e^{-t}$?

  (b) Find the radial Fourier transform of $h(t)$.

  (c) Does $x(t)$ have a radial Fourier transform? If so, find it; otherwise, give a reason why $X(\omega)$ does not exist; and, in any case, explain your answer.

8. Consider the analog signal $x(t) = [u(t + 1) - u(t - 1)]$, where $u(t)$ is the unit step signal.

  (a) Find the radial Fourier transform of $x(t)$, $X(\omega) = \mathcal{F}[x(t)](\omega)$.

  (b) Let $y(t) = x(t - 2)$; find $Y(\omega)$.

  (c) Find $\mathcal{F}[x(2t)]$.

  (d) Find $\mathcal{F}[x(t/5)]$.

  (e) Find $\mathcal{F}[\sin(t)x(t)]$.

9. Let H be a linear time-invariant (LTI) analog system; $y = Hx$; $h = H\delta$; and $X(\omega)$, $Y(\omega)$, and $H(\omega)$ are their respective radial Fourier transforms. Which of the following are true? Explain.

  (a) $Y(\omega)/X(\omega)$ is the Fourier transform of h.

  (b) $y(t)/h(t) = x(t)$.

  (c) $y(t) = x(t)*h(t)$, where * is the analog convolution operation.

10. Prove or disprove the following statement: If an periodic analog signal $x(t)$ is represented by a Fourier series, but this series does not converge to $x(t)$ for all t, then $x(t)$ is not continuous.

11. Prove or disprove the following statement: If $x(t) \in L^2(\mathbb{R})$ is an odd signal (i.e., $x(t) = -x(-t)$), and $X(\omega)$ is the radial Fourier transform of x, then $X(0) = 0$.

12. Suppose the analog signals x(t) and h(t) have radial Fourier transforms $X(\omega) = u(\omega + 1) - u(\omega - 1)$ and $H(\omega) = \exp(-\omega^2)$, respectively. Let the signal $y = x * h$.
    (a) Find $x(t)$.
    (b) Find $h(t)$.
    (c) Find $Y(\omega)$.
    (d) Find $y(t)$.

13. Suppose that $X(\omega)$ and $Y(\omega)$ are the radial Fourier transforms of $x(t)$ and $y(t)$, respectively, and let $h(n)$ be a discrete signal with

$$x(t) = \sum_{n=-\infty}^{\infty} h(n)y(t-n). \tag{5.141}$$

    (a) Find an expression for $X(\omega)$.
    (b) What kind of conditions should be imposed upon the discrete signal $h(n)$ so that your answer in (a) is mathematically justifiable? Explain.

14. Show that the radial Fourier transform for analog signals is a linear operation. Is it also translation invariant? Explain.

15. Show that if $F(\omega)$ is absolutely integrable, then the inverse Fourier transform $\mathcal{F}^{-1}[F(\omega)](t)$ exists.

16. Suppose that analog periodic signal x(t) has exponential Fourier series coefficients c_k:

$$c_k = \langle x(t), \phi_k(t) \rangle = \int_{t_0}^{t_0 + T} x(t) \frac{1}{\sqrt{T}} e^{-jk\Omega t} dt. \tag{5.142}$$

    Prove the following symmetry properties:
    (a) If $x(t)$ is real-valued and even, then the c_k are also real and even: $c_k = c_{-k}$.
    (b) If $x(t)$ is real and odd, then the c_k are purely imaginary and odd: $c_{-k} = -c_k$.

17. For analog signals $x(t)$ and $y(t) = x(t - a)$, show that the magnitudes of their radial Fourier transforms are equal, $|X(\omega)| = |Y(\omega)|$.

18. Prove or disprove: For all analog signals $x(t) \in L^2(\mathbb{R})$, if $x(t)$ is real-valued, then $X(\omega)$ is real-valued.

19. Let $x(t) \in L^1(\mathbb{R})$ be a real-valued analog signal and let $X(\omega)$ be its radial Fourier transform. Which of the following are true? Explain.
    (a) $X(\omega)$ is bounded: $X(\omega) \in L^\infty(R)$.
    (b) $|X(\omega)| \to 0$ as $|\omega| \to \infty$.
    (c) $X(\omega)$ is unbounded.

(d) $X(0) = 0$.

(e) $X(\omega)$ has a Fourier transform.

(f) $X(\omega)$ has an inverse Fourier transform.

(g) $X(\omega)$ has an inverse Fourier transform and it is identical to x(t).

(h) $X(\omega) \in L^1(\mathbb{R})$ also.

20. Let $x(t) \in L^2(\mathbb{R})$ be a real-valued analog signal and let $X(\omega)$ be its radial Fourier transform. Which of the following are true? Explain.

(a) $X(\omega)$ is bounded: $X(\omega) \in L^\infty(R)$.

(b) $|X(\omega)| \to 0$ as $|\omega| \to \infty$.

(c) $X(\omega)$ is unbounded.

(d) $X(0) = 0$.

(e) $X(\omega)$ has a Fourier transform.

(f) $X(\omega)$ has an inverse Fourier transform.

(g) $X(\omega)$ has an inverse Fourier transform and it is identical to $x(t)$.

(h) $X(\omega) \in L^2(\mathbb{R})$ also.

21. Let $x(t) \in L^1(\mathbb{R})$. Show that:

(a) Fourier transform $X(\omega)$ of $x(t)$ is bounded.

(b) $\|X\|_\infty \le \|x\|_1$.

22. Loosely speaking, an analog *low-pass filter H* is a linear, translation-invariant system that passes low frequencies and suppresses high frequencies. We can specify such a system more precisely with the aid of the Fourier transform. Let $h(t)$ be the impulse response of H and let $H(\omega) = \mathcal{F}(h(t))(\omega)$ be its Fourier transform. For a low-pass filter we require $|H(0)| = 1$ and $|H(\omega)| \to 0$ as $|\omega| \to \infty$.

(a) Show that if $|H(0)| \neq 1$ but still $|H(0)| \neq 0$ and $|H(\omega)| \to 0$ as $|\omega| \to \infty$, then we can convert H into a low-pass filter by a simple normalization;

(b) Show that, with an appropriate normalization, the Gaussian signal is a low-pass filter (sometimes we say that any system whose impulse response can be so normalized is a low-pass filter).

23. An analog *high-pass filter H* is a linear, translation-invariant system that suppresses low frequencies and passes high frequencies. Again, if $h(t)$ is the impulse response of H and $H(\omega) = \mathcal{F}(h(t))(\omega)$, then we stipulate that $|H(0)| = 0$ and $|H(\omega)| \to 1$ as $|\omega| \to \infty$. Explain why our Fourier theory might not accept analog high-pass filters.

24. An analog *bandpass filter H* passes a range of frequencies, suppressing both low and high frequencies.

(a) Formalize the idea of a bandpass filter using the spectrum of the impulse response of H.

(b) Give an example of a finite-energy bandpass filter.

(c) Let $h(t)$ be an analog low-pass filter and let $g(t)$ be an analog bandpass filter. What kind of filters are h * h, g * h, and g * g? Explain your answer.

    (d) Why would we not consider the case that $g(t)$ is an analog high-pass filter? Explain this too.

    (e) Formulate and formalize the concept of an analog *bandstop* (also *bandreject* or *notch*) filter. Can these be absolutely integrable signals? Finite-energy signals? Explain.

25. Suppose $h(t)$ is the impulse response for an analog filter H that happens to be a *perfect low-pass filter*. That is, for some $\omega_c > 0$, $|H(\omega)| = 1$ for $|\omega| \le \omega_c$, and $|H(\omega)| = 0$ for all $|\omega| > \omega_c$.

    (a) Show that as a time-domain filter, H is noncausal.

    (b) Explain why, in some sense, H is impossible to implement.

    (c) Show that $h(t) \in L^2(\mathbb{R})$, but $h(t) \notin L^1(\mathbb{R})$.

26. Suppose an analog signal, $x(t)$, has radial Fourier transform, $X(\omega)$, given by Figure 5.11
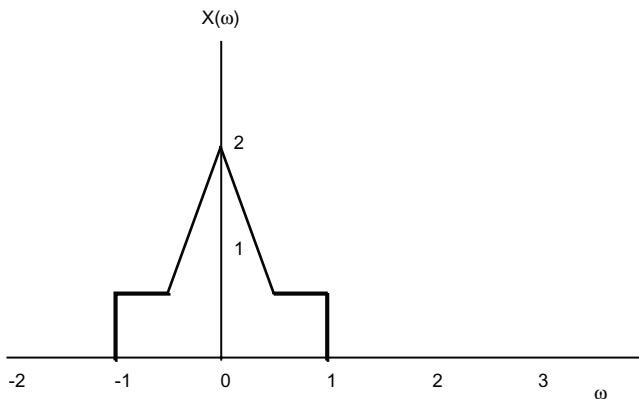

Fig. 5.11. Radial Fourier transform of signal $x(t)$.

Without attempting to compute $x(t)$, sketch $Y(\omega)$ for the following signals $y(t)$:

    (a) $y(t) = x(2t)$.

    (b) $y(t) = x(t/3)$.

    (c) $y(t) = (x * g)(t)$, where $g(t) = \exp(-t^2)$.

    (d) $y(t) = \cos(t)x(t)$.

    (e) $y(t) = \sin(t)x(t)$.

    (f) $y(t) = \exp(j5t)x(t)$.

27. Let $f(t)$, $h(t) \in L^2(\mathbb{R})$ and $F(\omega)$, $H(\omega)$ be their radial Fourier transforms.

    (a) If $g(t) = f(t)h(t)$, show that $g(t) \in L^2(\mathbb{R})$.

    (b) Show that $G(\omega) = (2\pi)^{-1}F(\omega) * H(\omega)$.

28. Develop an alternative approach to showing that signals with identical spectra must be the same. Let $f_1(t)$ and $f_2(t)$ have identical Fourier transforms; that is, $\mathcal{F}[f_1(t)] = \mathcal{F}[f_2(t)] = G(\omega)$.

(a) For an arbitrary $h(t)$ show that an alternative formulation of Parseval's relation holds:

$$2\pi \int_{-\infty}^{\infty} f_2(t)h(t)\, dt = \int_{-\infty}^{\infty} G(-\omega)H(\omega)\, d\omega. \qquad (5.143)$$

(b) Show that the above leads to

$$2\pi \int_{-\infty}^{\infty} [f_1(t) - f_2(t)]h(t)\, dt = 0. \qquad (5.144)$$

(c) Explain why it follows that $f_1(t) = f_2(t)$ for almost all t.

Generalized Fourier Transforms of Analog Signals

This chapter extends Fourier analysis to common signals that lie outside of the spaces $L^1(\mathbb{R})$ and $L^2(\mathbb{R})$.

The theory of $L^1(\mathbb{R})$ and $L^2(\mathbb{R})$ Fourier transforms is broad enough to encompass a large body of signal processing and analysis. The foundation provided for the transform allows us to discover the frequency content of analog signals. One might be content with the situation as it stands, but several common and practical functions are neither absolutely integrable nor of finite energy. For example:

- The simple sinusoids $f(t) = \sin(\omega_0 t)$ and $f(t) = \cos(\omega_0 t)$. It is difficult to imagine functions for which the notion of frequency content is any more straightforward, yet the radial Fourier transform

$$F(\omega) = \int\limits_{-\infty}^{\infty} f(t)e^{-j\omega t}dt = \mathcal{F}[f(t))](\omega) \tag{6.1}$$

  does not converge. Similar comments clearly apply to the complex exponential.
- The function $f(t) = c_0$, where c_0 is a positive or negative constant. Constant electrical signals are called direct current (DC) signals in engineering. Again, the notion of frequency content for this DC signal could hardly be more intuitive, but convergence of the Fourier integral fails.
- The unit step $u(t)$ and its close relative the signum, $\operatorname{sgn} t$ (see Figure 5.8), which clearly do not belong to the class of integrable or square-integrable functions.

Texts devoted to distributions and generalized Fourier transforms are Refs. 1–3. Mathematical analysis texts that also introduce the theory include Refs. 4–6.

6.1 DISTRIBUTION THEORY AND FOURIER TRANSFORMS

Our first encounter with useful integrals that defy solution using classical methods of calculus arose in Chapter 3, where integration of classically troublesome entities,

such as the derivative of the unit step, were elegantly handled through distributions. The theoretical framework employed test functions of rapid descent which were classically well-behaved and generated a calculus of distributions simply because the classical notions of derivatives could be applied directly to the test functions themselves. These developments suggest that if the troublesome signals listed above are treated as distributions, and the test functions have traditional Fourier transforms, then a theory of generalized Fourier transforms, embracing the selected distributions, can be formulated.

Consider replacing the complex exponential with some function $\Phi(t)$ which is sufficiently well-behaved to allow the integral over time, namely

$$\int_{-\infty}^{\infty} f(t)e^{-j\omega t} \, dt \to \int_{-\infty}^{\infty} f(t)\Phi(t) \, dt \tag{6.2}$$

to converge. Intuitively, one needs a $\Phi(t)$ which decays rapidly enough to counter the lack of integrability inherent in $f(t)$. Two key points follow:

- Each of the nonintegrable signals $f(t)$ under consideration is a function of slow growth (Chapter 3) and therefore represents a regular distribution of slow growth when set in the context of generalized integrals.
- The class of testing functions is Fourier transformable in the "regular" sense of Section 5.2; this is our link to frequency space.

The study of distributions in the time domain was based on the classical concept of integration by parts. Similarly, the classically derived Parseval relations extend the theory of distributions into the frequency domain. We propose the following:

Definition (Generalized Fourier Transform). Let $f(t)$ be a distribution of slow growth. Note that if $\phi(\alpha)$ is a testing function of rapid descent, we can define a Fourier transform,

$$\Phi(\beta) \;=\; \int_{-\infty}^{\infty} \phi(\alpha)e^{-j\beta\alpha} \, d\alpha. \tag{6.3}$$

By Parseval's theorem

$$\int_{-\infty}^{\infty} F(\omega)\phi(\omega) \, d\omega \;=\; \int_{-\infty}^{\infty} f(t)\Phi(t) \, dt. \tag{6.4}$$

The function $F(\omega)$ is the *generalized Fourier transform* of $f(t)$.

Remark. In the event that $f(t)$ is integrable, the generalized Fourier transform is merely an expression of Parseval's theorem for such functions. Consequently, $F(\omega)$ is a bona fide generalized Fourier transform encompassing both the integrable

functions (which are also covered by the Paresval relation) and the distributions of slow growth.

In the generalized Fourier transform, note that ω and t within the integrals (6.4) are merely continuous variables; the simple form of the generalized Fourier transform may be extended so that

$$\int_{-\infty}^{\infty} F(\omega)\phi(\omega) \ d\omega \ = \ \int_{-\infty}^{\infty} f(t)\Phi(t) \ dt \ = \ \int_{-\infty}^{\infty} F(t)\phi(t) \ dt \ = \ \int_{-\infty}^{\infty} f(\omega)\Phi(\omega) \ d\omega. \quad (6.5)$$

This is of more than academic interest and allows for greater dexterity when deriving the properties of the generalized Fourier transform.

6.1.1 Examples

How does our formulation of the generalized Fourier transform perform for the important, simple signals? Let us investigate the case of constant (DC) signals and impulses.

Example (DC Waveform). Let $f(t) = 1$ for all $t \in \mathbb{R}$. This signal represents a constant DC level for all values of t and is a function of slow growth. The generalized Fourier transform takes the form

$$\int_{-\infty}^{\infty} F(\omega)\phi(\omega) \ d\omega \ = \ \int_{-\infty}^{\infty} \Phi(t) \ dt \ = \ F[\Phi(t)](\omega)\big|_{\omega=0} \ = \ 2\pi\phi(-\omega)\big|_{\omega=0}. \quad (6.6)$$

The quantity following the last equality is simply $2\pi\phi(0)$, which can be written in terms of the Dirac delta:

$$\int_{-\infty}^{\infty} F(\omega)\phi(\omega) \ d\omega \ = \ 2\pi \int_{-\infty}^{\infty} \delta(\omega)\phi(\omega) \ d\omega. \quad (6.7)$$

Comparing both sides of (6.7), it is readily apparent that

$$F(\omega) \ = \ 2\pi\delta(\omega) \quad\quad\quad\quad (6.8)$$

represents the spectrum of the constant DC signal. This result supports the intuitively appealing notion that a constant DC level represents clusters its entire frequency content at the origin. We have already hinted at this in connection with the Fourier transform of the rectangular pulse in the limit of large width; in a sense, (6.8) is the ultimate expression of the scaling law for a rectangular pulse.

The time-dependent Dirac delta represents the converse:

Example (Impulse Function).   Consider a Dirac delta impulse, $f(t) = \delta(t)$. The generalized Fourier transform now reads

$$\int_{-\infty}^{\infty} F(\omega)\phi(\omega)\ d\omega = \int_{-\infty}^{\infty} \delta(t)\Phi(t)\ dt = F[\phi(t)](\omega)\big|_{\omega=0} = \int_{-\infty}^{\infty} \phi(t)\ dt$$

$$= \int_{-\infty}^{\infty} \phi(\omega)\ d\omega. \tag{6.9}$$

From a comparison both sides,

$$\mathcal{F}[\delta(t)](\omega) = 1 \tag{6.10}$$

for all $\omega \in \mathrm{R}$. The Dirac delta function's spectrum therefore contains equal contributions from all frequencies. Intuitively, this result is expected.

6.1.2   The Generalized Inverse Fourier Transform

The reciprocity in the time and frequency variables in (6.4) leads to a definition of a generalized inverse Fourier transform.

Definition (Generalized Inverse Fourier Transform).   Let $F(\omega)$ be a distribution of slow growth. If $\Phi(\beta)$ is a testing function of rapid descent, then it generates an inverse Fourier transform:

$$\phi(\alpha) = \int_{-\infty}^{\infty} \Phi(\beta)e^{j\beta\alpha}d\beta. \tag{6.11}$$

Once again, by Parseval's theorem

$$\int_{-\infty}^{\infty} F(\omega)\phi(\omega)\ d\omega = \int_{-\infty}^{\infty} f(t)\Phi(t)\ dt, \tag{6.12}$$

and *f(t)* is called the *generalized inverse Fourier transform* of $F(\omega)$. This definition is so intuitive it hardly needs to be written down.

No discussion of the generalized Fourier transform would be complete without tackling the remaining functions of slow growth which are central to many aspects of signal generation and analysis. These include the sinusoids and the appropriate piecewise continuous functions such as the unit step and signum functions. Their generalized spectra are most easily determined by judicious application of selected

properties of the generalized Fourier transform. Prior to completing that discussion, it is useful to illustrate some general properties of the generalized Fourier transform.

6.1.3   Generalized Transform Properties

In the previous examples we have emphasized that the generalized Fourier transform is an umbrella which encompasses standard, classical Fourier-integrable as well as slow growth functions considered as regular distributions. The properties of the classically defined Fourier transform demonstrated in Chapter 5 apply with little or no modification to the generalized transform. Naturally, the methods for proving them involve the nuances specific to the use of generalized functions. A general strategy when considering properties of the generalized Fourier transform is to begin with integrals (6.5) and allow the desired parameter (scale, time shift) or operator (differential) to migrate to the classical Fourier transform of the test function, where its effects are easily quantified. The reader should study the following examples carefully. The generalized Fourier transform is elegant but seductive; a common pitfall is to rearrange the generalized transform so it resembles the familiar classical integral and then "declare" a transform when in fact the classical integral will not coverge because the integrand is not integrable.

Proposition (Linearity). Let $f(t)$ represent the linear combination of arbitrary distributions of slow growth,

$$f(t) \ = \ \sum_{k \, = \, 1}^{N} a_k f_k(t) \,. \tag{6.13}$$

Then,

$$\int_{-\infty}^{\infty} F(\omega) \phi(\omega) \ d\omega \ = \ \sum_{k \, = \, 1}^{N} a_k \int_{-\infty}^{\infty} f_k(t) \Phi(t) \ dt \ = \ \int_{-\infty}^{\infty} \left\{ \sum_{k \, = \, 1}^{N} a_k F_k(\omega) \right\} \phi(\omega) \ d\omega. \tag{6.14}$$

The expected result follows:

$$F(\omega) \ = \ \sum_{k \, = \, 1}^{N} a_k F_k(\omega). \tag{6.15}$$

Proposition (Time Shift or Translation). Let $f(t)$ be a distribution of slow growth subjected to a time shift t_0 such that $f(t) \to f(t - t_0)$. Then,

$$\mathcal{F}[f(t - t_0)](\omega) \ = \ \mathcal{F}[f(t)] e^{-j\omega t_0}. \tag{6.16}$$

Use of the defining generalized Fourier transform relations leads to the following equalities (we reduce clutter in the integral by suppressing the (ω) suffix in $\mathcal{F}$):

$$\int_{-\infty}^{\infty} \mathcal{F}[f(t-t_0)]\phi(\omega)\, d\omega = \int_{-\infty}^{\infty} f(\alpha-t_0)\Phi(\alpha)\, d\alpha = \int_{-\infty}^{\infty} f(\gamma)\Phi(\gamma+t_0)\, d\gamma. \quad (6.17)$$

The change of variable, $\gamma \equiv \alpha - t_0$, in the last integral of (6.17) places the time shift conveniently within the classical Fourier transform of the test function. From here, matters are straightforward:

$$\int_{-\infty}^{\infty} f(\gamma)\Phi(\gamma+t_0)\, d\gamma = \int_{-\infty}^{\infty} \mathcal{F}[f(t)]\,\mathcal{F}^{-1}[\Phi(\gamma+t_0)]\, d\omega$$

$$= \int_{-\infty}^{\infty} \mathcal{F}[f(t)]\phi(\omega)e^{-j\omega t_0}\, d\omega \quad (6.18)$$

so that

$$\int_{-\infty}^{\infty} \mathcal{F}[f(t-t_0)]\phi(\omega)\, d\omega = \int_{-\infty}^{\infty} \mathcal{F}[f(t)]\phi(\omega)e^{-j\omega t_0}\, d\omega, \quad (6.19)$$

and the property is proven:

$$\mathcal{F}[f(t-t_0)](\omega) = \mathcal{F}[f(t)]e^{-j\omega t_0}. \quad (6.20)$$

We leave the remaining significant properties of the generalized Fourier transform to the exercises. As we have noted, they are identical to the properties of the standard integral transform, and the proofs are straightforward.

Remark. In the case of regular functions $f(t)$ considered in Chapter 5, the validity of time differentiation property,

$$\mathcal{F}\left[\frac{d}{dt}f(t)\right](\omega) = j\omega F(\omega), \quad (6.21)$$

was conditioned upon $\lim_{|t| \to \infty} f(t) = 0$. No such restriction applies to distributions of slow growth, since the convergence of the generalized Fourier transform is assured by the decay of the testing functions of rapid descent.

Using the properties of the generalized transform, we can resume calculating spectra for the remaining functions of slow growth. These are central to much of signal analysis. We cover the signum function, the unit step, and the sinusoids.

Example (Signum). Consider the case $f(t) = \text{sgn}(t)$. The differentiation property implies

$$\mathcal{F}\left[\frac{d}{dt}\text{sgn}(t)\right](\omega) = j\omega F(\omega) = \mathcal{F}[2\delta(t)], \qquad (6.22)$$

where we have used the recently derived transform of the Dirac delta function. From here, one is tempted to conclude that the desired spectrum $F(\omega) = \frac{2}{j\omega}$. However, a certain amount of care is required since in general $\omega F_1(\omega) = \omega F_2(\omega)$ does not imply $F_1(\omega) = F_2(\omega)$. This is another instance of unusual algebra resulting from the Dirac delta property, derived in Chapter 3: $\omega\delta(\omega) = 0$. Under the circumstances, this allows for the possibility of an additional term involving an impulse function, so that

$$\omega F_1(\omega) = \omega[F_2(\omega) + c_0\delta(\omega)], \qquad (6.23)$$

where c_0 is a constant to be determined. Returning to the example, with $F_1(\omega) \equiv F(\omega)$ and $\omega F_2(\omega) \equiv 2$, we obtain a complete and correct solution:

$$F(\omega) = \frac{2}{j\omega} + c_0\delta(\omega). \qquad (6.24)$$

A determination of c_0 can be made by appealing to symmetry. Since $\text{sgn}(t)$ is a real, odd function of t, its transform must be purely imaginary and odd in the frequency variable ω. Hence, we conclude that $c_0 = 0$. The spectrum is shown in Figure 6.1.

Based on this result, we can proceed to the unit step.

Example (Unit Step). Let $f(t) = u(t)$. Then,

$$\mathcal{F}[u(t)](\omega) = \pi\delta(\omega) + \frac{1}{j\omega}. \qquad (6.25)$$

This proof is left as an exercise. Note that the two terms above, $F_e(\omega)$ and $F_o(\omega)$, represent even and odd portions of the frequency spectrum. These may be obtained directly from even and odd components of $f(t)$, $f_e(t)$, and $f_o(t)$, respectively, in accordance with symmetries developed in Chapter 5. The Dirac delta impulse is a legacy of $f_e(t)$, which is not present in the signum function. The resulting spectrum Figure 6.1b is complex.

(a)

(b)
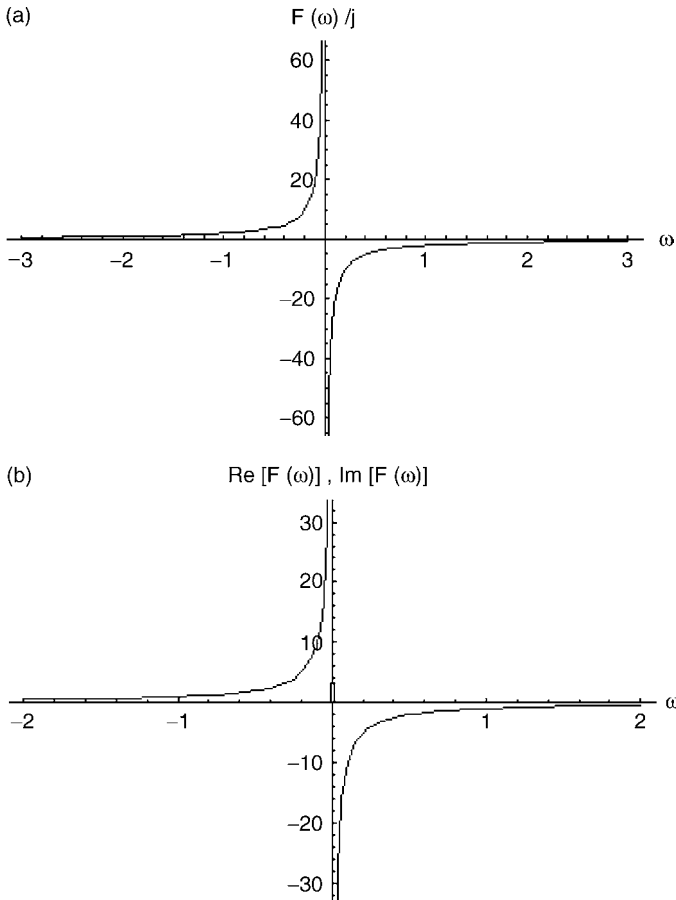
Fig. 6.1. (a) The Fourier transform of sgn(t) is purely imaginary and inversely proportional to ω. (b) The transform of the unit step consists of real Dirac delta function and an imaginary part, as shown.

Examples (Powers of t). The frequency differentiation property

$$\mathcal{F}[(-jt)^n f(t)](\omega) = \frac{d^n}{dt^n} F(\omega) \tag{6.26}$$

leads to several useful Fourier transforms involving powers of t and generalized functions. For integer $n \geq 0$

$$\mathcal{F}[t^n](\omega) = 2\pi j^n \cdot \frac{d^n \delta(\omega)}{d\omega^n}, \tag{6.27}$$

$$\mathcal{F}[t^n u(t)](\omega) = j^n \cdot \left[\pi \frac{d^n \delta(\omega)}{d\omega^n} + \frac{1}{j} \frac{(-1)^n n!}{\omega^{n+1}} \right], \tag{6.28}$$

$$\mathcal{F}[t^n \operatorname{sgn} t](\omega) = (-2)j^{n+1} \frac{(-1)^n n!}{\omega^{n+1}}. \tag{6.29}$$

The derivations are straightforward an left as an exercise. As expected, each of the above spectra contain singularities at $\omega = 0$ on account of the discontinuity in $f(t)$.

Integral powers of $|t|$ are easily handled. For even n,

$$\mathcal{F}[|t|^n](\omega) = \mathcal{F}[t^n](\omega), \tag{6.30}$$

so (6.27) applies. For odd n, note the convenient relation

$$\mathcal{F}[|t|^n](\omega) = \mathcal{F}[t^n \operatorname{sgn}(t)](\omega). \tag{6.31}$$

Remark. Treatment of fractional exponents $0 < n < 1$ and the theory of generalized Fourier transforms for $f(t)$ exhibiting logarithmic divergences is possible, but outside our scope.

Inverse integral powers of t, which are clearly neither integrable nor square integrable, readily yield generalized Fourier spectra. For example,

$$\mathcal{F}\left[\frac{1}{t}\right](\omega) = -j \cdot \pi \cdot \operatorname{sgn}(\omega) \tag{6.32}$$

follows from the application of the symmetry property to $\mathcal{F}[\operatorname{sgn}(t)](\omega)$. Repeated application of time differentiation leads to a more general result for integer $m > 0$:

$$\mathcal{F}\left[\frac{1}{t^m}\right](\omega) = \frac{-\pi}{(m-1)!} \cdot j^m \cdot \omega^{m-1} \cdot \operatorname{sgn}(\omega). \tag{6.33}$$

Example (Complex Exponential). Let $f(t) = e^{j\omega_0 t}$ represent a complex exponential with oscillations at a selected frequency ω_0. According to the frequency shift property of the generalized Fourier transform,

$$\mathcal{F}[g(t)e^{j\omega_0 t}](\omega) = G(\omega - \omega_0), \tag{6.34}$$

the simple substitution $g(t) = 1$—the constant DC signal—provides the desired result:

$$\mathcal{F}[e^{j\omega_0 t}](\omega) = 2\pi\delta(\omega - \omega_0). \qquad (6.35)$$

An example of this transform is shown in Figure 6.2a. Not surprisingly, the spectrum consists of an oscillation at a single frequency. In the limit $\omega_0 \to 0$, the spectrum reverts to $2\pi\delta(\omega)$, as fully expected.

Proposition (General Periodic Signal). Let $f(t)$ represent a periodic distribution of slow growth with period T. Then

$$\mathcal{F}[f(t)](\omega) = \frac{2\pi}{\sqrt{T}} \sum_{n=-\infty}^{\infty} c_n \delta(\omega - n\omega_0), \qquad (6.36)$$

where the c_n represent the exponential Fourier series coefficients for $f(t)$ and $\omega_0 = 2\pi T$.

This is almost trivial to prove using the linearity property as applied to an exponential Fourier series representation of the periodic signal:

$$f(t) = \frac{1}{\sqrt{T}} \sum_{n=-\infty}^{\infty} c_n e^{jn\omega_0 t}. \qquad (6.37)$$

This leads immediately to

$$\mathcal{F}[f(t)](\omega) = \frac{1}{\sqrt{T}} \sum_{n=-\infty}^{\infty} c_n \mathcal{F}[e^{jn\omega_0 t}] \qquad (6.38)$$

from which the desired result (6.36) follows.

This is an important conclusion, demonstrating that the Fourier series is nothing more than a special case of the generalized Fourier transform. Furthermore, upon application of the Fourier inversion, the sifting property of the Dirac delta readily provides the desired synthesis of $f(t)$:

$$\frac{1}{2\pi} \int_{-\infty}^{\infty} \mathcal{F}[f(t)] e^{j\omega t} d\omega = \sum_{n=-\infty}^{\infty} \frac{c_n}{\sqrt{T}} \int_{-\infty}^{\infty} \delta(\omega - n\omega_0) e^{j\omega t} d\omega \qquad (6.39)$$

which trivially reduces to the series representation of $f(t)$ as given in (6.37).
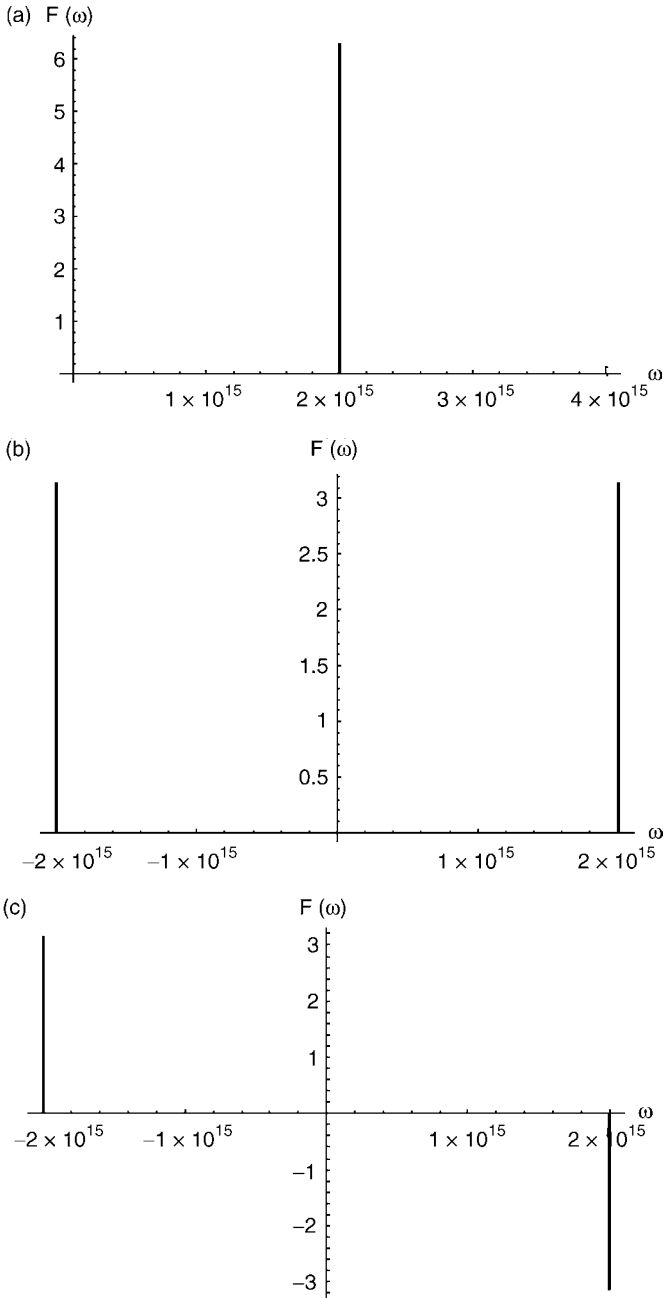
Fig. 6.2. Fourier transforms of (a) the complex exponential with fundamental frequency $\omega_0 = 2 \times 10^{15}$ rad/s, (b) a cosine of the same frequency, and (c) the corresponding sine wave.

Example (Cosine and Sine Oscillations). Let $f(t) = \cos(\omega_0 t)$. From the Euler relation—linking the sinusoids to the complex exponential—and the linearity property, we obtain

$$\mathcal{F}[\cos(\omega_0 t)](\omega) = \pi[\delta(\omega + \omega_0) + \delta(\omega - \omega_0)]. \tag{6.40}$$

Hence, the cosine exhibits a two-sided spectrum with contributions at $\omega = \pm\omega_0$, as Figure 6.2b illustrates. Note that in the process of forming a sinusoid, the spectral amplitude 2π inherent in the complex exponential has been redistributed equally amongst the positive and negative frequencies.

In the case of the sinusoid $f(t) = \sin(\omega_0 t)$, similar arguments demonstrate that

$$\mathcal{F}[\sin(\omega_0 t)](\omega) = j\pi(\delta(\omega + \omega_0) - \delta(\omega - \omega_0)). \tag{6.41}$$

The sine spectrum, shown in Figure 6.2c, is similar in form to the cosine but is, according to symmetry arguments, an odd function in frequency space. We will make use of both of the previous examples in the sequel. In particular, when we develop transforms that combine time- and frequency-domain information, the calculations of sinusoidal spectra will play an important role.

Generalized functions, particularly the Dirac delta function, arise repeatedly in applications and theoretical development of signal analysis tools. Far from being fringe elements in our mathematical lexicon, generalized functions provide the only mathematically consistent avenue for addressing the Fourier transform of several important waveforms. And, as we have just demonstrated, they link two analysis tools (the discrete Fourier series and the continuous Fourier transform) which initially appeared to be fundamentally distinct.

6.2 GENERALIZED FUNCTIONS AND FOURIER SERIES COEFFICIENTS

In this section, we apply generalized functions to develop an alternative technique for evaluating the Fourier coefficients of selected piecewise continuous periodic signals. We have encountered a number of such waveforms in earlier chapters, including the sawtooth wave and the train of rectangular pulses. In Chapter 5 we analyzed such waveforms by application of the the Fourier series expansion of periodic signals in terms of a sinusoidal orthonormal basis. There are no calculations performed in this section which could not, in principle, be performed using the well-established methods previously covered in this chapter and in Chapter 5, so

casual readers can safely skip this section without a loss of the essentials. Nonetheless, readers who master this section will emerge with the following:

- A method that affords the determination of Fourier series coefficients—for a certain class of periodic functions—without the use of integrals;
- Further experience applying generalized functions to Fourier analysis, including the Fourier expansion of a periodic train of impulse functions known as the *Dirac comb*; and
- An introduction to linear differential equations as they apply to Fourier analysis.

The central theme of these developments is the Dirac delta function and its role as the derivative of a step discontinuity. This discontinuity may appear in one or more of the derivatives of $f(t)$ (including the zeroth-order derivative), and this is the tie-in to differential equations. Our discussion is heuristic and begins with the Fourier series expansion of an impulse train. This forms the analytical basis for the other piecewise continuous functions considered in this section.

6.2.1 Dirac Comb: A Fourier Series Expansion

The term "Dirac comb" is a picturesque moniker for a periodic train of Dirac delta functions (Figure 6.3). The Dirac comb is a periodic generalized function, and it is natural to inquire into its Fourier series representations. The discussion had been deliberately slanted to emphasize the role of differential equations in selected problems where the Dirac comb is applicable. We derive the trigonometric and exponential Fourier series representations of the Dirac comb prior to examining some practical problems in the next section.
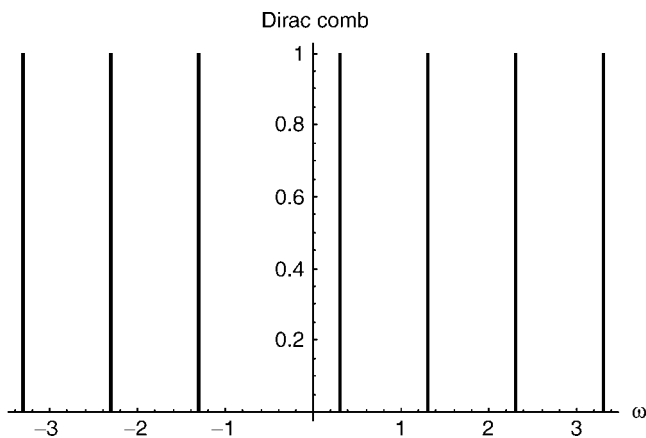
Fig. 6.3. A Dirac comb. By definition, the comb has unit amplitude. The version illustrated here has a unit period and is phase-shifted relative to the origin by an increment of 0.3.

6.2.1.1 *Dirac Comb: Trigonometric Fourier Series.* Let us revisit the periodic sawtooth wave discussed in Chapter 5. There is nothing sacred about our selection of the sawtooth wave to demonstrate the desired results other than the fact that its step transitions are such that a Dirac comb structure appear in the derivatives of the sawtooth wave. The Dirac comb is an odd function of period T with a sine Fourier series expansion:

$$x(t) = \sum_{k=1}^{\infty} b_k \sin(k\Omega t), \tag{6.42}$$

where $\Omega = (2\pi)/T$, and

$$b_k = -\frac{4h}{2\pi k}(-1)^k. \tag{6.43}$$

The signal $x(t)$ consists of a continuous portion $f(t)$ separated by periodically spaced steps of magnitude $-2h$:

$$x(t) = f(t) - 2h \sum_{m=-\infty}^{\infty} u\left(t - T\left(m + \frac{1}{2}\right)\right), \tag{6.44}$$

whose derivative is

$$x'(t) = \frac{2h}{T} - 2h \sum_{m=-\infty}^{\infty} \delta\left(t - \left(m + \frac{1}{2}\right)T\right). \tag{6.45}$$

Substituting the sine Fourier series representation for $x(t)$ into the left-hand side of (6.45) gives

$$\sum_{k=1}^{\infty} b_k \cdot k\Omega \cdot \cos(k\Omega t) = \frac{2h}{T} - 2h \sum_{m=-\infty}^{\infty} \delta\left(t - \left(m + \frac{1}{2}\right)T\right). \tag{6.46}$$

Therefore,

$$\sum_{m=-\infty}^{\infty} \delta\left(t - \left(m + \frac{1}{2}\right)T\right) = \frac{1}{T} + \frac{2}{T} \sum_{k=1}^{\infty} (-1)^k \cos(k\Omega t). \tag{6.47}$$

This is one form of the Dirac comb whose teeth are arranged along the t axis according to the sawtooth wave used in the derivation. A cleaner and more general

form of the Dirac comb may be obtained through a time shift of T/2, giving the basic series representation for a canonical Dirac comb with impulses placed at integer values of T:

$$\sum_{m = -\infty}^{\infty} \delta(t - mT) = \frac{1}{T} + \frac{2}{T} \sum_{k = 1}^{\infty} (-1)^k \cos(k\Omega(t + T/2))$$

$$= \frac{1}{T} + \frac{2}{T} \sum_{k = 1}^{\infty} \cos(k\Omega t). \qquad (6.48)$$

Note that the series representation for a Dirac comb of arbitrary phase shift relative to the origin can always be obtained from the canonical representation in (6.48) .

6.2.1.2 *Dirac Comb: Exponential Fourier Series.* The exponential Fourier series representation,

$$x(t) = \sum_{k = -\infty}^{\infty} c_k e^{jk\Omega t}, \qquad (6.49a)$$

can be derived directly from first principles or from the trigonometric form using the conversion derived in Chapter 5. The result is elegant:

$$c_n = c_{-n} = \frac{1}{\sqrt{T}} \qquad (6.49b)$$

for all integer n. Therefore,

$$\sum_{m = -\infty}^{\infty} \delta(t - mT) = \frac{1}{\sqrt{T}} \sum_{k = -\infty}^{\infty} e^{jk\Omega t}. \qquad (6.50)$$

6.2.2   Evaluating the Fourier Coefficients: Examples

The problem of finding Fourier series expansion coefficients for piecewise continuous functions from first principles, using the Fourier basis and integration, can be tedious. The application of a Dirac comb (particularly its Fourier series representations), to this class of functions replaces the integration operation with simpler differentiation.

We will proceed by example, considering first the case of a rectified sine wave and selected classes of rectangular pulse waveforms. In each case, we develop a differential equation that can then be solved for the Fourier expansion coefficients. As we proceed, the convenience as well as the limitations of the method will become apparent. Mastery of these two examples will provide the reader with sufficient understanding to apply the method to other piecewise continuous waveforms.

6.2.2.1 *Rectified Sine Wave.* Consider a signal

$$x(t) = |A_0 \sin \omega_0 t|, \tag{6.51}$$

where $\omega_0 = (2\pi)/T$, as in Figure 6.4. Now, $x(t)$ is piecewise continuous with discontinuities in its derivative at intervals of $T/2$ (*not* T). The derivative consists of continuous portions equal to the first derivative of the rectified sine wave, separated by step discontinuities of magnitude $\omega_0 A_0$:

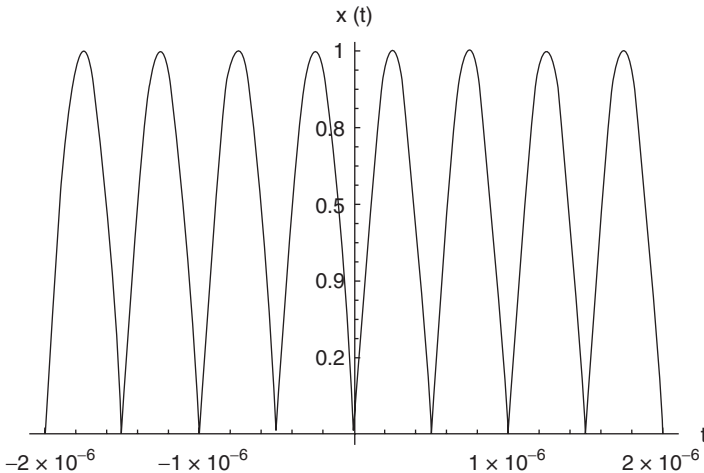$$x'(t) = \frac{d}{dt}|A_0 \sin \omega_0 t| + 2\omega_0 A_0 \sum_{n=-\infty}^{\infty} u(t - n\tau), \tag{6.52}$$

where $\tau = T/2$. Taking a further derivative,

$$x''(t) = -\omega_0^2 x(t) + 2\omega_0 A_0 \sum_{n=-\infty}^{\infty} \delta(t - n\tau), \tag{6.53}$$

brings in a train of impulses and—equally important—a term proportional to the original waveform. Substituting the trigonometric series representation of the impulse train and rearranging terms, we have the differential equation

$$x''(t) + \omega_0^2 x(t) = 2\omega_0 A_0 \left[\frac{1}{\tau} + \frac{2}{\tau} \sum_{n=1}^{\infty} \cos(n\Omega t) \right], \tag{6.54}$$

where $\Omega = ((2\pi)/T)$.

Fig. 6.4. A rectified sine wave. There is a discontinuity in the first derivative.

Remark. This is a second-order, linear differential equation for $x(t)$ whose presence in physical science is almost ubiquitous. The order refers to the highest derivative in the equation. Linearity implies no powers of $x(t)$ (or its derivative), greater than one. Due to the oscillatory nature of its solutions $x(t)$, it is termed the *wave equation*. In the form above, it contains a separate time-dependent term (in this case, representing the Dirac comb) on the right-hand side of (6.54). Depending on the physical context, this is referred to as the source term (in electromagnetic theory) or a forcing function (in circuit analysis and the study of dynamical systems). This equation is a major player in a number of disciplines. When no forcing function is present, the right-hand side vanishes, leaving the *homogeneous wave equation*

$$x''(t) + \omega_0^2 x(t) = 0 \tag{6.55}$$

whose solutions are the simple sinusoids of period T: $\sin(\Omega t)$ and $\cos(\Omega t)$, or linear combinations thereof.

Returning to the problem at hand, we can obtain expressions for the trigonometric Fourier series coefficients of $x(t)$ by substituting a trigonometric series representation,

$$x(t) = \frac{a_0}{2} + \sum_{n=1}^{\infty} [a_n \cos(n\Omega t)] + b_n \sin(n\Omega t), \tag{6.56}$$

and the second derivative

$$x''(t) = \sum_{n=1}^{\infty} -(n\Omega)^2 [a_n \cos(n\Omega t)] + b_n \sin(n\Omega t) \tag{6.57}$$

into (6.54). Then we solve the two resulting equations for a_n and b_n by equating the $\cos(n\Omega t)$ and $\sin(n\Omega t)$ components. So,

$$\omega_0^2 \cdot \frac{1}{2} a_0 = 2\omega_0 A_0 \frac{1}{\tau}, \tag{6.58}$$

giving

$$a_0 = \frac{4A_0}{\omega_0 \tau}, \tag{6.59}$$

and for $n \neq 0$,

$$-(n\Omega)^2 a_n + \omega_0^2 a_n = \frac{2}{\tau}. \tag{6.60}$$

Thus,

$$a_n = \frac{4A_0}{\pi}\left(\frac{1}{1-4n^2}\right). \tag{6.61}$$

The b_n vanish identically, as would be expected considering the even symmetry of $x(t)$, and this is confirmed by the governing equation:

$$(-(n\Omega)^2 + \omega_0^2) \cdot b_n = 0. \tag{6.62}$$

The exponential Fourier series representation can be obtained through these trigonometric coefficients or by direct substitution of the exponential Fourier series representation of the Dirac comb (6.50) into (6.54).

6.2.2.2 *Periodic- "Shaped" Rectangular Pulse.* Another problem we investigated in Section 5.1 is the periodic rectangular pulse train. Now let us consider a more general version of this waveform, consisting of a piecewise continuous portion denoted $p(t)$, with steps of magnitude A and B:

$$x(t) = p(t) + A_0 \sum_{n=-\infty}^{\infty} u[t-(p+nT)] - B_0 \sum_{n=-\infty}^{\infty} u[t-(q+nT)]. \tag{6.63}$$

In this notation, the pulse width is $d = q - p$. For the moment, we defer specification of a particular form for $p(t)$, but our experience with the previous example suggests that some restrictions will apply if we are to solve for the Fourier coefficients via a linear differential equation. Experience also suggests that the differential equation governing this situation will be of first order, since the Dirac comb appears when the first derivative is taken:

$$x'(t) = p'(t) + A_0 \sum_{n=-\infty}^{\infty} \delta[t-(p+nT)] - B_0 \sum_{n=-\infty}^{\infty} \delta[t-(q+nT)]. \tag{6.64}$$

Substituting the appropriate trigonometric Fourier series (6.48) for the impulse trains and expanding the cosines within the series leads to

$$x'(t) = p'(t) + \frac{(A_0 - B_0)}{T} + C(t) + S(t), \tag{6.65}$$

where

$$C(t) = \frac{2}{T} \sum_{n=1}^{\infty} \cos(n\omega_0 t)[A_0 \cos(n\omega_0 p) - B_0 \cos(n\omega_0 q)] \tag{6.66}$$

and

$$S(t) = \frac{2}{T} \sum_{n=1}^{\infty} \sin(n\omega_0 t)[A_0 \sin(n\omega_0 p) - B_0 \sin(n\omega_0 q)]. \tag{6.67}$$

Notice that for arbitrary choice of p and q, $x(t)$ is neither even nor odd; the expansion involves both sine and cosine components, as it should.

To complete this problem, $p(t)$ needs to be specified. If we are going to apply this technique successfully, we will have to restrict $p(t)$ so that the first-order differential equation governing $x(t)$ will be linear. One reasonable option is to specify that $p(t)$ is a linear function of t. Thus,

$$p'(t) = \frac{(B_0 - A_0)}{T}. \tag{6.68}$$

In this instance, the differential equation (6.65) is linear because $p(t)$ returns a constant upon differentiation. (From the previous example involving the rectified sine wave, it is obvious that $p(t)$ itself does not have to be a linear function of its independent variable in order to generate a linear governing differential equation for $x(t)$, but a recursion—as exhibited by the sinusoids—is necessary.) Returning to the problem at hand, we substitute the general Fourier series expansion for the derivative of $x(t)$ into (6.65) and solve for the Fourier coefficients,

$$a_n = \frac{-2}{n\omega_0 T}[A_0 \sin(n\omega_0 p) - B_0 \sin(n\omega_0 q)] \tag{6.69}$$

and

$$b_n = \frac{2}{n\omega_0 T}[A_0 \cos(n\omega_0 p) - B_0 \cos(n\omega_0 q)]. \tag{6.70}$$

As a check, notice that in the limit $A_0 = B_0$, $p = -q$ we generate the special case of a flat (zero-slope) rectangular pulse train of even symmetry, which was treated in Chapter 5. In this case, (6.69) predicts $b_n = 0$, as the even symmetry of $x(t)$ would dictate, and

$$a_n = \frac{4A_0}{n\omega_0 T} \sin[n\pi(d/T)]. \tag{6.71}$$

This is consistent with our previous derivation in Chapter 5 using the standard inner product with the Fourier basis.

Remarks. The problems associated with applying Fourier analysis to nonlinear differential equations can be appreciated in this example. Instead of equaling a constant, suppose that the derivative of $p(t)$ is proportional to some power, $p^n(t)$. Substituting the Fourier series for $p(t)$ would result in multiple powers of the Fourier coefficients, in various combinations, whose determination would be difficult, if not impossible. Furthermore, the example involving the rectified sine wave highlights the convenience associated with the fact that derivatives of the sinusoids are recursive: Up to multiplicative constants, one returns to the original function upon differentiating twice. These observations illustrate why the sinusoids (and their close relatives) figure so prominently in the solution of second-order linear differential equations.

6.3   LINEAR SYSTEMS IN THE FREQUENCY DOMAIN

Communication is the business of passing information from a source to a receiver as faithfully as possible. This entails preparation or encoding of the message, which is then impressed upon a waveform suitable for transmission across a channel to the receiver. At the receiver end, the signal must be decoded and distributed to the intended recipients. If all has gone well, they are provided with an accurate reproduction of the original information. The technical ramifications of each step are vast and involve the questions of analog versus digital encoding, the suitability of the transmission channel, and the design of suitable decoding apparatus—all of which are impacted in some way by the techniques described throughout this book.

This section is intended to provide a basic introduction to *filtering* and *modulation*, with an emphasis on the time and frequency domains implied by Fourier analysis. Filtering implies conditioning in the frequency domain; typically a given filter is designed to highlight or suppress portions of the spectrum. Filtering, in its ideal form, is conceptually simple, but in practice involves nuances and tradeoff due to restrictions imposed by the real world.

Modulation is an operation that inhabits the time domain; it is here that we connect the information-bearing message and a carrier signal, whose role is to aid in transporting the information across the designated channel. From the standpoint of our present knowledge base, the details of modulation are quite user-friendly, and we will present a somewhat detailed account of amplitude and frequency modulation—AM and FM—whose practical role in communications needs no introduction [7–9].

Since filtering and modulation involve the interaction of waveforms with linear systems, we rely extensively on the linear systems principles introduced in Chapter 3.

Two relatively simple theorems involving the Fourier transform establish the foundations of filtering and modulation. These are the *convolution theorem* and the *modulation theorem*, which we prove below. There are few electronic communication devices that do not, in some way, make use of the analytical mileage they provide.

6.3.1   Convolution Theorem

A *filter* is a linear system designed to suppress or enhance selected portions of a signal spectrum. In Chapter 3 we established an input–output relation for a linear, time-invariant system based on the system impulse response, denoted $h(t)$, and the input signal $f(t)$:

$$g(t) = \int_{-\infty}^{\infty} f(\tau)h(t-\tau)\, d\tau. \tag{6.72}$$

The convolution theorem relates the spectrum of the output $g(t)$ to those of the input and the system impulse response:

Theorem (Convolution).   Let $f_1(t)$ and $f_2(t)$ be two functions for which radial Fourier transforms $F_1(\omega)$ and $F_1(\omega)$ exist and let $f(t) = (f_1 * f_2)(t)$. Then the Fourier spectrum of $f(t)$ is

$$F(\omega) = F_1(\omega)F_2(\omega). \tag{6.73}$$

Proof: By definition,

$$F(\omega) = \int_{-\infty}^{\infty} e^{-j\omega t}\left[\int_{-\infty}^{\infty} f_1(\tau)f_2(t-\tau)\, d\tau\right] dt. \tag{6.74}$$

Interchanging the order of integration gives

$$F(\omega) = \int_{-\infty}^{\infty} f_1(\tau)\left[\int_{-\infty}^{\infty} e^{-j\omega t} f_2(t-\tau)\, dt\right] d\tau. \tag{6.75}$$

The time-shift property of the Fourier transform takes care of the integral with respect to t, so that

$$F(\omega) = \int_{-\infty}^{\infty} f_1(\tau)e^{-j\omega\tau}F_2(\omega)\, d\tau = F_1(\omega)F_2(\omega), \tag{6.76}$$

completing the proof.   ■

It is hard to imagine a simpler relationship between spectra. Set in the context of linear systems, the input and output spectra are linked:

$$G(\omega) = F(\omega)H(\omega), \tag{6.77}$$

so that $G(\omega)$ can be shaped or modified by an appropriately designed and implemented system transfer function $H(\omega)$. This forms the backbone of filter design. It will be considered in more detail following a proof of the modulation theorem, which is effectively a converse to the convolution theorem.

6.3.2 Modulation Theorem

Modulation is an operation whereby two or more waveforms, typically an information-bearing modulating signal $m(t)$ and a sinusoidal carrier $c(t)$, are multiplied to form a composite. The termwise product signal $f(t)$ is appropriate for transmission across a communication channel:

$$f(t) = m(t)c(t). \tag{6.78}$$

The modulation theorem relates the spectrum of the composite to those of the constituent modulating wave and carrier:

Theorem (Modulation). Let $f_1(t)$ and $f_2(t)$ be two functions for which Fourier transforms $F_1(\omega)$ and $F_2(\omega)$ exist. Let $f(t) = f_1(t)f_2(t)$. Then the Fourier transform of $f(t)$ is a convolution in the frequency domain:

$$F(\omega) = \frac{1}{2\pi} \int_{-\infty}^{\infty} F_1(\alpha)F_2(\omega - \alpha) \, d\alpha. \tag{6.79}$$

Proof: The Fourier transform of the time product,

$$F(\omega) = \int_{-\infty}^{\infty} e^{-j\omega t} f_1(t)f_2(t) \, dt, \tag{6.80}$$

can be rearranged by substitution of the inverse Fourier transform of $f_2(t)$:

$$F(\omega) = \frac{1}{2\pi} \int_{-\infty}^{\infty} f_1(t) \left[\int_{-\infty}^{\infty} F_2(\gamma)e^{j(\gamma - \omega)t} d\gamma \right] dt. \tag{6.81}$$

A change of variables, $\alpha = \omega - \gamma$, gives (noting carefully the signs and integration limits),

$$F(\omega) = \frac{-1}{2\pi} \int_{-\infty}^{\infty} f_1(t) \left[\int_{\infty}^{(-\infty)} F_2(\omega - \alpha)e^{-j\alpha t} \, d\alpha \right] dt = \frac{1}{2\pi} \int_{-\infty}^{\infty} F_1(\alpha)F_2(\omega - \alpha) \, d\alpha, \tag{6.82}$$

and the proof is complete. ■

The exact form of this spectrum depends heavily upon the nature of $f_1(t)$ and $f_2(t)$ and, in the framework of a modulated carrier signal, gives

$$F(\omega) = \frac{1}{2\pi} \int_{-\infty}^{\infty} M(\alpha)C(\omega - \alpha) \, d\alpha = \frac{1}{2\pi} \int_{-\infty}^{\infty} C(\alpha)M(\omega - \alpha) \, d\alpha. \tag{6.83}$$

The *productive* ↔ *convolution* relationship is one of the most elegant and useful aspects of the Fourier transform. It forms the basis for the design and application of linear filters considered in the next section.

Example (Damped Oscillations). When pure sinusoids are applied to a damped exponential (whose spectrum contained a pole along the imaginary axis; see Chapter 5), the pole acquires a real part. Consider

$$f(t) = e^{-\alpha t}\sin(\omega_0 t)u(t), \tag{6.84}$$

where α is a positive definite constant. Designating $f_1(t) = \sin(\omega_0 t)$ and $f_2(t) = e^{-\alpha t}u(t)$ then (6.79) gives

$$\mathcal{F}[f_1(t)f_2(t)](\omega) = \frac{1}{2\pi}\int_{-\infty}^{\infty}\left[\frac{\pi}{j}\{\delta(\gamma-\omega_0)-\delta(\gamma+\omega_0)\}\right]\frac{1}{\alpha+j(\omega_0-\gamma)}\,d\gamma. \tag{6.85}$$

This reduces, after some algebra, to

$$\frac{1}{2j}\left[\frac{1}{\alpha+j(\omega-\omega_0)}-\frac{1}{\alpha+j(\omega+\omega_0)}\right] = \frac{\omega_0}{(\alpha+j\omega)^2+\omega_0^2}. \tag{6.86}$$

There are poles in the complex plane located at

$$\omega = \pm\omega_0 + j\alpha \tag{6.87}$$

whose real parts are proportional to the frequency of oscillation. The imaginary part remains proportional to the decay. For $\cos(\omega_0 t)$, the spectrum is similar,

$$F(\omega) = \frac{\alpha+j\omega}{(\alpha+j\omega)^2+\omega_0^2} \tag{6.88}$$

but exhibits a zero at $\omega = j\alpha$. Note that it is impossible to distinguish the spectra of the sine and cosine on the basis of the poles alone.

6.4   INTRODUCTION TO FILTERS

To design a filter, it is necessary to specify a system transfer function $H(\omega)$ that will pass frequencies in a selected range while suppressing other portions of the input spectrum. A *filter design* is a specification of $H(\omega)$, including the frequency bands to be *passed*, those to be *stopped*, and the nature of the transition between these regions. In general, $H(\omega)$ is a complex-valued function of frequency,

$$H_0(\omega) = He^{-j\omega\Theta(\omega)}, \tag{6.89}$$

composed of a real-valued *amplitude spectrum* $H_0(\omega)$ and a *phase spectrum* $\Theta(\omega)$. In this chapter, we will work with the class of so-called *ideal filters,* whose transitions between the *stop bands* and the *pass bands* are unit steps:

Definition (Ideal Filter). An *ideal filter* is a linear, translation-invariant system with a transfer function of the form

$$H_0(\omega) \;=\; \sum_{n=1}^{N} a_n u(\omega - \omega_n) \tag{6.90}$$

and a zero phase spectrum across all frequencies: $\Theta(\omega) \;=\; 0$.

   The amplitude spectrum of an ideal filter is characterized by an integer number N transitions, each of which is a unit step of amplitude an at specified frequencies ω_n. The idealization is twofold:

- The unit step transitions are abrupt and perfectly clean. In practice, the transition exhibits rolloff—that is, it is gradual—and overshoot, which is signal processing parlance for oscillations or ripple near the corners of the step transitions, similar to Gibbs's oscillations.
- It is impossible to design and implement a filter whose phase spectrum is identically zero across all frequencies.

The nuisance imposed by a nonzero phase spectrum can be readily appreciated by the following simple illustration. Suppose an audio waveform $f(t)$ acts as an input to a linear system representing a filter with a transfer function $H(\omega)$; for the purposes of illustration we will assume that the amplitude spectrum is unity across all frequencies. The output signal $g(t)$ is characterized by a spectrum,

$$G(\omega) \;=\; e^{-j\omega\Theta(\omega)} F(\omega) \tag{6.91}$$

so that when $G(\omega)$ is inverted back to the time domain, the nonzero phase introduces time shifts in $g(t)$. If the input $f(t)$ were an audio signal, for example, $g(t)$ would sound distorted, because each nonzero phase would introduce a time shift that is a function of $\Theta(\omega)$. (Such *phasing* introduces a reverberation and was deliberately applied to audio entertainment during the so-called psychedelic era in the late 1960s. In more serious communication systems, such effects are not conducive to faithful and accurate data transmission.) In practice, there are ways to minimize phase distortion, but for the present discussion we will continue to inhabit the ideal world with zero phase.
   Filter types are classified according to the frequency bands they pass, and the user makes a selection based upon the spectral characteristics of the signal he intends to modify via application of the filter. A signal $m(t)$ whose spectrum is clustered around $\omega = 0$ is termed *baseband.* In audio signals, for example, the

power resides in the under-20-kHz range, and visual inspection of the spectrum shows a spread in the frequency domain whose nominal width is termed the *bandwidth*. The precise measure of bandwidth may depend upon the context, although a common measure of spectral spread is the 3-dB bandwidth:

Definition (3-dB Bandwidth).   The *3-dB bandwidth* occupied by a spectrum $F(\omega)$ is the frequency range occupied by the signal as measured at the point at which the squared magnitude $|F(\omega)|^2$ is equal to one-half its maximum value.

     The use of the squared magnitude allows the definition to encompass complex-valued spectra and eliminates any issues with +/– signs in the amplitude, which have no bearing on frequency spread. This definition of bandwidth applies equally well to baseband and bandpass spectra, but will be illustrated here with a Gaussian at baseband.

Example (3-dB Bandwidth of a Gaussian).   In the previous chapter we noted that the spectrum of a Gaussian pulse $f(t) = e^{-\alpha t^2}$ was a Gaussian of the form

$$F(\omega) = \sqrt{\frac{\pi}{\alpha}} e^{-\omega^2/4\alpha}. \tag{6.92}$$

According to the definition, the 3-dB bandwidth is the spread in frequency between the points defined by the condition

$$\frac{\pi}{\alpha} e^{-\omega^2/2\alpha} = \frac{1}{2}\frac{\pi}{\alpha} \tag{6.93}$$

or

$$\omega^2 = -2\alpha \ln\frac{1}{2} = 2\alpha \ln 2. \tag{6.94}$$

These points are $\omega = \pm\sqrt{2\ln 2}\sqrt{\alpha}$ so that the total 3-dB bandwidth is

$$\Delta\omega = 2\sqrt{2\ln 2}\sqrt{\alpha}. \tag{6.95}$$

As expected, large values of α result in a greater spectral spread. In communications systems it is common to describe performance in Hz (cycles/s), which scales the bandwidth accordingly,

$$\Delta f = \Delta\omega/2\pi. \tag{6.96}$$

The typical baseband audio signal is not exactly Gaussian, but occupies approximately 40 kHz (i.e., 2×20 kHz), a relatively small increment in (Hertz) frequency space. Television picture signals carry more information—including audio and visual signals—and occupy approximately 9 MHz.

There are other definitions of frequency spread which will be introduced when appropriate.

Much of analog and digital communication involves translating baseband signals in frequency space and filtering to suit the needs of a given system. Frequency translation will be discussed in the next subsection. Prior to that, we turn to an illustration of three common filter types and their uses.

6.4.1 Ideal Low-pass Filter

A low-pass filter is characterized by transitions $\omega_1 = -\omega_t$ and $\omega_2 = \omega_t$ with associated transition amplitudes $a_{1,2} = \pm 1$, as illustrated in Figure 6.5a. The ideal filter has created a passband in the interval $[-\omega_t, \omega_t]$, while suppressing all other frequencies by creating a stopband in those regions. The effect of low-pass filtering is to rid a signal of unwanted high frequencies, which can occur in several contexts. If we plan to sample and digitize a baseband signal, for example, frequencies above a certain limit will end up contaminating the reconstructed waveform since information from the high frequencies will be spuriously thrown into the lower frequency range. This phenomenon is known as aliasing—high frequencies are falsely identified with the lower—and the best course of action is to rid the signal of the offending spectral content prior to sampling.

Low-pass filters are useful when a baseband signal needs to be isolated from other signals present in the received waveform. In selected modulation schemes, the process in which a baseband signal is recovered at the receiver introduces an additional waveform residing near a higher frequency. This waveform is useless and the baseband signal can be isolated from it with a suitable low-pass filter.
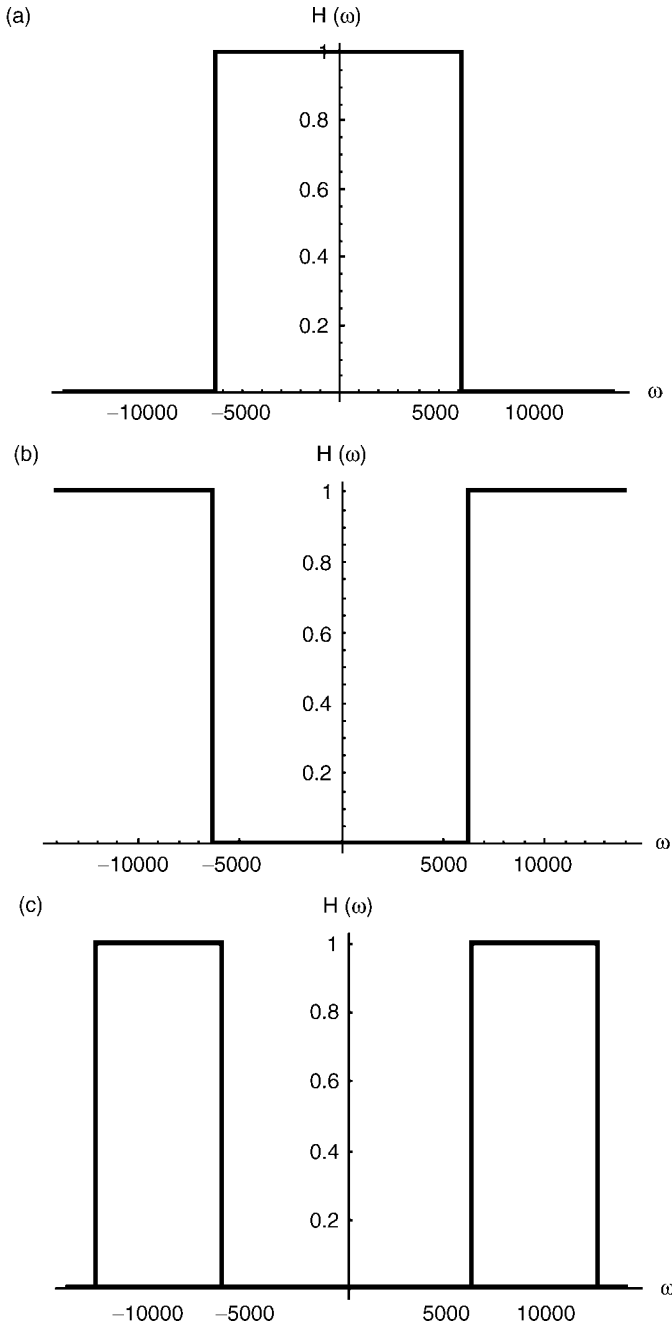
6.4.2 Ideal High-pass Filter

A high-pass filter passes all frequencies $|\omega| > \omega_t$. As with the low-pass filter, we locate transitions at $\omega_1 = -\omega_t$ and $\omega_2 = \omega_t$ but the associated transition amplitudes are $a_1 = -1$, $a_2 = -1$, as illustrated in Figure 6.5b. A primary application of high-pass filtering involves cutting out redundant portions of a signal spectrum to reduce overhead associated with bandwidth. In the forthcoming discussion on modulation, we will consider this in further detail.

6.4.3 Ideal Bandpass Filter

A bandpass filter is characterized by four transitions $\omega_1 = \omega_{t1}$, $\omega_1 = \omega_{t2}$, $\omega_1 = \omega_{t3}$, and $\omega_1 = \omega_{t4}$, with associated transition amplitudes $a_{1,2} = \pm 1$, $a_{3,4} = \pm 1$. As illustrated in Figure 6.5c, two passbands have been created which effectively isolate a band in the middle region of the spectrum.

Example (Shannon Function). The Shannon function

$$f(t) = \frac{\sin(2\pi t) - \sin(\pi t)}{\pi t} \tag{6.97}$$

Fig. 6.5. (a) Ideal filter types. (a) Ideal low-pass filter, shown with a transition frequency $f_t =$ 1 kHz. (b) Ideal high-pass filter. (c) Ideal bandpass filter, illustrated with passband widths of 1 kHz.

has the remarkable property of exhibiting and ideal two-sided bandpass spectrum. This is easily demonstrated. Note that the Shannon function is the difference of two sinc terms,

$$f_1(t) = \frac{\sin(2\pi t)}{\pi t} = 2\frac{\sin(2\pi t)}{2\pi t} \tag{6.98}$$

and

$$f_2(t) = \frac{\sin(\pi t)}{\pi t}, \tag{6.99}$$

each of which is integrable, so that one can evaluate the Fourier integral directly. Alternatively, we can apply the symmetry property

$$\mathcal{F}[F(t)](\omega) = 2\pi f(-\omega) \tag{6.100}$$

to the problem of the unit rectangular pulse supported on the interval $t \in [-a, a]$, whose spectrum was (see Chapter 5)

$$F(\omega) = 2a\frac{\sin(a\omega)}{a\omega}. \tag{6.101}$$

It follows immediately that the spectra of $f_1(t)$ and $f_2(t)$ are unit amplitude rectangular pulses of width 4π and 2π, respectively:

$$F_1(\omega) = u(\omega + 2\pi) - u(\omega - 2\pi), \tag{6.102}$$

$$F_2(\omega) = u(\omega + \pi) - u(\omega - \pi). \tag{6.103}$$

The composite spectrum of the Shannon function is the difference $F(\omega) = (F_2(\omega) - F_1(\omega))$ of two nested rectangular pulses, forming a perfect two-sided bandpass spectrum with transition frequencies $\omega_{t1} = -2\pi, \omega_{t2} = -\pi, \omega_{t3} = \pi, \omega_{t4} = 2\pi$. In terms of the unit step function,

$$F(\omega) = u(t + 2\pi) - u(t + \pi) + u(t - \pi) + u(t - 2\pi). \tag{6.104}$$

As expected given the properties of the Shannon function, the spectrum is a real function of even symmetry.

In general, bandpass filters are useful for isolating non-baseband spectra. For example, consider a multiuser communication link in which several operators are simultaneously transmitting information over several channels, each allocated to a given frequency range. Tuning in to a particular user typically involves some form of bandpass filter to isolate the desired channel.

Example (Derivative of a Gaussian). The Gaussian

$$g(t) = e^{-\alpha t^2} \tag{6.105}$$

exhibited a low-pass spectrum

$$\mathcal{F}[g(t)](\omega) = \sqrt{\frac{\pi}{\alpha}} e^{-\omega^2/\alpha}. \tag{6.106}$$

Multiplying the time-domain Gaussian by a pure sinusoid is one method of translating the bulk of the signal energy to higher frequencies to create a spectrum that approximates a bandpass filter (as we consider in the next section). Alternatively, one can induce the necessary waviness by taking the second derivative,

$$f(t) = -\frac{d^2}{dt^2} g(t) = 2\alpha[1 - 2\alpha t^2]e^{-\alpha t^2}. \tag{6.107}$$

Its spectrum,

$$F(\omega) = -(j\omega)(j\omega)\,\mathcal{F}[g(t)](\omega) = \omega^2 \sqrt{\frac{\pi}{\alpha}} e^{-\omega^2/(4\alpha)} \tag{6.108}$$

demonstrates bandpass characteristics in the form of two quasi-Gaussian pass bands centered about

$$\omega = \pm 2\sqrt{\alpha}. \tag{6.109}$$

The characteristic is hardly ideal, because it passes portions of all finite frequencies except at DC ($\omega = 0$), but as such could be used to eliminate any unwanted DC portion of a waveform. Note that the lobes are not perfect Gaussians due to the effect of the quadratic factor; thus the use of the term "centered" in connection with (6.109) is only approximate. This also complicates the calculation of 3-dB bandwidth, a matter that is taken up in the exercises.

Remark.   Both the Shannon function and the second derivative of the Gaussian are localized *atoms* in the time domain and make suitable *wavelets* (Chapter 11). In wavelet applications, their bandpass characteristics are used to advantage to select out features in the neighborhood of specific frequency.

6.5   MODULATION

The implications of the modulation theorem are far-reaching and quite useful. Most audio and video information begins as a baseband signal $m(t)$ whose frequency range is typically inappropriate for long-distance radio, TV, satellite, and optical fiber links. (Most often, a basic problem is attenuation in the channel, due to absorption in the transmission medium, at frequencies in the kHz regime.) There is also the question of multiple users. Whatever the medium, hundreds of audio and video programs are communicated simultaneously and must be so transferred without interference. Since the bandwidth of an individual audio or video signal is relatively small compared to the total bandwidth available in a given transmission medium, it

is convenient to allocate a slot in frequency space for each baseband signal. This allocation is called *frequency division multiplexing* (FDM). The modulation theorem makes this multichannel scheme possible.

Modulation theory is treated in standard communications theory books [7–9].

6.5.1 Frequency Translation and Amplitude Modulation

Let us reconsider the notion of modulation, where by our baseband signal $m(t)$ is multiplied by an auxiliary signal $c(t)$, to form a composite waveform $f(t)$. The composite is intended for transmission and eventual demodulation at the receiver end. Thus,

$$f(t) = m(t)c(t),\tag{6.110}$$

where $c(t)$ is a sinusoidal *carrier* wave,

$$c(t) = A_c \cos(\omega_c t) = A_c \cos(2\pi f_c t).\tag{6.111}$$

As this scheme unfolds, we will find that the carrier effectively translates the baseband information to a spectral region centered around the carrier frequency f_c. Multiplication by a sinusoid is quite common in various technologies. In various parts of the literature, the carrier signal is also referred to as the *local oscillator* signal, *mixing* signal, or *heterodyning* signal, depending upon the context.

The modulation theorem describes the Fourier transform of the composite signal. Let $m(t) = f_1(t)$ and $c(t) = f_2(t)$. Then

$$F_2(\omega) = \frac{2\pi}{\sqrt{T}}\left[\frac{\sqrt{T}}{2}\delta(\omega + \omega_c) + \frac{\sqrt{T}}{2}\delta(\omega + \omega_c)\right]$$

$$= \pi[\delta(\omega + \omega_c) + \delta(\omega + \omega_c)],\tag{6.112}$$

where we used the exponential Fourier series with $c_1 = c_{-1} = \sqrt{T}/2$. Designating the Fourier transform of $m(t)$ by $M(\omega)$, the spectrum of the composite signal is, according to the modulation theorem,
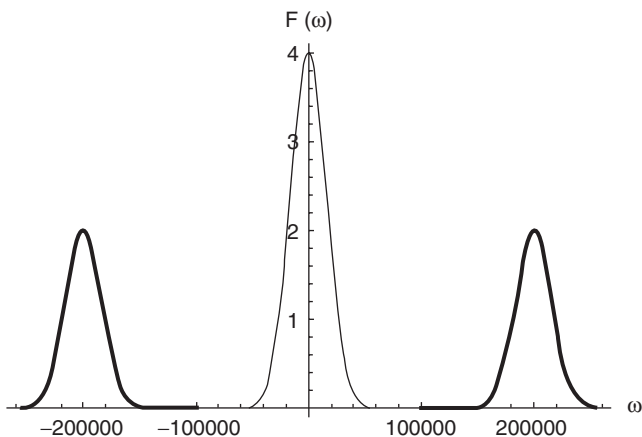
$$F(\omega) = \frac{1}{2}\int_{-\infty}^{\infty} M(\alpha)\delta(\omega + (\omega_c - \alpha))\, d\alpha + \frac{1}{2}\int_{-\infty}^{\infty} M(\alpha)\delta(\omega - (\omega_c - \alpha))\, d\alpha.\tag{6.113}$$

Using simple algebra to rearrange the arguments of the delta functionals and making use of their even symmetry, we can reduce the above to straightforward integrals:

$$F(\omega) = \frac{1}{2}\int_{-\infty}^{\infty} M(\alpha)\delta(\alpha - (\omega + \omega_c))\, d\alpha + \frac{1}{2}\int_{-\infty}^{\infty} M(\alpha)\delta(\alpha - (\omega - \omega_c))\, d\alpha\tag{6.114}$$

Equation (6.114) evaluates easily, resulting in

$$F(\omega) = \frac{1}{2}M(\omega + \omega_c) + \frac{1}{2}M(\omega - \omega_c).\tag{6.115}$$

Fig. 6.6. Frequency translation resulting from carrier modulation of a baseband Gaussian spectrum of amplitude 4. For purposes of illustration, f_c was set at 100 kHz, but most broadcast systems utilize carrier frequencies up to several orders of magnitude higher.

The composite spectrum consists of two facsimiles of the baseband spectra, translated in frequency so that they are centered around $\omega = \pm\omega_c$. The power in the original signal has been equally split between the two portions of the frequency-translated spectrum. The situation is illustrated in Figure 6.6 for a hypothetical Gaussian baseband spectrum.

6.5.2 Baseband Signal Recovery

Our emerging picture of multiuser communications systems consists of multiple baseband signals. Each baseband signal centers around a given carrier frequency, which is broadcast and available to end users. Each end user, in turn, can recover the desired information-bearing baseband signal in a number of ways.

One method of recovery requires the receiver to multiply the incoming composite signal by a local oscillator with frequency ω_s, giving

$$s(t) = [m(t)\cos(\omega_c t)]\cos(\omega_s t)$$
$$= \frac{m(t)}{2}\{\cos((\omega_c + \omega_s)\,t + \cos(\omega_c - \omega_s)t)\}. \tag{6.116}$$

Let us assume that the carrier and local oscillator frequencies differ by some amount $2\pi\Delta f$:

$$\omega_s = \omega_c + 2\pi\Delta f. \tag{6.117}$$

Then,

$$s(t) = \frac{m(t)}{2}[\cos\{2\omega_c + 2\pi\Delta f\}t + \cos(2\pi\Delta ft)]. \tag{6.118}$$

If the frequency deviation Δf is identically zero, this reduces to

$$s(t) \; = \; \frac{m(t)}{2} \cos(2\omega_c t) + \frac{m(t)}{2} . \qquad (6.119)$$

This is the sum of a half-amplitude baseband signal centered around $2\omega_c$ and a similar contribution residing at baseband.

Since systems are designed so that the carrier frequency is much larger than the highest frequency present in the baseband signal, these two contributions are well-separated in the frequency domain. The simple application of a low-pass filter to output described by (6.119) allows the user to eliminate the unwanted power near the frequency $2\omega_c$, leaving the half-amplitude baseband waveform intact. In the case of a multiuser channel, all of these double-frequency waves can be eliminated by a low-pass filter.

When $\Delta f = 0$, the local oscillator is said to be *synchornized* with the carrier. In practice, such precise tuning is not always possible, and a familiar problem with this technique is signal distortion and fading. This occurs, for instance, when the local oscillator drifts from the desired frequency. The source of this fading is evident in (6.118). A small amount of mistuning has little effect on the first term, since it is usually easy to maintain $\Delta f < f_c$; filtering removes this term. On the other hand, the second term is more sensitive to frequency adjustment. Any frequency deviation is going to cause distortion and undesired fading as $\cos(2\pi\Delta f t)$ periodically nears zero. Naturally, as Δf increases, the recovered baseband signal fades with greater frequency. Furthermore, the second term in (6.118) is effectively a baseband signal translated to an carrier frequency Δf. If this value gets too large—even a fraction of the typical baseband frequencies in $m(t)$—there is the possibility of translating a portion of the spectrum outside the passband of the low-pass filter used to retrieve $\frac{1}{2}m(t)$. This is not a trivial matter, because frequency deviations are usually specified as a percentage of the carrier frequency; so even a few percent can be a problem if the carrier frequency is relatively large.

6.5.3   Angle Modulation

Angle modulation is a method whereby the phase of the carrier wave is modulated by the baseband signal $m(t)$. That is,

$$f(t) \; = \; A_c \cos(\omega_c t + \phi_c(t)), \qquad (6.120)$$

where the *phase deviation*

$$\phi_c(t) \; = \; \phi_c[m(t)] \qquad (6.121)$$

is a function to be specified according to the application. The term angle modulation refers to the time-varying angle between the fixed carrier oscillation and the added phase $\phi_c(t)$. In practice, two functional relationships (6.121) are common. The first is a direct proportionality between the phase and the baseband modulation:

$$\phi_c(t) = \text{const} \times m(t), \tag{6.122}$$

which is referred to simply as *phase modulation* (PM). Another common arrangement makes the phase offset proportional to the integral of the baseband signal:

$$\phi_c(t) = \text{const} \times \int_{-\infty}^{t} m(\tau) \, d\tau, \tag{6.123}$$

which is called *frequency modulation* (FM), for reasons that will emerge as we proceed.

    This classification scheme can seem confusing at first glance. Bear in mind that both phase modulation and frequency modulation do, in their respective ways, modulate the phase of the carrier signal. Furthermore, the astute reader has probably wondered how it is possible to distinguish between a PM and an FM waveform by inspection. And, as a matter of fact, you cannot distinguish between them visually. Indeed, for most purposes in this book, the distinction is academic, since in either case $\phi_c(t)$ is simply some function of t. The distinction between PM and FM arises in the implementation. Without explicit knowledge as to how the phase offset $\phi_c(t)$ was constructed, FM and PM are effectively identical. For this reason, it is often sufficient to lapse into the generic label *angle modulation* to describe these waveforms. Of course, the end user, whose task it is to extract information (i.e., the baseband signal $m(t)$) from a given signal will find it of inestimable value to know whether a PM- or FM-style implementation was actually used in the transmission.

Example (Angle Modulation).   Much of this can be clarified by looking at a typical angle modulated signal. Consider a quadratic phase offset of the form

$$\phi_c(t) = \Omega t^2. \tag{6.124}$$

We illustrate the resulting angle modulated waveform (6.120) in Figure 6.7
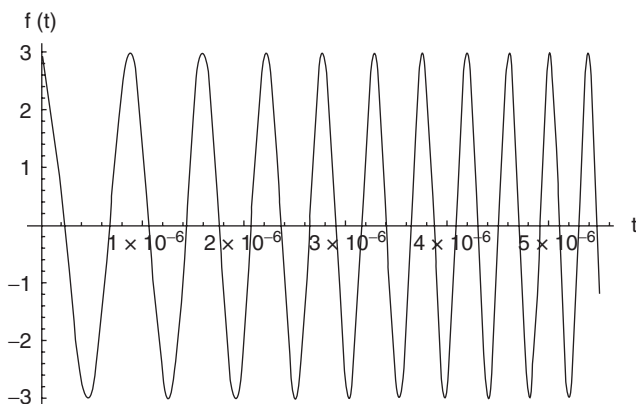
Fig. 6.7. Angle modulation. The illustrated waveform has a carrier frequency $f_c = 1$ MHz, amplitude $A_c = 3$, and $\Omega = 10^{12}$. The chirp induced by time-varying frequency is clearly in evidence.

Note the constant envelope (equal to A_c), which makes the class of *single-frequency* angle-modulated signals readily distinguishable from their amplitude-modulated counterparts (on the other hand, the superposition of multiple carriers can result in a time-varying envelope, as we will see). Furthermore, observe the apparent variation in frequency over time. This phenomenon, known as chirp, for its resemblance to the sound made by inhabitants of the avian world, is the most distinctive feature of angle modulated waveforms.

This motivates the following definition:

Definition (Instantaneous Frequency). Intuitively, the *instantaneous frequency* of a cosine-based angle modulated waveform (6.120) is defined

$$\omega(t) = \frac{d}{dt}[\omega_c t + \phi_c(t)] = \omega_c + \frac{d}{dt}\phi_c(t). \tag{6.125}$$

From this perspective, in which both carrier and time-varying phase effects are lumped into a general phase offset, the term *frequency* modulation makes sense. In the limit of vanishing or constant phase, the instantaneous frequency defaults to that of the carrier, as expected. According to (6.123), when employing an FM system, the baseband signal $m(t)$ is proportional to the second term in the instantaneous frequency defined in (6.125).

For the example in (6.124), the instantaneous frequency is a linear function of time, equal to $\omega_c + \Omega t$. This *linear chirp* is one of several common modulation schemes that involve higher-order polynomial or inverse powers of t and that are considered in the exercises.

More complicated signals, which may involve multiple frequency components, require the extra degree of freedom afforded by the complex exponential representation

$$f(t) = A(t)e^{j\Phi(t)}. \tag{6.126}$$

Taking the real part gives

$$f(t) = A(t)\cos\Phi(t), \tag{6.127}$$

leading to a general definition of instantaneous frequency:

$$\omega(t) \equiv \frac{d\Phi(t)}{dt}. \tag{6.128}$$

6.5.3.1   *Multiple Frequencies.* The time-varying amplitude $A(t)$ is a natural occurrence in signals that consist of multiple oscillations. For example, consider a simple composite signal consisting of two equal-amplitude pure oscillations represented by $\cos(\omega_1 t)$ and $\cos(\omega_2 t)$. Representing the composite as a sum of complex exponentials, it is easy to show that

$$f(t) = Ae^{j\omega_1 t} + Ae^{j\omega_2 t} = A\cos(\Delta t)e^{j\Sigma t}, \tag{6.129}$$

where Δ is the difference,

$$\Delta \equiv \frac{\omega_1 - \omega_2}{2}, \tag{6.130}$$

and the sum

$$\Sigma \equiv \frac{\omega_1 + \omega_2}{2} \tag{6.131}$$

is the average of the two pure oscillations. For this simple case, it is also the instantaneous frequency according to (6.128).

6.5.3.2   *Instantaneous Frequency versus the Fourier Spectrum.*   The instantaneous frequency should not be confused with the Fourier spectrum. This is general, but we will illustrate the point by examining the instantaneous and Fourier spectra of FM signals with sinusoidal phase deviation,

$$\phi_c(t) = k \cdot \sin(\omega_m t). \tag{6.132}$$

This is a useful analysis, since arbitrary information $m(t)$ can be decomposed into a spectrum of sinusoids. The spread of instantaneous frequencies is quantified by the *frequency deviation* defined as the maximum difference between the carrier frequency and the instantaneous frequency (6.128),

$$\Delta\omega \equiv sup[|\omega_c - \omega(t)|] = k\omega_m. \tag{6.133}$$

The derivation of (6.133) is straightforward and left as an exercise. It is common to express the amplitude k as the ratio $\Delta\omega / \omega_m$ and call it the *modulation index*. Equation (6.133) implies that the range of instantaneous frequency occupies a range $\omega_c \pm \Delta\omega$ implying a nominal bandwidth of instantaneous frequencies $2\Delta\omega$. This is intuitively appealing since it is directly proportional to the amplitude and frequency of the phase deviation. In the limit that either of these vanish, the signal reverts to a pure carrier wave.

We now turn to the Fourier spectrum. It can be shown that

$$f(t) = A_c\cos(\omega_c t + k \cdot \sin(\omega_m t)) \tag{6.134}$$

can be elegantly expressed as a superposition a carrier wave and an infinite set of discrete oscillations in multiples (harmonics) of ω_m:

$$f(t) = J_0(k)\cos(\omega_c t) - \sigma_{odd} + \sigma_{even}, \tag{6.135}$$

where

$$\sigma_{odd} \equiv \sum_{n=1}^{\infty} J_{2n-1}(k)[\cos(\omega_c - (2n-1)\omega_m)t - \cos(\omega_c + (2n-1)\omega_m)t] \tag{6.136}$$

and

$$\sigma_{\text{even}} \equiv \sum_{n=1}^{\infty} J_{2n}(k)[\cos(\omega_c - 2n\omega_m)t - \cos(\omega_c + 2n\omega_m)t].$$

In the exercises we lead the reader through the steps necessary to arrive at (6.135). The coefficients $J_p(k)$ are pth-order *Bessel functions of the first kind* and arise in a number of disciplines, notably the analysis of optical fibers, where good engineering treatments of the Bessel functions may be found [10]. Most scripted analysis tools make also them available as predefined functions. In general, they take the form of damped oscillations along the k axis [11]; by inspection of (6.135), they act as weights for the various discrete spectral components present in the signal. The carrier is weighted by the zeroth-order Bessel function, which is unity at the origin and, for k much smaller than unity, can be approximated by the polynomial,

$$J_0(k) \cong 1 - \frac{k^2}{4}. \tag{6.138}$$

The first *sideband* is represented by

$$J_1(k) \cong \frac{k}{2} - \frac{k^3}{16}. \tag{6.139}$$

The remaining sidebands, weighted by the higher-order Bessel functions for which $p > 1$, can be approximated as a single term,

$$J_p(k) \cong \frac{1}{p!}\left(\frac{k}{2}\right)^p \tag{6.140}$$

for small k. In the limit of zero phase deviation, the representation (6.135) reverts to a pure carrier wave $f(t) = \cos(\omega_c t)$, as expected. For k sufficiently small, but nonzero, the signal power consists mainly of the carrier wave and a single pair of sidebands oscillating at $\pm\omega_m$. Operation in this regime is termed *narrowband* FM.

In closing, we highlight the salient difference between Fourier spectral components and the instantaneous frequency: The spectrum of an FM signal with sinusoidal phase deviation is a superposition of Dirac impulses $\delta(\omega - (\omega_c \pm p\omega_m))$ for all integers p. On the other hand, the instantaneous frequency is continuous and oscillates through the range $\omega_c \pm \Delta\omega$.

The general case, in which information $m(t)$ is applied to the phase deviation, as given by (6.121), leads to analytically complex spectra that are beyond the scope of this discussion. But an appropriately behaved $m(t)$ can be naturally decomposed into pure Fourier oscillations similar to the sinusoids. So the simple case presented here is a foundation for the more general problem.

6.6 SUMMARY

This chapter has provided tools for studying the frequency content of important signals—sinusoids, constants, the unit step, and the like—for which the standard

Fourier analysis in Chapter 5 does not work. This generalized Fourier transform rests on the theory of distributions, which we covered in Chapter 3. The properties of the new transform are direct generalizations of those for the standard Fourier transform. An inverse transform exists as well. Further more, the generalized transform is equal to the standard transform for signals in the spaces $L^1(\mathbb{R})$ and $L^2(\mathbb{R})$.

The transform theory for generalized functions draws the links between the Fourier series and transform.

We applied the generalized transform to the study of communication systems. Understanding modulation schemes, for example, depends on spectral analysis of sinusoidal signals, and for this purpose the generalized transform makes the calculations particularly simple. We also considered the design of basic frequency selective linear, translation-invariant systems—filters. Chapter 9 will delve deeper into the theoretical and practical aspects of filter design using traditional Fourier analysis techniques.

Our next step is to develop the frequency theory task for the realm of discrete signals. Now, as we observed in the interplay between the ideas in Chapters 2 and 3, it is easier to justify a discrete summation (even if it has infinite limits) than an integration. Therefore, Chapter 7's mathematical work turns out to be much more concrete. With a discrete signal Fourier theory, computer implementations of frequency domain signal analysis becomes possible. We shall also build a link between analog and discrete signals through the famous Sampling Theorem, so our continuous domain results will appear once again.

REFERENCES

1. A. H. Zemanian, *Distribution Theory and Transform Analysis*, New York: Dover, 1987.

2. M. J. Lighthill, *Fourier Analysis and Generalized Functions*, New York: Cambridge University Press, 1958.

3. I. Halperin, *Introduction to the Theory of Distributions*, Toronto: University of Toronto Press, 1952.

4. R. Beals, *Advanced Mathematical Analysis*, New York: Springer-Verlag, 1987.

5. E. M. Stein and G. Weiss, *Introduction to Fourier Analysis on Euclidean Spaces*, Princeton, NJ: Princeton University Press, 1971.

6. L. Debnath and P. Mikusinski, *Introduction to Hilbert Spaces with Applications*, 2nd ed., San Diego, CA: Academic Press, 1999.

7. A. B. Carlson, *Communication Systems*, 3rd ed., New York: McGraw-Hill, 1986.

8. L. W. Couch III, *Digital and Analog Communication Systems*, 4th ed., Upper Saddle River, NJ: Prentice-Hall, 1993.

9. S. Haykin, *Communication Systems*, 3rd ed., New York: Wiley, 1994.

10. A. W. Snyder and J. D. Love, *Optical Waveguide Theory*, London: Chapman and Hall, 1983.

11. T. Okoshi, *Optical Fibers*, New York: Academic Press, 1982.

12. I. J. Schoenberg, Contribution to the problem of approximation of equidistant data by analytic functions, *Quarterly of Applied Mathematics*, vol. 4, pp. 45–99, 112–141, 1946.

13. M. Unser, Splines: A perfect fit for signal and image processing, *IEEE Signal Processing Magazine*, vol. 16, no. 6, pp. 22–38, November 1999.

PROBLEMS

1. Assume that $f(t)$ is a distribution of slow growth and prove the Fourier transform properties listed in Chapter 5.

2. Show that

(a)

$$F\left[\frac{d}{dt}\delta(t)\right](\omega) = j\omega, \tag{6.141}$$

(b)

$$F[t](\omega) = j2\pi \cdot \frac{d}{d\omega}(\delta(\omega)). \tag{6.142}$$

3. Show that

(a)

$$F[\cos(\omega_0 t)u(t)](\omega) = \frac{\pi}{2} \cdot [\delta(\omega - \omega_0) + \delta(\omega + \omega_0)] + j \cdot \frac{\omega_0}{(\omega_0^2 - \omega^2)}, \tag{6.143}$$

(b)

$$F[\sin(\omega_0 t)u(t)](\omega) = -j\frac{\pi}{2} \cdot [\delta(\omega - \omega_0) - \delta(\omega + \omega_0)] + \frac{\omega_0}{(\omega_0^2 - \omega^2)}. \tag{6.144}$$

4. Demonstrate the following generalized Fourier transforms, where $u(t)$ is the unit step.

(a)

$$F[u(t)](\omega) = \pi\delta(\omega) + \frac{1}{j\omega}, \tag{6.145}$$

(b)

$$F[(-jt)^n f(t)](\omega) = \frac{d^n}{dt^n}F(\omega), \tag{6.146}$$

(c)

$$F[t^n](\omega) = 2\pi j^n \cdot \frac{d^n \delta(\omega)}{d\omega^n}, \tag{6.147}$$

(d)

$$F[t^n u(t)](\omega) = j^n \cdot \left[\pi\frac{d^n \delta(\omega)}{d\omega^n} + \frac{1}{j}\frac{(-1)^n n!}{\omega^{n+1}}\right], \tag{6.148}$$

(e)

$$F[t^n \operatorname{sgn}(t)](\omega) = (-2)j^{n+1} \frac{(-1)^n n!}{\omega^{n+1}}. \tag{6.149}$$

5. A cosine-modulated signal $s(t) = m(t)\cos(\omega_c t)$ is recovered by multiplying it by $\cos(\omega_c t + \theta)$, where θ is a constant. (a) If this product is subjected to a low-pass filter designed to reject the contribution at $2\omega_c$, write the expression for the resulting waveform. (b) If the baseband signal $m(t)$ occupies a range $f \in [300, 3000]$ Hz, what is the minimum value of the carrier frequency ω_c for which it is possible to recover $m(t)$ according to the scheme in part a)? (c) What is the maximum value of the phase θ if the recovered signal is to be 95% of the maximum possible value?

6. The AM cosine-modulated signal $s(t) = m(t)\cos(\omega_c t)$ is recovered by multiplying by a periodic signal $\rho(t)$ with period k/f_c, where k is an integer. (a) Show that $m(t)$ may be recovered by suitably filtering the product $s(t)\rho(t)$. (b) What is the largest value of k for which it is possible to recover $m(t)$ if the baseband signal $m(t)$ occupies a range $f \in [0, 9000]$ Hz and the carrier frequency f_c is 1 MHz?

7. Consider two signals with *quadratic chirp*:

$$f_1(t) = a_1 \cos(bt^2 + ct), \tag{6.150}$$

$$f_2(t) = a_2 \cos(bt^2). \tag{6.151}$$

(a) Derive expressions for the instantaneous frequency of each. Comparing these, what purpose is served by the constant c?

(b) For convenience let $a_1 = b = c = 1$ and plot $f_1(t)$ over a reasonable interval (say, 10 to 30 s). Qualitatively, how is this plot consistent with the instantaneous frequency derived in part (a)?

(c) Let $a_2 = 1$ and plot the composite signal $f(t) = f_1(t) + f_2(t)$ over a 30-s interval. Are the effects of the instantaneous frequencies from part (a) still evident? Compared to the single waveform of part (b), what is the most noteworthy feature induced by superposing $f_1(t)$ and $f_2(t)$?

8. A signal exhibits *hyperbolic chirp*:

$$f(t) = a\cos\left(\frac{\alpha}{\beta - t}\right). \tag{6.152}$$

(a) Let $\alpha_1 = 1000$ and $\beta_1 = 900$, and plot $f(t)$ over a sufficiently large interval, say $t \in [0,3500]$.

(b) What qualitative effects are controlled by the parameters α and β? Let $\alpha_1 = 500$ and $\beta_1 = 740$ and replot $f(t)$.

(c) Derive an expression for the instantaneous frequency of $f(t)$ and plot your result using the signal parameters in part (a).

9. Consider an FM signal modulated by multiple cosines,

$$f(t) = \cos\left[\omega_c t + \sum_{n=1}^{N} k_n \cdot \cos(n \cdot \omega_m t)\right]. \qquad (6.153)$$

For $N = 1, 2$, derive expressions for

(a) The instantaneous frequency of $f(t)$.

(b) The frequency deviation.

10. Derive the Bessel function expansion for the sinusoidally modulated FM signal, (6.135). *Hint*: Make use of the identities

$$\cos(k \cdot \sin\omega_m t) = J_0(k) + 2\sum_{n=1}^{\infty} J_{2n}(k)\cos(2n \cdot \omega_m t), \qquad (6.154)$$

$$\sin(k \cdot \sin\omega_m t) = 2\sum_{n=1}^{\infty} J_{2n-1}(k)\sin((2n-1) \cdot \omega_m t) \qquad (6.155)$$

and the trigonometric relations

$$\cos x \cdot \cos y = \frac{1}{2}\cos(x - y) + \frac{1}{2}\cos(x + y), \qquad (6.156)$$

$$\sin x \cdot \sin y = \frac{1}{2}\cos(x - y) - \frac{1}{2}\cos(x + y). \qquad (6.157)$$

11. A carrier wave is angle modulated sinusoidally.

(a) In principle, how many values of the modulation index k result in a completely suppressed (i.e., zero) carrier wave? List the first five of these values.

(b) On the basis of your answer in (a), is the zeroth-order Bessel function perfectly periodic?

(c) Let $k = 0.1$ and plot the ratio $J_p(k)/J_0(k)$ as a function of the order p, for $p \in [0, 10]$. Qualitatively, what is the effect of increasing p? (Of course, for our purposes, only integer values of p are relevant.)

(d) For $k \in [0, 0.1]$, plot the ratios $J_1(k)/J_0(k)$ and $J_2(k)/J_0(k)$. What is happening to the amplitudes of the sidebands relative to the carrier as k is increased? Is this true for the remaining sidebands as well? Outside of the narrowband FM operating regime, can such behavior be expected for arbitrary k?

12. Consider a unit-amplitude FM carrier signal which is modulated by two sinusoids,

$$f(t) = \cos(\omega_c t + k_1 \cdot \sin\omega_1 t + k_2 \cdot \sin\omega_2 t). \qquad (6.158)$$

(a) Demonstrate the existence of sidebands at harmonics of the sum and difference frequencies $\omega_1 + \omega_2$ and $\omega_1 - \omega_2$ as well as at harmonics of ω_1 and ω_2.

(b) Show that in the limit of small k_1 and k_2 we may approximate $f(t)$ as a linear superposition of cosine and sine carrier waves,

$$f(t) \approx \cos\omega_c t - (k_1 \cdot \sin\omega_1 t + k_2 \cdot \sin\omega_2 t)\sin\omega_c t \tag{6.159}$$

Hint: Apply the approximations, valid for small x:

$$\cos x \cong 1, \tag{6.160}$$

$$\sin x \cong x. \tag{6.161}$$

13. As an application of Fourier transforms and their generalized extensions, this problem develops part of Schoenberg's Theorem on spline functions [12, 13]. We stated the theorem in Chapter 3: If $x(t)$ is a spline function of degree n having integral knots $K = \{m = k_m : m \in \mathbb{Z}\}$, then there are constants c_m such that

$$s(t) = \sum_{m=-\infty}^{\infty} c_m \beta_n(t-m). \tag{6.162}$$

In (6.162) the B-spline of order zero is

$$\beta_0(t) = \begin{cases} 1 & \text{if } -\dfrac{1}{2} < t < \dfrac{1}{2} \\ \dfrac{1}{2} & \text{if } |t| = \dfrac{1}{2} \\ 0 & \text{if otherwise} \end{cases} \tag{6.163}$$

and higher-order B-splines are defined as

$$\beta_n(t) = \underbrace{\frac{\beta_0(t) * \beta_0(t) * \ldots \beta_0(t)}{}}_{n+1 \text{ times}}. \tag{6.164}$$

(a) Explain why $\beta_n(t)$ has a Fourier transform.

(b) Let $B_n(\omega) = \mathcal{F}(\beta_n)(\omega)$ be the Fourier transform of $\beta_n(t)$. Following Ref. 13, show that

$$B_n(\omega) = \left[\frac{\sin\left(\dfrac{\omega}{2}\right)}{\dfrac{\omega}{2}}\right]^{n+1} = \left[\frac{e^{j\omega/2} - e^{-j\omega/2}}{j\omega}\right]^{n+1}. \tag{6.165}$$

(c) Let $y_n(t) = u(t)t^n$ be the one-sided polynomial of degree n. Show that

$$\frac{d^{n+1}}{dt^{n+1}} y_n(t) = n! \delta(t), \tag{6.166}$$

where $\delta(t)$ is the Dirac delta.

(d) Conclude that $Y_n(\omega) = n!/(j\omega)^{n+1}$.

(e) Next, show that

$$B_n(\omega) = \frac{Y_n(\omega)[e^{j\omega/2} - e^{-j\omega/2}]^{n+1}}{n!}. \tag{6.167}$$

(f) Use the binomial expansion from high-school algebra to get

$$B_n(\omega) = \frac{1}{n!} \sum_{k=0}^{n+1} \binom{n+1}{k} (-1)^k e^{-j\omega\left(k - \frac{n+1}{2}\right)} Y(\omega). \tag{6.168}$$

(g) Infer that

$$B_n(t) = \frac{1}{n!} \sum_{k=0}^{n+1} \binom{n+1}{k} (-1)^k y\left(t - k + \frac{n+1}{2}\right) \tag{6.169}$$

and that $\beta_n(t)$ is a piecewise polynomial of degree n.

(h) Show that $\dfrac{d^{n+1}}{dt^{n+1}} \beta_n(t) = n! \delta(t)$ is a sum of shifted Diracs.

(i) Show that an nth-order spline function on uniform knots is a sum of scaled, shifted B-splines.

Discrete Fourier Transforms

We have already discovered a rich theory of frequency transforms for analog signals, and this chapter extends the theory to discrete signals. In fact, the discrete world presents fewer mathematical subtleties. Several reasons compel us to cover the difficult theory first. It was historically prior, for one thing. Fourier developed his techniques for the practical solution of the heat equation long before engineers worried about pen-and-pencil computations for the frequency content of a sampled signal. Beginning with the treatment of analog frequency transforms furnishes—especially in the case of the classic Fourier series—a very clear foundation for comprehending the idea of the frequency content of a signal. A general periodic signal becomes a sum of familiar sinusoids, each with its well-known frequency value. Finally, it is easy to relate the discrete theory to analog notions and thereby justify the claims that such and such a value does represent the discrete signal spectral content at some frequency.

We begin frequency transforms for discrete signals by covering the discrete Fourier transform (DFT), which Chapters 2 and 4 have already introduced. Chapter 2 covered the DFT only very briefly, in the context of providing an example of an orthonormal subset of the discrete Hilbert space l^2. In studying the analysis of signal textures in Chapter 4, our statistical methods proved inadequate for characterizing certain periodic trends within signals. An example is separating the fine-scale roughness from the coarse-scale waviness of a signal. Although statistical techniques tend to obscure the repetitive appearance of signal features, there is no such problem with spectral texture measures. We found that the magnitude of the inner product of a discrete signal with an exponential provided a translation invariant measure of the presence of a discrete frequency component. Thus, two very different motivations already exist for our pursuit of discrete frequency theory, and the DFT in particular: The complex exponentials upon which it is based are orthogonal on finite intervals $[0, N-1] \subset \mathbb{Z}$, and it is very useful for signal texture analysis.

The discrete world's DFT is analogous to the analog Fourier series. It works with discrete periodic signals. The discovery of a fast algorithm for computing the DFT, called the fast Fourier transform (FFT), coincided with the phenomenal development of computing technology in the middle part of the twentieth century. The

FFT completely changed the nature of the signal processing discipline and the work habits—indeed the consciousness—of signal analysts [1]. By reducing the complexity of the computation from an $O(N^2)$ algorithm to an $O(N\log_2 N)$ problem, the FFT makes real-time frequency analysis of signals practical on digital computers.

Another discrete transform must be used when studying the frequencies within discrete aperiodic signals. It has a terrible name: the discrete-time Fourier transform (DTFT). Like the DFT, it extracts the frequency content of discrete signals. But unlike the DFT, the DTFT outputs a continuous range of frequencies from an aperiodic input signal. So similar are the acronyms that it is easily confused with the DFT, and, while its appellation boasts "discrete time," this is only a half-truth, because it in fact produces an analog result. Nevertheless, the awful moniker has stuck. We live with it. We repeat it. The DTFT is the discrete world's mirror image of the Fourier transform.

The next chapter covers a generalization of the DTFT, called the z-transform. It has applications in the stability analysis of discrete systems, solutions for discrete-time difference equations, and subsampling and upsampling operations.

This chapter's last sections develop the principles underlying the famous sampling theorem of Shannon[1] and Nyquist.[2] This result effectively builds a frequency analysis bridge between the world of analog signals and the world of discrete signals [2, 3].

7.1 DISCRETE FOURIER TRANSFORM

We have already made acquaintance with the discrete Fourier transform in Chapters 2 and 4. Now we seek a more formal foundation for the theory of the frequency content of discrete signals. All signal frequency analysis applications that rely on digital computers use the DFT, so we will have regular opportunities to refer back to this groundwork and even extend it in the later chapters of this book.

We first took note of the DFT in Chapter 2. The discrete complex exponentials, restricted to a finite interval, are an orthogonal set within the space of square-summable signals, l^2. Thus, if we consider the subspace of l^2 consisting of signals that are zero outside $[0, N-1]$, then the signals

$$u_k(n) = e^{\frac{-j2\pi kn}{N}}[u(n) - u(n-N)], \tag{7.1}$$

---

[1]Claude E. Shannon (1916–2001) first detailed the affinity between Boolean logic and electrical circuits in his 1937 Master's thesis at the Massachusetts Institute of Technology. Later, at Bell Laboratories, he developed much of theory of reliable communication, of which the sampling theorem is a cornerstone.
[2]Harry Nyquist (1887–1976) left Sweden at age 18 for the United States. As a Bell Laboratories scientist, he provided a mathematical explanation for thermal noise in an electrical resistance, discovered the relation between analog signal frequency and digital sampling rate that now bears his name, and acquired 138 patents.

form an orthogonal set on $[0, N − 1]$. We can normalize the family $\{u_k(n) \mid k = 0, 1, 2, ..., N − 1\}$ by dividing each signal in (7.1) by $N^{1/2}$. We don't need to consider $k > N − 1$, because these signals repeat themselves; this is due to the 2π-periodicity of the exponentials: $\exp(−j2\pi kn/N) = \exp[−j2\pi(k + N)/N]$.

Chapter 4 further acquainted us to the discrete Fourier transform through our study of signal texture. In particular, signals may have different periodic components within them: short-term variations, called roughness (in the parlance of surface metrology), and the long-term variations, called waviness. One way to distinguish and measure the two degrees of repetitiveness is to take the inner product over $[0, N − 1]$ of $x(n)$ with exponentials of the form (7.1). Any relatively large magnitude of the resulting inner product, $\langle x(n), \exp(2\pi nk/N)\rangle$ on $[0, N − 1]$ indicates a correspondingly large presence of a periodic component of discrete frequency $\omega = 2\pi k/N$. This idea could be augmented by performing a normalized cross-correlation of $x(n)$ with prototype signals $\exp(2\pi nk/N)$ as in Section 4.6.1.

7.1.1   Introduction

Our interest in the discrete Fourier transform is twofold. From the viewpoint of Hilbert spaces—where it furnishes a particularly elegant example of an orthogonal basis—we have a theoretical interest in exploring the discrete Fourier transform. From texture interpretation—the rich, seemingly endless field from which so many research endeavors arise—we acquire a practical interest in better understanding and applying the DFT. Let us then formally define the DFT, prove that it forms a complete representation of discrete periodic signals, and consider some examples.

Definition (Discrete Fourier Transform). Suppose $x(n)$ is a discrete signal and $N > 0$. Then the discrete signal $X(k)$ defined by

$$X(k) = \sum_{n=0}^{N-1} x(n) \exp\left(\frac{-2\pi jnk}{N}\right), \tag{7.2}$$

where $0 \leq k \leq N − 1$, is the *discrete Fourier transform* of $x(n)$ on the interval $[0, N − 1]$. Equation (7.2) is called the *analysis equation* for the DFT. In general, $X(k)$ is complex; the complex norm, $|X(k)|$, and complex phase, $\arg(X(k))$, for $0 \leq k < N$, are called the *discrete magnitude spectrum* and *discrete phase spectrum,* respectively, of $x(n)$.

DFT conventions vary widely. A popular notation is to use lowercase Latin letters for the time-domain discrete signal, $s(n)$, and the corresponding uppercase letter for the DFT, $S(k)$. Some authors like to use the hat mark: The DFT of $x(n)$ is $X(k)$ Also, the systems theory notation, $S = \mathcal{F}s$, is handy; $\mathcal{F}$ is the discrete system that accepts a signal $s(n)$ with period N and produces its DFT, $S(k)$. Note that the definition of the system $\mathcal{F}$ in this case depends on N. Different values for the period of the discrete input signals produce different discrete systems. We must register yet another warning about the varieties of DFT definitions in the literature. Equation

(7.2) is the most common definition of the DFT in the engineering research litera-
ture. There is also a discrete Fourier series (DFS) which multiplies each $X(k)$ in
(7.2) by N^{-1}. We introduce the DFS in Section 7.1.2, and there it becomes clear that
its particular formulation helps draw a link between analog and discrete frequency
transforms. Scientists often define the DFT with a positive exponent. Some authors
prefer to normalize the DFT coefficients by a factor of $N^{-1/2}$. Finally, when using
mathematical software packages, one must always be alert to the possibility that the
package indexes arrays beginning with one, not zero. In such a situation the DC
term of the DFT is associated with $k = 1$, the smallest periodic component with
$k = 2$ and $k = N$, and so on.

Example (Discrete Delta Signal). Consider the signal $x(n) = [\underline{1}, 0, 0, 0, 0, 0, 0, 0]$
on the interval $[0, 7]$. We have $X(k) = 1$, for $0 \le k < 8$. So the computation of
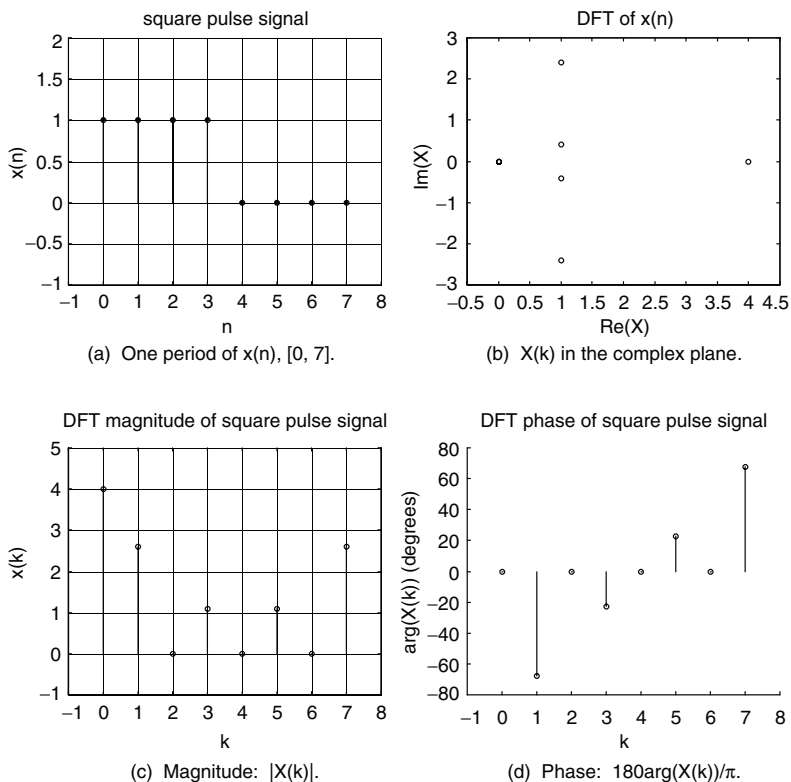the delta signal's transform is quite uncomplicated, unlike the case of the analog
Fourier series.

Example (Discrete Square Pulse). Consider the signal $x(n) = [1, \underline{1}, 1, 1, 0, 0, 0, 0]$.
Its DFT is $X(k) = [\underline{4}, 1-(1 + \sqrt{2})j, 0, 1 - (\sqrt{2} - 1)j, 0, 1 + (\sqrt{2} - 1)j, 0, 1 + (1 + \sqrt{2})j]$.
Note the symmetry: $X(k)$ and $X(8 - k)$ are complex conjugates for $0 < k \le 7$. If we
shift the square pulse so that $y(n) = [\underline{0}, 0, 1, 1, 1, 1, 0, 0]$, then $Y(k) = [\underline{4}, -(1 + \sqrt{2})-$
$j, 0, (\sqrt{2} - 1) + j, 0, (\sqrt{2} - 1) - j, 0, -(1 + \sqrt{2}) + j]$. Although the time-domain pulse
has translated, the zeros of the frequency-domain coefficients are in the same loca-
tions for both $X(k)$ and $Y(k)$. Indeed, there is a time shift property for the DFT, just
as we found for the analog Fourier transform and Fourier series. Since $x(n) = y(n -$
$m)$, where $m = 2$, we have $X(k) = Y(k)\exp(-2\pi jkm/8)$. The DFT can be visualized by
plotting the coefficients as points in the complex plane, or as separate plots of the
magnitude and the phase (Figure 7.1). Since the magnitude of the DFT coefficients
do not change with translation of the time-domain signal, it is most convenient to
plot the magnitude or the energy components of $X(k)$—$|X(k)|$ or $|X(k)|^2$, respectively.

Example (Ramp Pulse). Consider the signal $x(n) = [\underline{1}, 2, 3, 0, 0, 0]$ on $[0, 5]$, with
period $N = 6$. We find $X(k) = 1 + 2\exp(-\pi jk/3) + 3\exp(-\pi jk)$.

7.1.1.1 _Inversion Formula._ There is an inversion theorem for the DFT, and, as
we found in studying analog transforms, it is the key to understanding the basic
properties.

Theorem (DFT Inverse). Suppose $x(n)$ is a discrete signal and $X(k)$ is the DFT of
$x(n)$ on $[0, N - 1]$. Then

$$x(n) = \frac{1}{N} \sum_{k=0}^{N-1} X(k)\exp\left(\frac{2\pi jnk}{N}\right). \tag{7.3}$$

(a) One period of x(n), [0, 7].

(b) X(k) in the complex plane.

(c) Magnitude: |X(k)|.

(d) Phase: 180arg(X(k))/π.

Fig. 7.1. Some examples of the DFT computation. Panel (a) shows a single period of a simple square wave, $x(n)$. In panel (b), the DFT of $x(n)$, $X(k)$ is shown; note that there are only six distinct values, so the circled point at the origin represents three values: $X(2) = X(4) = X(6) = 0$. More revealing is the magnitude of the DFT, $|X(k)|$, shown in panel (c). The phase of $X(k)$ is shown in panel (d); note the linear progression of the phases of the nonzero $X(k)$ values. This clue indicates that DFT coefficients may be visualized as magnitudes associated with points on the unit circle of the complex plane.

Proof: We substitute the expression $X(k)$, given by (7.2) into the right-hand side of (7.3) and work through the exponential function algebra. This brute force attack gives

$$\frac{1}{N}\sum_{k=0}^{N-1}X(k)\exp\left(\frac{2\pi jnk}{N}\right) = \frac{1}{N}\sum_{k=0}^{N-1}\left(\sum_{r=0}^{N-1}x(r)\exp\frac{-2\pi jrk}{N}\right)\exp\left(\frac{2\pi jnk}{N}\right)$$

$$= \frac{1}{N}\sum_{r=0}^{N-1}\sum_{k=0}^{N-1}x(r)\exp\left(\frac{-2\pi jrk}{N}\right)\exp\left(\frac{2\pi jnk}{N}\right)$$

$$= \sum_{r=0}^{N-1}x(r)\left[\frac{1}{N}\sum_{k=0}^{N-1}\exp\left(\frac{2\pi j(n-r)k}{N}\right)\right], \qquad (7.4)$$

and it appears that we have quite a mess on our hands! However, the following lemma shows that the bracketed expression in (7.4) has a gratifying, simple form.

Lemma.   Let $N > 0$, and let p and k be integers. Then, if for some $m \in \mathbb{Z}$, we have $p = mN$, then

$$\frac{1}{N} \sum_{k=0}^{N-1} \exp\left(\frac{2\pi jpk}{N}\right) = 1; \tag{7.5a}$$

otherwise

$$\frac{1}{N} \sum_{k=0}^{N-1} \exp\left(\frac{2\pi jpk}{N}\right) = 0. \tag{7.5b}$$

Proof of lemma: Let $a = \exp(2\pi jp/N)$. Then, expanding the summation, for instance in (7.5a), gives

$$\frac{1}{N} \sum_{k=0}^{N-1} \exp\left(\frac{2\pi jpk}{N}\right) = \frac{1}{N}\left(1 + a + a^2 + \cdots + a^{N-1}\right). \tag{7.6}$$

But if $p = mN$, then $a = \exp(2\pi jmN/N) = \exp(2\pi jm) = 1$. In this case, the right-hand side of (7.6) is unity. If $p/N \notin \mathbb{Z}$, then $a \neq 1$ and $1 - a \neq 0$. This implies $1 + a + a^2 + \cdots + a^{N-1} = (1 - a^N)/(1 - a)$. However, $aN = 0$, and in this case the right-hand side of (7.6) is zero, proving the lemma.   ∎

Let us then continue proving the theorem. The term $(n - r)$ in the bracketed expression in (7.4) is either an integral multiple of N or it is not. Suppose $p = (n - r) = mN$ for some $m \in \mathbb{Z}$; by the lemma, therefore, the bracketed expression is unity. But since $0 \le n, r \le N - 1$, we know that $p = n - r$ is a multiple of N only if $n - r = 0$, that is, $n = r$. So the bracketed sum in (7.4) is zero unless $n = r$:

$$\frac{1}{N} \sum_{k=0}^{N-1} \exp\left(\frac{2\pi j(n-r)k}{N}\right) = \begin{cases} 0 & n \neq r, \\ 1 & \text{otherwise.} \end{cases} \tag{7.7}$$

Thus, the whole expression in (7.4) reduces to $x(n)$, and the proof of the theorem is complete.   ∎

Definition (Inverse DFT).   Equation (7.3) is called the *synthesis equation* for the DFT. The expression (7.3) is also called the *inverse discrete Fourier transform* (IDFT).

The first term, $X(0)$, is often called the DC (direct current) component of the DFT for $x(n)$, since it contains no periodic (i.e., alternating current) component. This whispers of Fourier analysis's electrical engineering heritage, although

nowadays everyone—engineers, scientists, even university business school professors running trend analyses—uses the term. Note that when $x(n)$ is reconstructed from its DFT, the synthesis equation summation begins with the factor $X(0)/N$, which is the average value of $x(n)$ on the interval $[0, N-1]$.

Corollary (Discrete Fourier Basis). Let K be the set of discrete signals supported on the interval $[0, N-1]$, and let $u(n)$ be the unit step signal. Then K is a Hilbert subspace of l^2, and the windowed exponential signals, $\{u_k(n) \mid 0 \le k \le N-1\}$, where

$$u_k(n) = \frac{\exp(2\pi jkn/N)}{\sqrt{N}}[u(n) - u(n-N)], \tag{7.8}$$

form an orthonormal basis for K.

Proof: Recall from Section 2.7.1 that a Hilbert subspace is an inner product subspace that is complete in the sense that every Cauchy sequence of elements converges to a subspace element. This is easy to show for K. So let us consider the windowed exponentials (7.8). Note that if $0 \le k, l \le N-1$, then

$$\langle u_k, u_l \rangle = \sum_{n=0}^{N-1} \frac{\exp(j2\pi kn/N)}{\sqrt{N}} \overline{\frac{\exp(j2\pi ln/N)}{\sqrt{N}}} = \frac{1}{N} \sum_{n=0}^{N-1} \exp[j2\pi(k-l)n/N]. \tag{7.9}$$

The theorem's lemma shows that the sum on the right-hand side of (7.9) is zero unless $k = l$, in which case it is unity. But this is precisely the orthonormality condition. We must show too that the orthonormal set is complete; that is, we need to show the other sense of completeness, which specifies that every element of the subspace K is arbitrarily close to a linear combination of elements of $\{u_k(n) \mid 0 \le k \le N-1\}$. Let $X(k)$ be given by (7.2). For $0 \le n \le N-1$, the theorem implies

$$x(n) = \frac{1}{N} \sum_{k=0}^{N-1} X(k) \exp\left(\frac{2\pi jnk}{N}\right) = \frac{1}{\sqrt{N}} \sum_{k=0}^{N-1} X(k) u_k(n). \tag{7.10}$$

This shows that $x(n)$ is a linear combination of the $\{u_k(n)\}$. ∎

Corollary (DFT for Discrete Periodic Signals). Suppose $x(n)$ is a discrete signal with period $N > 0$: $x(n) = x(n + N)$ for all n. Then,

$$x(n) = \frac{1}{N} \sum_{k=0}^{N-1} X(k) \exp\left(\frac{2\pi jnk}{N}\right). \tag{7.11}$$

for all n.

Proof: Note that on the finite interval $[0, N − 1]$, the theorem implies (7.11). But $x(n) = x(n + N)$, and the right-hand side of (7.11) is also periodic with period N, so the corollary holds.   ■

Corollary (DFT Uniqueness). Suppose $x(n)$ and $y(n)$ are discrete signals, and $X(k)$ and $Y(k)$ are their respective DFTs on $[0, N − 1]$. If $X = Y$ on $[0, N − 1]$, then $x(n) = y(n)$ on $[0, N − 1]$.

Proof: If $X(k) = Y(k)$ for all $0 \le k \le N − 1$, then both $x(n)$ and $y(n)$ are given by the same inversion formula (7.3). So $x(n) = y(n)$ for all $0 \le n \le N − 1$.   ■

So the transform's uniqueness on an interval follows from the inversion equation. We followed a similar roundabout route toward showing transform uniqueness with the analog Fourier series and Fourier transform. In the analog world, the integration of signals, possibly containing discontinuities, complicates the uniqueness propositions, of course. Supposing Riemann integration, we can claim uniqueness only up to a finite number of impulse discontinuities. And, allowing the more robust Lebesgue integration, we can only claim that signals that are equal, except perhaps on a set of measure zero, have identical transforms. However, with discrete signals, owing to the finite sums used in computing the DFT, the transform values are truly unique.

Corollary (DFT Uniqueness). Suppose $x(n)$ and $y(n)$ discrete signals, both with period equal to N. If their DFTs are equal, $X(k) = Y(k)$ for all $0 \le k \le N − 1$, then $x(n) = y(n)$ for all n.

Proof: Combine the proofs of the previous two corollaries.   ■

If $X(k) = Y(k)$ for all $0 \le k \le N − 1$, then both $x(n)$ and $y(n)$ are given by the same inversion formula (7.3). So $x(n) = y(n)$ for all $0 \le n \le N − 1$.

The DFT Uniqueness Corollary encourages us to characterize the DFT as the appropriate transform for periodic discrete signals. If a signal $x(n)$ has period $N > 0$, then, indeed, the synthesis equation provides a complete breakdown of $x(n)$ in terms of a finite number of exponential components. But, the DFT is also applied to the restriction of aperiodic discrete signals to an interval, say $s(n)$ on $[a, b]$, with $b − a = N − 1$. In this case, the analysis equation (7.2) is used with $x(n) = s(a − n)$. Of course, the synthesis equation does not give $s(n)$; rather, it produces the periodic extension of $s(n)$ on $[a, b]$.

7.1.1.2 *Further Examples and Some Useful Visualization Techniques.*
Therefore, let us explore a few examples of the DFT's analysis and synthesis equations before proceeding to link the DFT to the frequency analysis of analog signals. These examples show that it is quite straightforward to compute the DFT analysis equations coefficients $X(k)$ for a trigonometric signal $x(n)$. It is not necessary, for instance, to explicitly perform the sum of products in the DFT analysis equation (7.2).

Example (Discrete Sinusoids). Consider the discrete sinusoid $x(n) = \cos(\omega n)$. Note that $x(n)$ is periodic if and only if ω is a rational multiple of 2π: $\omega = 2\pi p/q$ for some $p, q \in \mathbb{Z}$. If $p = 1$ and $q = N$, then $\omega = 2\pi/N$, and $x(n)$ is periodic on $[0, N-1]$ with fundamental period N. Signals of the form $\cos(2\pi kn/N)$ are also periodic on $[0, N-1]$, but since $\cos(2\pi kn/N) = \cos(2\pi(N-k)n/N)$, they are different only for $k = 1$, $2, ..., \lfloor N/2 \rfloor$. We recall these facts from the first chapter and note that a like result holds for discrete signals $y(n) = \sin(\omega n)$, except that $\sin(2\pi kn/N) = -\sin(2\pi(N-k)n/N)$. We can explicitly write out the DFT synthesis equations for the discrete sinusoids by observing that

$$\cos\left(\frac{2\pi nk}{N}\right) = \frac{1}{2}\exp\left(\frac{2\pi jnk}{N}\right) + \frac{1}{2}\exp\left(\frac{2\pi jn(N-k)}{N}\right), \qquad (7.12a)$$

$$\sin\left(\frac{2\pi nk}{N}\right) = \frac{1}{2j}\exp\left(\frac{2\pi jnk}{N}\right) - \frac{1}{2j}\exp\left(\frac{2\pi jn(N-k)}{N}\right), \qquad (7.12b)$$

for $0 \le k \le \lfloor N/2 \rfloor$. Equations (7.12a) and (7.12b) thereby imply that $X(k) = X(N-k) = N/2$ with $X(m) = 0$, for $0 \le m \le N-1$, $m \ne k$; and $Y(k) = -Y(N-k) = (-jN/2)$, with $Y(m) = 0$, for $0 \le m \le N-1$, $m \ne k$. The factor of N in the expressions for $X(k)$ and $Y(k)$ ensures that the DFT synthesis equation (7.3) holds for $x(n)$ and $y(n)$, respectively.

Example (Linear Combinations of Discrete Sinusoids). If we multiply a discrete sinusoid by a constant scale factor, $v(n) = Ax(n) = A\cos(\omega n)$, then the DFT coefficients for $v(n)$ are $V(k) = AX(k)$. This is a *scaling* property of the DFT. This is clear from the analysis (7.2) and synthesis (7.3) equations. Furthermore, if $v(n) = x(n) + y(n)$, then $V(k) = X(k) + Y(k)$, where $V(k)$, $X(k)$, and $Y(k)$ are the DFT coefficients of $v(n)$, $x(n)$, and $y(n)$, respectively. This is a *superposition* property of the DFT. Thus, it is easy to find the DFT synthesis equation for a linear combinations of discrete sinusoids from this linearity property and the previous example.

Example (Phase of Discrete Sinusoids). If the sinusoid $x(n) = \cos(\omega n)$ has period $N > 0$, then so does $y(n) = \cos(\omega n + \phi)$. Since $y(n) = [\exp(j\omega n + j\phi) + \exp(-j\omega n - j\phi)]/2 = [\exp(j\phi)\exp(j\omega n) + \exp(-j\phi)\exp(-j\omega n)]/2$, we can use the scaling and superposition properties of the previous example to find the DFT coefficients of $Y(k)$ in terms of $X(k)$. Notice also that the sinusoidal signal's phase shift, ϕ, does not change the complex magnitude of the DFT coefficients. This property we noted in our study of textured signal periodicity in Chapter 4.

A common and useful notation allows us to write the DFT is a more compact form.

Definition (Phase Factor). For $N > 0$, the Nth root of unity, $W_N = e^{-2\pi j/N}$, is called the *phase factor* of order N.

The fast Fourier transform algorithms in Section 7.1.4 exploit the symmetries of the phase factor that appear in the DFT analysis and synthesis equations.

Now, the powers of W_N, $(W_N)^k = e^{-2\pi jk/N}$, $0 \le k < N$, all lie on the unit circle in the complex plane: $(W_N)^k = e^{-2\pi jk/N} = \cos(2\pi k/N) - j\sin(2\pi k/N)$. Then we can rewrite the DFT analysis and synthesis equations as follows:
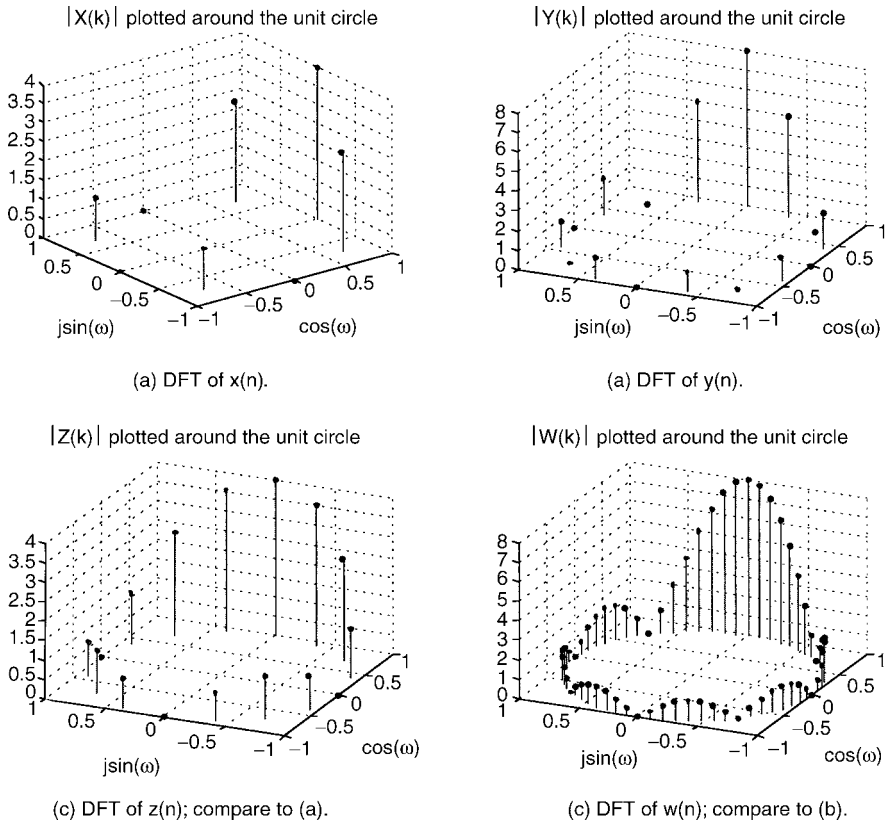
$$X(k) = \sum_{n=0}^{N-1} x(n)W_N^{nk}, \tag{7.13}$$

$$x(n) = \frac{1}{N}\sum_{k=0}^{N-1} X(k)W_N^{-nk}. \tag{7.14}$$

Thus, $X(k)$ is a polynomial of degree $N - 1$ in $(W_N)^k$, and $x(n)$ is a polynomial of degree $N - 1$ in $(W_N)^{-n}$. That is, if we define the complex polynomials, $P(z) = x(0) + x(1)z + x(2)z^2 + \cdots + x(N-1)z^{N-1}$ and $p(z) = (1/N)[X(0) + X(1)z + X(2)z^2 + \cdots + X(N-1)z^{N-1}]$, then $X(k) = P((W_N)^k)$, and $x(n) = p((W_N)^{-n})$. The DFT of $x(n)$ is just the complex polynomial $P(z)$ evaluated at specific points on the unit circle, namely $(W_N)^k = e^{-2\pi jk/N}$, $0 \le k < N$. Similarly, the IDFT is the complex polynomial $p(z)$ evaluated at points $(W_N)^{-n}$ on the unit circle, $0 \le n < N$. In fact, these are the same points, just iterated in the opposite order. We will extend this idea of representing the DFT as a complex polynomial restricted to a set of discrete points in the next chapter; in fact, the concept of the z-transform carries it to the extreme. For now we just want to clarify that the DFT coefficients can be thought of as functions of an integer variable k or of points on the unit circle $z = \cos(2\pi k/N) - j\sin(2\pi k/N)$. This idea enables us to better visualize some of the behavior of the transform for specific signals. For example, we may study the transforms of square pulse signals for various periods N and various duty cycles (percent of non zero coefficients) as in Figure 7.2.

For square pulse signals, such as in Figure 7.2, there is a closed-form expression for the DFT coefficients. Suppose $x(n)$ has period $N > 0$, and $x(n)$ is zero except for the first M values, $x(0) = x(1) = \cdots = x(M - 1) = 1$, with $0 < M < N - 1$. Then $X(k)$ is a partial geometric series in $(W_N)^k$: $X(k) = 1 + (W_N)^k + (W_N)^{2k} + \cdots + (W_N)^{k(M-1)}$. Assuming that $(W_N)^k \ne 1$, we calculate

$$X(k) = \frac{1 - \left(W_N^k\right)^M}{1 - W_N^k} = \frac{W_N^{kM/2}\left(W_N^{-kM/2} - W_N^{kM/2}\right)}{W_N^{k/2}\left(W_N^{-k/2} - W_N^{k/2}\right)} = \frac{W_N^{kM/2}\left(e^{\pi jkM/N} - e^{-\pi jkM/N}\right)}{W_N^{k/2}\left(e^{\pi jk/N} - e^{-\pi jk/N}\right)}$$

$$= \frac{W_N^{kM/2}\left(2j\sin(\pi kM/N)\right)}{W_N^{k/2}\left(2j\sin(\pi k/N)\right)} = W_N^{k(M-1)/2}\frac{\left(\sin(\pi kM/N)\right)}{\left(\sin(\pi k/N)\right)} \tag{7.15}$$

Thus, for $k = 0$, $X(k) = M$, and for $0 < k < M - 1$, the DFT coefficient $X(k)$ is given by the product of a complex $2N$th root of unity and a ratio of sinusoids: $\sin(\pi kM/N)$ and $\sin(\pi k/N)$. Since $\sin(\pi kM/N)$ oscillates M times faster than $\sin(\pi k/N)$, there are

|X(k)| plotted around the unit circle

(a) DFT of x(n).

|Y(k)| plotted around the unit circle

(a) DFT of y(n).

|Z(k)| plotted around the unit circle

(c) DFT of z(n); compare to (a).

|W(k)| plotted around the unit circle

(c) DFT of w(n); compare to (b).

Fig. 7.2. Visualizing the DFT around the unit circle of the complex plane. We set $\omega = 2\pi k/N$ and plot the DFT magnitudes of some signals relative to $\cos(\omega)$ and $\sin(\omega)$ around the unit circle in the complex plane. In part (a), $|X(k)|$ for $x(n) = [\underline{1}, 1, 1, 1, 0, 0, 0, 0]$. In part (b), $|Y(k)|$ for $y(n) = [\underline{1}, 1, 1, 1, 1, 1, 1, 1, 0, 0, 0, 0, 0, 0, 0, 0]$. In part (c), $|Z(k)|$ for $z(n) = [\underline{1}, 1, 1, 1, 0, 0, 0, 0, 0, 0, 0, 0, 0, 0, 0, 0]$. In part (d), $w(n)$ has period $N = 64$, with $w(n) = 1$ for $0 \le n \le 7$, and $w(n) = 0$ otherwise. Note that the size of the square pulse within the signal's period determines the number of lobes, and the number of analysis equation summands determines the detail within the lobes.

M lobes in the discrete magnitude spectrum $|X(k)|$, if we count the big lobe around $k = 0$ twice (Figure 7.2).

7.1.1.3   Simple Applications.
Let us briefly show how to use the DFT in applications on real sampled signal data. This section shows how the magnitudes of DFT coefficients indicate significant periodic trends in the original analog signal. As an example, we perform a discrete Fourier analysis of the solar disturbances associated with sunspots. Most people are aware that sunspot numbers increase dramatically during these solar disturbances, affect high-frequency radio communication on earth, and tend to occur in approximately 11-year cycles.

Since discrete signals arise from sampling analog signals, the first step is to suppose $x(n) = x_a(nT)$, where $x_a(t)$ is an analog signal, $T > 0$ is the sampling interval, and $x_a(t)$ has period NT. If we write $x(n)$ in terms of its DFT synthesis equation (7.3), then we see that the sinusoidal components of smallest frequency are for $k = 1$ and $k = N - 1$: $\cos(2\pi n/N)$, $\sin(2\pi n/N)$, $\cos(2\pi(N - 1)n/N)$, and $\sin(2\pi(N - 1)n/N)$. These discrete sinusoids come from sampling analog sinusoids with fundamental period NT, for example, $\sin(2\pi n/N) = \sin(2\pi t/(NT))|_{t=Tn}$. But this is precisely the analog sinusoid with fundamental frequency $1/NT$ Hz.

Application (Wolf Sunspot Numbers). The first chapter introduced the Wolf sunspot numbers as an example of a naturally occurring, somewhat irregular, but largely periodic signal. From simple time-domain probing of local signal extrema, we can estimate the period of the sunspots. The DFT is a more powerful tool for such analyses, however. Given the Wolf sunspot numbers over some 300 years, a good estimate of the period of the phenomenon is possible. Figure 7.3 shows the time-domain sunspot data from 1700 to 1996. The sampling interval T is 1 year ($T = 1$), and we declare 1700 to be year zero for Wolf sunspot number data. Thus, we perform a frequency analysis of the signal, using the DFT on $w(n)$ over the interval $[1700-1700, 1996-1700] = [0, N - 1]$. Figure 7.3 shows the DFT, $W(k)$, and its magnitude; there is a huge peak, and for that the rest of the analysis is straightforward. Brute force search finds the maximum magnitude $|W(k)|$ for $0 < k < (1996 - 1700 + 1)/2$ at time instant $k = k_0$. We do not need to consider higher k values, since the terms above $k = 148 = \lfloor 297/2 \rfloor$ represent discrete frequencies already counted

Wolf Sunspot Numbers: 1700 - 1996

(a)
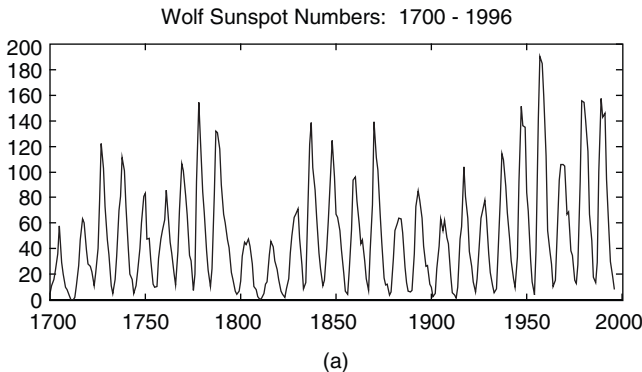
Fig. 7.3. Wolf sunspot numbers. Signal $w(n)$ is the Wolf sunspot number, a composite figure equal to $10G + S$, where G is the average number of sunspot groups and S is the average number of spots reported by a team of international observers. In panel (a), the time-domain plot of $w(n)$ from 1700 to 1996 is shown; note the periodicity. Panel (b) plots the DFT coefficients $W(k)$ in the complex plane but this representation does not aid interpretation. The power of the DFT signal, $P(k) = |W(k)|^2$, appears in panel (c), with the DC term zeroed. The maximum power value occurs at $k = 27$, which represents a sinusoidal component with a period of $297/27 = 11$ years.
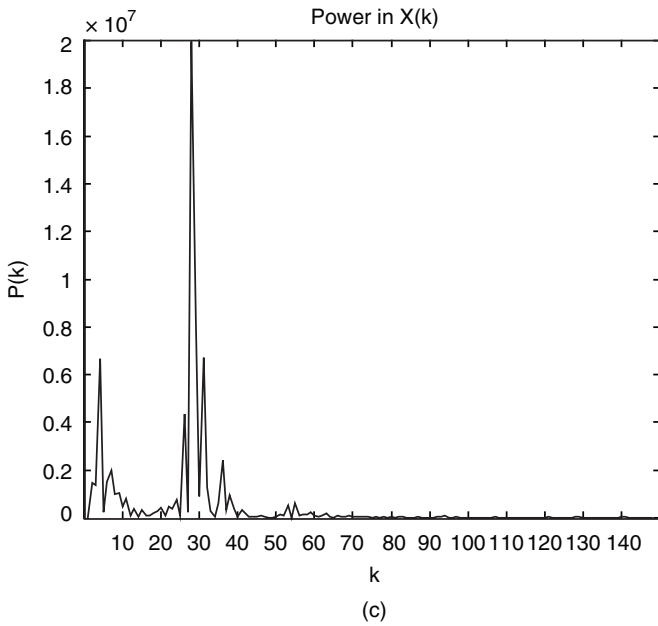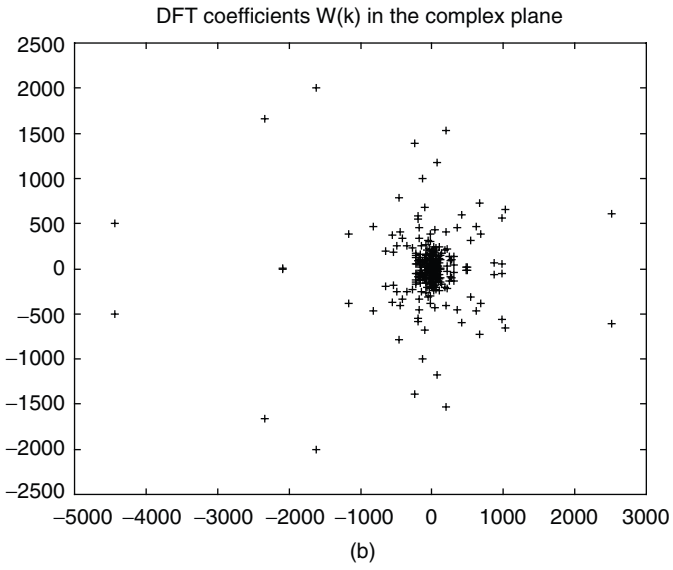
DFT coefficients W(k) in the complex plane

(b)

Power in X(k)

(c)

Fig. 7.3 (*Continued*)

among the lower k values. The frequency resolution of the DFT on $N = 297$ samples, each separated by $T = 1$ year, is $1/NT$. Therefore, the biggest periodic component in the sunspot cycle is k_0/NT cycles/year, and this corresponds to a sunspot period of NT/k_0 years.

This same analysis serves other oscillatory signal analysis applications considered already: electrocardiology, manufactured surface waviness analysis, and tone detection. We will consider its further practical uses, strengths, and weaknesses in Chapter 9.

Note that the theoretical presentation of the DFT proceeds in a completely formal manner. A modest amount of algebra, along with the nice properties of the complex exponential signal, are just enough to develop a complete theory. There are no subtleties concerning discontinuities such as we had to overcome with the analog Fourier series. The discrete nature of the signals and the decomposition of a discrete periodic signal into a finite set of discrete exponentials demand no exotic tools such as distributions or Dirac delta functions. The complex exponential signal's elegance and a little algebra are sufficient to develop the entire theory. We could now prove a bunch of theorems about properties of the DFT. But our goal is develop the tools, the understanding, and the fundamental insights of signal analysis; we should not think to just throw the theory at the reader. Before proceeding to a lengthy list of the DFT's properties, let's explore the links that the DFT shares with the tools we already know for the frequency analysis of analog signals. In particular, we shall show that a discrete signal's DFT coefficients approximate certain of the Fourier series coefficients for an analog periodic source signal.

7.1.2 The DFT's Analog Frequency-Domain Roots

Perhaps the clearest insight into how the discrete Fourier transform reveals the frequency content of a discrete signal is to explore its relationship to the Fourier series for analog periodic signals. We begin by defining a variant of the DFT that takes a form very similar to the analog Fourier series.

Definition (Discrete Fourier Series). Suppose $x(n)$ is a discrete signal and $N > 0$. Then the discrete signal $c(k) = c_k$, defined by

$$c(k) = \frac{1}{N} \sum_{n=0}^{N-1} x(n) \exp\left(\frac{-2\pi jnk}{N}\right) \tag{7.16}$$

where $0 \le k \le N - 1$, is the *discrete Fourier series* (DFS) of $x(n)$ on the interval $[0, N - 1]$. Equation (7.16) is called the DFS *analysis equation* for $x(n)$.

Note that if $x(n)$ has DFT coefficients $X(k)$ and DFS coefficients $c(k)$ on $[0, N - 1]$, then $X(k) = c(k)/N$. Except for the factor N, the DFT and the DFS share an

identical theory. Corresponding to the DFT's synthesis equation, there is a DFS *synthesis equation*:

$$x(n) = \sum_{k=0}^{N-1} c(k) \exp\left(\frac{2\pi jnk}{N}\right),$$ (7.17)

where $c(k)$ are the DFS analysis equation coefficients for $x(n)$ on $[0, N-1]$. Equation (7.17) also defines the inverse discrete Fourier series (IDFS). The two concepts are so similar that in the literature one must pay close attention to the particular form of the definitions of the DFT and DFS.

The next theorem clarifies the relationship between the DFS and the analog Fourier series. This shows that these discrete transforms are in fact simple approximations to the FS coefficients that we know from analog signal frequency theory. We are indeed justified in claiming that the DFS and DFT provide a frequency-domain description of discrete signals.

Theorem (Relation Between DFS and FS). Let $x_a(t)$ be an analog signal with period $T > 0$. Suppose $N > 0$, $\Delta t = T/N$, $F = 1/T$, and $x(n) = x_a(n\Delta t)$ is a discrete signal that samples $x_a(t)$ at intervals Δt. Finally, let $c(k)$ be the kth DFS coefficient (7.16) for $x(n)$, and let $c_a(k)$ is the kth analog Fourier series coefficient for $x_a(t)$ on $[0, T]$. That is,

$$c_a(k) = \frac{1}{T}\int_0^T x(t)e^{-j2\pi kFt}\,dt,$$ (7.18)

where $0 < k < N-1$. Then, $c(k)$ is the trapezoidal rule approximation to the FS integral (7.18) for $c_a(k)$, using the intervals $[0, \Delta t]$, $[\Delta t, 2\Delta t]$, ..., $[(N-1)\Delta t, N\Delta t]$.

Proof: The integrand in (7.18) is complex, but the trapezoidal rule can be applied to both its real and imaginary parts. Suppose we let $y(t) = x_a(t)\exp(-j2\pi kFt)$ be the integrand. Recalling the trapezoidal rule from calculus (Figure 7.4), we can see that a typical trapezoid has a base of width Δt and average height $[y(n\Delta t) + y((n+1)\Delta t)]/2$. In other words, an approximation to $c_a(k)$ is

$$\hat{c}_a(k) = \frac{1}{T}\left\{\left[\left(\frac{y(0\cdot\Delta t)+y(1\cdot\Delta t)}{2}\right)\Delta t + \left(\frac{y(1\cdot\Delta t)+y(2\cdot\Delta t)}{2}\right)\Delta t + \cdots + \left(\frac{y((N-1)\cdot\Delta t)+y(N\cdot\Delta t)}{2}\right)\Delta t\right]\right\}.$$ (7.19)

Collecting terms inside the braces of (7.18) and observing that $y(0) = y(N\Delta t) = y(T)$ gives
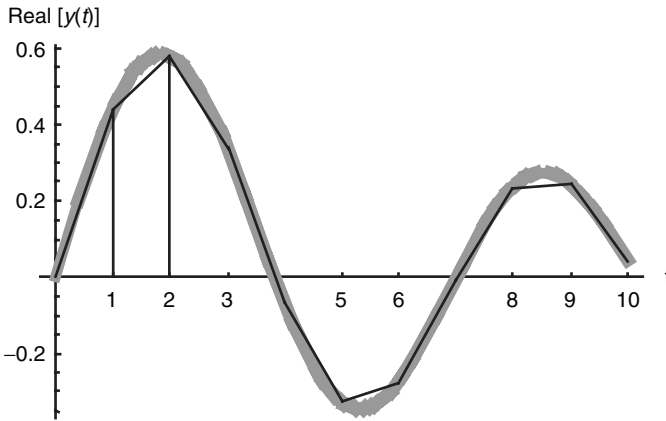
Fig. 7.4. Approximating the Fourier series integral by the trapezoidal rule. The signal $x_a(t)$ has period $T > 0$. The trapezoidal rule applies to the real and imaginary parts of the integrand in the Fourier series analysis equation, $y(t) = x_a(t)\exp(-j2\pi kFt)$. It is necessary to include sufficient trapezoids to span an entire period of the analog signal $x(t)$; in this illustration $T = 10$.

$$\hat{c}_a(k) = \frac{\Delta t}{T} \sum_{n=0}^{N-1} x_a(n\Delta t)\exp(-j2\pi kFn\Delta t) = \frac{1}{N} \sum_{n=0}^{N-1} x(n)\exp\left(\frac{-j2\pi kn}{N}\right) = c(k). \quad (7.20)$$

This shows that the trapezoidal rule approximation to the FS integral is precisely the DFS coefficient $c(k)$ and completes the proof.   ∎

Thus, the DFS is a straightforward approximation of the analog Fourier series components. And the DFT is just the DFS scaled by the period of the discrete signal. Again, these transforms are appropriate for discrete periodic signals. Of course, one may take any discrete signal, $x(n)$, restrict it to a finite interval, $[0, N-1]$, where $N > 0$, and then perform the DFT analysis equation computation for the $x(n)$ values for $0 \le n < N$. The result is N complex numbers, $X(0), X(1), \dots, X(N-1)$. This is like computing the DFT for the periodic extension of $x(n)$. The result of computing the IDFT on $X(0), X(1), \dots, X(N-1)$, is not the original signal $x(n)$; it is $x_p(n) = (1/N)$ $[X(0) + X(1)e^{2\pi jkn/N} + \cdots + X(N-1)e^{2\pi j(N-1)n/N}$, which is periodic with period N. Another transform is necessary for the study of frequency in aperiodic signals—the discrete-time Fourier transform (DTFT). As the DFT is the discrete world's replica of the Fourier series, so the counterpart to Fourier transform for discrete signals is the DTFT. Before considering the aperiodic case, however, let us explain some of the properties of the DFT and how these lead to efficient algorithms for its computation.

7.1.3 Properties

This section explains the many elegant properties of the discrete Fourier transform. Generally speaking, these theorems on linearity, symmetry, and conservation of signal

energy result from the special algebraic characteristics of the complex exponential function. Interesting in themselves, they are useful as well in analyzing signals. As an example, the energy in DFT coefficients does not change as the underlying periodic signal is translated. This property we noted in Chapter 4, and its motivation was our search for a translation-invariant, spatial-frequency-based texture indicator. Our further studies of the properties of DFT, especially its computational symmetries, will lead to the fast Fourier transform (FFT) algorithm. For signals with certain periods— especially powers of two—the FFT offers a dramatic reduction in the computational burden of computing discrete frequency components with the DFT.

Let us begin with some basic properties of the DFT. We have already noted that the DFT of a signal $x(n)$ on $[0, N-1]$, $N > 0$, has period N.

Proposition (Linearity, Time Shift, and Frequency Shift). Let $x(n)$ and $y(n)$ be periodic signals with period $N > 0$, let a and b be constants, and let $X(k)$ and $Y(k)$ be their DFTs, respectively. Then:

(a) (Linearity) The DFT of $ax(n) + by(n)$ is $aX(k) + bY(k)$.

(b) (Time Shift) The DFT of $x(n-m)$ is $(W_N)^{km}X(k)$.

(c) (Frequency Shift) The IDFT of $X(k-m)$ is $(W_N)^{-nm}x(n)$.

In other words, delaying a time-domain signal by m samples is equivalent to multiplying each DFT coefficient in the frequency domain, $X(k)$, by the factor $(W_N)^{km} = e^{-2\pi jkm/N}$. And delaying the frequency-domain signal $X(k)$ by m samples reflects a time-domain multiplication of each value $x(n)$ by $(W_N)^{-nm}$.

Proof: Linearity is easy and left as an exercise. Let $z(n) = x(n-m)$ and let $r = n-m$. Let's apply the DFT analysis equation directly to $z(n)$:

$$Z(k) = \sum_{n=0}^{N-1} z(n)\exp\left(\frac{-j2\pi kn}{N}\right) = \exp\left(\frac{-j2\pi km}{N}\right)\sum_{n=0}^{N-1} x(n-m)\exp\left(\frac{-j2\pi k(n-m)}{N}\right)$$

$$= W_N^{kM}\sum_{n=0}^{N-1} x(n-m)\exp\left(\frac{-j2\pi k(n-m)}{N}\right) = W_N^{kM}\sum_{r=-m}^{N-1-m} x(r)\exp\left(\frac{-j2\pi kr}{N}\right)$$

$$= W_N^{kM}\sum_{r=0}^{N-1} x(r)\exp\left(\frac{-j2\pi kr}{N}\right) = W_N^{kM}X(k). \qquad (7.21)$$

Since $x(r)$ and $\exp(-2\pi jkr/N)$ both have period N, the summation over r in (7.21) may start at any index; in particular, if we start the summation at $r = 0$, we have precisely the DFT analysis formula for $X(k)$. The proof of the frequency shift property is similar and is left as an exercise. ∎

Definition (Discrete Convolution). Let $x(n)$ and $y(n)$ be periodic signals with period $N > 0$. Then the signal $z(n)$ defined by

$$z(n) = \sum_{k=0}^{N-1} x(k)y(n-k) \tag{7.22}$$

is called the *discrete convolution* of x and y: $z = x * y$.

Note that the definition of discrete convolution can be extended to the case where one of the signals (or both) is not periodic. The expression (7.22) is computed for the periodic extension of the signals over $[0, N-1]$. We then have the following theorem that relates convolutions of discrete signals to the termwise products of their DFTs. Although we are working with frequency transforms of a greatly different formal nature, the comparison to the analog Fourier transform's Convolution Theorem is striking.

Theorem (Convolution in Time). Let $x(n)$ and $y(n)$ be periodic signals with period $N > 0$, $X(k)$ and $Y(k)$ their DFTs, and $z(n) = x * y$. Then the DFT of $z(n)$ is $Z(k) = X(k)Y(k)$.

Proof: A direct attack is fruitful. We write out the expression for $Z(k)$ according to the DFT analysis equation, insert the convolution formula for z in terms of x and y, and then separate the terms.

$$Z(k) = \sum_{n=0}^{N-1} z(n)W_N^{kn} = \sum_{n=0}^{N-1} (x * y)(n)W_N^{kn} = \sum_{n=0}^{N-1} \left(\sum_{m=0}^{N-1} x(m)y(n-m) \right) W_N^{kn}. \tag{7.23}$$

Interchanging the order of summation in (7.23) is the key step. This permits us to collect m-summation terms associated with x and n-summation terms associated with y together and expose the product of their DFTs.

$$Z(k) = \sum_{m=0}^{N-1} \sum_{n=0}^{N-1} x(m)y(n-m)W_N^{kn} = \sum_{m=0}^{N-1} x(m) \sum_{n=0}^{N-1} y(n-m)W_N^{kn}$$

$$= \sum_{m=0}^{N-1} x(m)W_N^{km} \sum_{n=0}^{N-1} y(n-m)W_N^{k(n-m)} = \sum_{m=0}^{N-1} x(m)W_N^{km} \sum_{r=0}^{N-1} y(r)W_N^{kr} = X(k)Y(k). \tag{7.24}$$

We let $r = n - m$ for a change of summation variable in the penultimate summation of (7.24). Since $y(n)$ is periodic with period N, the summation from $r = -m$ to $N - 1 - m$ is the same as the summation from $r = 0$ to $N - 1$. ∎

Theorem (Convolution in Frequency). That is, let $x(n)$ and $y(n)$ be periodic signals with period $N > 0$; let $X(k)$ and $Y(k)$ be their DFTs, and let $z(n) = x(n)y(n)$ be the termwise product of x and y. Then the DFT of $z(n)$ is $Z(k) = (1/N)X(k) * Y(k)$, where $X(k) * Y(k)$ is the discrete convolution of $X(k)$ and $Y(k)$.

Proof: Similar to the Convolution in Time Theorem. ∎

Proposition (Symmetry). Let signal $x(n)$ have period $N>0$ and $X(k)$ be its DFT. Then:

(a) The DFT of $x^*(n)$, the complex conjugate of $x(n)$, is $X^*(N-k)$, and the DFT of $x^*(N-n) = x^*(-n)$ is $X^*(k)$.

(b) The DFT of $x_e(n) = (1/2)(x(n) + x^*(N-n))$, the even part of $x(n)$, is $\text{Re}[X(k)]$, the real part of $X(k)$.

(c) The DFT of $x_o(n) = (1/2)(x(n) - x^*(N-n))$, the odd part of $x(n)$, is $j\text{Im}[X(k)]$, where $\text{Im}[X(k)]$ is the imaginary part of $X(k)$.

(d) The DFT of $\text{Re}[x(n)]$ is $X_e(k) = (1/2)(X(k) + X^*(N-k))$, the even part of $X(k)$.

(e) The DFT of $j\text{Im}[x(n)]$ is $X_o(k) = (1/2)(X(k) - X^*(N-k))$, the odd part of $X(k)$.

Proof: Easy. ∎

Proposition (Real Signals). Let signal $x(n)$ be real-valued with period $N > 0$, and let $X(k)$ be its DFT. Then:

(a) $X(k) = X^*(N-k)$.

(b) The DFT of $x_e(n)$ is $\text{Re}[X(k)]$.

(c) The DFT of $x_o(n)$ is $j\text{Im}[X(k)]$.

Proof: Also easy. ∎

Theorem (Parseval's). Let $x(n)$ have period $N > 0$ and let $X(k)$ be its DFT. Then

$$\sum_{m=0}^{N-1} x(n)\overline{x}(n) = \frac{1}{N} \sum_{k=0}^{N-1} X(k)\overline{X}(k). \tag{7.25}$$

Proof: Although it seems to lead into a messy triple summation, here again a stubborn computation of the frequency-domain energy for $X(k)$ on the interval $[0, N-1]$ bears fruit. Indeed,

$$\sum_{k=0}^{N-1} X(k)\overline{X}(k) = \sum_{k=0}^{N-1}\left(\sum_{m=0}^{N-1} x(m)W_N^{km} \overline{\sum_{n=0}^{N-1} x(n)W_N^{kn}}\right)$$

$$= \sum_{k=0}^{N-1}\left(\sum_{m=0}^{N-1} x(m)W_N^{km} \left(\sum_{n=0}^{N-1} \overline{x(n)}\,\overline{W_N^{kn}}\right)\right)$$

$$= \sum_{k=0}^{N-1}\sum_{m=0}^{N-1}\sum_{n=0}^{N-1} x(m)\overline{x(n)}W_N^{k(m-n)}$$

$$= \sum_{m=0}^{N-1}\sum_{n=0}^{N-1} x(m)\overline{x(n)} \sum_{k=0}^{N-1} W_N^{k(m-n)}. \tag{7.26}$$

The last summation at the bottom in (7.26) contains a familiar expression: the partial geometric series in $(W_N)^{m-n}$ of length N. Recall from the lemma within the proof of the DFT Inverse Theorem (Section 7.1.1.1) that this term is either N or 0, according to whether $m = n$ or not, respectively. Thus, the only products $x(m)x^*(n)$ that will contribute to the triple sum in (7.26) are those where $m = n$, and these are scaled by the factor N. Therefore,

$$\sum_{k=0}^{N-1} X(k)\overline{X}(k) = \sum_{m=0}^{N-1}\sum_{n=0}^{N-1} x(m)\overline{x(n)} \sum_{k=0}^{N-1} W_N^{k(m-n)} = N \sum_{n=0}^{N-1} x(n)\overline{x(n)}, \qquad (7.27)$$

and the proof is complete.   ∎

We have explored some of the theory of the DFT, noted its specific relation to the analog Fourier series, and considered its application for finding the significant periodicities in naturally occurring signals. In particular, we presented an example that uncovered the period of the sunspot cycle by taking the DFT of the discrete signal giving Wolf sunspot numbers over several centuries. We know from Chapter 4's attempts to analyze signals containing significant periodicities (textures, speech, tone detection, and the like) that pure time-domain methods—such as statistical approaches—can prove quite awkward. We do need the DFT for computer implementation, and the next section explores, therefore, the efficient computation of the DFT on digital computers.

7.1.4 Fast Fourier Transform

The fast Fourier transform (FFT) has been known, it turns out, since the time of Gauss.[3] Only recently, however, has it been widely recognized and utilized in signal processing and analysis. Indeed, its original rediscovery in the 1960s marks the beginning of an era in which digital methods supplanted analog methods in signal theory and applications.

7.1.4.1 Computational Cost.

Let us begin by studying the computational costs incurred in the DFT analysis and synthesis equations. Clearly, if the time-domain signal, $x(n)$ on $[0, N - 1]$, is complex-valued, then the operations are nearly identical. The IDFT computation requires an additional multiplication of a complex value by the factor $(1/N)$, as an inspection of the equations shows:

$$X(k) = \sum_{n=0}^{N-1} x(n)\exp\left(\frac{-2\pi jnk}{N}\right) = \sum_{n=0}^{N-1} x(n)W_N^{nk}, \qquad (7.28a)$$

$$x(n) = \frac{1}{N}\sum_{k=0}^{N-1} X(k)\exp\left(\frac{2\pi jnk}{N}\right) = \frac{1}{N}\sum_{k=0}^{N-1} X(k)W_N^{-nk}. \qquad (7.28b)$$

---

[3]Gauss, writing in a medieval form of Latin, made progress toward the algorithm in his notebooks of 1805. [M. T. Heideman, D. H. Johnson, and C. S. Burrus, 'Gauss and the history of the fast Fourier transform,' *IEEE ASSP Magazine*, vol. 1, no. 4, pp. 14–21, October 1984.]

But the principal computational burden lies in computing the complex sum of complex products in (7.28a) and (7.28b).

Consider the computation of $X(k)$ in (7.28a). For $0 \leq k \leq N - 1$, the calculation of $X(k)$ in (7.28a) requires N complex multiplications and $N - 1$ complex sums. Computing all N of the $X(k)$ values demands N^2 complex multiplications and $N^2 - N$ complex additions. Digital computers implement complex arithmetic as floating point operations on pairs of floating point values. Each complex multiplication, therefore, requires four floating point multiplications and two floating point additions; and each complex addition requires two floating point additions. So the total floating point computation of an N-point FFT computation costs $4N^2$ multiplications and $2(N^2 - N) + 2N^2$ additions. Other factors to consider in an FFT implementation are:

- Storage space and memory access time for the $x(n)$ and $X(k)$ coefficients;
- Storage space and memory access time for the $(W_N)^{kn}$ values;
- Loop counting and termination checking overheads.

Ultimately, as N becomes large, however, the number of floating point additions and multiplications weighs most significantly on the time to finish the analysis equation. Since the number of such operations—whether they are complex operations or floating point (real) operations—is proportional to N^2, we deem the DFT an order-N^2, or $O(N^2)$ operation.

FFT algorithms economize on floating point operations by eliminating duplicate steps in the DFT and IDFT computations. Two properties of the phase factor, W_N, reveal the redundancies in the complex sums of complex products (7.28a) and (7.28b) and make this reduction in steps possible:

- Phase factor periodicity: $(W_N)^{kn} = (W_N)^{k(n + N)}$;
- *Phase factor symmetry:* $[(W_N)^{kn}]^* = (W_N)^{k(N - n)}$.

Two fundamental approaches are decimation-in-time and decimation-in-frequency.

7.1.4.2 *Decimation-in-Time.* Decimation-in-time FFT algorithms reduce the DFT into a succession of smaller and smaller DFT analysis equation calculations. This works best when $N = 2^p$ for some $p \in \mathbb{Z}$. The N-point DFT computation resolves into two $(N/2)$-point, each of which resolves into two $(N/4)$-point DFTs, and so on.

Consider, then, separating the computation of $X(k)$ in (7.28a) into even and odd n within $[0, N - 1]$:

$$X(k) = \sum_{m=0}^{(N/2)-1} x(2m)W_N^{2km} + \sum_{m=0}^{(N/2)-1} x(2m+1)W_N^{(2m+1)k}$$

$$= \sum_{m=0}^{(N/2)-1} x(2m)W_N^{2km} + W_N^k \sum_{m=0}^{(N/2)-1} x(2m+1)W_N^{2km} \qquad (7.29)$$

Note the common $(W_N)^{2km}$ phase factor in both terms on the bottom of (7.29). This leads to the key idea for the DFT's time-domain decimation:

$$W_N^2 = \exp\left(\frac{-2\pi j}{N}\right)^2 = \exp\left(\frac{-4\pi j}{N}\right) = \exp\left(\frac{-2\pi j}{N/2}\right) = W_{\left(\frac{N}{2}\right)}. \tag{7.30}$$

We set $y(m) = x(2m)$ and $z(m) = x(2m + 1)$. Then $y(m)$ and $z(m)$ both have period $N/2$. Also, (7.30) allows us to write (7.29) as a sum of the $N/2$-point DFTs of $y(m)$ and $z(m)$:

$$X(k) = \sum_{m=0}^{(N/2)-1} y(m)W_{\left(\frac{N}{2}\right)}^{km} + W_N^k \sum_{m=0}^{(N/2)-1} z(m)W_{\left(\frac{N}{2}\right)}^{km} = Y(k) + W_N^k Z(k). \tag{7.31}$$

From (7.31) it is clear that an N-point DFT is the computational equivalent of two $N/2$-point DFTs, plus $N/2$ complex multiplications, plus $N/2$ complex additions. Figure 7.5 illustrates the process of decomposing an 8-point DFT into two 4-point DFTs.

Does this constitute a reduction in computational complexity? The total cost in complex operations is therefore $2(N/2)^2 + 2(N/2) = N + N^2/2$ complex operations. For large N, the $N^2/2$ term, representing the DFT calculations, dominates. But the division by two is important! Splitting the $Y(k)$ and $Z(k)$ computations in the same way reduces the computation of the two DFTs to four $N/4$-point DFTs, plus $2(N/4)$ complex multiplications, plus $2(N/4)$ complex additions. The grand total cost
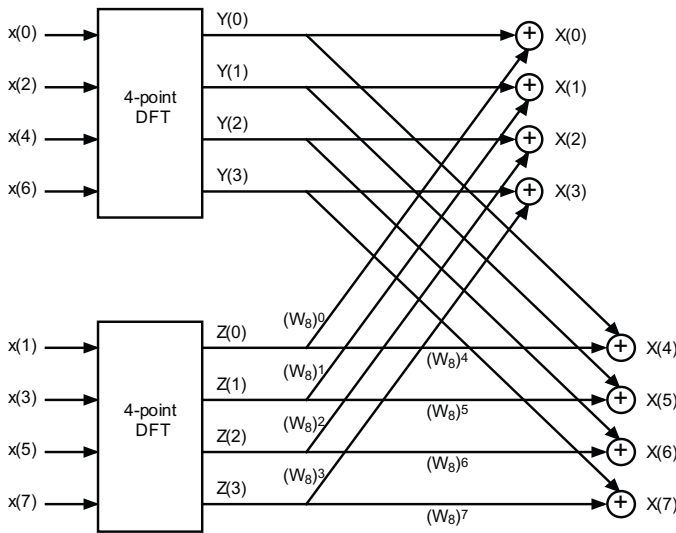
Fig. 7.5. The time domain decimation of an 8-point DFT. An 8-point analysis problem decomposes into two preliminary 4-point problems, followed by a scalar multiplication and a summation. This is only the first stage, but it effectively halves the number of complex operations necessary for computing the DFT of $x(n)$ on $[0, 7]$.
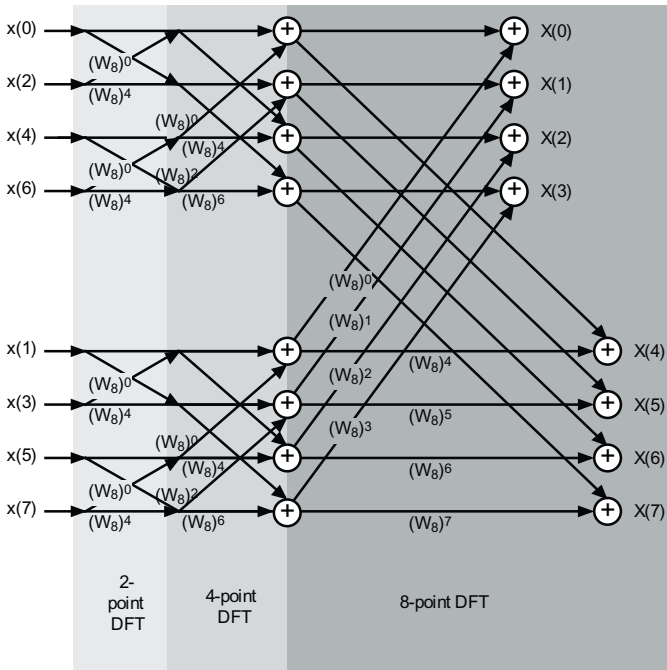
Fig. 7.6. Fully decimated 8-point DFT. Further decomposition steps expose an elementary operation that recurs throughout the computation. Notice also that the original data elements must be sorted in bit-reversed order at the beginning of the algorithm. Binary index numbers are used; that is, $x(000)$ is followed by $x(100)$, instead of $x(001)$, with which it swaps places. Next comes $x(010)$, since its bit-reversed index stays the same. But the next signal value must be $x(110)$, which swaps places with $x(011)$. This computational trick allows the in-place computation of DFT coefficients.

$N + [N + 4(N/4)^2] = N + N + N^2/4 = 2N + N^2/4$. The next iteration trims the cost to $3N + N^2/8$. And this can continue as long as N contains factors of two—$\log_2 N$ times. Thus, the fully executed decimation-in-time reduces the computational burden of an N-point DFT from $O(N^2)$ to $O(N\log_2 N)$.

Figure 7.6 illustrates the process of decomposing an 8-point DFT down to the final 2-point problem.

It turns out that a single basic operation underlies the entire FFT algorithm. Consider the 8-point problem in Figure 7.6. It contains three DFT computation stages. Four two-point problems comprise the first stage. Let us examine the structure of the first stage's operation. Pairs of the original signal elements are multiplied by either $(W_8)^0 = 1$ or $(W_8)^4 = -1$, as shown in Figure 7.7a. Thereafter, pairs of the two-point DFT coefficients are similarly multiplied by either of two possible powers of W_8: $(W_8)^0 = 1$ or $(W_8)^4 = -1$ again, or, $(W_8)^2$ and $(W_8)^6$.
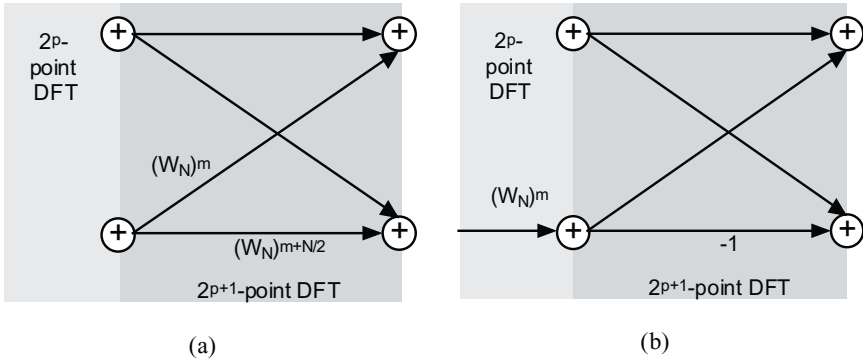
Fig. 7.7. (a), The butterfly operation or its equivalent, simpler form (b), occurs throughout the FFT computation.

Indeed, at any of the later stages of computation, the multiplying phase factors always assume the form $(W_8)^m$ and $(W_8)^{m+4}$. Because their ratio is $(W_8)^{m+4-m} = (W_8)^4 = -1$, we may further simplify the rudimentary operation (Figure 7.7b), eliminating one complex multiplication. The resulting crisscross operation is called a butterfly, which the flow graph vaguely resembles. Some aesthetically pleasing term does seem appropriate: The butterfly operation reveals an elegant structure to the DFT operation, and the algorithms in Section 7.1.4.4 make efficient use of this elegance.

Now let us consider the rearrangement of the original signal values $x(0)$, $x(1)$, $x(2)$, $x(3)$, $x(4)$, $x(5)$, $x(6)$, $x(7)$ into the proper order for the four initial butterflies: $x(0)$, $x(4)$, $x(2)$, $x(6)$, $x(1)$, $x(5)$, $x(3)$, $x(7)$. This represents a bit-reversed reading of the indices of the data, because we observe that if the indices of the signal values are written in binary form, that is, $x(0) = x(000)$, $x(1) = x(001)$, and so on, then the necessary rearrangement comes from reading the binary indices backwards: $x(000)$, $x(100)$, $x(010)$, $x(110)$, $x(001)$, $x(101)$, $x(011)$, $x(111)$. At each of the three stages of the computation, we maintain eight complex values, beginning with the original signal data in bit-reversed order. Then we perform butterfly operations, with the index difference between value pairs doubling at each stage.

Now let us consider another approach to the efficient computation of the DFT by splitting the frequency domain values $X(k)$ into smaller and smaller groups.

7.1.4.3 *Decimation-in-Frequency.* Suppose again that we are faced with the problem of computing the DFT coefficients $X(k)$ for a signal $x(n)$ on $[0, N-1]$. In the previous section, we split the DFT analysis equation sum over $0 \leq n \leq N-1$ into two sums: for n even and for n odd. Now we divide the frequency-domain values $X(k)$ for $0 \leq k \leq N-1$ into even k and odd k. The result is an alternative, efficient algorithm for computing DFT coefficients called the decimation-in-frequency FFT.

Again, suppose that N is a power of 2, and let us consider DFT coefficients $X(k)$ where $k = 2m$. We have

$$X(2m) = \sum_{n=0}^{N-1} x(n)W_N^{2mn} = \sum_{n=0}^{(N/2)-1} x(n)W_N^{2mn} + \sum_{n=N/2}^{N-1} x(n)W_N^{2mn}$$

$$= \sum_{n=0}^{(N/2)-1} x(n)W_N^{2mn} + \sum_{n=0}^{(N/2)-1} x\left(n+\frac{N}{2}\right)W_N^{2m(n+\frac{N}{2})} \tag{7.32}$$

Not unexpectedly, phase factor properties fortuitously apply. We observe that $(W_N)^{2m(n+N/2)} = (W_N)^{2mn}(W_N)^{mN} = (W_N)^{2mn}(W_{N/2})^{mn}$. Hence, for $0 \le m < N/2$, we have

$$X(2m) = \sum_{n=0}^{(N/2)-1} x(n)W_N^{2mn} + \sum_{n=0}^{(N/2)-1} x\left(n+\frac{N}{2}\right)W_N^{2m(n+\frac{N}{2})}$$

$$= \sum_{n=0}^{(N/2)-1} x(n)W_{N/2}^{mn} + \sum_{n=0}^{(N/2)-1} x\left(n+\frac{N}{2}\right)W_{N/2}^{2mn}$$

$$= \sum_{n=0}^{(N/2)-1} \left[x(n) + x\left(n+\frac{N}{2}\right) \right] W_{N/2}^{2mn}. \tag{7.33}$$

This last result shows that the $X(k)$ coefficients, for k even, can be calculated by an $(N/2)$-point DFT. Turning to the remaining $X(k)$, for $k = 2m + 1$ odd, we find

$$X(2m+1) = \sum_{n=0}^{(N/2)-1} x(n)W_N^{(2m+1)n} + \sum_{n=N/2}^{N-1} x(n)W_N^{(2m+1)n}$$

$$= \sum_{n=0}^{(N/2)-1} x(n)W_N^{(2m+1)n} + \sum_{n=0}^{(N/2)-1} x\left(n+\frac{N}{2}\right)W_N^{(2m+1)(n+N/2)}$$

$$= \sum_{n=0}^{(N/2)-1} x(n)W_N^{(2m+1)n} + W_N^{(2m+1)(N/2)} \sum_{n=0}^{(N/2)-1} x\left(n+\frac{N}{2}\right)W_N^{(2m+1)n}$$

$$\tag{7.34}$$

Now it is time to invoke the phase factor properties: $(W_N)^{(2m+1)(n+N/2)} = (W_N)^{2mn}(W_N)^{m(N/2)} = -1$. Therefore, (7.34) simplifies to

$$X(2m+1) = \sum_{n=0}^{(N/2)-1} x(n)W_N^{(2m+1)n} - \sum_{n=0}^{(N/2)-1} x\left(n+\frac{N}{2}\right)W_N^{(2m+1)n}$$

$$= \sum_{n=0}^{(N/2)-1}\left[x(n)-x\left(n+\frac{N}{2}\right)\right]W_N^{(2m+1)n}$$

$$= \sum_{n=0}^{(N/2)-1}\left[x(n)-x\left(n+\frac{N}{2}\right)\right]W_N^{2mn}W_N^{n}$$

$$= \sum_{n=0}^{(N/2)-1}\left[x(n)-x\left(n+\frac{N}{2}\right)\right]W_{N/2}^{mn}W_N^{n}$$

$$= \sum_{n=0}^{(N/2)-1}\left[W_N^{n}\left\{x(n)-x\left(n+\frac{N}{2}\right)\right\}\right]W_{N/2}^{mn}. \tag{7.35}$$

This shows that we can calculate $X(k)$ for k odd by an $(N/2)$-point DFT of the complex signal $y(n) = (W_N)^n[x(n) - x(n + (N/2))]$. Together (7.33) and (7.35) demonstrate that an N-point DFT computation can be replaced by two $(N/2)$-point DFT computations. As in the decimation-in-time strategy, we can iterate this divide-and-compute strategy as many times as N is divisible by two. The decimation-in-frequency result is an $O(N\log_2 N)$ algorithm too.

7.1.4.4 *Implementation.* This section considers FFT implementation in a modern high-level language, C++, and in assembly language on a representative digital signal processor, the Motorola 56000/56001.

Let's examine a C++ implementation of a radix-2 decimation-in-time algorithm, drawn from a classic FORTRAN coding of the FFT [4]. This algorithm uses the new standard template library contained in the header file <complex>. It replaces the traditional C++ complex arithmentic library, <complex.h>, which defines complex numbers as instances of a class whose member variables are two double-precision floating point numbers. The new template library allows us to construct complex numbers using the C++ float data type, for example, by declaring:

```
complex<float> x;
```

Specifying the `float` data type in the template conserves memory space.

Figure 7.8 shows the C++ implementation of the FFT.

Most references present FFT algorithms in FORTRAN [6–8], but also in C [9, 10]. The FFT can be implemented on a special computer architecture—called a shuffle-exchange network—that interconnects multiple processors in a manner similar to the FFT's butterfly flow diagram. This facilitates either the butterfly operation or the bit-reversed ordering of data, but not both at once, because interprocessor communication bottlenecks occur. Nevertheless, it is still possible to improve the FFT algorithm by an additional $O(N^{1/2})$ [11].

```
#include <math.h>
#include <stdlib.h>
#define PI 3.14159265358979
#include <use_ansi.h>
#include <complex>        //ISO/ANSI std template library
using namespace std;
int fft(complex<double> *x, int nu)
{ // sanity check to begin with:
  if (x == NULL || nu <= 0)
    return 0;
  int N = 1 << nu;            //N=2**nu
  int halfN = N >> 1;         //N/2
  complex<double> temp, u, v;
  int i, j, k;
  for (i = 1, j = 1; i < N; I++){  //bit-reversing data:
    if (i < j){ temp = x[j-1]; x[j-1] = x[i-1]; x[i-1] = temp;}
    k = halfN;
    while (k < j){j -= k; k >>= 1;}
    j += k;
  }
  int mu, M, halfM, ip;
  double omega;
  for (mu = 1; mu <= nu; mu++) {
    M = 1 << mu;        // M = 2**mu
    halfM = M >> 1;     // M/2
    u = complex<double>(1.0, 0.0);
    omega = PI/(double)halfM;
    w = complex<double>(cos(omega), -sin(omega));
    for (j = 0; j < halfM;j++){
      for (i = j; i < N; i += M){
        ip = i + halfM;
        temp = x[ip]*u;
        x[ip] = x[i] - temp;
        x[i] += temp;
      }
      u  * = w;
    }
    u  * = w;
  }
  return 1;
}
```

Fig. 7.8. A C++ implementation of the FFT. This algorithm uses the complex data type in the ISO/ANSI standard template library [5].

```
;Radix-2 decimation in time FFT macro call
fftr2a    macro points, data, coeff
          move #points/2, n0
          move #1,n2
          move #points/4, n6
          move #-1,m0
          move m0,m1
          move m0,m4
          move m0,m5
          move #0,m6              ; addr mod for bit-rev addr
          do   #@cvi (@log (points)/@log(2)+0.5),_end_pass
          move #data,r0
          move r0,r4
          lua  (r0)+n0,r1
          move #coef,r6
          lua  (r1)-,r5
          move n0,n1
          move n0,n4
          move n0,n5
          do   n2,_end_grp
          move x:(r1),x1    y:(r6),y0  ;sin and cos tables
          move x:(r5),a     y:(r6),b   ;load data values
          move x:(r6)+n6,x0
          do   n0,_end_bfy
          mac  x1,y0,b      y:(r1)+,y1 ;decim in time begins
          macr -x0,y1,b     a:x:(r5)+  y:(r0),a
          subl b,a          x:(r0),b   b,y: (r4)
          mac  -x1,x0,b     x:(r0)+,a  a,y: (r5)
          macr -y1,y0,b     x:(r1),x1
          subl b,a          b,x:(r4)+  y:(r0),b
_end_bfy
          move a,x:(r5)+n5      y:(r1)+n1,y1
          move x:(r0)+n0,x1    y:(r1)+n1,y1
_end_grp
          move n0,b1              ; div bfys/group by 2
          lsr  b            n2,a1
          lsl  a            b1,n0
          move a1,n2
_end_pass
          endm
```

Fig. 7.9. An Assembly language implementation of the FFT on the Motorola 56001 DSP chip [12]. The *X* and *Y* memory banks contain the input data's real and imaginary components, respectively. The *X* and *Y* memory banks also hold the cosine and sine tables for the exponential function implementation. The algorithm bit-reverses the output data stream.

It is interesting to examine the implementation of the FFT on a DSP processor (Figure 7.9). Let us now briefly describe some architectural features of this processor that support the implementation of digital signal processing algorithms. These features include:

- Multiple memory areas (*X* and *Y*) and data paths for two sets of signal data.
- No-overhead loop counting.
- A multiply-accumulate operation that runs in parallel with *X* and *Y* data movements.
- Built-in sine and cosine tables (in the case of the 56001) to avoid trigonometric function library calls.
- Addressing modes that support memory indexing needed for convolution operations.

The FFT code in Figure 7.9 explois these processing features for a compact implementation of decimation-in-time algorithm.

There are also FFT algorithms for $N \neq 2^n$. These general radix algorithms are more complicated, consume more memory space, and are less speedy than the dyadic decimation-in-time and decimation-in-frequency computations. Nevertheless, they are superior to the DFT and useful when the success of an application depends on fast frequency component computations. Another method, Goertzal's algorithm, uses a convolutional representation of the DFT's analysis equation as the basis for a fast computation. This algorithm is attractive for digital signal processors, because of their special hardware. Some of the exercises explore these FFT algorithms.

7.2 DISCRETE-TIME FOURIER TRANSFORM

In our study of signals and their frequency-domain representations, we have yet to cover one possibility: the class of discrete aperiodic signals. The frequency transform tool that applies to this case is the discrete-time Fourier transform (DTFT). It turns out that not all aperiodic discrete signals have DTFTs. We demonstrate that the transform exists for the important classes of absolutely summable and square-summable signals.

There is a generalization of the DTFT—the *z*-transform—which provides additional analytical capabilities suitable for those signals for which there is no DTFT. We cover the *z*-transform in Chapter 8. Chapter 9 explains a variety of applications of both the DTFT and the *z*-transform.

7.2.1 Introduction

We start the discussion with a formal definition—the mathematician's style at work once again. The definition involves an infinite sum, and so, as with the Fourier transform's infinite integral, for a given signal there are questions of the validity of the transform operation. We momentarily set these concerns aside to review a few examples. Then we turn to the important question of when the DTFT sum converges

and prove an inversion result. The DTFT is an important theoretical tool, since it provides the frequency domain characterization of discrete signals from the most important signal spaces we know from Chapter 2: the absolutely summable (l^1) signals and the square summable (l^2) signals.

7.2.1.1   *Definition and Examples.*

Let us begin with the abstract definition of the DTFT and follow it with some simple examples. These provide some indication of the transform's nature and make the subsequent theorems more intuitive. The DTFT's definition does involve an infinite sum; for a given signal, therefore, we must eventually provide answers to existential questions about this operation.

Definition (Discrete-Time Fourier Transform). If $x(n)$ is a discrete signal, then the analog signal discrete signal $X(\omega)$ defined by

$$X(\omega) = \sum_{n=-\infty}^{+\infty} x(n)\exp(-jn\omega), \tag{7.36}$$

where $\omega \in \mathbb{R}$, is the *radial discrete-time Fourier transform* (DTFT) of $x(n)$. The units of ω are radians/second. We often refer to (7.36) as the DTFT analysis equation for $x(n)$. If we take $\omega = 2\pi f$, then we can define the (Hertz) DTFT also:

$$X(f) = \sum_{n=-\infty}^{+\infty} x(n)\exp(-j2\pi nf). \tag{7.37}$$

Generally, here, and in most texts, the DTFT takes the form (7.36) and, unless otherwise specified, we use the radial form of the transform.

Like the analog Fourier series, the DTFT is a transform that knows not what world it belongs in. The Fourier series, we recall from Chapter 4, transforms a periodic analog signal, $x(t)$, into a discrete signal: the Fourier coefficients $c(k) = c_k$. And the DTFT maps a discrete signal, $x(n)$, to an analog signal, $X(\omega)$. This prevents the FS and the DTFT from being considered bona fide systems. Both the Fourier transform and the DFT, however, can be viewed as systems. The FT maps analog signals to analog signals, and it may be considered a partial function on the class of analog signals. We know from Chapter 4's study of the FT that the absolutely integrable (L^1) signals, for example, are in the domain of the the FT system. Also, the DFT maps discrete signals of period N to discrete signals of period N. We surmise (rightly, it turns out) that, owing to the doubly infinite sum in the analysis equation, the study of the DTFT will involve much more mathematical subtlety than the DFT.

Clearly, the DTFT sum exists whenever the signal $x(n)$ is finitely supported; that is, it is zero outside some finite interval. So for a wide—and important—class of signals, the DTFT exists. Without worrying right now about the convergence of the analysis equation (7.36) for general signals, we proceed to some examples of the radial DTFT.

Example (Discrete Delta Signal). Consider the signal $\delta(n)$, the discrete delta function. This signal is unity at $n = 0$, and it is zero for $n \neq 0$. For any $\omega \in \mathbb{R}$, all of the summands in (7.36) are zero, save the $n = 0$ term, and so we have $X(\omega) = 1$ for all $\omega \in \mathbb{R}$.

Example (Discrete Square Pulse). Consider the signal $h(n) = [1, 1, \underline{1}, 1, 1]$, which is unity for $-2 \leq n \leq 2$ and zero otherwise. We recognize this signal as the impulse response of a Moving Average System. If $y = Hx = h * x$, then the system H averages the five values around $x(n)$ to produce $y(n)$. We calculate

$$H(\omega) = \sum_{n=-\infty}^{+\infty} h(n)\exp(-jn\omega) = \sum_{n=-2}^{+2} \exp(-jn\omega)$$

$$= e^{2j\omega} + e^{j\omega} + 1 + e^{-j\omega} + e^{-2j\omega} = 1 + 2\cos(\omega) + 2\cos(2\omega). \tag{7.38}$$

The notation might cause confusion, but we will use $H(\omega)$ for the DTFT of discrete signal $h(n)$ and simply H for the system with impulse response $h(n)$. Figure 7.10 plots $H(\omega)$.

**Example (Exponential Signal).** Consider the signal $x(n) = 2^{-n}u(n)$, and its DTFT analysis equation,
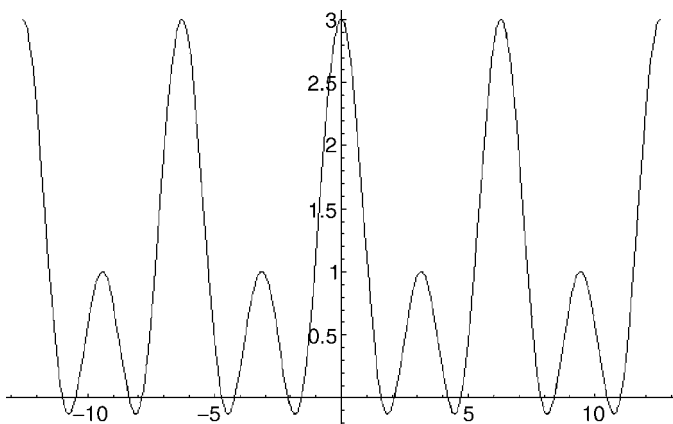
Fig. 7.10. Graph of $H(\omega)$ where $h(n) = [1, 1, \underline{1}, 1, 1]$. $H(\omega)$ is a 2π-periodic analog signal, and it assumes a maximum value at $\omega = 0$. In general, $H(\omega)$ is complex, and in such cases we prefer to plot $|H(\omega)|$ and $\arg(H(\omega))$ on one period: $[0, 2\pi]$ or $[-\pi, \pi]$.

$$X(\omega) = \sum_{n=-\infty}^{+\infty} x(n)\exp(-jn\omega) = \sum_{n=0}^{+\infty}\left(\frac{1}{2}\right)^n \exp(-jn\omega) = \sum_{n=0}^{+\infty}\left(\frac{e^{-j\omega}}{2}\right)^n$$

$$= \frac{1}{1-\left(\dfrac{e^{-j\omega}}{2}\right)} = \frac{1}{1-\dfrac{\cos(\omega)}{2}+j\dfrac{\sin(\omega)}{2}} = \frac{1-\dfrac{\cos(\omega)}{2}-j\dfrac{\sin(\omega)}{2}}{\left(1-\dfrac{\cos(\omega)}{2}\right)^2+\left(\dfrac{\sin(\omega)}{2}\right)^2}. \qquad (7.39)$$

Signal $x(n)$ is a geometric series of the form $1 + a + a^2 + \cdots$, where $a = (1/2)\exp(-j\omega)$. Since $|a| = 1/2 < 1$, the step from an infinite sum to the simple quotient $1/(1 - a)$ on the bottom left side of (7.39) is justified. Figure 7.11 shows the magnitude and phase of the DTFT of $x(n)$.

Notice that the DTFT (7.36) appears to be in the form of an l^2 inner product. Given $x(n)$, we can informally write $X(\omega) = \langle x(n), \exp(j\omega n)\rangle$, because the l^2 inner
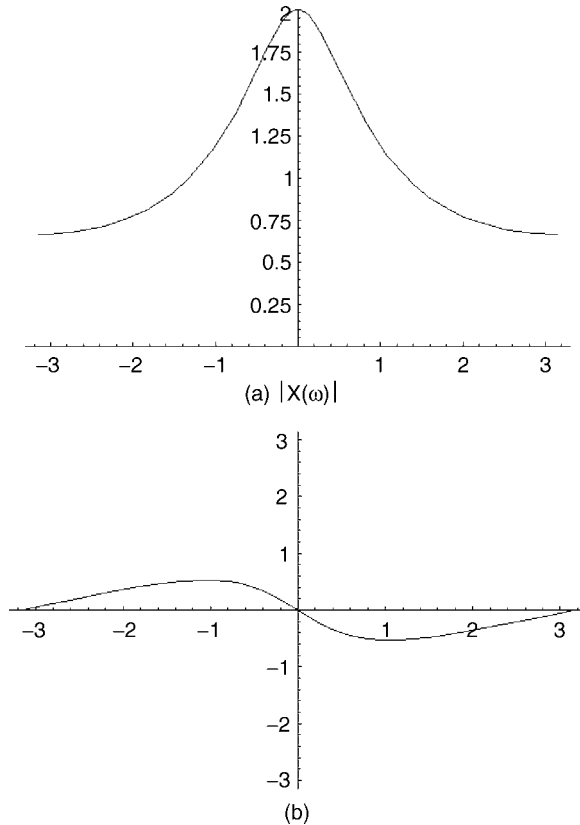
Fig. 7.11. DTFT of $x(n) = 2^{-n}u(n)$. Panel (a) shows $|X(\omega)|$ on $[-\pi, \pi]$. Panel (b) plots $\arg(X(\omega))$.

product, like the DTFT analysis equation, is precisely the sum of all products of terms $x(n)\exp(-j\omega n)$. Conceptually (and still informally), then, for each ω the DTFT $X(\omega)$ measures the similarity between $x(n)$ and $\exp(j\omega n)$. So $X(\omega)$ is the spectral content of the discrete signal $x(n)$ for radial frequency ω. We cannot formalize this intuition unless we know more about the convergence of the analysis equation sum. The signal $\exp(j\omega n)$ is not square-summable, so we do not know, without more investigation, whether the inner product-like sum converges. The convergence of the DTFT analysis equation is a question that we must therefore address, and fortunately, there are satisfactory answers.

7.2.1.2   *Existence.* Let us consider two of the most important classes of discrete signals: absolutely-summable signals and square-summable signals. Do representatives of these function spaces always have discrete-time Fourier transforms? Guaranteeing a transform for l^2 signals, like the case of the analog L^2 Fourier transforms in Chapter 5, requires some care. There is, however, a very easy existence proof for the DTFT of l^1 signals.

Theorem (DTFT Existence for Absolutely Summable Signals). Suppose $x(n) \in l^1$. Then the DTFT of $x(n)$, $X(\omega)$, exists and converges absolutely and uniformly for all $\omega \in \mathbb{R}$.

Proof: To show absolute convergence of the analysis equation, we need to show that

$$\sum_{n=-\infty}^{+\infty} \left| x(n)\exp(-jn\omega) \right| = \sum_{n=-\infty}^{+\infty} |x(n)|\left|\exp(-jn\omega)\right| = \sum_{n=-\infty}^{+\infty} |x(n)| < \infty. \qquad (7.40)$$

But the last term in (7.40) is precisely the l^1 norm of $x(n)$, and this must be finite, since $x(n) \in l^1$. So the analysis equation formula for $X(\omega)$ does indeed converge to a limit for any ω. We recall from real and complex analysis [13, 14] that the uniform convergence of the series (7.36), means that for every $\varepsilon > 0$ there is an $N > 0$ such that if $m, n > N$, then for all ω:

$$\left| \sum_{k=m}^{k=n} x(k)\exp(-jk\omega) \right| < \varepsilon. \qquad (7.41)$$

The main point of uniform convergence is that the Cauchy criterion (7.41) applies to all ω, independent of N, which depends only on the choice of ε. If N must vary with ε, then ordinary, but not uniform, convergence exists. Now, (7.40) shows convergence for all ω; the interval $[-\pi, \pi]$ is closed and bounded, hence it is *compact*; and a convergent series on a compact subset of the real line is uniformly convergent on that subset. Therefore, since we know that $X(\omega)$ is periodic with period $[-\pi, \pi]$, the DTFT analysis equation series converges uniformly to $X(\omega)$ for all ω. ∎

Corollary (Continuity of DTFT). Suppose $x(n) \in l^1$. Then the DTFT of $x(n)$, $X(\omega)$, is continuous.

Proof: It is the sum of a uniformly convergent series, and each partial sum in the series,

$$S_N(\omega) = \sum_{n=-N}^{n=N} x(n)\exp(-jn\omega), \tag{7.42}$$

is a continuous function of ω. ∎

Now consider a signal $x(n) \in l^2$. We are familiar with the signal space l^2 from Chapter 2: It is the Hilbert space of square-summable discrete signals. It has an inner product, $\langle x, y \rangle$, which measures how alike are two l^2 signals; a norm, $\|x\|_2$, which derives from the inner product, $\|x\|_2 = (\langle x, x \rangle)^{1/2}$; and orthonormal bases, $\{e_i : i \in \mathbb{N}\}$, which allow us to decompose signals according to their similarity to the basis elements, $\langle e_i, x \rangle$. Thus, Hilbert spaces extend the convenient analytical tools (which one finds, for example, in finite-dimensional vector spaces), to the doubly infinite "vectors" of signal processing and analysis—discrete signals. Let us next show that for square-summable signals the DTFT exists.

Theorem (DTFT Existence for Square-Summable Signals). Suppose $x(n) \in l^2$. Then the DTFT of $x(n)$, $X(\omega)$, exists for all $\omega \in \mathbb{R}$.

Proof: Let $\omega \in \mathbb{R}$ and consider the partial DTFT analysis equations sums,

$$X_N(\omega) = \sum_{n=-N}^{+N} x(n)\exp(-jn\omega), \tag{7.43}$$

where $N \in \mathbb{N}$, the natural numbers. (We shall use the notation $X_N(\omega)$ for DTFT partial sums quite a bit.) Let H be the Hilbert space of square-integrable analog signals (cf. Chapter 3) on $[-\pi, \pi]$: $H = L^2[-\pi, \pi]$. For each N, $X_N(\omega)$ has period 2π and is square-integrable on $[-\pi, \pi]$:

$$\left\|X_N(\omega)\right\|_H^2 = \int_{-\pi}^{\pi} \left| \sum_{n=-N}^{N} x(n)\exp(-jn\omega) \right|^2 d\omega < \infty; \tag{7.44}$$

hence, $X_N(\omega) \in L^2[-\pi, \pi]$. Let us denote the L^2-norm on H of a square-integrable signal, $s(t)$, by $\|s(t)\|_H$. We wish to show that $(X_N(\omega): N \in \mathbb{N})$ is an $L^2[-\pi, \pi]$ Cauchy sequence; that is, given $\varepsilon > 0$, we can choose $N > M$ both sufficiently large so that $\|X_N - X_M\|_H < \varepsilon$. This would imply that the limit of the sequence $(X_N(\omega))$, which is the series sum of the analysis equation for $x(n)$, does in fact converge to an element of H: $X(\omega)$. Note that

$$X_N(\omega) - X_M(\omega) = \sum_{n=M+1}^{N} x(n)\exp(-jn\omega) + \sum_{n=-M-1}^{-N} x(n)\exp(-jn\omega). \tag{7.45}$$

Thus, using the orthogonality of signals $\exp(-jwn)$ on $[-\pi, \pi]$ and the properties of the inner product on H, we find

$$\left\| X_N(\omega) - X_M(\omega) \right\|_H^2$$

$$= \left\langle \sum_{n=M+1}^{N} x(n)e^{-j\omega n} + \sum_{n=-M-1}^{-N} x(n)e^{-j\omega n}, \ \sum_{m=M+1}^{N} x(m)e^{-j\omega m} + \sum_{m=-M-1}^{-N} x(m)e^{-j\omega m} \right\rangle$$

$$= \left\langle \sum_{n=M+1}^{N} x(n)e^{-j\omega n}, \ \sum_{m=M+1}^{N} x(m)e^{-j\omega m} + \sum_{m=-M-1}^{-N} x(m)e^{-j\omega m} \right\rangle$$

$$+ \left\langle \sum_{n=-M-1}^{-N} x(n)e^{-j\omega n}, \ \sum_{m=M+1}^{N} x(m)e^{-j\omega m} + \sum_{m=-M-1}^{-N} x(m)e^{-j\omega m} \right\rangle$$

$$= \left\langle \sum_{n=M+1}^{N} x(n)e^{-j\omega n}, \ \sum_{m=M+1}^{N} x(m)e^{-j\omega m} \right\rangle + \left\langle \sum_{n=M+1}^{N} x(n)e^{-j\omega n}, \ \sum_{m=-M-1}^{-N} x(m)e^{-j\omega m} \right\rangle$$

$$+ \left\langle \sum_{n=-M-1}^{-N} x(n)e^{-j\omega n}, \ \sum_{m=M+1}^{N} x(m)e^{-j\omega m} \right\rangle + \left\langle \sum_{n=-M-1}^{-N} x(n)e^{-j\omega n}, \ \sum_{m=-M-1}^{-N} x(m)e^{-j\omega m} \right\rangle$$

$$= \sum_{n=M+1}^{N} \sum_{m=M+1}^{N} x(n)\bar{x}(m) \left\langle e^{-j\omega n}, e^{-j\omega m} \right\rangle + \sum_{n=M+1}^{N} \sum_{m=-M-1}^{-N} x(n)\bar{x}(m) \left\langle e^{-j\omega n}, e^{-j\omega m} \right\rangle$$

$$+ \sum_{n=-M-1}^{-N} \sum_{m=M+1}^{N} x(n)\bar{x}(m) \left\langle e^{-j\omega n}, e^{-j\omega m} \right\rangle + \sum_{n=-M-1}^{-N} \sum_{m=-M-1}^{-N} x(n)\bar{x}(m) \left\langle e^{-j\omega n}, e^{-j\omega m} \right\rangle$$

$$= 2\pi \sum_{n=M+1}^{N} x(n)\bar{x}(n) + 0 + 0 + 2\pi \sum_{n=-M-1}^{-N} x(n)\bar{x}(n). \tag{7.46}$$

We have used $\langle \exp(-j\omega n), \exp(-j\omega m) \rangle = 2\pi\delta_{n,m}$, where $\delta_{n,m}$ is the Kronecker delta, to simplify the first and last double summations and to discard the two middle double summations in (7.46). Now, since $x(n) \in l^2$, it has a finite l^2-norm; in other words,

$$\left\| x(n) \right\|^2 = \sum_{n=-\infty}^{\infty} x(n)\bar{x}(n) < \infty. \tag{7.47}$$

This means that for $\varepsilon > 0$, we can find $N > M$ sufficiently large so that

$$\sum_{n=M+1}^{N} x(n)\bar{x}(n) < \varepsilon \tag{7.48a}$$

and

$$\sum_{n=-M-1}^{-N} x(n)\bar{x}(n) < \varepsilon. \tag{7.48b}$$

Together, (7.48a) and (7.48b) imply that (7.46) can be made arbitrarily small. Thus the sequence $(X_N(\omega): N \in \mathbb{N})$ is Cauchy in $H = L^2[-\pi, \pi]$. Since H is a Hilbert space, this Cauchy sequence converges to a signal, the DTFT of $x(n)$, $X(\omega) \in H$. ∎

7.2.1.3   Inversion. This section studies the problem of finding an inverse for the DTFT. Those frequency transforms covered so far—the Fourier series, the Fourier transform, and the discrete Fourier transform—all have inverses, assuming, in the case of the FS and FT that our signals belong to certain function spaces. So we expect no exceptions from the frequency transform for discrete aperiodic signals. Now, the DTFT of a discrete signal $x(n)$ is a periodic function $X: \mathbb{R} \to \mathbb{C}$, so the inverse must transform a periodic analog signal into a discrete signal. One transform, familiar from Chapter 5, does precisely this—the Fourier series. For an analog periodic signal, the FS finds a discrete set of frequency coefficients. We shall see that there is in fact a very close relationship between the inverse relation for the DTFT and the analog FS.

Our first theorem provides a simple criterion for the existence of an inverse.

Theorem (Inverse DTFT). Suppose that $x(n)$ has a DTFT, $X(\omega)$, and that the analysis equation for $X(\omega)$ converges uniformly on $[-\pi, \pi]$. Then, for all $n \in \mathbb{Z}$,

$$x(n) = \frac{1}{2\pi} \int_{-\pi}^{+\pi} X(\omega) \exp(j\omega n)\, d\omega \cdot \tag{7.49}$$

Proof: The stipulation that the analysis equation's convergence be uniform is critical to the proof. The DTFT analysis equation for $x(n)$ is a limit of partial sums:

$$X(\omega) = \lim_{N \to \infty} X_N(\omega) = \lim_{N \to \infty} \sum_{n=-N}^{+N} x(n) \exp(-jn\omega) = \sum_{n=-\infty}^{+\infty} x(n) \exp(-jn\omega). \tag{7.50}$$

After changing the dummy summation variable, we insert (7.50) directly into the integrand of (7.49):

$$\frac{1}{2\pi} \int_{-\pi}^{+\pi} X(\omega) \exp(j\omega n)\, d\omega = \frac{1}{2\pi} \int_{-\pi}^{+\pi} \left(\lim_{N \to \infty} \sum_{m=-N}^{+N} x(m) \exp(-jm\omega) \right) \exp(j\omega n)\, d\omega. \tag{7.51}$$

The uniform convergence of the limit in (7.51) permits us to interchange the integration and summation operations [13]:

$$\frac{1}{2\pi} \int_{-\pi}^{+\pi} X(\omega) \exp(j\omega n)\, d\omega = \frac{1}{2\pi} \lim_{N \to \infty} \sum_{m=-N}^{+N} x(m) \int_{-\pi}^{+\pi} \exp[j\omega(n-m)]\, d\omega$$

$$= \frac{1}{2\pi} \sum_{m=-\infty}^{+\infty} x(m) \delta_{m,n} = x(n), \tag{7.52}$$

where $\delta_{n,m}$ is the Kronecker delta. ∎

Corollary (Inverse DTFT for Absolutely Summable Signals). If $x(n) \in l^1$, then for all $n \in \mathbb{Z}$,

$$x(n) = \frac{1}{2\pi} \int_{-\pi}^{+\pi} X(\omega) \exp(j\omega n) \, d\omega, \tag{7.53}$$

where $X(\omega)$ is the DTFT of $x(n)$.

Proof: The analysis equation sum for $X(\omega)$ converges uniformly by the DTFT Existence Theorem for Absolutely Summable Signals in the previous section. Hence the Inverse Theorem above implies that the formula (7.53) is valid.   ∎

Definition (Inverse Discrete-Time Fourier Transform). If $X(\omega)$ is a 2π-periodic analog signal and $x(n)$, as defined by (7.53), exists, then $x(n)$ is the *inverse discrete-time Fourier transform* (IDTFT) of $X(\omega)$. Equation (7.53) is also called the DTFT *synthesis equation*.

This last result (7.53) highlights an intriguing aspect of the DTFT. Equation (7.53) says that if $x(n)$ is absolutely summable, then $x(n)$ is the nth Fourier series coefficient for $X(\omega)$. To understand this, recall that if the analog signal $y(s) \in L^1[0, T]$ has period $T > 0$, then the Fourier series analysis equation gives (unnormalized) Fourier coefficients,

$$c_k = \frac{1}{T} \int_{-T/2}^{+T/2} y(s) \exp(-2\pi jkFs) \, ds, \tag{7.54}$$

where $F = 1/T$. The companion synthesis equation reconstructs $y(s)$ from the c_k:

$$y(s) = \sum_{k=-\infty}^{+\infty} c_k \exp(2\pi jkFs). \tag{7.55}$$

The reconstruction is not perfect, however. When $y(s)$ contains a discontinuity at $s = s_0$, then the synthesis equation converges to a value midway between the left- and right-hand limits of $y(s)$ at $s = s_0$. We can easily transpose (7.55) to the form of the DTFT analysis equation. We need only set $x(k) = c_k$, $\omega = -2\pi Fs$, and $X(\omega) = y(s) = y(-\omega/(2\pi F))$. Therefore, analog periodic signals have discrete spectral components given by the Fourier series coefficients. And discrete aperiodic signals have continuous periodic spectra given by their 2π-periodic DTFTs. There is more than an affinity between the discrete aperiodic signals and the analog periodic signals; there is, as we shall see in a moment, a Hilbert space isomorphism.

Now, we have found an inversion relation for the DTFT and defined the synthesis equation for absolutely summable signals, but what about l^2 signals? This is our most important l^p space, since it supports an inner product relation. Is there an

inverse relation similar to (7.53) for square-summable discrete signals? The following theorem helps to answer this question in the affirmative, and it is one step toward showing the essential sameness of l^2 and $L^2[-\pi, \pi]$.

Theorem (DTFT Existence for Square-Summable Signals). If $x(n) \in l^2$, then there is an analog signal $y(s) \in L^2[-\pi, \pi]$ such that

$$x(n) = \frac{1}{2\pi} \int_{-\pi}^{+\pi} y(s) \exp(jsn) \, ds, \tag{7.56a}$$

for all $n \in \mathbb{Z}$, and

$$y(s) = \sum_{n=-\infty}^{+\infty} x(n) \exp(-jsn), \tag{7.56b}$$

Proof: Recall the Riesz–Fischer Theorem from Chapter 2. Suppose we take $H = L^2[-\pi, \pi]$ as the Hilbert space and $\{e_n(s): n \in \mathbb{Z}\} = \{(2\pi)^{-1/2}\exp(-jsn): n \in \mathbb{Z}\}$ as the orthonormal set in H which Riesz–Fischer presupposes. Then the Riesz–Fischer result states that if $x(n) \in l^2$, then there is a $w(s) \in H$ such that $\langle w, e_n(s) \rangle = x(n)$, and $w = \Sigma x(n) e_n(s)$. Furthermore, w is unique in the following sense: Any other $h \in H$ for which this holds can differ from w only on a set of measure zero; in other words, $\|w - h\|_2 = 0$, where $\| \cdot \|_2$ is the norm on $L^2[-\pi, \pi]$:

$$\|y\|_2 = \left(\int_{-\pi}^{+\pi} |y(s)|^2 ds \right)^{\frac{1}{2}}. \tag{7.57}$$

Continuing to apply this previous abstract theorem to our present concrete problem, we must have a $w(s) \in H$ such that

$$x(n) = \langle w, e_n \rangle = \langle w, \exp(-jsn) \rangle = \int_{-\pi}^{+\pi} w(s) \frac{\exp(jsn)}{\sqrt{2\pi}} \, ds \tag{7.58}$$

and

$$w(s) = \sum_{n=-\infty}^{+\infty} x(n) e_n(s) = \sum_{n=-\infty}^{+\infty} x(n) \frac{\exp(-jsn)}{\sqrt{2\pi}}. \tag{7.59}$$

Setting $y(s) = (2\pi)^{1/2} w(s)$ completes the proof. ∎

How exactly does this help us answer the question of whether square-summable discrete signals have DTFTs? Briefly, $x(n) \in l^2$ does have a DTFT: We take $X(\omega) = y(\omega)$, where y is the $L^2[-\pi, \pi]$ signal guaranteed by the theorem. The problem is that $X(\omega)$ need not be continuous; therefore, there are many possible choices for $X(\omega)$ in

$L^2[-\pi, \pi]$ that obey the DTFT synthesis equation. The various choices may differ on a set of measure zero, so that the norm of their difference, computed with an integral of adequate power (such as the Lebesgue integral) is zero. This should be no surprise. We recall Chapter 5's lesson, for example, that the Fourier series sum of a signal converges to the midpoint of a signal discontinuity. The FS imperfectly recovers the original periodic analog signal. If $x(n) \in l^1$, on the other hand, then the convergence of the DTFT analysis equation (or, alternatively, the convergence of the Fourier series sum) is uniform, so that $X(\omega)$ is continuous and pointwise unique on $[-\pi, \pi]$.

Corollary (Embedding of l^2 into $L^2[-\pi, \pi]$). For $x(n) \in l^2$, then set $\mathcal{F}(x) = (2\pi)^{-1/2}X(\omega) \in L^2[-\pi, \pi]$. Then $\mathcal{F}$ is a Hilbert space isomorphism between l^2 and (the equivalence classes of signals that are equal almost everywhere) its image $\mathcal{F}[l^2]$.

Proof: The theorem guarantees that a unique (up to a set of measure zero) $X(\omega)$ exists, so $\mathcal{F}$ is well-defined. It is also clear that the DTFT is a linear mapping from l^2 to $L^2[-\pi, \pi]$, and so too is $\mathcal{F}$ (exercise). We need to show as well that $\langle x, y \rangle = \langle \mathcal{F}x, \mathcal{F}y \rangle$, for all $x, y \in l^2$. Let $Y(\omega)$ be the DTFT of $y(n)$. Working from within the realm of $L^2[-\pi, \pi]$, we find

$$\langle X, Y \rangle = \int_{-\pi}^{+\pi} X(\omega)\overline{Y}(\omega)\, d\omega = \int_{-\pi}^{+\pi} \left[\sum_{n=-\infty}^{+\infty} x(n)\exp(-j\omega n) \right] \left[\sum_{k=-\infty}^{+\infty} \overline{y}(k)\exp(j\omega k) \right] d\omega$$

$$= \int_{-\pi}^{+\pi} \left[\sum_{n=-\infty}^{+\infty} \sum_{k=-\infty}^{+\infty} x(n)\overline{y}(k)\exp^{-j\omega(n-k)} \right] d\omega. \tag{7.60}$$

Since $x, y \in l^2$, the partial sums $X_N(\omega)$ and $Y_N(\omega)$ converge absolutely; for example, we have $|x(n)\exp(-j\omega n)| = |x(n)|$, and $\Sigma|x(n)|^2 = (\|x\|_2)^2 < \infty$. This justifies the step to a double summation of products [13]. And, because the double sum on the bottom of (7.60) converges on the closed set $[-\pi, \pi]$, it converges uniformly. This allows us to interchange the summation and integration operations, obtaining

$$\langle X, Y \rangle = \sum_{n=-\infty}^{+\infty} \sum_{k=-\infty}^{+\infty} \int_{-\pi}^{+\pi} x(n)\overline{y}(k)\exp^{-j\omega(n-k)}\, d\omega = 2\pi \sum_{n=-\infty}^{+\infty} x(n)\overline{y}(n)$$

$$= 2\pi \langle x(n), y(n) \rangle. \tag{7.61}$$

Only the terms with $n = k$ in the integral of (7.61) are nonzero. Finally, since $\mathcal{F}(x) = (2\pi)^{-1/2}X(\omega)$, $\langle \mathcal{F}x, \mathcal{F}y \rangle = \langle x, y \rangle$. ∎

An embedding therefore exists from the discrete Hilbert space l^2 into the continuous Hilbert space $L^2[-\pi, \pi]$. This Hilbert subspace of $L^2[-\pi, \pi]$, the image of l^2 under $\mathcal{F}$, $\mathcal{F}[l^2]$, is essentially just like l^2. Is it the case, perhaps owing to the intricacies

of its analog signal elements, that the full Hilbert space, $L^2[-\pi, \pi]$, is fundamentally more complex than l^2? The requisite tools of formal analog theory—Dirac delta functions, Lebesgue integration, questions of separability, and so on—make it tempting to conclude that $L^2[-\pi, \pi]$ ought to be a richer mathematical object than the drab, discrete l^2. Moreover, the embedding that we have given is a straightforward application of the abstract Riesz–Fischer theorem; no technical arguments using the specific characteristics of $L^2[-\pi, \pi]$ signals are necessary. So it might well be concluded that the orthogonal complement, $\mathcal{F}[l^2]^\perp$, is indeed nontrivial.

No, the truth is quite the opposite: The mapping $\mathcal{F}(x(n)) = (2\pi)^{-1/2}X(\omega)$ from l^2 into $L^2[-\pi, \pi]$ is indeed a Hilbert space isomorphism. We can show this if we can find a set of signals in the image of l^2 under the embedding relation, $\mathcal{F}$, that is dense in $L^2[-\pi, \pi]$. In general, questions of orthogonality and finding embeddings (also called injections) of one Hilbert space into another tend to admit easier answers. But showing that one or another set of orthogonal elements spans the entire Hilbert space—the question of completeness—is quite often a daunting problem. Fortunately, we already have the crucial tool in hand, and the next corollary explains the result.

Corollary (Isomorphism of l^2 and $L^2(-\pi, \pi)$). Let $x(n) \in l^2$, let $X(\omega)$ be the DTFT of $x(n)$, and set $\mathcal{F}(x) = (2\pi)^{-1/2}X(\omega) \in L^2[-\pi, \pi]$. Then $\mathcal{F}$ is a Hilbert space isomorphism.

Proof: Consider some $Y(\omega) \in L^2[-\pi, \pi]$. We need to show that Y is arbitrarily close to some element of the image of $\mathcal{F}$, $\mathcal{F}[l^2]$. From Chapter 5, Y has a Fourier series representation,

$$Y(\omega) = \sum_{k=-\infty}^{+\infty} c_k \exp(2\pi jkF\omega) = \sum_{k=-\infty}^{+\infty} c_k \exp(jk\omega)$$

$$= \lim_{K\to\infty} \sum_{k=-K}^{+K} c_k \exp(jk\omega) = \lim_{K\to\infty} Y_K(\omega), \tag{7.62}$$

where

$$c_k = \frac{1}{T} \int_{-T/2}^{+T/2} Y(\omega)\exp(-2\pi jkF\omega)\,d\omega = \frac{1}{2\pi} \int_{-\pi/2}^{+\pi/2} Y(\omega)\exp(-jk\omega)\,d\omega. \tag{7.63}$$

Since $T = \pi - (-\pi) = 2\pi$ and $F = 1/T = 1/(2\pi)$, (7.62) shows that see that $Y(\omega)$ is really the limit of the $Y_K(\omega)$. But each $Y_K(\omega)$ is a linear combination of exponentials, $\exp(jk\omega)$, which are in the image, $\mathcal{F}[l^2]$. Since Y was arbitrary, this implies that the span of the exponentials is dense in $L^2[-\pi, \pi]$, or, equivalently, that its closure is all of $L^2[-\pi, \pi]$. ∎

The next section contains an extended study of a single example that illustrates some of the convergence problems that arise when taking the DTFT of a signal that is not absolutely summable.

7.2.1.4   *Vagaries of X(ω) convergence in L²[−π, π].*   The search for those classes of discrete signals, $x(n)$, that have a DTFT leads to difficulties with the convergence of the analysis equation sum. We have just shown that absolutely summable and square-summable discrete signals have DTFTs; if $x(n) \in l^2$, however, we cannot guarantee that the DTFT, $X(\omega)$, is unique. Now we explore in some detail an example of a square-summable signal that is not in l^1. Its DTFT is not unique, due to the presence of discontinuities in $X(\omega)$. Moreover, its convergence is tainted by spikes near the points of discontinuity that persist even as the partial analysis equation sums converge (in the l^2 norm) to $X(\omega)$.

Example (Discrete Sinc Signal).   Consider the signal $x(n)$ defined as follows:

$$x(n) = \frac{\mathrm{sinc}(n)}{\pi} = \begin{cases} \dfrac{\sin(n)}{\pi n} & \text{if } n \neq 0, \\[2ex] \dfrac{1}{\pi} & \text{if } n = 0. \end{cases} \tag{7.64}$$

Although $x(n) \notin l^1$, since its absolute value decays like n^{-1}, we do find $x(n) \in l^2$, because $|x(n)|^2$ is dominated by $(\pi n)^{-2}$, which does converge. If we let $\tilde{X}(\omega) = 1$ for $|\omega| \leq 1$ and $\tilde{X}(\omega) = 0$ otherwise, then

$$x(n) = \frac{1}{2\pi} \int_{-\pi}^{+\pi} \tilde{X}(\omega) \exp(j\omega n) \, d\omega \cdot \tag{7.65}$$

Thus, the IDTFT of $\tilde{X}(\omega)$ is $x(n)$. Figure 7.12 shows $\tilde{X}(\omega)$ and the discrete signal that results from its IDTFT.

Is $\tilde{X}(\omega)$ the DTFT of $x(n)$? Not exactly, but let us study the situation further. Since (7.65) is a Fourier series analysis equation, and $x(n)$ is a FS coefficient for $\tilde{X}(\omega)$, we can consider the limit of the corresponding Fourier series sum, $X(\omega)$. Then $X(\omega)$ converges for $\pm\omega = 1$ to $X(\omega) = 1/2$, the midpoint between the discontinuities:

$$X(\omega) = \lim_{N \to \infty} \sum_{n=-N}^{n=+N} x(n) \exp(-j\omega n)$$

$$= \sum_{n=-\infty}^{n=+\infty} x(n) \exp(-j\omega n) = \begin{cases} 1 & \text{if } |\omega| < 1, \\ 0 & \text{if } |\omega| > 1, \\ 1/2 & \text{if } |\omega| = 1. \end{cases} \tag{7.66}$$

This is an unlucky result: for each $\omega \in [-\pi, \pi]$ the partial sums in (7.66) have a limit, but it is $X(\omega)$, not $\tilde{X}(\omega)$. The convergence of the partial sums in (7.66) is not uniform,

(a) $\tilde{X}(\omega)$

(b) $x(n)$
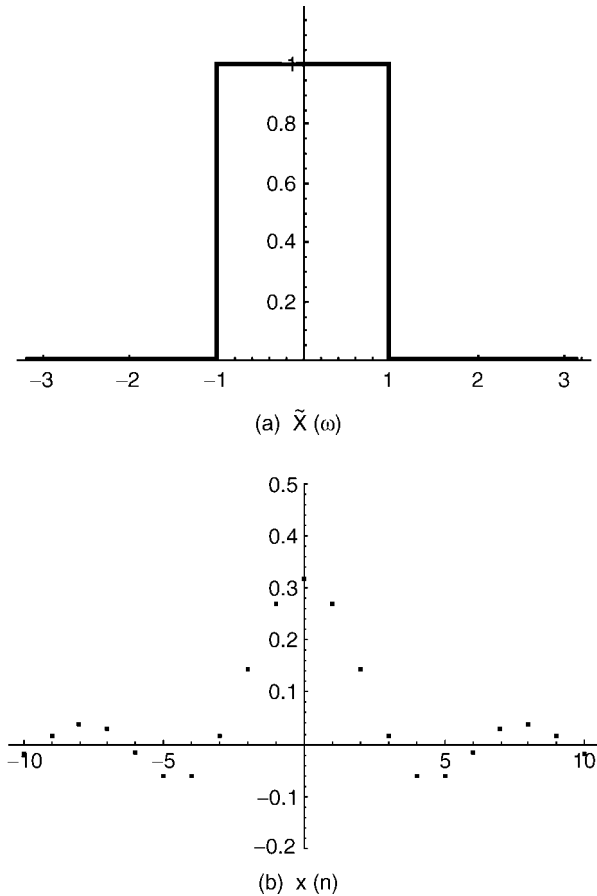
Fig. 7.12. Panel (a) shows a square pulse signal on $[-\pi, \pi]$. The result of applying the IDTFT to this pulse is shown in panel (b).

as it would be if $x(n)$ were absolutely summable. Instead, the convergence is in the $L^2[-\pi, \pi]$ norm, $\| \cdot \|_2$, and it allows the limit of the DTFT analysis equation, $X(\omega)$, to differ from the signal from which we derived $x(n)$ in the first place, $\tilde{X}(\omega)$.

Example (Gibbs Phenomenon). Examining the partial sums of (7.62) exposes a further feature of convergence under $\| \cdot \|_2$, namely the Gibbs[4] phenomenon. Spikes appear near the step edges in $\tilde{X}(\omega)$ and do not diminish with increasingly long partial sums (Figure 7.13).

[4]Josiah W Gibbs (1839–1903), an American chemist, physicist, and professor at yale University. Gibbs devised the vector dot product, $v \cdot w$, and the cross product, $v \times w$, and investigated the famous spike in Fourier series convergence. Although he was the first scientist of international stature from the United States, Yale neither appreciated his capabilities nor remunerated him for his service. Gibbs supported himself on an inheritance over the cource of a decade at Yale.
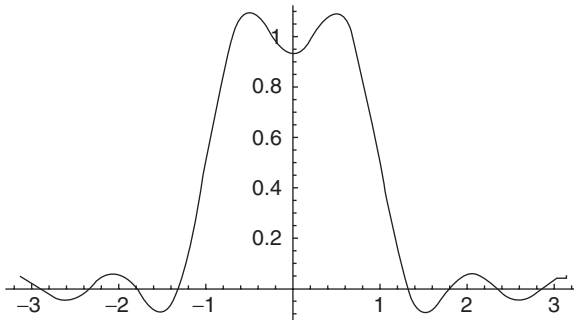
(a) Partial DTFT sum, $X_N(\omega)$, N = 5;
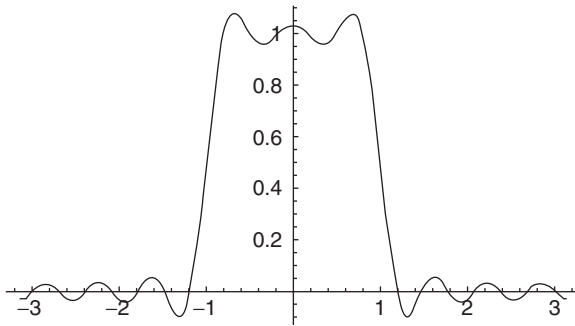
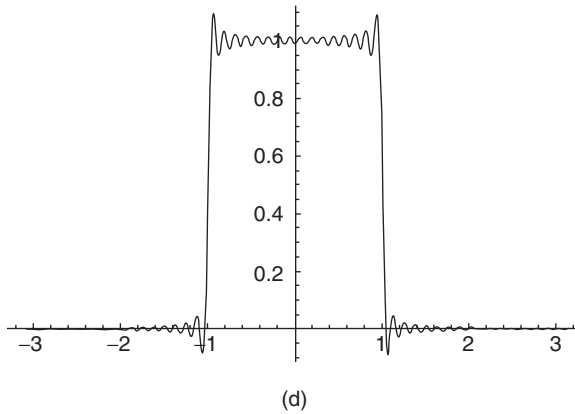
(b) $X_N(\omega)$, N = 10;
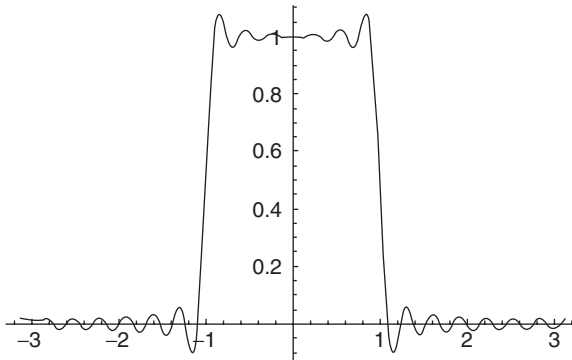
(c) $X_N(\omega)$, N = 20;

Fig. 7.13. A study of partial DTFT analysis equation sums for the square-summable signal $x(n) = \pi^{-1}\sin(n)$. Panel (a) shows $X_5(\omega)$; panel (b) shows $X_{10}(\omega)$; panel (c) shows $X_{20}(\omega)$; and panel (d), $X_{50}(\omega)$, shows a persistent ringing effect at the discontinuities.

(d)

Fig. 7.13 (*Continued*)

Although its name has a supernatural resonance, there are specific, clearly defin-able reasons for the Gibbs phenomenon. In fact, it occurs whenever there is a dis-continuity in a square integrable signal on $[-\pi, \pi]$. To more clearly grasp the reasons for the phenomenon, let us consider the partial DTFT sums, $X_N(\omega)$:

$$X_N(\omega) = \sum_{n=-N}^{n=+N} x(n)\exp(-j\omega n) = \sum_{n=-N}^{n=+N}\left\{\frac{1}{2\pi}\int_{-\pi}^{+\pi} X(\Omega)\exp(j\Omega n)\ d\Omega\right\}\exp(-j\omega n)$$

$$= \frac{1}{2\pi}\sum_{n=-N}^{n=+N}\left\{\int_{-\pi}^{+\pi} X(\Omega)\exp(j(\Omega-\omega)n)\ d\Omega\right\}. \tag{7.67}$$

The IDTFT of $X(\omega)$ replaces $x(n)$ in the finite summation of (7.67). $X(\omega)$ itself is the limit of these partial DTFT sums as $N \to \infty$. (We already know the definition of $X(\omega)$: It is the step function equal to unity on $[-1, 1]$ and zero elsewhere on $[-\pi, +\pi]$. It is thus possible to simplify the integral in (7.67), but we resist in order to show how the following development does not depend on the specific nature of $X(\omega)$.) Next, we set $\theta = \Omega - \omega$ toward a change of the integration variable, thereby giving

$$X_N(\omega) = \frac{1}{2\pi}\sum_{n=-N}^{n=+N}\left\{\int_{-\pi-\omega}^{\pi-\omega} X(\theta+\omega)\exp(j\theta n)\ d\theta\right\}$$

$$= \frac{1}{2\pi}\sum_{n=-N}^{n=+N}\left\{\int_{-\pi}^{\pi} X(\theta+\omega)\exp(j\theta n)\ d\theta\right\} \tag{7.68}$$

Note that the integrand is 2π-periodic, which permits us to take the limits of integration from $[-\pi, +\pi]$ instead of $[-\pi - \omega, \pi - \omega]$. Let us now interchange the finite summation and integration operations in (7.68) to obtain

$$X_N(\omega) = \int_{-\pi}^{\pi} X(\theta+\omega) \left\{ \frac{1}{2\pi} \sum_{n=-N}^{n=+N} \exp(j\theta n) \right\} d\theta = \int_{-\pi}^{\pi} X(\theta+\omega) D_N(\theta) d\theta. \qquad (7.69)$$

Therefore, the partial DTFT synthesis equation sums, $X_N(\omega)$, are given by the cross-correlation on $[-\pi, +\pi]$ of X and the Dirichlet[5] kernel of order N, $D_N(\theta)$. Chapter 5 introduced the Dirichlet kernel in connection with the problem of the Fourier series sum's convergence . It is an algebraic exercise to show that

$$D_N(\theta) = \frac{1}{2\pi} \sum_{n=-N}^{n=+N} \exp(j\theta n) = \frac{1}{2\pi} \frac{\sin\left(N\theta + \dfrac{\theta}{2}\right)}{\sin\left(\dfrac{\theta}{2}\right)} = \frac{1}{2\pi} + \frac{1}{\pi} \sum_{n=1}^{n=N} \cos(\theta n), \qquad (7.70)$$

and therefore, for any $N > 0$,

$$\int_{0}^{\pi} D_N(\theta)\ d\theta = \frac{1}{2} = \int_{-\pi}^{0} D_N(\theta)\ d\theta \cdot \qquad (7.71)$$

Now, from (7.70) the Dirichlet kernel is an even function. So changing the variable of integration in (7.69) shows $X_N(\omega)$ to be a convolution of X and $D_N(\theta)$:

$$X_N(\omega) = \int_{-\pi}^{\pi} X(\theta+\omega) D_N(\theta)\ d\theta = \int_{-\pi}^{\pi} X(\theta) D_N(\omega-\theta)\ d\theta \cdot \qquad (7.72)$$

Now we understand the root cause of the Gibbs phenomenon. Because $X(\theta)$ in (7.72) is zero for $|\theta| > 1$, has discontinuities at $\theta = \pm 1$, and is unity for $|\theta| < 1$, the convolution integral produces a response that has a spike near the discontinuity. The spike's height is roughly the sum of the area of $D_N(\theta)$ under its main hump (Figure 7.14) plus the tail of the Dirichlet kernel that overlaps with the nonzero part of X.

The crux of the problem is how the first peak in the evaluation of the convolution integral behaves as $N \to \infty$. Empirically, as evidenced by Figure 7.13, the convolution generates a spike that shrinks in width but does not diminish in height. Clearly, the height of $D_N(\theta)$ does increase as $\theta \to 0$. Hence, it would appear that the area under the Dirichlet kernel between the first two zero crossings, $\pm\theta_N$, where $\theta_N = \pi/(N + 1/2)$, does not fall below some positive value. In fact, this area

---

[5]Peter Gustav Lejeune Dirichlet (1805–1859) studied convergence kernels for the Fourier series and problems in potential theory. He provided a proof of Fermat's Last Theorem for the case $n = 5$.
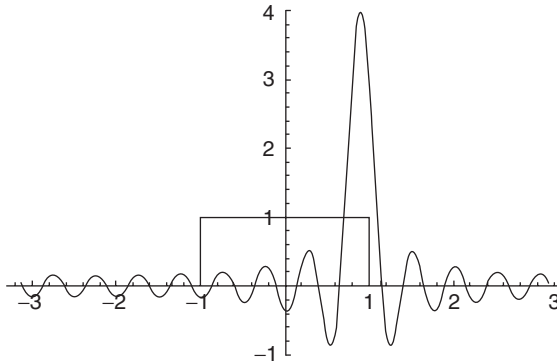
Fig. 7.14. Convolution with $D_N(\theta)$ at a discontinuity. A convolution integral of the analog signal X with the Dirichlet kernel of order N (here, $N = 12$) gives the partial DTFT summation for X, $X_N(\omega)$. The output is equal to the area under $D_N(\theta)$ that overlaps the nonzero area of the square pulse signal X.

remains constant! As $N \rightarrow \infty$, its decreasing width is perfectly balanced by the increasing height. Let us investigate:

$$\int_{-\theta_N}^{+\theta_N} D_N(\theta)\, d\theta = 2 \int_0^{\theta_N} D_N(\theta)\, d\theta = \frac{1}{\pi} \int_0^{\theta_N} \frac{\sin\left(N\theta + \dfrac{\theta}{2}\right)}{\sin\left(\dfrac{\theta}{2}\right)}\, d\theta. \tag{7.73}$$

Making the change of integration variable $\Omega = N\theta + \theta/2$, we find

$$\int_{-\theta_N}^{+\theta_N} D_N(\theta)\, d\theta = \frac{1}{\pi} \int_0^{\pi} \frac{\sin(\Omega)}{\sin\left(\dfrac{\Omega}{2N+1}\right)} \frac{2}{2N+1}\, d\Omega = \frac{2}{\pi} \int_0^{\pi} \frac{\sin(\Omega)}{\Omega} \frac{\left(\dfrac{\Omega}{2N+1}\right)}{\sin\left(\dfrac{\Omega}{2N+1}\right)}\, d\Omega. \tag{7.74}$$

As $N \rightarrow \infty$, $\Omega/(2N + 1) \rightarrow 0$; taking the limit of (7.74) as $N \rightarrow \infty$ and interchanging the limit and integration operations on the right-hand side of (7.74) gives

$$\lim_{N \to \infty} \int_{-\theta_N}^{+\theta_N} D_N(\theta)\, d\theta = \frac{2}{\pi} \int_0^{\pi} \frac{\sin(\Omega)}{\Omega} \lim_{N \to \infty} \frac{\left(\dfrac{\Omega}{2N+1}\right)}{\sin\left(\dfrac{\Omega}{2N+1}\right)}\, d\Omega = \frac{2}{\pi} \int_0^{\pi} \frac{\sin(\Omega)}{\Omega}\, d\Omega \tag{7.75}$$

showing that the between the first zero crossings of $D_N(\theta)$ is constant. The area under $\mathrm{sinc}(\Omega)$ from 0 to π is approximately 1.85194, so the convolution integral (7.72) for the partial DTFT summation, $X_N(\omega)$, evaluates to approximately

$(2/\pi)(1.85194) = 1.17898$. To find the approximate value of the convolution integral (7.72) at one of the Gibbs spikes, we must add the main hump's contribution to the area under the small oscillations in the tail of $D_N(\theta)$. What is this latter value? Figure. 7.14 shows the situation; these small osciallations overlap with the nonzero part of $X(\omega)$ and affect the convolution result. We know from (7.71) that the entire integral of $D_N(\theta)$ over $[-\pi, \pi]$ is unity. Thus, the integral over $[-1, 1]$ is also near unity, since (exercise) the areas of the oscillations decrease like $1/n$. So, we have

$$1 = \int_{-\theta_N}^{+\theta_N} D_N(\theta) \, d\theta + 2 \int_{+\theta_N}^{\pi} D_N(\theta) \, d\theta \approx 1.17898 + 2 \int_{+\theta_N}^{\pi} D_N(\theta) \, d\theta, \qquad (7.76)$$

and therefore the maximum of the convolution, $X_N(\omega_{max})$, approximates to

$$X_N(\omega_{max}) = \int_{-\pi}^{\pi} X(\theta) D_N(\omega_{max} - \theta) \, d\theta \approx \int_{-\theta_N}^{+\theta_N} D_N(\theta) \, d\theta + \int_{+\theta_N}^{\pi} D_N(\theta) \, d\theta$$

$$\approx 1.17898 - \frac{0.17898}{2} = 1.08949. \qquad (7.77)$$

A careful review of this analysis should convince the reader that

- Any step discontinuity in $X(\omega)$ will produce the same result.
- The amount of overshoot around the discontinuity is approximately 9% of the step height of the discontinuity.

The first point follows from the fact that for sufficiently high N values, the Dirichlet kernel's main peak will be so narrow that $X(\omega)$ will appear flat before and after the jump. That is, $D_N(\theta)$ localizes the discontinuity of $X(\omega)$. The second point is perhaps easier to witness from the present example. The size of the Gibbs phenomenon's spike is given by an integral, which is a linear operation, and so scaling the step height causes the convolution's output to scale accordingly. The rich Fourier analysis literature provides further explanations and generalizations of the Gibbs phenomenon [15–17].

7.2.1.5 *Some Final Points.* This section concludes our preliminary study of the DTFT by stating two theoretical results.

Not all of our abstract l^p signal spaces support a DTFT; however, we have the following result [18]:

Theorem (DTFT Existence for *p*-Summable Signals). Suppose $x(n) \in l^p$, for $1 < p < 2$. Then there exists an $X(\omega) \in L^q[-\pi, \pi]$, where p and q are conjugate exponents (that is, $p^{-1} + q^{-1} = 1$), such that the values $x(n)$ are the Fourier series coefficients for $X(\omega)$.

Thus, we have a rich variety of signal spaces whose members have DTFTs. In signal analysis, the limiting cases—l^1 and l^2—are the most important. For $x(n) \in l^1$, the partial sums, $X_N(\omega)$, converge uniformly on $[-\pi, \pi]$ to a continuous signal, $X(\omega)$. Because $X(\omega)$ is continuous on a closed interval, $[-\pi, \pi]$, it is also bounded: $X(\omega) \in L^\infty$. The partial DTFT sums, $X_N(\omega)$, converge pointwise when $x(n)$ is absolutely summable. This is not the case for square-summable signals; we have seen that pointwise convergence does not necessarily occur for $x(n) \in l^2$. A long-standing problem has been to characterize the set of points for which the Fourier series of an $L^2[-\pi, \pi]$ signal converges. Many mathematicians supposed that convergence occurs almost everywhere, and in 1966 Carleson finally proved [19] the following theorem:

Theorem (Carleson's).   If $X(\omega) \in L^2[-\pi, \pi]$, then the Fourier series for X converges almost everywhere to $X(\omega)$.

This result was soon generalized by Hunt to any $L^p[-\pi, \pi]$, $1 < p < \infty$ [20]. The exceptional case is $L^1[-\pi, \pi]$. And what a exception it is: In 1926, Kolmogorov[6] found an unbounded, discontinuous function, $f \in L^1[-\pi, \pi]$, whose Fourier series diverges everywhere from f [21, 22].

7.2.2 Properties

Let us enumerate the properties of the discrete-time Fourier transform. We assume throughout that discrete signals, say $x(n)$, belong to some signal space that supports a DTFT operation. Many of these are similar in flavor to the properties of previously covered transforms: the Fourier series, Fourier transform, and discrete Fourier transform. Consequently, we leave several of the proofs as exercises.

Proposition (Linearity, Time-Shift, and Frequency Shift).   Let $x(n)$ and $y(n)$ be discrete signals and let $X(\omega)$ and $Y(\omega)$ be their DTFTs, respectively. Then

(a) (Linearity) The DTFT of $ax(n) + by(n)$ is $aX(\omega) + bY(\omega)$.
(b) (Time Shift) The DTFT of $x(n - m)$ is $\exp(-j\omega m)X(\omega)$.
(c) (Frequency Shift) The IDTFT of $X(\omega - \theta)$ is $\exp(-j\theta n)x(n)$.

Proof: Exercise.   ∎

---

[6]A. N. Kolmogorov (1903−1987), professor of mathematics at Moscow State University, investigated problems of topology and analysis and established the axiomatic approach to probability theory.

Proposition (Frequency Differentiation). Suppose $x(n)$ is a discrete signal, $X(\omega)$ is its DTFT, and the partial sums $X_N(\omega)$ converge uniformly on $[-\pi, \pi]$ to $X(\omega)$. Then the DTFT of $nx(n)$ is $jdX(\omega)/d\omega$.

Proof: To prove transform properties, one may work from either end of a proposed equality; in this case, it is easier to manipulate the derivative of the DTFT. To wit,

$$j\frac{d}{d\omega}X(\omega) = j\frac{d}{d\omega}\sum_{n=-\infty}^{\infty} x(n)\exp(-jn\omega) = j\sum_{n=-\infty}^{\infty} x(n)\frac{d}{d\omega}\exp(-jn\omega). \qquad (7.78)$$

The interchange of the differentiation and infinite summation operations is valid because the DTFT analysis equation is uniformly convergent. Taking the derivative of the summand in (7.78) and pulling the constants through the summation gives

$$j\frac{d}{d\omega}X(\omega) = j\sum_{n=-\infty}^{\infty} x(n)(-jn)\exp(-jn\omega) = \sum_{n=-\infty}^{\infty} nx(n)\exp(-jn\omega). \qquad (7.79)$$

This is precisely the DTFT analysis equation for the signal $nx(n)$. ∎

Without a doubt, the most important property of the DTFT is the Convolution-in-Time Theorem. This result shows that convolving two signals in the time domain is equivalent to multiplying their frequency domain representations. Since we are dealing with aperiodic signals, there is no need to redefine convolution for a finite interval, as we did with the DFT in (7.22). The convolution-in-time property is the key to understanding signal filtering—the selective suppression of frequency bands within a signal. We shall resort to this theorem many times in the chapters that follow.

Theorem (Convolution in Time). Let $x(n)$ and $y(n)$ be signals, let $X(\omega)$ and $Y(\omega)$ be their DTFTs, and let $z = x * y$. If the convolution sum for $z(n)$ converges absolutely for each integer n, then the DTFT of $z(n)$ is $Z(\omega) = X(\omega)Y(\omega)$.

Proof: Among all of the theoretical investigations into all of the transforms studied so far, we should note a distinct computational compatibility between the transform integral (or summation) and the convolution operation. The DTFT is no exception. We substitute the expression for the convolution, $z = x * y$, directly into the DTFT analysis equation for $Z(\omega)$:

$$Z(\omega) = \sum_{n=-\infty}^{\infty} z(n)\exp(-j\omega n) = \sum_{n=-\infty}^{\infty} (x * y)(n)\exp(-j\omega n)$$

$$= \sum_{n=-\infty}^{\infty} \left(\sum_{k=-\infty}^{\infty} x(k)y(n-k) \right) \exp(-j\omega n)$$

$$= \sum_{n=-\infty}^{\infty} \sum_{k=-\infty}^{\infty} x(k)y(n-k)\exp(-j\omega (n-k))\exp(-j\omega k)$$

$$= \sum_{k=-\infty}^{\infty} \sum_{n=-\infty}^{\infty} x(k)y(n-k)\exp(-j\omega (n-k))\exp(-j\omega k)$$

$$= \sum_{k=-\infty}^{\infty} x(k)\exp(-j\omega k) \sum_{n=-\infty}^{\infty} y(n-k)\exp(-j\omega (n-k))$$

$$= X(\omega) \sum_{n=-\infty}^{\infty} y(n-k)\exp(-j\omega (n-k))$$

$$= X(\omega) \sum_{m=-\infty}^{\infty} y(m)\exp(-j\omega m) = X(\omega)Y(\omega). \tag{7.80}$$

We use the absolute convergence of the convolution sum to justify writing the iterated summation as a double summation and to subsequently switch the order to the summation. A routine change of summation variable, $m = n - k$, occurs in the last line of (7.80). ∎

There is an important link back to our results on linear, translation-invariant systems. Recall from Chapter 2 that the convolution relation characterizes LTI systems. If H is LTI, then the output, $y = Hx$, is the convolution of $h = H\delta$ with x: $y = h * x$. Thus we have the following corollary.

Corollary (Convolution in Time). If H is an LTI system, h is the impulse response of H, and $y = Hx$, then $Y(\omega) = X(\omega)H(\omega)$, assuming their DTFTs exist.

Proof: Note that $y = h * x$ and apply the theorem. ∎

We shall establish yet another transform Convolution Theorem when we study the z-transform in Chapter 8. The next theorem is a companion result. It establishes for the DTFT a familiar link: Multiplication in the time domain equates with convolution in the frequency domain. This theorem has a z-transform variant, too.

Theorem (Convolution in Frequency). Suppose $x(n)$ and $y(n)$ are discrete signals; $X(\omega)$, $Y(\omega) \in L^2[-\pi, \pi]$ are their respective DTFTs; and $z(n) = x(n)y(n)$ is their

termwise product. Then the DTFT of $z(n)$, $Z(\omega)$, is given by the scaled convolution of $X(\omega)$ and $Y(\omega)$ in $L^2[-\pi, \pi]$:

$$Z(\omega) = \frac{1}{2\pi} \int_{-\pi}^{+\pi} X(\theta)Y(\omega-\theta)\,d\theta. \tag{7.81}$$

Proof: The right-hand side of (7.81) is the integral of the product of infinite summations whose terms contain the complex exponential—for instance, $\exp(-j\theta n)$. We have already witnessed numerous cases where the summands cancel owing to the 2π-periodicity of the exponential. Therefore, let us work from the $L^2[-\pi, \pi]$ side of (7.81). Indeed, we compute,

$$\frac{1}{2\pi} \int_{-\pi}^{+\pi} X(\theta)Y(\omega-\theta)\,d\theta = \frac{1}{2\pi} \int_{-\pi}^{+\pi} \sum_{n=-\infty}^{\infty} x(n)\exp(-j\theta n) \sum_{k=-\infty}^{\infty} y(k)\exp[-j(\omega-\theta)k]\,d\theta$$

$$= \frac{1}{2\pi} \sum_{n=-\infty}^{\infty} \sum_{k=-\infty}^{\infty} x(n)y(k)\exp(-j\omega k) \int_{-\pi}^{+\pi} \exp(-j\theta n)\exp(j\theta k)\,d\theta$$

$$= \frac{1}{2\pi} \sum_{n=-\infty}^{\infty} \sum_{k=-\infty}^{\infty} x(n)y(k)\exp(-j\omega k) \int_{-\pi}^{+\pi} \exp[-j\theta(n-k)]\,d\theta. \tag{7.82}$$

Once again the last integral is zero, unless $n = k$; in this case it evaluates to 2π. Thus, all of the terms of the double summation on the bottom of (7.82) are zero, save those where $n = k$. Our strategy works, and we find

$$\frac{1}{2\pi} \int_{-\pi}^{+\pi} X(\theta)Y(\omega-\theta)\,d\theta = \frac{1}{2\pi} \sum_{n=-\infty}^{\infty} \sum_{k=-\infty}^{\infty} x(n)y(k)\exp(-j\omega k) \int_{-\pi}^{+\pi} \exp[-j\theta(n-k)]\,d\theta$$

$$= \frac{2\pi}{2\pi} \sum_{n=-\infty}^{\infty} x(n)y(n)\exp(-j\omega n) = \sum_{n=-\infty}^{\infty} z(n)\exp(-j\omega n) = Z(\omega) \tag{7.83}$$

which completes the proof. ∎

Note that the above proof allows for the case that the signal $y(n)$ may be complex-valued. This observation gives us the following corollary.

Corollary.   Again let $x(n)$ and $y(n)$ be discrete signals, and let $X(\omega)$, $Y(\omega) \in L^2[-\pi, \pi]$ be their respective DTFTs. Then,

$$\sum_{n=-\infty}^{\infty} x(n)\bar{y}(n) = \frac{1}{2\pi} \int_{-\pi}^{+\pi} X(\theta)\bar{Y}(\theta)\,d\theta. \tag{7.84}$$

Proof: Before commencing with the proof, let us observe that the left-hand side of (7.84) is the l^2 inner product of $x(n)$ and $y(n)$, and the right-hand side is just the inner product of $X(\omega)$ and $Y(\omega)$ scaled by the factor $(2\pi)^{-1}$. Well, in the course of establishing the embedding isomorphism from l^2 into $L^2[-\pi, \pi]$ as Hilbert spaces, we already proved this result. Nonetheless, we can convey some of the symmetry properties and computational mechanics of the DTFT by offering another argument. So set $w(n) = \bar{y}(n)$ and $z(n) = x(n)w(n) = x(n)\bar{y}(n)$. By the theorem, then, the DTFT of $z(n)$ is

$$Z(\omega) = \frac{1}{2\pi} \int_{-\pi}^{+\pi} X(\theta)W(\omega - \theta)\, d\theta. \tag{7.85}$$

Therefore,

$$Z(0) = \left(\sum_{n=-\infty}^{+\infty} z(n)e(-j\omega n)\right)\Bigg|_{\omega=0} = \sum_{n=-\infty}^{+\infty} x(n)\bar{y}(n) = \frac{1}{2\pi} \int_{-\pi}^{+\pi} X(\theta)W(-\theta)\, d\theta. \tag{7.86}$$

What is $W(-\theta)$ in the integral on the right-hand side of (7.86)? By the algebra of complex conjugates, however, we find

$$\bar{Y}(\theta) = \overline{\left[\sum_{n=-\infty}^{+\infty} y(n)e(-j\theta n)\right]} = \sum_{n=-\infty}^{+\infty} \bar{y}(n)e(j\theta n) = \sum_{n=-\infty}^{+\infty} \bar{y}(n)e[-j(-\theta)n] = W(-\theta). \tag{7.87}$$

Putting (7.86) and (7.87) together establishes the theorem's result.   ∎

Corollary (Parseval's Theorem). If $x(n) \in l^2$, then $\|x(n)\|_2 = (2\pi)^{-1}\|X(\omega)\|_2$.

Proof: Take $x(n) = y(n)$ in the previous corollary. (Observe that the two norms in the statement of Parseval's theorem are taken in two different Hilbert spaces: l^2 and $L^2[-\pi, \pi]$.)   ∎

Note that Parseval's theorem too follows from our earlier Hilbert space isomorphism. Many frequency transform theorems at first glance appear to be almost miraculous consequences of the properties of the exponential function, or its sinusoidal parts, or the definition of the particular discrete or analog transform. But in fact they are mere instances of Hilbert space results. That very general, very abstract, partly algebraic, partly geometric theory that we studied in Chapters 2 and 3 provides us with many of the basic tools for the frequency domain processing and analysis of signals.

Parseval's theorem shows that signal energy in the time domain is proportional to signal energy in the frequency domain. This has some practical applications. In Chapter 9 we shall consider frequency-domain analysis of signals. We sought methods for discovering the periodicities of signals in Chapter 4, and to some extent we were

successful in applying statistical and structural methods toward this end. Using discrete Fourier transforms, such as the DFT or the DTFT, we can obtain a description of the signal in terms of its frequency content. Then, in order to decide whether one or another frequency is present in the time-domain signal, we examine the frequency-domain representation for significant values at certain frequencies. But what constitutes a significant value? We can threshold signals in the frequency domain, just as we did in the time domain in Chapter 4. But, again, how do we set the threshold for what constitutes a significant frequency component? Parseval's theorem tells us that we can look for a sufficient portion of the signal's energy within a frequency range. We know that the overall frequency-domain energy is proportional to the overall time-domain energy, and the time-domain energy is computable from the signal values. Thus, we can select a threshold for the frequency domain based on some percentage of time-domain energy. Since we know that the total frequency domain energy is proportional to time-domain energy, we do not even have to examine other bands once the threshold is exceeded in some range of frequencies.

As with the DFT, there are a variety of DTFT symmetry properties. At this stage in our exposition, these are routine, and we leave them as exercises. The next section covers a property of the DTFT that applies to linear, translation-invariant systems. It turns out that with the DTFT, we can show that LTI systems have a very benign effect on exponential signals.

7.2.3 LTI Systems and the DTFT

Let us return to the idea of a discrete, linear, translation-invariant system. We introduced discrete LTI systems in the second chapter, and there we showed that LTI systems are characterized by the convolution relation. The system output, $y = Hx$, is the convolution of the input with a fixed signal, $y = h * x$, where $h = H\delta$. The discrete signal $h(n)$ is called the impulse response of the LTI system H. There is a close, important relationship between LTI systems and the DTFT.

Recall that an eigenvector for a finite-dimensional linear map, T, is a vector $\mathbf{v}$ for which $T\mathbf{v} = a\mathbf{v}$, for some constant a. Similarly, we can define an eigenfunction for a system, to be a signal for which $y = Hx = ax$, for some constant value a.

Theorem (Eigenfunctions of LTI Systems). If H is an LTI system, $y = Hx$, where $x(n) = \exp(j\omega n)$, then $x(n)$ is an eigenfunction of the system H.

Proof: By the Convolution Theorem for LTI systems, we have

$$y(n) = (h * x)(n) = \sum_{k=-\infty}^{+\infty} h(k)x(n-k) = \sum_{k=-\infty}^{+\infty} h(k)\exp[j\omega(n-k)]$$

$$= \exp(j\omega n) \sum_{n=-\infty}^{+\infty} h(k)\exp(-j\omega k) = \exp(j\omega n)H(\omega), \qquad (7.88)$$

where $H(\omega)$ is the DTFT of $h(n)$. ∎

The theorem inspires the following definition.

Definition (Frequency Response of LTI Systems). If H is an LTI system, and $h = H\delta$, is the impulse response of H, then $H(\omega)$, the DTFT of $h(n)$, is called the *frequency response* of H.

Note that we have a notational conflict, in that we are using the uppercase H to denote both the LTI system and its frequency response. Of course, writing the frequency response as a function of ω helps to distinguish the two. The context usually makes clear which is the system and which is the frequency-domain representation of the impulse response. So we persist in using the notation, which is a widespread signal theory convention.

It is the behavior of $H(\omega)$ as a function of ω that determines how an LTI system, H, affects the frequencies within a discrete signal. The Eigenfunctions Theorem showed that if $x(n) = \exp(j\omega n)$ is an exponential signal, and $y = Hx$, then $y(n) = x(n)H(\omega)$. So the magnitude of the output, $|y(n)|$, is proportional to the magnitude of the input, $|x(n)|$, and the constant of proportionality is $|H(\omega)|$. Thus, if $|H(\omega)|$ is small, then the system suppresses exponential signals of radial frequency w. And if $|H(\omega)|$ is large, then H passes exponentials $\exp(j\omega n)$. What is meant, however, by the "frequencies within a discrete signal?" If the input signal consists of a pure exponential, $x(n) = \exp(j\omega n) = \cos(\omega n) + j\sin(\omega n)$, of frequency ω radians/second, then the frequency component within the signal is the exponential. It consists of a real and an imaginary sinusoidal component. And, by the theorem, the system's frequency response determines how the system affects the frequency components of $x(n)$. Furthermore, suppose the input signal consists of a sum of scaled exponentials,

$$x(n) = \sum_{k=M}^{N} c_k \exp(j\omega_k n). \tag{7.89}$$

By linearity we have

$$y(n) = H[x(n)] = H\left[\sum_{k=M}^{N} c_k \exp(j\omega_k n)\right] = \sum_{k=M}^{N} c_k H\left[\exp(j\omega_k n)\right]$$

$$= \sum_{k=M}^{N} c_k H\left[\exp(j\omega_k n)\right] = \sum_{k=M}^{N} c_k \exp(j\omega_k n)H(\omega_k) = \sum_{k=M}^{N} H(\omega_k)c_k \exp(j\omega_k n).$$

$$\tag{7.90}$$

Thus, the output consists of the sum of $x(n)$'s frequency components, each further attenuated or amplified by its corresponding value, $H(\omega_k)$. But is it still correct to refer to a general signal's frequency components?

Within certain classes of aperiodic signals, it is indeed possible to approximate them arbitrarily well with sums of exponentials, such as in (7.89). If we can show this, then this justifies the above characterization of the frequency response as admitting and suppressing the various frequency components within a signal (7.90). Let us state our desired result as a theorem.

Theorem (Frequency Components of Aperiodic Signals). Let the signal $x(n)$ have DTFT $X(\omega)$. If $x(n)$ is absolutely summable or square-summable, then it can be approximated arbitrarily well by linear combinations of exponential signals of the form $\{\exp(jn\omega) : \omega = \pi(2m - M)/M$ for some m, $0 < m < M - 1$, $1 < M\}$.

Proof: The key idea is to approximate the synthesis equation integral representation for $x(n)$ in terms of $X(\omega)$:

$$x(n) = \frac{1}{2\pi} \int_{-\pi}^{+\pi} X(\omega) \exp(j\omega n)\, d\omega. \tag{7.91}$$

The trapezoidal rule approximates $x(n)$ by dividing the interval $[-\pi, \pi]$ into $N > 0$ segments of equal width, $2\pi/N$, and summing the areas of the trapezoidal regions. Let $y(n, \omega) = X(\omega)\exp(j\omega n)$. Then, $y(n, -\pi) = y(n, \pi)$, and after some simplification, we get

$$x(n) \approx \frac{1}{M}\big[y(n,-\pi) + y(n,-\pi+2\pi/M) + y(n,-\pi+4\pi/M) + \cdots + y(n,\pi-2\pi/M)\big]$$

$$= \frac{1}{M}\sum_{m=0}^{M-1} y(n,-\pi+2\pi m/M) = \frac{1}{M}\sum_{m=0}^{M-1} X(-\pi+2\pi m/M)\exp[jn(-\pi+2\pi m/M)]$$

$$= \frac{1}{M}\sum_{m=0}^{M-1} X(-\pi+2\pi m/M)\exp\left[jn\pi\left(\frac{2m-M}{M}\right)\right]. \tag{7.92}$$

Since (7.92) is a linear combination of terms of the form $A_m\exp(jn\omega)$, where A_m is a constant, and $\omega = \pi(2m - M)/M$, the proof is complete. ∎

Now, it is possible to investigate the effect an LTI system H, where $h = H\delta$, has on an aperiodic input signal $x(n)$. We first closely approximate $x(n)$ by a linear combination of exponential terms, $\exp(jn\omega)$, $\omega = \pi(2m - M)/M$, as given by the Frequency Components Theorem. By the Eigenfunctions Theorem, the various component exponential terms scale according to the value of the DTFT of $h(n)$, $H(\omega)$:

$$y(n) = (h * x)(n) = \left(h * \sum_{m=0}^{M-1} A_m \exp\left[jn\frac{\pi(2m-M)}{M}\right]\right)(n)$$

$$= \sum_{m=0}^{M-1} A_m \exp\left[jn\frac{\pi(2m-M)}{M}\right]H\left(\frac{\pi(2m-M)}{M}\right) = \sum_{m=0}^{M-1} A_m \exp\left(jn\omega_m\right)H(\omega_m).$$

$$\tag{7.93}$$

Depending on the value of $H(\omega_m)$ at various values of ω_m, then, the frequency components of $x(n)$ are attenuated or amplified by the LTI system H.

Example (Perfect High-Frequency Attenuation System). Let us explore a system H that removes all frequency components above a certain fixed radial frequency, ω_c, from a discrete aperiodic signal, $x(n)$. There is a practical need for such systems. They remove noise from signals prior to segmentation and classification, as we noted in Chapter 4. If the time-domain filter $h(n)$ removes all frequency components above ω_c, the DTFT of $h(n)$, $H(\omega)$, must be zero for $|\omega| > |\omega_c|$, as Figure 7.15 shows. We can compute $h(n)$ for the square pulse in Fig. 7.15(a) as follows.

$$h(n) = \frac{1}{2\pi} \int_{-\pi}^{+\pi} X(\omega) exp(jn\omega) \, d\omega = \frac{1}{2\pi} \int_{-\omega_c}^{+\omega_c} exp(jn\omega) \, d\omega$$

$$= \frac{1}{2\pi} \frac{exp(jn\omega)}{jn} \bigg|_{-\omega_c}^{+\omega_c} = \frac{\sin(n\omega_c)}{\pi n} = \frac{\omega_c}{\pi} \mathrm{sinc}(n\omega_c). \qquad (7.94)$$

However flawless it may be in the frequency domain, as a time-domain noise removal filter, $h(n)$ is quite imperfect. Two fundamental problems render it physically impossible to implement:

- It has infinite support.
- The system H is non causal: $h(n) = 0$ for $n < 0$.

The first point means that we can never finish the convolution sum necessary to calculate the output $y = Hx$. Of course, we can come very close to approximating the

(a)   (b)
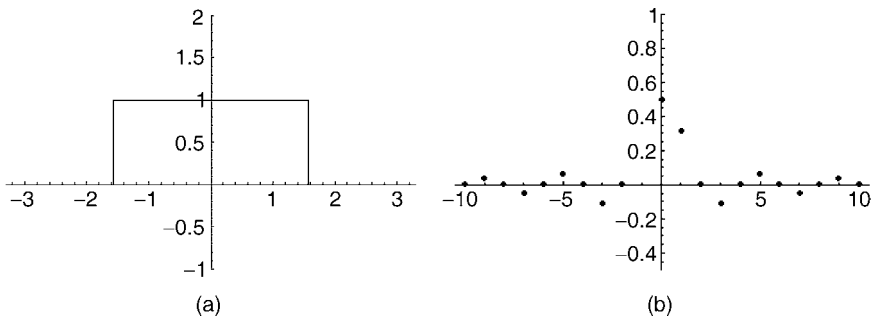
Fig. 7.15. Perfect high-frequency removal. The system with impulse response $h(n)$ and DTFT $H(\omega)$ will remove all frequencies above ω_c if $H(\omega) = 0$ for $|\omega| > \omega_c$. We also expect that H will perfectly preserve frequencies within the range $[-\omega_c, \omega_c]$; in other words, if $|\omega| \leq \omega_c$, then $H(\omega) = 1$. Thus, $H(\omega)$ resembles a square pulse centered in $[-\pi, \pi]$, as in panel (a). Here, $\omega_c = \pi/2$. The time-domain sinc signal in (b) gives rise to such a frequency-domain representation.

perfect filter output by prolonging the summation until further terms are negligible. But worse is the non causality. This implies that computing the convolution $y = h *$ x requires future values of the input signal $x(n)$. In the next chapter we shall uncover filter design techniques that avoid these problems.

7.3   THE SAMPLING THEOREM

Presentations of signal theory throughout the text have alternated between analog developments and discrete developments. We have worked either in the analog world or in the discrete world. Sampling an analog signal at regular intervals produces a discrete signal, but so far nothing has been proffered as an interconnection between the analog source and the discrete result. However, now have the theoretical tools in hand to effect a unification of the two realms of signal theory. The unification takes place using not time domain methods, but rather frequency-domain methods. Perhaps this is not so unexpected. After all, we noted that the discrete-time Fourier transform very much resembles the analog Fourier series and that there is a Hilbert space isomorphism between the analog space $L^2[-\pi, \pi]$ (or, more precisely, its equivalence classes of signals equal almost everywhere) and the discrete space l^2.

7.3.1   Band-Limited Signals

One of the key ideas in linking the analog and discrete worlds is the notion of a bandlimited analog signal. This means, informally, that the frequency-domain representation of the signal has finite support. Physically, this is a realistic assumption, as no physical signal can have frequency components that go arbitrarily high in frequency. Nature can only shake so fast.

Definition (Band-Limited Signal).   An analog signal $x(t)$ is *band-limited* if its Fourier transform, $X(\omega)$, exists and has finite support.

To discover the connection to band-limited signals, let us consider anew the operation of sampling an analog signal. If $x(t)$ is a continuous, absolutely integrable analog signal and $T > 0$, then it may be sampled at intervals T to produce the discrete signal $s(n) = x(nT)$. Let us suppose that $s(n) \in l^1$ so that the DTFT sum converges uniformly to $S(\omega)$,

$$S(\omega) = \sum_{n=-\infty}^{+\infty} s(n) \exp(-jn\omega), \tag{7.95}$$

and, hence, that $s(n)$ is represented by the DTFT synthesis equation,

$$s(n) = \frac{1}{2\pi} \int_{-\pi}^{+\pi} S(\omega) \exp(j\omega n) \, d\omega \tag{7.96}$$

Because $x(t) \in L^1$, $x(t)$ is represented by the FT's synthesis equation,

$$x(t) = \frac{1}{2\pi} \int_{-\infty}^{+\infty} X(\omega) \exp(j\omega t) \, d\omega \qquad (7.97)$$

where $X(\omega)$ is the radial Fourier transform of $x(t)$. Since $s(n) = x(nT)$, we get another representation of $s(n)$:

$$s(n) = x(nT) = \frac{1}{2\pi} \int_{-\infty}^{+\infty} X(\omega) \exp(j\omega nT) \, d\omega \qquad (7.98)$$

Now we have a derivation of the discrete signal values from both a discrete frequency representation (7.96) and from an analog frequency representation (7.98). The observation is both easy and important. (The reason that we did not take note of this earlier is that only now do we have Fourier and inverse Fourier transforms for both analog and discrete signals!) The key to discovering the hidden bond between the analog and discrete signal domains lies in finding mathematical similarities in the integrands of the DTFT and FT synthesis equations.

Connecting the two integrands in (7.96) and (7.98) involves both the sampling interval, T, and the bandwidth of the original analog signal, $x(t)$. Since the IFT integral (7.98) has infinite limits, and the IDTFT integral has finite limits, the prospects for relating the two integrands seem dim. Note, however, that if the FT of $x(t)$ is band-limited, then the nonzero values of $X(\omega)$ are confined to an interval, $[-b, +b]$, where $b > 0$. The FT integral representation of $s(n)$ becomes

$$s(n) = x(nT) = \frac{1}{2\pi} \int_{-b}^{+b} X(\omega) \exp(j\omega nT) \, d\omega \qquad (7.99)$$

A change of integration variable, $\theta = \omega T$, converts (7.99) into the form

$$s(n) = x(nT) = \frac{1}{2\pi T} \int_{-bT}^{+bT} X\left(\frac{\theta}{T}\right) \exp[jn\theta] \, d\theta \qquad (7.100)$$

Now, if the interval $[-bT, bT] \subseteq [-\pi, \pi]$, then the integrals (7.96) and (7.100) are comparable. Suppose we choose T small enough so that this is true; we space the discrete samples of $x(t)$ so close together that $bT < \pi$. Since $X(\theta/T)$ is zero outside $[-bT, bT]$,

$$s(n) = x(nT) = \frac{1}{2\pi} \int_{-\pi}^{+\pi} \frac{1}{T} X\left(\frac{\theta}{T}\right) \exp[jn\theta] \, d\theta \qquad (7.101)$$

(Observe carefully that none of this analysis would be valid without $x(t)$ being band-limited.) Now there are two different representations of the discrete signal $x(n)$: one (7.96) dependent on $S(\omega)$, the DTFT of $s(n)$, and another (7.101) dependent on a

scaled, amplified portion of the FT of $x(t)$: $T^{-1}X(\theta/T)$. We know that the DTFT is unique, since it is invertible, and therefore we have $S(\omega) = T^{-1}X(\omega/T)$.

Let us summarize. If the analog signal, $x(t)$, is band-limited, then a sufficiently high sampling rate, T, guarantees that the DTFT of $s(n) = x(nT)$ and the (scaled, amplified) FT of $x(t)$ are equal.

In principle, this fact allows us to reconstruct $x(t)$ from its discrete samples. Suppose, again, that $s(n) = x(nT)$ and that T is so small that $bT < \pi$, where $X(\omega)$ is zero outside $[-b, b]$. From the samples, $s(n)$, we compute the DTFT, $S(\omega)$. Now, by the preceding considerations, $S(\omega) = T^{-1}X(\omega/T)$; in other words, $TS(\omega T) = X(\omega)$. Now we can compute $x(t)$ as the IFT of $X(\omega)$. So, indeed, the samples of a band-limited analog signal can be chosen close enough together that the original signal can be recovered from the samples.

The next section we will give this abstract observation some practical value.

7.3.2 Recovering Analog Signals from Their Samples

Now let us work toward a precise characterization of the conditions under which an analog signal is recoverable by discrete samples. One outcome of this will be an elucidation of the concept of aliasing, which occurs when the conditions for ideal reconstruction are not completely met.

In the previous section we studied the relationship between the DTFT and the FT for band-limited signals $x(t)$ and discrete signals $s(n) = x(nT)$, $T > 0$. The next theorem relaxes the assumption that $x(t)$ is band-limited.

Theorem (DTFT and FT). Suppose that $x(t) \in L^1$ is an analog signal, $T > 0$, and $s(n) = x(nT)$. If $s(n) \in l^1$ so that the DTFT sum converges uniformly to $S(\omega)$, then

$$S(\omega) = \frac{1}{T} \sum_{k=-\infty}^{+\infty} X\left(\frac{\omega + 2\pi k}{T}\right). \tag{7.102}$$

Proof: Continuing the development of the previous section, we set $\theta = \omega T$ for a change of integration variable:

$$s(n) = x(nT) = \frac{1}{2\pi} \int_{-\infty}^{+\infty} X(\omega)\exp(j\omega nT)\,d\omega = \frac{1}{2\pi T} \int_{-\infty}^{+\infty} X\left(\frac{\theta}{T}\right)\exp(j\theta n)\,d\theta. \tag{7.103}$$

Let $Y(\theta) = T^{-1}X(\theta/T)$. Then,

$$s(n) = x(nT) = \frac{1}{2\pi} \int_{-\infty}^{+\infty} X(\omega)\exp(j\omega nT)\,d\omega = \frac{1}{2\pi} \int_{-\infty}^{+\infty} Y(\theta)\exp(j\theta n)\,d\theta. \tag{7.104}$$

If we assume that $x(t)$ is band-limited, then X—and hence Y—have finite support; this reduces (7.104) to a finite integral as in the previous section. Let us not assume here that $x(t)$ is band-limited and instead investigate how (7.104) can be written as a

sum of finite integrals. Indeed, we can break (7.104) up into 2π-wide chunks as follows:

$$s(n) = \frac{1}{2\pi} \int_{-\infty}^{+\infty} Y(\theta) \exp(j\theta n)\, d\theta = \frac{1}{2\pi} \sum_{k=-\infty}^{\infty} \int_{-\pi+2\pi k}^{\pi+2\pi k} Y(\theta) \exp(j\theta n)\, d\theta \qquad (7.105)$$

The insight behind this is that the chunk of $Y(\theta)$ corresponding to $k = 0$ should look like $S(\omega)$ on $[-\pi, \pi]$, and the others, corresponding to $k = 0$, should be negligible if T is small and $x(t)$ is approximately band-limited. Now set $\phi = \theta - 2\pi k$ to get

$$s(n) = \frac{1}{2\pi} \sum_{k=-\infty}^{\infty} \int_{-\pi}^{\pi} Y(\phi+2\pi k) \exp[j(\phi+2\pi k)n]\, d\phi$$

$$= \frac{1}{2\pi} \sum_{k=-\infty}^{\infty} \int_{-\pi}^{\pi} Y(\phi+2\pi k) \exp(j\phi n)\, d\phi = \frac{1}{2\pi} \int_{-\pi}^{\pi} \sum_{k=-\infty}^{\infty} Y(\phi+2\pi k) \exp(j\phi n)\, d\phi$$

$$(7.106)$$

The interchange of the order of the summation and the integration is allowable, because the sum converges uniformly to $Y(\theta)$ on $\mathbb{R}$. Now we have (7.106) in the form of the DTFT synthesis equation (7.96) for $s(n)$:

$$s(n) = \frac{1}{2\pi} \int_{-\pi}^{\pi} S(\omega) \exp(j\omega n)\, d\omega = \frac{1}{2\pi} \int_{-\pi}^{\pi} \sum_{k=-\infty}^{\infty} Y(\omega+2\pi k) \exp(j\omega n)\, d\omega \qquad (7.107)$$

Since the DTFT is invertible, together (7.107) entails

$$S(\omega) = \sum_{k=-\infty}^{\infty} Y(\omega+2\pi k) = \frac{1}{T} \sum_{k=-\infty}^{\infty} X\left(\frac{\omega+2\pi k}{T}\right) \qquad (7.108)$$

as desired.   ∎

Equation (7.108) shows that $S(\omega)$, the DTFT of $s(n)$, is the sum of an infinite number of copies of $Y(\omega)$, each translated by $2\pi k$ (Figure 7.16). Note that the sum of shifted copies of $Y(\omega)$ is 2π-periodic. The situation of interest is when there is no overlap in the shifted $Y(\omega)$ components in Figure 7.16. In this case, $Y(\omega)$ resembles a single period of the DTFT of $s(n)$, $S(\omega)$. We may recover $x(t)$ from the discrete samples, because we then know that $X(\omega) = TY(T\omega)$, and $x(t)$ derives from $X(\omega)$ via the FT synthesis equation. What criteria are necessary for there to be no overlap of the shifted versions of $Y(\omega)$? The famous Shannon–Nyquist theorem answers this question.

Theorem (Shannon–Nyquist Sampling Theorem). Suppose that $x(t) \in L^1$ is an analog signal, $T > 0$, and $s(n) = x(nT)$. If $s(n) \in l^1$, so that the DTFT sum converges uniformly to $S(\omega)$, then $x(t)$ may be recovered from the samples $s(n)$ if
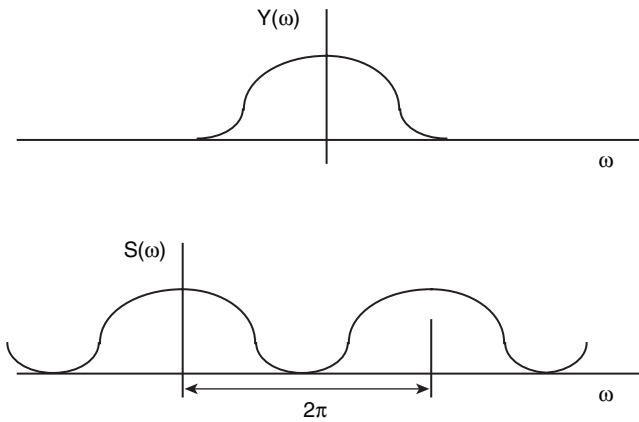
Fig. 7.16. $S(\omega)$ is the sum of shifted copies of $Y(\omega)$. If Y decays quickly in the frequency domain, then its translated copies overlap only slightly or not at all.

- $x(t)$ is band-limited.
- The sampling frequency $F = T^{-1} > 2F_{max}$, where $|X(\omega)| = 0$ for $\omega > 2\pi F_{max}$.

Proof: We deduce a series of equivalent criteria that prevent overlap. Now, since the difference between two translates is 2π, no overlap occurs when all of the nonzero values of $Y(\omega)$ lie within $[-\pi, \pi]$. Thus, $Y(\omega) = 0$ for $|\omega| > b > 0$, for some $b < \pi$. This means that $X(\omega) = 0$ for $|\omega| > |b/T|$, since $Y(\omega) = T^{-1}X(\omega/T)$. Equivalently, for no overlap, it must be the case that $x(t)$ is band-limited, and its nonzero spectral values within $[-\pi/T, \pi/T]$. Let $0 < B$ be the least upper bound of $\{\omega : X(\omega) > 0 \text{ or } X(-\omega) > 0\}$. Then $B < \pi/T$. But, B is measured in radians per second, and to give it in hertz we need to use the radians-to-hertz conversion formula, $\omega = 2\pi f$. Thus, the criterion for no overlap becomes $2\pi F_{max} < \pi/T$, where F_{max} is the maximum frequency component of $x(t)$ in hertz, and T is the sampling period $s(n) = x(nT)$. Finally, this means precisely that $2F_{max} < 1/T = F$. ∎

When the analog signal $x(t)$ is not band-limited, aliasing is inevitable, because the shifted versions of $Y(\omega)$ must overlap. When $x(t)$ is band-limited and the sampling interval is too large, the shifted versions of $Y(\omega)$ overlap with one another and in their summation produce artifacts that are not part of the shape of the true analog spectrum of $x(t)$. Figure 7.17 illustrates a situation with aliasing.

These results motivate the following definition [3].

Definition (Nyquist Rate). If a signal $x(t)$ is band-limited, then its *Nyquist rate* is $F = 2F_{max}$, where F_{max} is the least upper bound of values ω, where $|X(\omega)| \neq 0$.

Thus, sampling at intervals T such that $1/T$ is above the Nyquist rate permits perfect reconstruction of the analog signal $x(t)$ from its discrete samples, $s(n) = x(nT)$.
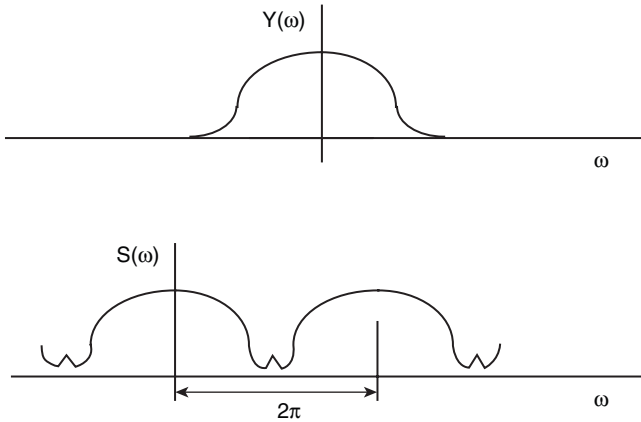
Fig. 7.17. Aliasing occurs when the shifted copies of $Y(\omega)$ overlap. In this situation, a single period of the spectrum of $s(n)$, $S(\omega)$, is *not* an exact replica of $X(\omega)$. High frequency components are added into some of the low frequency components. The result is that the reconstructed analog signal does not equal the original time domain signal, $x(t)$.

We now know, in principle, the conditions under which an analog signal may be reconstructed from its discrete samples. The next two sections limn out the theory of sampling. Section 7.3.3 provides an elegant reconstruction formula; it shows how to rebuild the analog signal from a simple set of interpolating signals. Section 7.3.4 casts a shadow on all these proceedings, however. A central result, the Uncertainty Principle, informs us that a signal with good frequency-domain behavior (as regards sampling and reconstruction) must have poor time-domain characteristics.

7.3.3   Reconstruction

The next theorem gives a formula for reconstructing, or interpolating, an analog signal from its samples. The conditions discovered above for ideal reconstruction must apply, of course. And there are some qualifications to this result that should be kept in mind:

- It assumes that perfect discrete samples are obtained in the sampling operation.
- The interpolating signals are not finitely supported.
- There are an infinite number of signals that must be summed to achieve perfect reconstruction.

Clearly, there are practical concerns with implementing analog signal reconstruction using this method. The reconstruction derives from evaluating the Fourier transform synthesis equation integral over a single period of the DTFT of $s(n)$, the signal samples.

Theorem (Shannon–Nyquist Interpolation Formula). Suppose that $x(t) \in L^1$ is an analog signal, $T > 0$, and $s(n) = x(nT)$. Let $s(n) \in l^1$ so that the DTFT sum converges uniformly to $S(\omega)$. Also, let $2F_{max} < F = 1/T$, where F_{max} is the maximum frequency component of $x(t)$ in hertz. Then $x(t)$ may be recovered from $s(n)$ by the following sum:

$$x(t) = \sum_{n=-\infty}^{+\infty} s(n)\operatorname{sinc}\left(\frac{\pi t}{T} - n\pi\right) \tag{7.109}$$

Proof: The criterion for reconstruction applies, $x(t)$ is band-limited, and we find $x(t)$ from the IFT integral:

$$x(t) = \frac{1}{2\pi} \int_{-\infty}^{+\infty} X(\omega)\exp(j\omega t)\, d\omega = \frac{1}{2\pi} \int_{-\pi/T}^{+\pi/T} X(\omega)\exp(j\omega t)\, d\omega \tag{7.110}$$

Now, the DTFT of $s(n)$ is given by (7.108) for all $\omega \in \mathbb{R}$, and (because there is no overlap of the shifted versions of the Fourier transform) for $\omega \in [-\pi/T, \pi/T]$, we have $TS(\omega) = X(\omega/T)$, whence

$$x(t) = \frac{T}{2\pi} \int_{-\pi/T}^{+\pi/T} S(T\omega)\exp(j\omega t)\, d\omega \tag{7.111}$$

Inserting the DTFT analysis equation sum for $S(T\omega)$ in (7.111) and interchanging integration and summation gives

$$x(t) = \frac{T}{2\pi} \int_{-\pi/T}^{+\pi/T} \left[\sum_{n=-\infty}^{\infty} s(n)\exp(-jT\omega n) \right] \exp(j\omega t)\, d\omega$$

$$= \frac{T}{2\pi} \sum_{n=-\infty}^{\infty} s(n) \int_{-\pi/T}^{+\pi/T} \exp(-jT\omega n)\exp(j\omega t)\, d\omega$$

$$= \frac{T}{2\pi} \sum_{n=-\infty}^{\infty} s(n) \int_{-\pi/T}^{+\pi/T} \exp[j\omega(t - Tn)]\, d\omega \tag{7.112}$$

The last definite integral evaluates to a sinc signal:

$$x(t) = \frac{T}{2\pi} \sum_{n=-\infty}^{\infty} s(n) \int_{-\pi/T}^{+\pi/T} \exp[j\omega(t - Tn)]\, d\omega = \sum_{n=-\infty}^{\infty} s(n) \frac{\sin\left[\frac{\pi}{T}(t - Tn)\right]}{\left[\frac{\pi}{T}(t - Tn)\right]}$$

$$= \sum_{n=-\infty}^{\infty} s(n)\operatorname{sinc}\left(\frac{\pi t}{T} - \pi n\right) \tag{7.113}$$

and the proof is complete. ∎

Another way to interpret this result is to note that, for a given sampling interval T, the set of the analog sinc functions, $\text{sinc}(\pi t/T - \pi n)$, span the space of band-limited signals.

7.3.4 Uncertainty Principle

The concept of a band-limited signal demands further scrutiny. If it was not at the beginning of this discussion, it is certainly clear now how important band-limited signals are for signal processing. Whenever the motivation is to cast an analog signal in digital form and reproduce it—perhaps with some intermediate processing steps applied—then a major consideration is how well discrete samples can represent the original signal. Technologies such as compact disc players succeed or fail based on whether they can sample signals fast enough to beat the Nyquist rate. In analyzing a signal, we also begin with a real-world—analog—signal; then we sample it, process it, and load it into a computer. In the computer, software algorithms build a structural description of the signal and then attempt to classify, identify, and recognize the signal or its fragments. Admittedly, the algorithms may destroy the original form of the signal. But the representation by the interpolation formula is useful, since the coefficients of the expansion indicate a certain signal similarity to the interpolating sinc functions. These may be a basis for classification. And this whole classification procedure gets started with an observation that the source analog signals enjoy a strict limitation on the extent of their frequency content.

This does beg the question, How common are band-limited signals? A signal, $x(t)$, is band-limited when $X(\omega) = \mathcal{F}[x(t)]$ has finite support. If the signal is band-limited, but still has high-frequency components, then a proportionately higher sampling frequency is necessary for ideal signal reconstruction. So, in general, we seek signals whose spectral values are concentrated, or localized, about the origin, $\omega = 0$. We confess that real signals—be they analog or discrete—do not continue unabated forever in the time domain; they must eventually die out. And for practical reasons, such as available memory in a signal analysis system, this time-domain locality is an important consideration. But can we also expect good frequency-domain behavior from finitely supported analog signals?

It is easy to see that a nonzero signal cannot be finitely supported in both domains, because if $x(t)$ and $X(\omega)$ have finite support, then $x(t) = x(t)[u(t + a) - u(t - a)]$ for some $a > 0$. The FT of $x(t)$ is therefore the convolution of the FT of $x(t)$ and the analog boxcar signal $b(t) = u(t + a) - u(t - a)$. But $B(\omega)$ is a sinc-type function, and since $X(\omega)$ is nonzero, the convolution of the two in the frequency domain does not have finite support, a contradiction.

Let us state and prove another famous result, the Uncertainty Principle, which shows that there is an insurmountable tradeoff between frequency-domain locality and time-domain locality. First, however, we need to define the concept of the locality of a signal in the time and frequency domains. We invoke concepts from statistics; namely, the locality of a signal is associated with the second moment, or the variance, of its values.

Definition (Time- and Frequency-Domain Locality). The *time-domain locality* of a signal $x(t)$ is

$$\Delta_t^2(x) = \int\limits_{-\infty}^{+\infty} |x(t)|^2 \, t^2 dt, \qquad (7.114a)$$

and its *frequency-domain locality* is

$$\Delta_\omega^2(X) = \int\limits_{-\infty}^{+\infty} |X(\omega)|^2 \, \omega^2 d\omega \qquad (7.114b)$$

The uncertainty principle holds for signals that decay faster than the reciprocal square root signal. This is necessary for the convergence of the second-order moment integral.

Theorem (Uncertainty Principle). Suppose that $x(t)$ is an analog signal, $\|x\|_2 = 1$, and $x^2(t)t \to 0$ as $t \to \infty$. Then

$$\sqrt{\frac{\pi}{2}} \le \Delta_t(x)\Delta_\omega(X). \qquad (7.115)$$

Proof: The idea is to apply the analog Cauchy–Schwarz inequality to $tx(t)x'(t)$:

$$\left| \int\limits_{-\infty}^{+\infty} tx(t)x'(t)\, dt \right|^2 \le \int\limits_{-\infty}^{+\infty} |tx(t)|^2 dt \int\limits_{-\infty}^{+\infty} |x'(t)|^2 dt = \Delta_t^2(x) \int\limits_{-\infty}^{+\infty} |x'(t)|^2 \qquad (7.116)$$

Now, $x'(t)$ has radial FT $j\omega X(\omega)$, so the analog version of Parseval's formula (Chapter 5) implies that

$$\int\limits_{-\infty}^{+\infty} |x'(t)|^2 = \frac{1}{2\pi} \Delta_\omega^2(X). \qquad (7.117)$$

Hence,

$$\left| \int\limits_{-\infty}^{+\infty} tx(t)x'(t)\, dt \right|^2 \le \Delta_t^2(x)\frac{1}{2\pi}\Delta_\omega^2(X). \qquad (7.118)$$

The integral in (7.118) is our focus; using the chain rule on its integrand and then integrating it by parts gives

$$\int_{-\infty}^{+\infty} tx(t)x'(t)\,dt = \frac{1}{2}\int_{-\infty}^{+\infty} t\frac{\partial x^2(t)}{\partial t}x'(t)\,dt = \frac{1}{2}tx^2(t)\Big|_{-\infty}^{\infty} - \frac{1}{2}\int_{-\infty}^{+\infty} x^2(t)\,dt \qquad (7.119)$$

Now, $x^2(t)t \to 0$ as $t \to \infty$ and $\|x\|_2 = 1$ imply

$$\int_{-\infty}^{+\infty} tx(t)x'(t)\,dt = \frac{1}{2}\int_{-\infty}^{+\infty} t\frac{\partial x^2(t)}{\partial t}x'(t)\,dt = 0 - \frac{1}{2}\int_{-\infty}^{+\infty} x^2(t)\,dt = -\frac{1}{2}\|x\|^2 = -\frac{1}{2}. \quad (7.120)$$

Hence, from (7.118),

$$\left|-\frac{1}{2}\right|^2 = \frac{1}{4} \le \Delta_t^2(x)\frac{1}{2\pi}\Delta_\omega^2(X), \qquad (7.121)$$

from which (7.115) follows.   ∎

   In the exercises, it is shown that the Gaussian signal achieves this lower bound in the product of joint time- and frequency- domain locality.
   Thinking about the Fourier transform and the Uncertainty Principle, we can understand how poor is its joint locality. Allowing that we may Fourier transform signals of slow decay (Chapter 6) using the generalized FT, the FT of a sinusoid is a pair of pulses in the frequency domain. Also, the FT of a pulse $\delta(t)$ is the constant $\omega = 1$. Thus, signals with extreme locality in one domain transform into signals with no locality whatsoever in the other domain. We will discover the problems that this lack of joint locality causes when we work through frequency-domain applications in Chapter 9. Chapters 10 and 11 develop transformation theories—very modern theories, it turns out—that furnish good local time and frequency decompositions of signals. Finally, in the last chapter, we apply these short-time Fourier and wavelet transforms to signal analysis problems.

7.4   SUMMARY

The detailed investigation and intense interest in discrete frequency transforms is a relatively recent phenomenon, and this is an altogether curious circumstance in view of the very tractable nature of the mathematical underpinnings. Analog theory—as some readers now just catching their breath would doubtlessly urge—is much more difficult. Historically, discrete frequency transforms have been explored since the time of Gauss, but it is only with the development of digital computers that the fast computational methods have attracted wide interest and investigation.

Most of the exercises are basic problems that reinforce the concepts developed in the text. The next chapter considers an extension of the DTFT, called the *z*-transform. Chapter 9 considers applications of frequency-domain analysis to signal interpretation problems.

REFERENCES

1. J. W. Cooley and J. W. Tukey, An algorithm for the machine calculation of complex Fourier series, *Mathematics of Computation,* vol. 19, pp. 297–301, 1965.

2. C. E. Shannon, A mathematical theory of communication, *Bell Systems Technical Journal,* vol. 27, pp. 379–423 and pp. 623–656, 1948.

3. H. Nyquist, Certain topics in telegraph transmission theory, *Transactions of the AIEE,* vol. 47, pp. 617-644, 1928.

4. J. W. Cooley, P. A. Lewis, and P. D. Welch, Historical notes on the fast Fourier transform, *IEEE Transactions on Audio and Electroacoustics,* vol. AU-15, pp. 76–79, June 1967.

5. P. J. Plauger, *The C++ Standard Library*, PTR Publishers, 1997.

6. DSP Committee of the IEEE Society for Acoustics, Speech, and Signal Processing, *Programs for Digital Signal Processing*, New York: IEEE Press, 1979.

7. W. H. Press, B. P. Flannery, S. A. Teukolsky, and W. T. Vetterling, *Numerical Recipes*, Cambridge: Cambridge University Press, 1986.

8. C. S. Burrus and T. W. Parks, *DFT/FFT and Convolution Algorithms: Theory and Implementation*, New York: Wiley, 1985.

9. S. D. Stearns and R. A. David, *Signal Processing Algorithms in FORTRAN and C*, Englewood Cliffs, NJ: Prentice-Hall, 1988.

10. W. H. Press, B. P. Flannery, S. A. Teukolsky, and W. T. Vetterling, *Numerical Recipes in C*, Cambridge: Cambridge University Press, 1988.

11. H. S. Stone, *High-Performance Computer Architecture*, Reading, MA: Addison-Wesley, 1987.

12. *DSP56000/56001 Digital Signal Processor User's Manual*, Motorola, Inc., 1990.

13. M. Rosenlicht, *Introduction to Analysis*, New York: Dover, 1986.

14. E. Hille, *Analytic Function Theory*, vol. I, Waltham, MA: Blaisdell, 1959.

15. H. S. Carslaw, *An Introduction to the Theory of Fourier's Series and Integrals*, 3rd ed., New York: Dover, 1950.

16. H. F. Davis, *Fourier Series and Orthogonal Functions*, New York: Dover, 1963.

17. J. S. Walker, *Fourier Analysis*, New York: Oxford University Press, 1988.

18. D. C. Champeney, *A Handbook of Fourier Theorems*, Cambridge: Cambridge University Press, 1987.

19. L. Carleson, On convergence and growth of partial sums of Fourier series, *Acta Mathematica,* vol. 116, pp. 135–157, 1966.

20. R. A. Hunt, in *Orthogonal Expansions and Their Continuous Analogues*, Carbondale, IL: Southern Illinois University Press, pp. 235–255, 1968.

21. A. Zygmund, *Trigonometric Series*, vols. 1–2, Cambridge: Cambridge University Press, 1959.

22. Y. Katznelson, *An Introduction to Harmonic Analysis,* New York: Dover, 1976.

PROBLEMS

1. 1.For each of the following signals, $x(n)$, and intervals, $[0, N - 1]$, find the discrete Fourier transform (DFT), $X(k)$:

   (a) $x(n) = \cos(\pi n/3)$ on $[0, 5]$

   (b) $x(n) = \sin(\pi n/3)$ on $[0, 5]$

   (c) $x(n) = \cos(\pi n/3)$ on $[0, 11]$

   (d) $x(n) = 3\sin(\pi n/3) + \cos(4\pi n/3)$ on $[0, 11]$

   (e) $x(n) = \exp(4\pi n/5)$ on $[0, 9]$

   (f) $x(n) = \cos(2\pi n/5 + \pi/4)$ on $[0, 4]$

2. Let $X = \mathcal{F}x$ be the system that accepts a signal of period $N > 0$ at its input and outputs the DFT of x.

   (a) Show that the system $\mathcal{F}$ is linear. That is, suppose that discrete signals $x(n)$ and $y(n)$ both have period $N > 0$. Show that the DFT of $s(n) = x(n) + y(n)$ is $S(k) = X(k) + Y(k)$, where $X(k)$ and $Y(k)$ are the DFTs of $x(n)$ and $y(n)$, respectively.

   (b) Show that the system $\mathcal{F}$ is not translation-invariant.

3. We may apply either the DFT or IDFT equation to transform a signal $x(n)$. Suppose that $x(n)$ has period $N > 0$.

   (a) Show that the DFT and the IDFT of $x(n)$ both have period N.

   (b) Show that if $X(k)$ is the DFT of $x(n)$, then the DFT of $X(k)$ is $Nx(-k)$.

4. Suppose the discrete signal, $x(n)$, has support on the finite interval, $[0, N -1]$, where $N > 0$.

   (a) Show that the signal $x_p(n)$ defined by

   $$x_p(n) = \sum_{k=-\infty}^{\infty} x(n - kN) \qquad (7.122)$$

   is periodic with period N and is identical to $x(n)$ on $[0, N - 1]$.

   (b) Suppose we perform the DFT analysis equation calculation for $x(n)$'s values on $[0, N - 1]$, giving $X(0), X(1), \ldots, X(N - 1)$. Then define $y(n) = (1/N)[X(0) + X(1)e^{2\pi jkn/N} + \cdots + X(N - 1)e^{2\pi j(N-1)n/N}$. Show that $y(n) = x_p(n)$ for all n.

5. Some of the first examples in this chapter showed that the delta signal $\delta(n)$ has DFT $\Delta(k) = 1$, and the signal signal $x(n) = [\underline{1}, 1, 1, 1, 0, 0, 0, 0]$ has DFT $X(k) = [\underline{4}, 1 - (1 + \sqrt{2})j, 0, 1 - (\sqrt{2} - 1)j, 0, 1 + (\sqrt{2} - 1)j, 0, 1 + (1 + \sqrt{2})j]$ on the interval $[0, 7]$. Find the DFT of the following signals, using only the properties of the DFT and without explicitly computing the DFT analysis equation's summation of products.

   (a) $y(n) = x(n - 1) = [\underline{0}, 1, 1, 1, 1, 0, 0, 0]$

   (b) $y(n - k)$ for some $0 < k < 8$

    (c) $y(n) = x(n) + \delta(n) = [\underline{2}, 1, 1, 1, 0, 0, 0, 0]$

    (d) $y(n) = x(n) + \delta(n - 3)$

6. Prove the Convolution in Frequency Theorem. That is, let $x(n)$ and $y(n)$ be periodic signals with period $N > 0$; let $X(k)$ and $Y(k)$ be their DFTs; and let $z(n) = x(n)y(n)$, the termwise product of x and y. Show that the DFT of $z(n)$ is $Z(k) = (1/N)X(k)*Y(k)$, where $X(k)*Y(k)$ is the discrete convolution of $X(k)$ and $Y(k)$.

7. Let signal $x(n)$ be real-valued with period $N > 0$, and let $X(k)$ be its DFT. Prove the following symmetry properties:

    (a) $\mathrm{Re}[X(k)] = \mathrm{Re}[X^*(N - k)] = \mathrm{Re}[X^*(-k)]$

    (b) $\mathrm{Im}[X(k)] = -\mathrm{Im}[X^*(N - k)]$

    (c) $|X(k)| = |X(N - k)|$

    (d) $\arg(X(k)) = -\arg(X(n - k))$.

8. Suppose the DTFT, $X(\omega)$, of the signal $x(n)$ exists. Show that $X(\omega)$ is periodic with period 2π.

9. Suppose that H is a linear, translation-invariant (LTI) system, and let $h(n)$ be its impulse response.

    (a) Suppose H is a finite impulse response (FIR) system. Show that the DTFT of $h(n)$, $H(\omega)$, exists.

    (b) Suppose H is stable: if $x(n)$ is bounded, then $y = Hx$ is also bounded. Show that $H(\omega)$ exists.

10. Consider the two Hilbert spaces, l^2 and $L^2[a, b]$, where $a < b$. (Consider two signals in $L^2[a, b]$ to be the same if they are equal except on a set of Lebesgue measure zero.)

    (a) Show that there is an isomorphism between the discrete Hilbert space l^2 and the analog Hilbert space $L^2[a, b]$.

    (b) Give an explicit definition of a mapping, G, between them that effects the isomorphism.

    (c) The shifted impulses $\{u(n - k): k \in \mathbb{Z}\}$ constitute an orthogonal basis set for l^2; find, therefore, their image under G and show that it is an orthogonal basis as well.

    (d) Are the exponential signals $\{\exp(j\omega n): k \in \mathbb{Z}\}$ an orthogonal basis set for $L^2[a, b]$? Explain.

11. Derive the following properties of the Dirichlet kernel, $D_N(\theta)$.

    (a) Use the properties of the exponential function $\exp(j\theta n)$ to show

$$D_N(\theta) = \frac{1}{2\pi} \sum_{n=-N}^{n=+N} \exp(j\theta n) = \frac{1}{2\pi} + \frac{1}{\pi} \sum_{n=1}^{n=N} \cos(\theta n).$$

    (b) Use the closed-form expression for the partial geometric series summation to show

$$D_N(\theta) = \frac{1}{2\pi} \frac{\sin\left(N\theta + \dfrac{\theta}{2}\right)}{\sin\left(\dfrac{\theta}{2}\right)}.$$

(c) Use (a) to prove

$$\int_0^\pi D_N(\theta)\, d\theta = \frac{1}{2} = \int_{-\pi}^0 D_N(\theta)\, d\theta.$$

(d) From (b), show that $D_N(\theta)$ has its first two zero crossings at the points $\theta_N = \pm\pi/(N + 1/2)$. What is $D_N(0)$?

(e) Use (b) to sketch $D_N(\theta)$ for various values of N. Explain how $D_N(\theta)$ may be considered as the high-frequency sinusoid $\sin(N\theta + \theta/2)$ bounded above by the cosecant envelope $[\csc(\theta/2)]/(2\pi)$ and below by $-[\csc(\theta/2)]/(2\pi)$.

12. Consider the mapping $\mathcal{F}$ that takes $x(n) \in l^2$ to $X(\omega) \in L^2[-\pi, \pi]$, where $X(\omega)$ is the DTFT of $x(n)$. Show that $\mathcal{F}$ is linear, but not quite an isomorphism. Explain how to modify $\mathcal{F}$ so that it becomes a Hilbert space isomorphism.

13. Find the DTFT of the following signals.

(a) $e_k(n) = \delta(n - k)$

(b) $b(n) = [1, 1, 1, \underline{1}, 1, 1, 1]$

(c) $a(n) = b(n) + e_2(n) + 4e_{-3}(n)$

(d) $s(n) = (1/3)^n u(n)$

(e) $x(n) = (5)^n u(2 - n)$

(f) $h(n) = s(n) + 4b(n)$

(g) $y(n) = (x*h)(n)$

14. Find the IDTFT of the following signals.

(a) $E_k(\omega) = \exp(j\omega k)$

(b) $S(\omega) = 3\sin(-7j\omega)$

(c) $C(\omega) = 2\cos(3j\omega)$

(d) $P(\omega) = S(\omega)C(\omega)$

15. Let $x(n)$ and $y(n)$ be discrete signals and $X(\omega)$ and $Y(\omega)$ be their respective DTFTs. Then show the following linearity, time shift, frequency shift, and time reverse properties:

(a) The DTFT of $ax(n) + by(n)$ is $aX(\omega) + bY(\omega)$.

(b) The DTFT of $x(n - m)$ is $\exp(-j\omega m)X(\omega)$.

(c) The IDTFT of $X(\omega - \theta)$ is $\exp(-j\theta n)x(n)$.

(d) The DTFT of $x(-n)$ is $X(-\omega)$.

16. Let the signal $x(n)$ be real-valued and let $X(\omega)$ be its DTFT. If $z \in \mathbb{C}$, then let z^* be the complex conjugate of z, let $\text{Real}(z)$ be its real part, let $\text{Imag}(z)$ be its imaginary part, and let $\arg(z) = \tan^{-1}[\text{Imag}(z)/\text{Real}(z)]$ be the argument of z. Prove the following symmetry properties:

(a) $\text{Real}(X(\omega)) = \text{Real}(X(-\omega))$

(b) $-\text{Imag}(X(\omega)) = \text{Imag}(X(-\omega))$

(c) $X(\omega) = X^*(-\omega)$

(d) $|X(\omega)| = |X(-\omega)|$

(e) $\arg(X(\omega)) = -\arg(X(-\omega))$

17. Let the signal $x(n)$ be real-valued and $X(\omega)$ be its DTFT. If $x_e(n) = [x(n) + x(-n)]/2$ is the even part of $x(n)$, and $x_o(n) = [x(n) - x(-n)]/2$ is the odd part of $x(n)$, then find

(a) The DTFT of $x_e(n)$

(b) The DTFT of $x_o(n)$

18. Let the signal $x(n)$ be real-valued and let $X(\omega)$ be its DTFT. Show the following symmetry properties, which use the notation of the previous two problems:

(a) The DTFT of $x^*(n)$ is $X^*(-\omega)$, and the DTFT of $x^*(-n)$ is $X^*(\omega)$.

(b) The DTFT of $x_e(n)$ is $\text{Real}(X(\omega))$, and the DTFT of $x_o(n)$ is $j[\text{Imag}(X(\omega))]$.

(c) The DTFT of $\text{Real}(X(n))$ is $X_e(\omega)$, and the DTFT of $j[\text{Imag}(X(n))]$ is $X_o(\omega)$.

19. We know that the perfect high-frequency removal (low-pass) filter has impulse response

$$h(n) = \frac{\omega_c}{\pi} \text{sinc}(n\omega_c) = \frac{\omega_c}{\pi} \frac{\sin(n\omega_c)}{n\omega_c} = \frac{\sin(n\omega_c)}{n\pi}.$$

(a) Consider the discrete system whose frequency response, $G(\omega)$, is unity for $|\omega| > \omega_c$ and zero otherwise. Explain why G may be considered a perfect high-pass filter. Find the time-domain filter, $g(n)$, corresponding to $G(\omega)$. Is $g(n)$ physically implementable? Explain.

(b) Consider the discrete system whose frequency response, $P(\omega)$, is unity for $\omega_h \geq |\omega| \geq \omega_l$ and zero otherwise. Explain the description of P as being an ideal bandpass filter. Find the time-domain filter, $g(n)$, corresponding to $G(\omega)$. Is $g(n)$ physically implementable? Explain.

(c) If $h(n)$ is an ideal time-domain low-pass filter, it is possible to approximate it by a finitely supported filter by zeroing terms above $n = N > 0$. In signal analysis applications, such as Chapter 4 considered, explain the possible uses of such a filter. For what types of applications is this filter useful? What applications are not served by this filter?

(d) Consider the questions in part (c) for perfect high-pass and bandpass filters.

20. Analog signal $x(t)$ has radial FT $X(\omega)$ shown below.
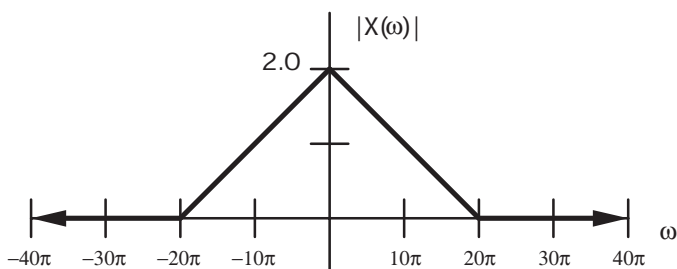
(a) What is the Nyquist rate for this signal in hertz?

(b) If $s(n) = x(nT)$, where $1/T = F = 15$ hertz, sketch the DTFT of s, $S(\omega)$.

(c) Sketch the radial FT of an ideal low-pass filter H such $y = Hs$ is not aliased when sampled at $F_S = 15$ hertz.

The remaining problems extend some of the ideas in the text.

21. Suppose we are given a formula for the DTFT of a discrete signal $h(n)$: $H(\omega) = P(\omega)/Q(\omega)$, where P and Q are both polynomials in ω. Develop two methods to find $h(n)$.

22. Show that a nonzero signal $x(n)$ cannot be finitely supported in both the time and frequency domains.

(a) Show that there is a $k > 0$ such that $x(n) = x(n)[u(n + k) - u(n - k)] = x(n)b(n)$, where $u(n)$ is the discrete unit step signal.

(b) Find the discrete-time Fourier transform of $b(n)$: $B(\omega)$.

(c) Apply the Convolution-in-Frequency Theorem to the product $x(n)b(n)$ to find an equivalent expression for $X(\omega)$.

(d) Derive a contradiction from the two expressions for $X(\omega)$.

23. Let $g(t) = A\exp(-\sigma t^2)$. Use the conditions for equality in the analog Schwarz inequality, and find constants A and σ so that

$$\sqrt{\frac{\pi}{2}} \leq \Delta_t (g)\Delta_\omega(G)$$

The *z*-Transform

The *z*-transform generalizes the discrete-time Fourier transform. It extends the domain of the DTFT of $x(n)$, the periodic analog signal $X(\omega)$, which is defined for $\omega \in \mathbb{R}$, to a function defined on $z \in \mathbb{C}$, the complex plane.

The motivations for introducing the *z*-transform are diverse:

- It puts the powerful tools of complex analysis at our disposal.
- There are possibilities for analyzing signals for which the DTFT analysis equation does not converge.
- It allows us to study linear, translation-invariant systems for which the frequency response does not exist.
- Some specialized operations such as signal subsampling and upsampling are amenable to *z*-transform techniques.
- It provides a compact notation, convenient for describing a variety of systems and their properties.

Having listed these *z*-transform benefits, we hasten to add that very often a series of *z*-transform manipulations concludes with a simple restriction of the transform to the DTFT. So we will not be forgetting the DTFT; on the contrary, it is the basic tool that we will be using for the spectral analysis of aperiodic discrete signals for the remainder of the book.

The development of *z*-transform theory proceeds along lines similar to those used in Chapter 7 for the DTFT. Many of the proofs of *z*-transform properties, for example, are very like the corresponding derivations for the DTFT. We often leave these results as exercises, and by now the reader should find them straightforward. This is a short chapter. It serves as a bridge between the previous chapter's theoretical treatment of discrete Fourier transforms and the diverse applications—especially filter design techniques—covered in Chapter 9.

Texts on systems theory introduce the *z*-transform and its analog world cousin, the Laplace transform [1, 2]. Books on digital signal processing [3–7] cover the *z*-transform in more detail. Explanations of the transform as a discrete filter design tool may also be found in treatments oriented to specific applications [8–10]. The

z-transform was applied in control theory [11–13] long before it was considered for the design of digital filters [14]. Specialized treatises include Refs. 15 and 16.

8.1 CONCEPTUAL FOUNDATIONS

The z-transform has a very elegant, abstract definition as a power series in a complex variable. This power series is two-sided; it has both positive and negative powers of z, in general. Furthermore, there may be an infinite number of terms in the series in either the positive or negative direction. Like the DTFT, the theory of the z-transform begins with an investigation of when this doubly-infinite summation converges. Unlike the DTFT, however, the z-transform enlists a number of concepts from complex analysis in order to develop its existence and inversion results. This section introduces the z-transform, beginning with its abstract definition and then considering some simple examples.

Readers may find it helpful to review the complex variables tutorial in Chapter 1 (Section 1.7) before proceeding with the z-transform.

8.1.1 Definition and Basic Examples

The z-transform generalizes the DTFT to a function defined on complex numbers. To do this, we replace the complex exponential in the DTFT's definition with $z \in \mathbb{C}$. A simple change it is, but we shall nevertheless face some interesting convergence issues. For our effort, we will find that many of the properties of the DTFT carry through to the extended transform, and they provide us with tools for analyzing signals and systems for which the DTFT is not well-suited.

Definition (z-Transform). If $x(n)$ is a discrete signal and $z \in \mathbb{C}$, then its z-*transform,* $X(z)$, is defined by

$$X(z) = \sum_{n=-\infty}^{+\infty} x(n)z^{-n}. \tag{8.1}$$

To avoid some notation conflicts, the fancy-z notation, $X = \mathcal{Z}(x)$, is often convenient for writing the z-transform of $x(n)$. The signal $x(n)$ and the complex function $X(z)$ are called a z-transform pair. We also call (8.1) the z-transform *analysis equation.* Associated with a z-transform pair is a *region of convergence* (the standard acronym is ROC): $\text{ROC}_X = \{z \in \mathbb{C}: X(z) \text{ exists}\}$. Sometimes as $|z|$ gets large, the value $X(z)$ approaches a limit. In this case, it is convenient to indicate that $\infty \in \text{ROC}_X$. The notation $\mathbb{C}^+$ is useful for the so-called *extended complex plane*: $\mathbb{C}$ augmented with a special element, ∞.

Let us postpone, for a moment, convergence questions pertaining to the z-transform sum. Note that taking the restriction of complex variable z to the unit circle, $z = \exp(j\omega)$, and inserting this in (8.1), gives the DTFT. The DTFT is the restriction of the z-transform to the unit circle of the complex plane, $|z| = 1$: $X[\exp(j\omega)] = X(\omega)$, where the first "$X$" is the z-transform, and the second "X" is the DTFT of $x(n)$, respectively.

There is another form of the z-transform that uses only the causal portion of a signal.

Definition (One-sided z-Transform). If $x(n)$ is a discrete signal and $z \in \mathbb{C}$, then its *one sided z-transform*, $X^+(z)$, is defined by

$$X^+(z) = \sum_{n=0}^{+\infty} x(n)z^{-n}, \tag{8.2}$$

The one-sided, or unilateral, z-transform is important for the specialized problem of solving linear, constant-coefficient difference equations. Typically, one is given difference equations and initial conditions at certain time instants. The task is to find all the discrete signal solutions. The one-sided z-transform agrees with the standard two-sided transform on signals $x(n) = 0$ for $n < 0$. The linearity property is the same, but the shifting property differs. These ideas and an application are considered in the problems at the end of the chapter.

As with the DTFT, the infinite sum in the z-transform summation (8.1) poses convergence questions. Of course, the sum exists whenever the signal $x(n)$ has finite support; the corresponding z-transform $X(z)$ is a sum of powers (positive, zero, and negative) of the complex variable z. Let us consider some elementary examples of finding the z-transforms of discrete signals. Finding such z-transform pairs, $x(n)$ and $X(z)$, is typically a matter of finding the z-transform of a signal $y(n)$ which is similar to $x(n)$ and then applying the z-transform properties to arrive at $X(z)$ from $Y(z)$.

Example (Discrete Delta). Let us start simple by considering the discrete delta signal, $\delta(n)$. For any $z \in \mathbb{C}$, only the summand corresponding to $n = 0$ is nonzero in (8.1), and thus $\Delta(z) = Z(\delta)(z) = 1$ for all $z \in \mathbb{C}$.

Example (Square Pulse). Again, let us consider the impulse response of the moving average system, H. It has impulse response $h(n) = [1, 1, \underline{1}, 1, 1]$; in other words, $h(n) = 1$ for $-2 \le n \le 2$, and $h(n) = 0$ otherwise. We write immediately

$$H(z) = \sum_{n=-\infty}^{+\infty} h(n)z^{-n} = \sum_{n=-2}^{+2} z^{-n} = z^{2n} + z^n + 1 + z^{-n} + z^{-2n}. \tag{8.3}$$

Note that $H(z)$ exists for all $z \in \mathbb{C}$, $z \ne 0$. Thus, a signal, $x(n)$, whose DTFT converges for all $\omega \in \mathbb{R}$ may have a z-transform, $X(z)$, which does not converge for all $z \in \mathbb{C}$. In general, a finitely supported signal, $x(n)$, that is nonzero for positive time instants will not have a z-transform, $X(z)$, which exists for $z = 0$.

Example (Causal Exponential Signal). Consider the signal $x(n) = a^n u(n)$. We calculate

$$X(z) = \sum_{n=-\infty}^{+\infty} x(n)z^{-n} = \sum_{n=0}^{\infty} a^n z^{-n} = \sum_{n=0}^{\infty} \left(\frac{a}{z}\right)^n = \frac{1}{1-\frac{a}{z}} = \frac{z}{z-a}, \tag{8.4}$$

where the geometric series sums in (8.4) to $z/(z-a)$ provided that $|a/z| < 1$. Thus, we have $\mathrm{ROC}_X = \{z \in \mathbb{C}: |a/z| < 1\} = \{z \in \mathbb{C}: |a| < |z|\}$. In other words, the region of

convergence of the z-transform of $x(n) = a^n u(n)$ is all complex numbers lying outside the circle $|z| = a$. In particular, the unit step signal, $u(n)$, has a z-transform, $U(z) = 1/(1 - z^{-1})$. We may take $a = 1$ above and find thereby that $\mathrm{ROC}_U = \{z \in \mathbb{C} : 1 < |z|\}$.

This example shows that a z-transform can exist for a signal that has no DTFT. If $|a| > 1$ in the previous example, for instance, then the analysis equation for $x(n)$ does not converge. But the z-transform, $X(z)$, does exist, as long as z lies outside the circle $|z| = a$ in the complex plane. Also, the ROC for this example was easy to discover, thanks to the geometric series form taken by the z-transform sum. There is a companion example, which we need to cover next. It illustrates the very important point that the ROC can be the only distinguishing feature between the z-transforms of two completely different signals.

Example (Anti-causal Exponential Signal). Consider the signal $y(n) = -a^n u(-n - 1)$. Now we find

$$Y(z) = \sum_{n=-\infty}^{+\infty} y(n)z^{-n} = \sum_{n=-\infty}^{-1} -a^n z^{-n} = -\sum_{n=1}^{\infty} \left(\frac{z}{a}\right)^n = -\frac{z}{a}\sum_{n=0}^{\infty} \left(\frac{z}{a}\right)^n$$

$$= -\left(\frac{\dfrac{z}{a}}{1 - \dfrac{z}{a}}\right) = \frac{z}{z - a},$$
(8.5)

with the convergence criterion $|z/a| < 1$. In this case, we have $\mathrm{ROC}_Y = \{z \in \mathbb{C} : |z/a| < 1\} = \{z \in \mathbb{C} : |z| < |a|\}$. The region of convergence of the z-transform of $y(n) = -a^n u(-n - 1)$ is all complex numbers lying inside the circle $|z| = a$.

The upshot is that we must always be careful to specify the region of convergence of a signal's z-transform. In other words, given one algebraic expression for $X(z)$, there may be multiple signals for which it is the z-transform; the deciding factor then becomes the region of convergence.

8.1.2 Existence

Demonstrating the convergence of the z-transform for a particular signal makes use of complex variable theory. In particular, the z-transform is a Laurent series [17, 18].

Definition (Power and Laurent Series). A complex power series is a sum of scaled powers of the complex variable z:

$$\sum_{n=0}^{+\infty} a_n z^n.$$
(8.6)

A Laurent series is a two-sided series of the form

$$\sum_{n=-\infty}^{+\infty} a_n z^{-n} = \sum_{n=1}^{+\infty} a_n z^{-n} + \sum_{n=-\infty}^{0} a_n z^{-n}, \tag{8.7}$$

where the a_n are (possibly complex) coefficients. (Most mathematics texts do not use the negative exponent in the definition—their term z^n has coefficient a_n; our definition goes against the tradition so that its form more closely follows the definition of the *z*-transform.) One portion of the series consists of negative powers of *z*, and the other part consists of non-negative powers of *z*. We say the Laurent series (8.7) converges for some $z \in \mathbb{C}$ if both parts of the series converge.

Obviously, we are interested in the situation were the Laurent series coefficients are the values of a discrete signal, $x(n) = a_n$. From complex variable theory, which we introduced in the first chapter, the following results are relevant to Laurent series convergence. We prove the first result for the special case where the *z*-transform of $x(n)$ contains only non-negative powers of *z*; that is, it is a conventional power series in *z*. This will happen when $x(n) = 0$ for $n > 0$.

The next definition identifies upper and lower limit points within a sequence.

Definition (lim sup and lim inf). Let $A = \{a_n : 0 \le n < \infty\}$. Define $A_N = A \setminus \{a_n : 0 \le n < N\}$, which is the set A after removing the first N elements. Let κ_N be the least upper bound of A_N. Then the limit, κ, of the sequence $\{\kappa_N : N > 0\}$ is called the *lim sup* of A, written

$$\kappa = \lim_{N \to \infty} \{\kappa_N : N > 0\} = \lim_{n \to \infty} \sup A = \lim_{n \to \infty} \sup\{a_n : 0 \le n < \infty\}. \tag{8.8}$$

Similarly, if we let λ_N be the greatest lower bound of A_N, then the limit of the sequence $\{\lambda_N : N > 0\}$ is called the *lim inf* [1] of A:

$$\lambda = \lim_{N \to \infty} \{\lambda_N : N > 0\} = \lim_{n \to \infty} \inf A = \lim_{n \to \infty} \inf\{a_n : 0 \le n < \infty\}. \tag{8.9}$$

Sometimes a sequence of numbers does not have a limit, but there are convergent subsequences within it. The lim sup is the largest limit of a convergent subsequence, and the lim inf is the smallest limit of a convergent subsequence, respectively. The sequence has a limit if the lim sup and the lim inf are equal. Readers with advanced calculus and mathematical analysis background will find these ideas familiar [19–21]. We need the concept of the lim sup to state the next theorem. Offering a convergence criterion for a power series, it is a step toward finding the ROC of a *z*-transform.

Theorem (Power Series Absolute Convergence). Suppose $x(n)$ is a discrete signal; its *z*-transform, $X(z)$, has only non-negative powers of *z*,

$$X(z) = \sum_{n=0}^{+\infty} a_n z^n; \tag{8.10}$$

---

[1] These are indeed the mathematical community's standard terms. The lim sup of a sequence is pronounced "lim soup," and lim inf sounds just like its spelling.

and

$$\kappa = \lim_{n\to\infty} \sup\{|a_n|^{1/n} : 1 \le n < \infty\}. \tag{8.11}$$

Then $X(z)$ converges absolutely for all z with $|z| < \kappa^{-1}$ and diverges for all $|z| > \kappa^{-1}$. (This allows A to be unbounded, in which case $\kappa = \infty$ and, loosely speaking, $\kappa^{-1} = 0$.)

Proof: Consider some z such that $|z| < \kappa^{-1}$, and choose $\lambda > \kappa$ so that λ^{-1} lies between these two values: $|z| < \lambda^{-1} < \kappa^{-1}$. Because $\kappa = \lim \sup A$, there is an N such that $|a_n|^{1/n} < \lambda$ for all $n > N$. But this implies that $|a_n z^n| < |z\lambda|^n$ for $n > N$. Since $|z\lambda| < 1$ by the choice of λ, the power series (8.10) is bounded above by a convergent geometric series. The series must therefore converge absolutely. We leave the divergence case as an exercise. ∎

Definition (Radius of Convergence). Let $\rho = \kappa^{-1}$, where κ is given by (8.11) in the Power Series Absolute Convergence Theorem. Then ρ is called the *radius of convergence* of the complex power series (8.10).

Corollary (Power Series Uniform Convergence). Suppose $x(n)$ is a discrete signal; its z-transform, $X(z)$, has only non-negative powers of z as in the theorem (8.10); and κ is defined as in (8.11). Then for any $0 < R < \rho = \kappa^{-1}$, $X(z)$ converges uniformly in the complex disk $\{z \in \mathbb{C} : |z| < R < \rho = \kappa^{-1}\}$.

Proof: For any disk of radius R, $0 < R < \rho$, the proof of the theorem implies that there is a convergent geometric series that bounds the power series (8.10). Since the convergence of the dominating geometric series does not depend on z, the sum of the series in z (8.10) can be made arbitrarily close to its limit independent of z. The convergence is therefore uniform. ∎

Corollary (Analyticity of the Power Series Limit). Again, if $x(n)$ is a discrete signal; its z-transform, $X(z)$, has the form (8.10); and $\rho = \kappa^{-1}$ is given by (8.11), then $X(z)$ is an analytic function, the derivative $X'(z) = dX(z)/dz$ can be obtained by termwise differentiation of the power series (8.10), and $\text{ROC}_X = \text{ROC}_{dX/dz}$.

Proof: This proof was given already in Section 1.7, where we assumed the uniform convergence of the power series. From the Uniform Convergence Corollary, we know this to be the case within the radius of convergence, ρ; the result follows. ∎

Finally, we consider the situation that most interests us, the Laurent series. The z-transform assumes the form of a Laurent series. We have, in fact, already developed the machinery we need to discover the region of convergence of a z-transform. We apply the Power Series Convergence Theorems above for both parts of the Laurent series: the negative and non-negative powers of z.

Theorem (z-Transform Region of Convergence). Let $x(n)$ be a discrete signal and let $X(z) = X_1(z) + X_2(z)$ be its z-transform (which may be two-sided). Suppose

$X(z) = X_1(z) + X_2(z)$, where $X_2(z)$ consists on non-negative powers of z, and $X_1(z)$ contains only negative powers of z. Then $X(z)$ converges absolutely within an annulus of the complex plane, $\text{ROC}_X = \{z \in \mathbb{C}: \rho_1 < |z| < \rho_2\}$, where ρ_1 and ρ_2 are the radii of convergence of $X_1(z)$ and $X_2(z)$, respectively. The convergence of the z-transform Laurent series is uniform within any closed annulus contained in ROC_X, and its limit, $X(z)$ is analytic within this same closed annulus.

Proof: $X(z)$'s true power series portion, $X_2(z)$, converges inside some circle $|z| = \rho_2$, where ρ_2 is the radius of convergence. The $X_1(z)$ portion of $X(z)$ converts to power series form by setting $w = z^{-1}$. Then the radius of convergence may be found for the power series $Y(w) = X_1(w^{-1}) = X_1(z)$. $Y(w)$ converges inside some circle of radius R_1, say, which means $X_1(z)$ converges outside the circle $\rho_1 = 1/R_1$. The region formed by intersecting the exterior of the circle $|z| = \rho_1$ and the interior of the circle $|z| = \rho_2$ is the annulus we seek. ∎

Example. Suppose $x(n)$ is given as follows:

$$x(n) = \begin{cases} 3^{-n} & \text{for } n \geq 0, \\ -4^n & \text{for } n < 0. \end{cases} \tag{8.12}$$

Let $x_1(n) = a^n u(n)$, where $a = 1/3$, and $x_2(n) = -b^n u(-n - 1)$, where $b = 4$. Then $x(n) = x_1(n) + x_2(n)$. We have computed the z-transforms of signals of this form in earlier examples. We have $X(z) = X_1(z) + X_2(z)$, where $X_1(z)$ converges outside the circle $|z| = 1/3$, and $X_2(z)$ converges inside the circle $|z| = 4$ (Figure 8.1).
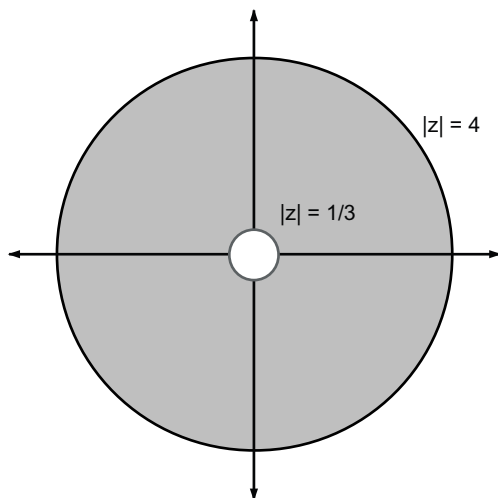
Fig. 8.1. The region of convergence of the z-transform of $x(n) = 3^{-n}u(n) - 4^n u(-n-1)$ is an open annulus in the complex plane. The causal portion of $x(n)$ produces a power series in z^{-1}, which converges outside the circle $|z| = 1/3$. The anti-causal part of $x(n)$ produces a power series in z, which converges inside the circle $|z| = 4$.

Let us now turn to the basic properties of the z-transform. The above example made tacit use of the linearity property. The z-transform properties we cover resemble very closely those of our previously studied transforms, especially the DTFT. One subtlety is the region of convergence, which we must account for during algebraic and analytic operations on the transformed signals.

8.1.3 Properties

The properties of the z-transform closely resemble those of the discrete transform that it generalizes—the discrete-time Fourier transform. With the z-transform, there is a twist, however; now the region of convergence of the transform figures prominently in validating the properties. We divide this section's results into two categories: basic properties and those that rely on the principles of contour integration in the complex plane.

8.1.3.1 Basic Properties. This theorems herein are much like those we developed for the DTFT. Their proofs are also similar, involve familiar methods, and we leave them as exercises for the most part. One caveat in dealing with the z-transform is the region of convergence; one must always be careful to specify this annulus and to consider the special cases of $z = 0$ and $z = \infty$.

Proposition (Linearity, Time Shift, Frequency Shift, and Time Reversal). Let $x(n)$ and $y(n)$ be discrete signals and let $X(z)$ and $Y(z)$ be their z-transforms, respectively. Then

- (a) (Linearity) The z-transform of $ax(n) + by(n)$ is $aX(z) + bY(z)$, and its region of convergence contains $\text{ROC}_X \cap \text{ROC}_Y$.
- (b) (Time Shift) The z-transform of $x(n - m)$ is $z^{-m}X(z)$, and its region of convergence is ROC_X, except, perhaps, that it may include or exclude the origin, $z = 0$, or the point at infinity, $z = \infty$;
- (c) (Frequency Shift, or Time Modulation) Let $a \in \mathbb{C}$. Then the z-transform of $a^n x(n)$ is $Y(z) = X(z/a)$ with $\text{ROC}_Y = |a|\text{ROC}_X$.
- (d) (Time Reversal) If $Z[x(n)] = X(z)$, and $y(n) = x(-n)$, then $Z[y(n)] = Y(z) = X(z^{-1})$, with $\text{ROC}_Y = \{z \in \mathbb{C}: z^{-1} \in \text{ROC}_X\}$.

Proof: In (a), the formal linearity is clear, but it is only valid where both transforms exist. If $a \neq 0$, then the ROC of $aX(z)$ is ROC_X, and a similar condition applies to $Y(z)$. However, when the two transforms are added, cancellations of their respective terms may occur. This expands the sum's ROC beyond the simple intersection of ROC_X and ROC_Y. Also in (b), multiplication of $X(z)$ by z^k for $k > 0$ may remove from ROC_X. However, if $X(z)$ contains only powers $z^{-|n|}$, for $n > k$, then multiplication by z^k will have no effect on ROC_X. Similarly, multiplication of $X(z)$ by z^k for $k < 0$ may remove 0 from ROC_X, and so on. The other cases are just as straightforward to list. Toward proving (c), let us remark that the power series expansion for $X(z/a)$ will have a new region of convergence that is scaled by $|a|$ as follows: If $\text{ROC}_X = \{z: r_1 < |z| < r_2\}$, then $\text{ROC}_Y = \{z: |a|r_1 < |z| < |a|r_2\}$. Time reversal is an exercise. ∎

Proposition (Frequency Differentiation). Suppose $x(n)$ is a discrete signal, and $X(z)$ is its z-transform. Then the z-transform of $nx(n)$ is $-zdX(z)/dz$. The region of convergence remains the same, except that ∞ may be deleted or 0 may be inserted.

Proof: Similar to the Frequency Differentiation Property of the DTFT. Note that within the region of convergence, the z-transform Laurent series is differentiable. Since we multiply by a positive power of z, will be deleted from the ROC if the highest power of z in $X(z)$ is z^0. Similarly, 0 may be inserted into the ROC if the lowest power of z in $X(z)$ is z^{-1}. ∎

Example. Suppose $x(n) = -na^n u(-n - 1)$. Find $X(z)$. We already know from the example of the anti-causal exponential signal in Section 8.1.1 that the z-transform of $-a^n u(-n - 1)$ is $(1 - a/z)^{-1}$, with ROC $= \{z \in \mathbb{C}: |z| < |a|\}$. Thus, the frequency differentiation property applies and we have

$$X(z) = -z \frac{d}{dz}\left(1 - \frac{a}{z}\right)^{-1} = z\left(1 - \frac{a}{z}\right)^{-2} \frac{d}{dz}\left(1 - \frac{a}{z}\right) = \frac{az}{(z-a)(z-a)}. \tag{8.13}$$

Also, $\text{ROC}_X = \{z \in \mathbb{C}: |z| < |a|\}$. The properties are useful in finding the z-transforms of new signals.

The z-transform is not without a convolution theorem. Sometimes signal processing systems must deal with signals or system impulse responses for which the DTFT does not converge. A useful tool in this instance is the z-transform. And (not unexpectedly by this point!) there is a convolution result for the z-transform; it finds use in studying LTI systems, questions of stability, subsampling, and interpolation operations for discrete signals.

Theorem (Convolution in Time). Let $x(n)$ and $y(n)$ be signals; let $X(z)$ and $Y(z)$ their z-transforms, respectively; and let $w = x * y$. Then the z-transform of $w(n)$ is $W(z) = X(z)Y(z)$, and $\text{ROC}_W \supseteq \text{ROC}_X \cap \text{ROC}_Y$.

Proof: The proof of the DTFT Convolution-in-Time Theorem extends readily to the z-transform:

$$W(z) = \sum_{n=-\infty}^{\infty} w(n)z^{-n} = \sum_{n=-\infty}^{\infty} (x * y)(n)z^{-n} = \sum_{n=-\infty}^{\infty} \left(\sum_{k=-\infty}^{\infty} x(k)y(n-k) \right)z^{-n}$$

$$= \sum_{n=-\infty}^{\infty} \sum_{k=-\infty}^{\infty} x(k)y(n-k)z^{-(n-k)}z^{-k} = \sum_{k=-\infty}^{\infty} \sum_{n=-\infty}^{\infty} x(k)y(n-k)z^{-(n-k)}z^{-k}$$

$$= \sum_{k=-\infty}^{\infty} x(k)z^{-k} \sum_{n=-\infty}^{\infty} y(n-k)z^{-(n-k)} = X(z)Y(z). \tag{8.14}$$

If $x \in \text{ROC}_X \cap \text{ROC}_Y$, then the z-transform's Laurent series converges absolutely. This justifies the step from an iterated summation to a double summation as well as the interchange in the order of summation in (8.14). Hence, $\text{ROC}_W \supseteq \text{ROC}_X \cap \text{ROC}_Y$. ∎

Corollary (LTI System Function). Suppose H is a discrete LTI system $y = Hx$; its impulse response is $h = H\delta$; and $X(x)$, $Y(z)$, and $H(z)$ are the z-transforms of $x(n)$, $y(n)$, and $h(n)$, respectively. Then, $Y(z) = H(z)X(z)$.

Proof: The output signal $y = h * x$ by the Convolution Theorem for LTI Systems, and the result follows from the theorem. ∎

Definition (System or Transfer Function). Let H be a discrete LTI system $y = Hx$ and $h = H\delta$ its impulse response. Then the z-transform of $h(n)$, $H(z)$ is called the system function or the transfer function for the system H.

Remark. For our multiple uses of the uppercase "H," we once again ask the reader's indulgence. Here, both the system itself and its impulse response, a complex-valued function of a complex variable, are both denoted "H."

8.1.3.2 *Properties Involving Contour Integration.* With the DTFT synthesis equation, we can identify a time-domain signal $x(n)$ with the analog Fourier Series coefficients of its DTFT, $X(\omega)$. The interconnection is at once elegant and revealing. The z-transform is like the DTFT, in that it is a discrete transform with an inversion relation which involves a continuous domain integration operation. However, because the domain of definition of the z-transform is a region in the complex plane, the inversion formula becomes quite exotic: It depends on a complex contour integral.

Readers who skimmed the material in Section 1.7 may wish to review it more carefully before proceeding with the next several theorems.

Theorem (Inversion). Suppose $x(n)$ is a discrete signal and $X(z)$ is its z-transform. If C is any simple, counterclockwise, closed contour of the complex plane; the origin is in the interior of C; and $C \subseteq \text{ROC}_X$, then

$$x(n) = \frac{1}{2\pi j} \oint_C X(z) z^{n-1} dz. \tag{8.15}$$

Proof: The integrand in (8.15) contains a power of z, and the contour is closed; this suggests the Cauchy integral theorem from Section 1.7.3.

$$\frac{1}{2\pi j} \oint_C X(z) z^{n-1} dz = \frac{1}{2\pi j} \oint_C \left[\sum_{k=-\infty}^{k=+\infty} x(k) z^{-k} \right] z^{n-1} dz = \frac{1}{2\pi j} \sum_{k=-\infty}^{k=+\infty} x(k) \oint_C z^{n-k-1} dz.$$

$$\tag{8.16}$$

Once again, inserting the analysis equation directly into the integral and then interchanging the order of summation and integration pays off. Since the *z*-transform is absolutely and uniformly convergent within its ROC, the order of summation and integration is unimportant in (8.16). Recall, from Section 1.7.3, the Cauchy integral theorem:

$$\frac{1}{2\pi j}\oint_C z^m \, dz = \begin{cases} 0 & \text{if} \quad m \neq -1, \\ 1 & \text{if} \quad m = -1. \end{cases} \tag{8.17}$$

As a consequence, all terms in the summation of are zero except for the one where $n = k$. This implies that

$$x(n) = \frac{1}{2\pi j}\oint_C X(z)z^{n-1} \, dz, \tag{8.18}$$

as desired.   ∎

Equation (8.18) is the *z*-transform synthesis equation.

Example (Unit Circle Contour). Suppose now that $Z(x(n)) = X(z)$ and that ROC_X contains the unit circle: $C = \{z : |z| = 1\} \subseteq \text{ROC}_X$. Then, $z = \exp(j\omega)$ on C, $\omega \in [-\pi, +\pi]$; $dz = j\exp(j\omega) \, d\omega$; and evaluating the inverse *z*-transform contour integral gives

$$\frac{1}{2\pi j}\oint_C X(z)z^{n-1} \, dz = \frac{1}{2\pi j}\oint_{|z|=1} X(z)z^{n-1} \, dz = \frac{1}{2\pi j}\int_{-\pi}^{+\pi} X(e^{j\omega})(e^{j\omega})^{n-1} \, je^{j\omega} \, d\omega$$

$$= \frac{1}{2\pi}\int_{-\pi}^{+\pi} X(e^{j\omega})(e^{j\omega})^n \, d\omega = \frac{1}{2\pi}\int_{-\pi}^{+\pi} X(\omega)\exp(jn\omega) \, d\omega. \tag{8.19}$$

In (8.19), $X(e^{j\omega})$ is the *z*-transform evaluated at $z = \exp(j\omega)$, and $X(\omega)$ is the DTFT of $x(n)$ evaluated at ω, $-\pi \leq \omega \leq \pi$. This example thus shows that if C is the unit circle and it lies within ROC_X, then the inverse *z*-transform relation reduces to the IDTFT.

Prominent among the *z*-transform's basic properties in the previous section, the Convolution-in-Time Theorem linked convolution in time to simple multiplication in the *z*-domain. The next theorem is its counterpart for *z*-domain convolutions. Although this results lacks the aesthetic appeal of the DTFT's Convolution-in-Frequency Theorem, it will nevertheless prove useful for discrete filter design applications in the next chapter.

Theorem (Convolution in the *z*-Domain). Let $s(n) = x(n)y(n)$ be the termwise product of $x(n)$ and $y(n)$; $Z(x(n)) = X(z)$, with $\text{ROC}_X = \{z \in \mathbb{C} : r_X < |z| < R_X\}$; and $Z(y(n)) = Y(z)$, where $\text{ROC}_Y = \{z \in \mathbb{C} : r_Y < |z| < R_Y\}$. Then, $\text{ROC}_S \supseteq \{z \in \mathbb{C} : r_X r_Y < |z| < R_X R_Y\}$. Furthermore, let C be a simple, closed contour of the complex plane whose interior contains the origin. If $\text{ROC}_{X(w)} \cap \text{ROC}_{Y(z/w)}$ contains C, then

$$S(z) = \frac{1}{2\pi j}\oint_C X(w)Y\left(\frac{z}{w}\right)w^{-1} \, dw. \tag{8.20}$$

Proof: The z-transform analysis equation for $S(z)$ is

$$S(z) = \sum_{n=-\infty}^{+\infty} s(n)z^{-n} = \sum_{n=-\infty}^{+\infty} x(n)y(n)z^{-n} = \sum_{n=-\infty}^{+\infty} \left[\frac{1}{2\pi j} \oint_C X(w)w^{n-1} \right] y(n)z^{-n},$$

(8.21)

where the z-transform synthesis equation (8.18), with dummy variable of integration w, replaces $x(n)$ inside the sum. This substitution is valid for any simple, closed path C, when $C \subseteq \mathrm{ROC}_X$. Summation and integration may change order in , so long as $z \in \mathrm{ROC}_S$, where uniform convergence reigns:

$$S(z) = \frac{1}{2\pi j} \oint_C X(w) \sum_{n=-\infty}^{+\infty} y(n) \left(\frac{z}{w} \right)^{-n} w^{-1}dw = \frac{1}{2\pi j} \oint_C X(w)Y \left(\frac{z}{w} \right) w^{-1}dw. \quad (8.22)$$

When does $S(z)$ exist? We need $C \subseteq \mathrm{ROC}_X = \{w \in \mathbb{C}: r_X < |w| < R_X\}$ and $z/w \in \mathrm{ROC}_Y = \{z \in \mathbb{C}: r_Y < |z| < R_Y\}$. The latter occurs if and only if $r_Y < |z/w| < R_Y\}$; this will be the case if $|w|r_Y < |z| < |w|R_Y$ for $w \in \mathrm{ROC}_X$. Hence ROC_S includes $\{z \in \mathbb{C}: r_Xr_Y < |z| < R_XR_Y\}$. The contour integral in (8.22) will exist whenever $w \in C$ and $z/w \in \mathrm{ROC}_Y$; in other words, $C \subseteq \mathrm{ROC}_X \cap \mathrm{ROC}_{Y(z/w)}$, as stated. ∎

Corollary (Parseval's Theorem). Suppose that $x(n), y(n) \in l^2$, $\mathcal{Z}(x(n)) = X(z)$, and $\mathcal{Z}(y(n)) = Y(z)$. If C is a simple, closed contour whose interior contains the origin, and $C \subseteq \mathrm{ROC}_X \cap \mathrm{ROC}_{Y*(1/w*)}$, then

$$\langle x,y \rangle = \sum_{n=-\infty}^{+\infty} x(n)y*(n) = \frac{1}{2\pi j} \oint_C X(w)Y* \left(\frac{1}{w*} \right) w^{-1}dw. \quad (8.23)$$

Proof: The inner product $\langle x, y \rangle$ exists, since x and y are square-summable, and if $s(n) = x(n)y*(n)$, then $s(n) \in l^1$ (Cauchy–Schwarz). If $\mathcal{Z}(s(n)) = S(z)$, then

$$S(z) = \sum_{n=-\infty}^{+\infty} x(n)y*(n)z^{-n}, \quad (8.24)$$

so that

$$\langle x,y \rangle = \sum_{n=-\infty}^{+\infty} x(n)y*(n) = S(1). \quad (8.25)$$

It is an easy exercise to show that $\mathcal{Z}(y*(n)) = Y*(z*)$; and together with the Convolution in z-Domain Theorem (8.22), this entails

$$\langle x,y \rangle = S(1) = \frac{1}{2\pi j} \oint_C X(w)Y* \left(\frac{1}{w*} \right) w^{-1}dw, \quad (8.26)$$

completing the proof. ∎

8.2 INVERSION METHODS

Given a complex function of a complex variable, $X(z)$, there are three methods for finding the time domain signal, $x(n)$, such that $Z[x(n)] = X(z)$. These approaches are:

- Via the inverse *z*-transform relation, given by the contour integral (8.15).
- Through an expansion of $X(z)$ into a Laurent series; then the $x(n)$ values read directly from the expansion's coefficient of z^{-n}.
- By way of algebraic manipulation (especially using partial fractions) of $X(z)$ into a form in which its various parts are readily identified as the *z*-transforms of known discrete signals. This approach relies heavily on the *z*-transform's basic properties (Section 8.2.1).

Actually, the second two methods are the most useful, because the contour integrals prove to be analytically awkward. This section considers some examples that illustrate each of these *z*-transform inversion tactics.

8.2.1 Contour Integration

Let us look first at the easiest nontrivial example using contour integration in the complex plane to discover the discrete signal $x(n)$ whose *z*-transform is the given complex function $X(z)$. On first reading, this section can be reviewed casually. But those readers who accepted our invitation—several chapters back—to skip the complex variables tutorial should note that those ideas are key to this approach for *z*-transform inversion.

Example (Inversion by Contour Integration). Suppose $X(z) = z/(z - a)$, $a \neq 0$, with $\text{ROC}_X = \{z \in \mathbb{C}: |a| < |z|\}$. Of course, we already know the signal whose *z*-transform is $X(z)$; it is the causal exponential signal $a^n u(n)$ from the example in Section 8.1.1. But, in order to learn the technique, let us proceed with pretenses toward discovery. From the *z*-transform synthesis equation (8.15), we may choose the contour C to be a circle outside $z = |a|$ and immediately write

$$x(n) = \frac{1}{2\pi j} \oint_C X(z) z^{n-1} dz = \frac{1}{2\pi j} \oint_C \frac{z^n}{(z - a)} dz. \qquad (8.27)$$

Is the contour integral (8.27) easy to evaluate? To the fore, from complex analysis, comes a powerful tool: the Cauchy residue theorem (Section 1.7.3). Assume that C is a simple, closed curve; $a_m \notin C$, $1 < m < M$; $f(z)$ is a complex function, which is analytic (has a derivative df/dz) on and within C, except for poles ($|f(z)| \to \infty$ near a pole) at each of the a_m. The residue theorem then states that

$$\frac{1}{2\pi j} \oint_C f(z) \, dz = \sum_{m=1}^{M} \text{Res}(f(z), a_m). \qquad (8.28a)$$

Recall that the residue of $f(z)$ at the pole $z = p$ is given by

$$\text{Res}(f(z), p) = \begin{cases} \dfrac{1}{(k-1)!} g^{(k-1)}(p) & \text{if } p \in \text{Interior}(C), \\ 0 & \text{otherwise,} \end{cases} \tag{8.28b}$$

where k is the order of the pole, $g(z)$ is the nonsingular part of $f(z)$ near p, and $g^{(k-1)}$ (p) is the $(k-1)$th derivative of $g(z)$ evaluated at $z = p$. (Complex function $f(z)$ has a pole of order $(k-1)$ at $z = 0$ if there exists $g(z)$ such that $f(z) = g(z)/(z-p)^k$, $g(z)$ is analytic near $z = p$, and $g(p) \neq 0$.) Let us continue the example. To find $x(n)$, $n \geq 0$, we set $f(z) = z^n/(z-a)$, as in (8.27). Note that $f(z)$ is analytic within C, except for a first-order pole at $z = a$. Therefore, $g(z) = z^n$, and we have $\text{Res}(f(z), a) = g^{(0)}(a) = x(n) = a^n$. For non-negative values of n, computing the contour integral (8.27) is generally quite tractable. Elated by this result, we might hope to deduce values $x(n)$, $n < 0$, so easily. When $n < 0$, however, there are multiple poles inside C: a pole at $z = a$ and a pole of order n at $z = 0$. Consider the case $n = -1$. We set $f(z) = z^{-1}/(z-a)$. Thus, the pole at $z = p = 0$ is of order $k = 1$, since $g(z) = (z-a)^{-1}$ is analytic around the origin. Therefore, $\text{Res}(f(z), z = 0) = g^{(0)}(p) = g^{(0)}(0) = (-a)^{-1}$. There is another residue, and we must sum the two, according to (8.28b). We must select a different analytic part of $f(z)$ near the pole at $z = a$; we thus choose $g(z) = z^{-1}$, so that $g(z)$ is analytic near $z = a$ with $f(z) = g(z)/(z-a)^1$. Consequently, this pole is also first order. Since $g^{(0)}(a) = a^{-1} = \text{Res}(f(z), z = a)$, we have $x(-1) = \text{Res}(f(z), z = 0) + \text{Res}(f(z), z = a) = (-a)^{-1} + a^{-1} = 0$. Now let us turn our attention to the case $n = -2$. Now $f(z) = z^{-2}/(z-a)$, whence the pole at $z = 0$ is of order 2. Still, by (8.28b), $x(-2) = \text{Res}(f(z), z = 0) + \text{Res}(f(z), z = a)$, but now $f(z)$ has a pole of order 2 at $z = 0$. First, we set $g(z) = (z-a)^{-1}$ as before, but now we find $\text{Res}(f(z), z = 0) = g^{(1)}(0) = -1(0-a)^{-2} = -a^{-2}$. For the pole at $z = a$, we put $g(z) = z^{-2}$ and verify that $\text{Res}(f(z), z = a) = a^{-2}$. Thus, coincidentally, $x(-2) = -a^{-2} + a^{-2} = 0$. It is possible to show that, indeed, $x(n) = 0$ for $n < 0$. Therefore, $x(n) = a^n u(n)$ for all n.

The lesson of the example is that z-transform inversion by complex contour integration is sophisticated, easy, and fun for $n > 0$ where the integrand in (8.27) has first order poles, but tedious when there are higher-order poles. We seek simpler methods.

8.2.2 Direct Laurent Series Computation

Let us now try to exploit the idea that the z-transform analysis equation is a two-sided power, or Laurent, series in the complex variable z. Given by the z-transform inversion problem are a complex function of z, $X(z)$, and a region of convergence, ROC_X. The solution is to find $x(n)$ so that $Z(x(n)) = X(z)$. Direct Laurent series computation solves the inversion problem by algebraically manipulating $X(z)$ into a form that resembles the z-transform analysis equation (8.1). Then the $x(n)$ values read off directly as the coefficients of the term z^{-n}. Not just any algebraic fiddling will do; the method can go awry if the algebraic manipulations do not stay in consonance with the information furnished by ROC_X.

Once again, we consider a well-known example to learn the technique.

Example (Laurent Series Computation for Causal Discrete Signal). Suppose $X(z) = z/(z - a)$, $a \neq 0$, with $\text{ROC}_X = \{z \in \mathbb{C}: |a| < |z|\}$. Of course, we already know the signal whose z-transform is $X(z)$; it is the causal exponential signal $a^n u(n)$. Performing long division on $X(z)$ produces a Laurent series:

$$X(z) = \frac{z}{z - a} = z - a \; \overline{\left) \begin{matrix} 1 + az^{-1} + a^2 z^{-2} + a^2 z^{-2} + \cdots \\ z \end{matrix} \right.} \tag{8.29}$$

Using the z term in $z - a$ as the principal divisor produces a quotient that is a Laurent expansion. Since ROC_X is the region outside the circle $|z| = a$, we see by inspection that $x(n) = u(n)a^n$.

Now we consider the same $X(z)$, but allow that ROC_X is inside the circle $|z| = a$.

Example (Laurent Series Computation for Anti-causal Discrete Signal). Suppose $X(z) = z/(z - a)$, $a \neq 0$, with $\text{ROC}_X = \{z \in \mathbb{C}: |z| < |a|\}$. Performing long division again, but this time using the $-a$ term in $z - a$ as the principal divisor, produces a different Laurent series:

$$X(z) = \frac{z}{z - a} = -a + z \; \overline{\left) \begin{matrix} -a^{-1} z - a^{-2} z^2 - a^{-3} z^3 - a^{-4} z^4 - \cdots \\ z \end{matrix} \right.} \tag{8.30}$$

The algebraic manipulation takes into account the fact that ROC_X is the region inside the circle $|z| = a$, and the expansion is in positive powers of z. This means that $x(n)$ is anti-causal: $x(n) = -u(-n - 1)a^n$.

The next example complicates matters a bit more.

Example (Quadratic Denominator). Suppose $X(z) = z(z - 2)^{-1}(z - 1)^{-1}$, with $\text{ROC}_X = \{z \in \mathbb{C}: |2| < |z|\}$. Attacking the problem directly with long division gives

$$X(z) = \frac{z}{(z - 2)(z - 1)} = z^2 - 3z + 2 \; \overline{\left) \begin{matrix} z^{-1} + 3z^{-2} + 7z^{-3} + 15z^{-4} - \cdots \\ z \end{matrix} \right.} \tag{8.31}$$

We observe that $x(n) = u(n)(2^n - 1)$ from the derived form of the Laurent series (8.31). We can check this result by using linearity. Note that $X(z) = z(z - 2)^{-1} - z(z - 1)^{-1}$. The first term is the z-transform of $u(n)2^n$, and its radius of convergence is $\{z \in \mathbb{C}: 2 < |z|\}$. The second term is the z-transform of $u(n)1^n$, with $\text{ROC} = \{z \in \mathbb{C}: 1 < |z|\}$. Therefore, their difference, $u(n)(2^n - 1^n)$, has z-transform $z(z - 2)^{-1} - z(z - 1)^{-1}$, whose radius of convergence equals $\{z \in \mathbb{C}: 2 < |z|\} \cap \{z \in \mathbb{C}: 1 < |z|\} = \{z \in \mathbb{C}: 2 < |z|\} = \text{ROC}_X$.

Our method of checking this last example leads to the table lookup technique of the section.

8.2.3   Properties and *z*-Transform Table Lookup

The last method for computing the inverse *z*-transform is perhaps the most common. We tabulate a variety of *z*-transforms for standard signals and use the various properties of the transform to manipulate a given $X(z)$ into a form whose components are *z*-transforms of the known signals. Typically, then, $x(n)$ is a linear combination of these component signals. One standard trick that is useful here is to break up a complicated rational function in z, $X(x) = P(z)/Q(z)$, where P and Q are polynomials, into a sum of simpler fractions that allows table lookup. This is called the partial fractions method, and we will consider some examples of its use as well.

Example. Suppose $X(z) = (1 - az)^{-1}$, with $\mathrm{ROC}_X = \{z \in \mathbb{C}: |z| < |a|^{-1}\}$. From a direct computation of the *z*-transform, we know that $Z[a^n u(n)] = z/(z - a)$, with ROC $= \{z \in \mathbb{C}: |z| > |a|\}$. Let $y(n) = a^n u(n)$ and $x(n) = y(-n)$. The time-reversal property implies

$$X(z) = \frac{z^{-1}}{(z^{-1} - a)} = \frac{1}{(1 - az)}, \tag{8.32}$$

with $\mathrm{ROC}_X = \{z \in \mathbb{C}: z^{-1} \in \mathrm{ROC}_Y\} = \{z \in \mathbb{C}: |z| < |a|^{-1}\}$, as desired.

Table 8.1 provides a list of common signals, their *z*-transforms, and the associated regions of convergence. These pairs derive from

TABLE 8.1. Signals, Their *z*-Transforms, and the Region of Convergence of the *z*-Transform

$x(n)$	$X(z)$	ROC_X
$\delta(n - k)$	z^{-k}	$k > 0 : \{z \in \mathbb{C}^+: z \neq 0\}$
		$k < 0 : \{z \in \mathbb{C}^+ : z \neq \infty\}$
$a^n u(n)$	$z/(z - a)$	$\{z \in \mathbb{C} : |a| < |z|\}$
$-a^n u(-n - 1)$	$z/(z - a)$	$\{z \in \mathbb{C} : |z| < |a|\}$
$a^{-n} u(-n)$	$\dfrac{1}{(1 - az)}$	$\{z \in \mathbb{C} : |z| < |a|^{-1}\}$
$-a^{-n} u(n-1)$	$\dfrac{1}{(1 - az)}$	$\{z \in \mathbb{C}^+ : |z| > |a|^{-1}\}$
$na^n u(n)$	$az/(z^2 - 2az + a^2)$	$\{z \in \mathbb{C}^+ : |a| < |z|\}$
$-na^n u(-n - 1)$	$az/(z^2 - 2az + a^2)$	$\{z \in \mathbb{C} : |z| < |a|\}$
$\cos(an)u(n)$	$\dfrac{z^2 - \cos(a)z}{z^2 - 2\cos(a)z + 1}$	$\{z \in \mathbb{C} : 1 < |z|\}$
$\sin(an)u(n)$	$\dfrac{\sin(a)z}{z^2 - 2\cos(a)z + 1}$	$\{z \in \mathbb{C} : 1 < |z|\}$
$u(n)/(n!)$	$\exp(z)$	$\{z \in \mathbb{C}\}$
$n^{-1}u(n-1)(-1)^{n+1}a^n$	$\log(1 + az^{-1})$	$\{z \in \mathbb{C}^+ : |a| < |z|\}$

- Basic computation using the z-transform analysis equation;
- Application of transform properties;
- Standard power series expansion from complex analysis.

Example. Suppose that

$$X(z) = \frac{z^2 - \left(\dfrac{\sqrt{2}}{2}\right)z}{(z^2 - \sqrt{2}z + 1)},$$

(8.33)

with $\text{ROC}_X = \{z \in \mathbb{C}: |z| > 1\}$. The table entry, $\cos(an)u(n)$, applies immediately. Taking $a = \pi/4$ gives $x(n) = \cos(\pi n/4)u(n)$. Variants of a z-transform pair from Table 8.1 can be handled using the transform properties. Thus, if

$$Y(z) = \frac{1 - \left(\dfrac{\sqrt{2}}{2}\right)z^{-1}}{(z^2 - \sqrt{2}z + 1)},$$

(8.34)

then $Y(z) = z^{-2}X(z)$, so that $y(n) = x(n + 2) = \cos[\pi(n + 2)/4]u(n + 2)$ by the time shift property.

Example (Partial Fractions Method). Suppose that we are given a rational function in the complex variable z,

$$X(z) = \frac{2z^2}{2z^2 - 3z + 1},$$

(8.35)

where $\text{ROC}_X = \{z \in \mathbb{C}: |z| > 1\}$. The partial fraction technique factors the denominator of (8.35), $2z^2 - 3z + 1 = (2z - 1)(z - 1)$, with an eye toward expressing $X(z)$ in the form

$$X(z) = 2z \frac{z}{2z^2 - 3z + 1} = 2z\left[\frac{A}{2z - 1} + \frac{B}{z - 1}\right],$$

(8.36)

where A and B are constants. Let us concentrate on finding the inverse z-transform of $Y(z) = X(z)/(2z)$, the bracketed expression in (8.36). Table 8.1 covers both of its terms: they are of the form $(1 - az)^{-1}$. The sum of these fractions must equal $z(2z^2 - 3z + 1)^{-1}$, so $A(z - 1) + B(2z - 1) = z$. Grouping terms involving like powers of z produces two equations: $A + 2B = 1$, $A + B = 0$. Hence,

$$\frac{X(z)}{2z} = \frac{z}{2z^2 - 3z + 1} = \left[\frac{-1}{2z - 1} + \frac{1}{z - 1}\right] = \left[\frac{1}{1 - 2z} - \frac{1}{1 - z}\right] = Y(z).$$

(8.37)

Now, $y(n) = -2^{-n}u(n - 1) + u(n - 1) = (1 - 2^{-n})u(n - 1)$ by linearity and Table 8.1. Also, $\text{ROC}_Y = \{z \in \mathbb{C}^+: |z| > 2^{-1}\} \cap \{z \in \mathbb{C}^+: |z| > 1\} = \{z \in \mathbb{C}^+: |z| > 1\}$.

Therefore, the z-transform of $x(n) = 2y(n + 1) = (2 - 2^{-n})u(n)$ is $2zY(z)$ by the time shift property.

Example (Partial Fractions, Multiple Roots in Denominator). Now suppose that the denominator of $X(z)$ has multiple roots:

$$X(z) = \frac{z}{(z-1)(z+2)^2}. \tag{8.38}$$

It turns out that a partial fractions expansion of $X(z)/z$ into, say,

$$\frac{X(z)}{z} = \frac{1}{(z-1)(z+2)^2} = \frac{A}{(z-1)} + \frac{B}{(z+2)^2} \tag{8.39}$$

does not work, in general. Rather, the partial fractions arithmetic is satisfactory when $X(z)/z$ is broken down as follows:

$$\frac{X(z)}{z} = \frac{1}{(z-1)(z+2)^2} = \frac{A}{(z-1)} + \frac{B}{(z+2)^2} + \frac{C}{(z+2)}. \tag{8.40}$$

The solutions are $A = 1/7$, $B = 2/7$, and $C = -1/7$. Applying linearity, time shift, and Table 8.1 completes the example. This is left as an exercise.

8.2.4 Application: Systems Governed by Difference Equations

The above theory applies directly to the study of linear, translation-invariant systems where a difference equation defines the input–output relation. Chapter 2 introduced this kind of system (Sections 2.4.2 and 2.10). We shall see here and in Chapter 9 that:

- For such systems, the transfer function $H(z)$ is a quotient of complex polynomials.
- Difference equations govern a wide variety of important signal processing systems.
- Recursive algorithms very efficiently implement these systems on digital computers.
- The filters that arise from difference equations can be derived straightforwardly from equivalent analog systems.
- For almost any type of filter—low-pass, high-pass, bandpass, or band-reject— a difference equation governed system can be devised that very well approximates the required frequency selection behavior.

In fact, the filters within almost all signal analysis systems derive from difference equations, and we describe them by the z-transform of their impulse response.

Suppose that the difference equation for a system H is

$$y(n) = b_0 x(n) + b_1 x(n-1) + \cdots + b_M x(n-M)$$
$$- a_1 y(n-1) - a_2 y(n-2) - \cdots - a_N y(n-N). \tag{8.41}$$

We see that $y(n)$ can be computed from its past N values, $\{y(n) \mid 1 \le n \le N\}$, the current input value $x(n)$, and the past M values of input signal $\{x(n) \mid 1 \le n \le M\}$. Collecting output terms on the left-hand side and input terms on the right-hand side of (8.41), taking the z-transform of both sides, and finally applying the shift property, we have

$$Y(z)\left[1 + \sum_{k=1}^{N} a_k z^{-k} \right] = X(z)\left[\sum_{m=0}^{M} b_m z^{-m} \right]. \tag{8.42}$$

Hence,

$$H(z) = \frac{Y(z)}{X(z)} = \frac{\left[\displaystyle\sum_{m=0}^{M} b_m z^{-m} \right]}{\left[1 + \displaystyle\sum_{k=1}^{N} a_k z^{-k} \right]}, \tag{8.43}$$

confirming that the system function for H is a rational function of a single complex variable.

Now the methods of z-transform inversion come into play. The partial fractions technique converts the rational function (8.43) into a sum of simpler terms to which table lookup applies. Thus, we can find the impulse response $h(n)$ of the LTI system H. Finally, we can compute the response of H to an input signal $x(n)$ by convolution $y(n) = (h * x)(n)$.

Example (Smoothing System). The system H smoothes input signals by weighting the previous output value and adding it to the weighted input value as follows:

$$y(n) = Ay(n-1) + Bx(n). \tag{8.44}$$

By z-transforming both sides of (8.44), we get

$$Y(z) = Az^{-1} Y(z) + BX(z), \tag{8.45}$$

so that

$$H(z) = \frac{Y(z)}{X(z)} = \frac{B}{1 - Az^{-1}}. \tag{8.46}$$

Assuming that the system is causal, so that $h(n) = 0$ for $n < 0$, we have

$$h(n) = BA^n u(n), \tag{8.47}$$

by Table 8.1.

8.3   RELATED TRANSFORMS

This section introduces two other transforms: the chirp z-transform (CZT) and the Zak transform (ZT). A short introduction to them gives the reader insight into recent research efforts using combined analog and discrete signal transformation tools.

8.3.1   Chirp *z*-Transform

The CZT samples the z-transform on a spiral contour of the complex plane [7, 22]. The CZT transform has a number of applications [23]:

- It can efficiently compute the discrete Fourier transform (DFT) for a prime number of points.
- It can be used to increase the frequency resolution of the DFT, zooming in on frequency components (Chapter 9).
- It has been applied in speech [8, 24], sonar, and radar signal analysis [6, 25], where chirp signals prevail and estimations of their parameters—starting frequency, stopping frequency, and rate of frequency change—are crucial.

8.3.1.1 *Definition.* Recall that evaluating the z-transform $X(z)$ of $x(n)$ on the unit circle $z = \exp(j\omega)$ gives the discrete-time Fourier transform: $X(\omega) = [Z(x)](e^{j\omega})$. If $N > 0$ and $x(n)$ is finitely supported on the discrete interval $[0, N-1]$, then $X(z)$ becomes

$$X(z) = \sum_{n=0}^{N-1} x(n)z^{-n}. \tag{8.48}$$

Furthermore, if $\omega = 2\pi k/N$, $0 \le k < N$, so that $z = \exp(2\pi jk/N)$, then the DTFT analysis equation (8.48) becomes a discrete Fourier transform of $x(n)$. So we are evaluating the z-transform $X(z)$ on a discrete circular contour of the complex plane. The idea behind the CZT is evaluate the z-transform on a discrete spiral—as distinct from purely circular—contour. We use the notation and generally follow the presentation of Ref. 7.

Definition (Chirp *z*-Transform). Let $A = A_0\exp(2\pi j\theta_0)$; $W = W_0\exp(2\pi j\phi_0)$; M, $N > 0$ be natural numbers; $x(n) = 0$ outside $[0, N-1]$; and set $z_k = AW^{-k}$ for $0 \le k < M$. The chirp z-transform of $x(n)$ with respect to A and W is

$$X_{A,W}(k) = \sum_{n=0}^{N-1} x(n)z_k^{-n} = \sum_{n=0}^{N-1} x(n)A^{-n}W^{nk}. \tag{8.49}$$

If $A = 1$, $M = N$, and $W = \exp(-2\pi j/N)$, then the CZT gives the DFT of order N for the signal $x(n)$ (exercise). Figure 8.2 shows a typical discrete spiral contour for a CZT.

Further note that if $W_0 > 1$, then the contour spirals inward, whereas $W_0 < 1$ means the contour winds outward (Figure 8.2).
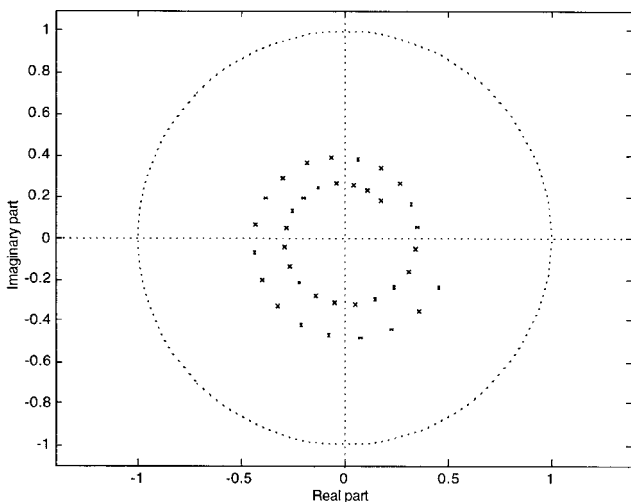
Fig. 8.2. Discrete spiral path for a CZT. Innermost point is $A = (.25)\exp(j\pi/4)$. Ratio between the M = 37 contour samples is $W = (0.98)\exp(-j\pi/10)$. Unit circle $|z| = 1$ is shown by dots.

8.3.1.2 *Algorithm.*

An efficient implementation of the CZT, as a weighted convolution of two special functions, is possible as follows. Using our earlier notation, define the discrete signals $v(n)$ and $y(n)$ by

$$v(n) = W^{\frac{n^2}{2}}, \tag{8.50a}$$

$$y(n) = x(n)v(n)A^{-n}. \tag{8.50b}$$

Since

$$nk = \frac{n^2 + k^2 - (k-n)^2}{2}, \tag{8.51}$$

we calculate

$$X_{A,W}(k) = \sum_{n=0}^{N-1} x(n)A^{-n}W^{\frac{n^2+k^2-\frac{(k-n)^2}{2}}{2}} = W^{\frac{k^2}{2}}\sum_{n=0}^{N-1} y(n)v(k-n). \tag{8.52}$$

Equation (8.52) gives $X_{A,W}(k)$ as the convolution of $y(n)$ and $v(n)$, but weighted by the factor $v(k)$. Now, thanks to the convolution theorem for the DFT, we can compute discrete convolutions by Fourier transforming both signals, taking the frequency-domain product term-by-term, and then inverse transforming the result. Hence, if we have an efficient fast Fourier transform algorithm available, then a CZT may much more efficiently compute the DFT for a problematic—even prime—order N.

Here are the steps in the CZT algorithm [7]:

(i) First, we define $y(n)$:

$$y(n) = \begin{cases} A^{-n}W^{2/2}x(n) & \text{if } n \in [0, N-1], \\ 0 & \text{otherwise.} \end{cases} \tag{8.53}$$

(ii) Next, we determine the size of the FFT operation to perform. Inspecting the convolution equation (8.52), where k ranges between 0 and $M-1$, we see that we need $v(n)$ values for $-N+1 \leq n \leq M-N$, for a total of $M-N-(-N+1)+1 = M$ samples. Since $y(n)$ is supported on $[0, N-1]$, the convolution result will be supported on $[0, (M-1)+(N-1)] = [0, M+N-2]$. So the full $y*v$ requires $(M+N-2)+1 = M+N-1$ samples (of which, for the CZT, we only care about M of them). Thus, we pick a power 2^P (or another FFT-suitable composite integer L), so that $M+N-1 \leq L$. This will be the order of the fast forward transforms and of the inverse transform after pointwise multiplication in the frequency domain.

(iii) We set $v(n)$ to be L-periodic such that

$$v(n) = \begin{cases} W^{-n^2/2} & \text{if } n \in [0, M-1], \\ W^{-(L-n)^2/2} & \text{if } n \in [L-N+1, L-1], \\ 0 & \text{otherwise.} \end{cases} \tag{8.54}$$

(iv) Compute the FFTs, $Y(k)$ and $V(k)$, of $y(n)$ and $v(n)$, respectively.

(v) Compute $G(k) = Y(k)V(k)$, for $0 \leq k \leq L-1$.

(vi) Compute the inverse FFT of $G(k)$: $g(n)$.

(vii) Set

$$X_{A,W}(k) = W^{\frac{k^2}{2}} g(k) \qquad \text{for} \qquad 0 \leq k \leq M-1. \tag{8.55}$$

Evidently, the computational burden within the algorithm remains the three fast transforms [7]. Each of these requires on the order of $L\log_2(L)$ operations, depending, of course, on the particular FFT available. So we favor the CZT when $L\log_2(L)$ is much less than the cost of a full-convolution MN operation.

8.3.2   Zak Transform

The Zak transform (ZT) is an important tool in Chapter 10 (time-frequency analysis). The transform and its applications to signal theory are covered in Refs. 26 and 27.

8.3.2.1   *Definition and Basic Properties.*   The Zak transform maps an analog signal $x(t)$ to a two-dimensional function having independent variables in both time and frequency. We know that restricting the z-transform to the unit circle $|z| = 1$

gives the discrete-time Fourier transform. The idea behind the Zak transform is that discrete signals generally come from sampling analog signals $x(n) = x_a(nT)$, for some $T > 0$, and that we can compute a DTFT for a continuum of such sampled analog signals.

Definition (Zak Transform). Let $a > 0$ and $x(t)$ be an analog signal. Then the Zak transform with parameter a of $x(t)$ is

$$X_a(s,\omega) = \sqrt{a} \sum_{k=-\infty}^{\infty} x(as - ak)\exp(2\pi j\omega k). \tag{8.56}$$

Remark. We use a fancy $\mathcal{Z}_a$ for the map taking an analog signal to its Zak transform: $(\mathcal{Z}_a x)(s, \omega) = X_a(s, \omega)$. Our transform notation uses the sign notation $x(s - k)$ following [28]. Generally, we take $a = 1$ and omit it from the notation: $(\mathcal{Z}x)(s, \omega) = X(s, \omega)$; this is the form of the definition we use later in several parts of Chapter 10.

Proposition (Periodicity). If $X_a(s, \omega)$ is the ZT of $x(t)$, then

$$X_a(s+1,\omega) = \exp(2\pi j\omega)X_a(s,\omega), \tag{8.57a}$$

$$X_a(s,\omega+1) = X_a(s,\omega). \tag{8.57b}$$

Proof: Exercise. ∎

Observe that with parameter s fixed $y(-k) = x(s - k)$ is a discrete signal. If we further set $z = \exp(2\pi j\omega)$, then the ZT summation with $a = 1$ becomes

$$X(s,\omega) = \sum_{k=-\infty}^{\infty} y(-k)\exp(2\pi j\omega k) = \sum_{k=-\infty}^{\infty} y(k)\exp(-2\pi j\omega k) = \sum_{k=-\infty}^{\infty} y(k)z^{-k}. \tag{8.58}$$

Equation (8.58) is the z-transform of $y(k)$ evaluated on the unit circle. More precisely, it is the DTFT of $y(k)$ with 2π frequency dilation.

8.3.2.2   *An Isomorphism.* We now show an interesting isomorphism between the Hilbert space of finite-energy analog signals $L^2(\mathbb{R})$ and the square-integrable two-dimensional analog signals on the unit square $S = [0, 1] \times [0, 1]$.

The Zak transform is in fact a unitary map from $L^2(\mathbb{R})$ to $L^2(S)$; that is, $\mathcal{Z}$ is a Hilbert space map that takes an $L^2(\mathbb{R})$ orthonormal basis to an $L^2(S)$ orthonormal basis in a one-to-one and onto fashion [27, 28].

Lemma. Let $b(t) = u(t) - u(t - 1)$ be the unit square pulse, where $u(t)$ is the analog step function. Then $\{b_{m,n}(t) = \exp(2\pi jmt)b(t - n) \mid m, n \in \mathbb{Z}\}$ is a basis for $L^2(\mathbb{R})$. Moreover, $\{e_{m,n}(s, t) = \exp(2\pi jms)\exp(2\pi jnt) \mid m, n \in \mathbb{Z}\}$ is a basis for $L^2(S)$.

Proof: Apply Fourier series arguments to the unit intervals on $\mathbb{R}$. The extension of Fourier series to functions of two variables is outside our one-dimensional perspective, but is straightforward, and can be found in advanced Fourier analysis texts (e.g., Ref. 29.) ∎

Theorem (Zak Isomorphism). The Zak transform $\mathcal{Z}: L^2(\mathbb{R}) \to L^2(S)$ is unitary.

Proof: Let's apply the ZT to the Fourier basis on $L^2(\mathbb{R})$, $\{b_{m,n}(t) \mid m, n \in \mathbb{Z}\}$ of the lemma:

$$(\mathcal{Z}b_{m,n})(s,\omega) = \sum_{k=-\infty}^{\infty} b_{m,n}(s-k)\exp(2\pi j\omega k)$$

$$= \exp(2\pi jms)\exp(-2\pi jn\omega) \sum_{k=-\infty}^{\infty} b(s-n-k)\exp(2\pi j\omega(n-k))$$

$$= \exp(2\pi jms)\exp(-2\pi jn\omega)(\mathcal{Z}b)(s,\omega) = e_{m,-n}(s,\omega)(\mathcal{Z}b)(s,\omega). \quad (8.59)$$

Let us reflect on the last term, $(\mathcal{Z}b)(s, \omega)$ for $(s, \omega) \in S$. We know that

$$(\mathcal{Z}b)(s,\omega) = \sum_{k=-\infty}^{\infty} b(s-k)\exp(2\pi j\omega k). \qquad (8.60)$$

On the interior of S, $(0, 1) \times (0, 1)$, we have $b(s - k) = 0$ for all $k \neq 0$. So only one term counts in the infinite sum (8.60), namely $k = 0$, and this means $(\mathcal{Z}b)(s, \omega) = 1$ on the unit square's interior. On the boundary of S, we do not care what happens to the ZT sum, because the boundary has (two-dimensional) Lebesgue measure zero; it does not affect the $L^2(S)$ norm. Thus, $\mathcal{Z}$ sends $L^2(\mathbb{R})$ basis elements $b_{m,n}$ to $L^2(S)$ basis elements $e_{m,-n}$, and is thus unitary. ∎

8.4 SUMMARY

The z-transform extends the discrete-time Fourier transform from the unit circle to annular regions complex plane, called regions of convergence. For signal frequency, the DTFT is the right inspection tool, but system properties such as stability can be investigated with the z-transform. Readers may recall the Laplace transform from system theory and differential equations work; it bears precisely such a relationship to the analog Fourier transform (Chapter 5). The Laplace transform extends the definition of the Fourier transform, whose domain is the real numbers, to regions of the complex plane.

The next chapter covers frequency-domain signal analysis, including both analog and digital filter design. It most assuredly explores further z-transform techniques.

This chapter closed with an introduction to two related tools: the chirp z-transform and the Zak transform. The CZT is a discretized z-transform computed on a custom contour. If the contour follows the unit circle, then the CZT can be used to

save some computational steps that we would ordinarily suffer when computing a DFT of difficult (prime) order. Or, careful contour selection with the CZT gives more frequency coefficients in a narrow application range than the Fourier transform. The Zak transform's isomorphism property effectively converts questions about $L^2(\mathbb{R})$ analog signals into questions about finite-energy signals on the unit square. Analytically, the unit square, even though it is two-dimensional, is often easier to deal with. This benefit of the ZT makes it especially powerful when we study frames based on windowed Fourier atoms in Chapter 10.

8.4.1   Historical Notes

Kaiser [14] introduced the *z*-transform into the signal processing discipline from control theory only in the early 1960s. At the time, digital computer applications had stimulated interest in discrete transforms, filtering, and speech processing. Filters are systems that pass some frequency ranges while suppressing others, and they are common at the front end of a signal analysis system that must interpret oscillatory data streams. It turns out—as we shall see in the next chapter—that very good filters can be built out of simple recursive structures based on difference equations. The *z*-transform readily gives the system function for such difference equations as a rational function of a single complex variable: $H(z) = B(z)/A(z)$. We have developed straightforward algebraic methods for inverting such rational functions, which in turn reveals the system impulse response and allows us to calculate the system response to various inputs.

In the late 1960s, Bluestein [30] first showed how to compute the DFT using a chirped linear filtering operation. The formalization of CZT algorithm and many of its original applications are due to Rabiner, Schafer, and Rader [22, 23].

The ZT arrives relatively late to signal theory from physics [31], where Zak developed it independently for solid-state applications. Janssen introduced it into the mainstream signal analysis literature [26]. The transform has been many places—indeed, Gauss himself may have known of it [28].

8.4.2   Guide to Problems

Readers should find most problems straightforward. Problems 2 and 3 explore some of the limit ideas and radius of converge concepts used in the chapter. There is a *z*-transform characterization of stable systems, which is developed in the later problems. Finally, some computer programming tasks are suggested.

REFERENCES

1. A. V. Oppenheim, A. S. Willsky, and S. H. Nawab, *Signals and Systems*, 2nd ed., Upper Saddle River, NJ: Prentice-Hall, 1997.
2. J. A. Cadzow and H. F. Van Landingham, *Signals, Systems, and Transforms.* Englewood Cliffs, NJ: Prentice-Hall, 1983.

3. H. Baher, *Analog and Digital Signal Processing.* New York: Wiley, 1990.

4. J. G. Proakis and D. G. Manolakis, *Digital Signal Processing*, 2nd ed., New York: Macmillan, 1992.

5. R. A. Roberts and C. T. Mullis, *Digital Signal Processing*. Reading, MA: Addison-Wesley, 1987.

6. A. V. Oppenheim and R. W. Shafer, *Discrete-Time Signal Processing*, Englewood Cliffs, NJ: Prentice-Hall, 1989.

7. L. R. Rabiner and B. Gold, *Theory and Application of Digital Signal Processing*, Englewood Cliffs, NJ: Prentice-Hall, 1975.

8. T. Parsons, *Voice and Speech Processing*, New York: McGraw-Hill, 1987.

9. M. Akay, *Biomedical Signal Processing*, San Diego, CA: Academic Press, 1994.

10. F. Scherbaum, *Of Poles and Zeros: Fundamentals of Digital Seismology*, Dordrecht, The Netherlands: Kluwer, 1996.

11. C. H. Wilts, *Principles of Feedback Control*, Reading, MA: Addison-Wesley, 1960.

12. C. L. Phillips and H. T. Nagle, Jr., *Digital Control System Analysis and Design*, Englewood Cliffs, NJ: Prentice-Hall, 1984.

13. K. Ogata, *Discrete-Time Control Systems*, Englewood Cliffs, NJ: Prentice-Hall, 1987.

14. J. F. Kaiser, Design methods for sampled data systems, *Proceedings of the First Annual Allerton Conference on Circuits and System Theory*, pp. 221–236, 1963. Also in L. R. Rabiner and C. M. Rader, eds., *Digital Signal Processing*, New York: IEEE Press, 1972.

15. E. I. Jury, *Theory and Applications of the Z-Transform Method*, Malabar, FL: Krieger, 1982.

16. R. Vich, *Z-Transform Theory and Applications*, Boston: D. Reidel, 1987.

17. E. Hille, *Analytic Function Theory*, vol. I, Waltham, MA: Blaisdell, 1959.

18. L. V. Ahlfors, *Complex Analysis,* 2nd ed., New York: McGraw-Hill, 1966.

19. M. Rosenlicht, *An Introduction to Analysis*, New York: Dover, 1978.

20. W. F. Rudin, *Real and Complex Analysis*, 2nd ed., New York: McGraw-Hill, 1974.

21. R. Beals, *Advanced Mathematical Analysis*, New York: Springer-Verlag, 1987.

22. L. R. Rabiner, R. W. Shafer, and C. M. Rader, The chirp *z*-transform algorithm, in L. R. Rabiner and C. M. Rader, eds., *Digital Signal Processing*, New York: IEEE Press, pp. 322–328, 1972.

23. L. R. Rabiner, R. W. Shafer, and C. M. Rader, The chirp *z*-transform algorithm and its applications, *Bell System Technical Journal*, vol. 48, pp. 1249–1292, May 1969.

24. R. W. Shafer and L. R. Rabiner, System for automatic formant analysis of voiced speech, *Journal of the Acoustical Society of America*, vol. 47, no. 2, pp. 634–648, February 1970.

25. M.I. Skolnik, *Introduction to Radar Systems*, 2nd ed., New York: McGraw-Hill, 1986.

26. A. J. E. M. Janssen, The Zak transform: A signal transform for sampled time-continuous signals, *Philips Journal of Research*, vol. 43, no. 1, pp. 23–69, 1988.

27. C. E. Heil and D. F. Walnut, Continuous and discrete wavelet transforms, *SIAM Review*, vol. 31, pp. 628–666, December 1989.

28. I. Daubechies, *Ten Lectures on Wavelets*, Philadelphia: SIAM, 1992.

29. A. Zygmund, *Trigonometric Series*, vols. I & II, 2nd ed., Cambridge: Cambridge University Press, 1985.

30. L. I. Bluestein, A linear filtering approach to the computation of the discrete Fourier transform, *IEEE Transactions on Audio and Electroacoustics*, vol. AU-18, pp. 451–455,

December 1970. Reprinted in L. R. Rabiner and C. M. Rader, eds., *Digital Signal Processing*, New York: IEEE Press, 1972.

31. J. Zak, Finite translations in solid state physics, *Physics Review Letters*, vol. 19, pp. 1385–1397, 1967.

PROBLEMS

1. Find the z-transform and ROC for each of the following signals:

   (a) $x(n) = u(n-5) - u(n+2)$, where $u(n)$ is the discrete unit step signal. Can one simply apply the linearity and shift properties to $x(n)$ for the right answer?

   (b) $\delta(n-4) + u(n)$, where $\delta(n)$ is the discrete impulse.

   (c) $x(n) = 3^n u(-n) + n2^{-n} u(n)$.

   (d) $x(n) = u(n)[n2^{n-1}]$.

   (e) $x(n) = u(n)[n2^{n-1} + n]$.

   (f) $x(n) = 1/n!$

   (g) $x(n) = u(-n-1)(1/3)^n$.

   (h) $x(n) = u(n)(-1/5)^n + u(-n-1)(1/2)^n$.

2. Consider the lim sup and lim inf of a sequence, $A = \{a_n: 0 \le n < \infty\}$. Suppose we have defined elements of the sequence as follows: $a_0 = 0$; $a_n = 1 + 1/n$, if n is even; and $a_n = -1 - 1/n$, if n is odd.

   (a) Show that the sequence A has no limit.

   (b) Show that the lim sup A is 1.

   (c) Show that the lim inf of A is -1.

   (d) Let $A_N = A \setminus \{a_n: 0 \le n < N\}$ and κ_N be the least upper bound of A_N. Show that $\kappa_N \le \kappa_M$ if $M < N$.

   (e) Show that a sequence $B = \{b_n: 0 \le n < \infty\}$ has a limit if and only if its lim inf and its lim sup are equal. What about the cases where the limit is $\pm \infty$?

   (f) Show that

$$\lim_{n \to \infty} \inf\{b_n: 0 \le n < \infty\} = - \lim_{n \to \infty} \sup\{-b_n: 0 \le n < \infty\}. \tag{8.61}$$

3. Suppose $Z(x(n)) = X(z)$ has only non-negative powers of z:

$$X(z) = \sum_{n=0}^{+\infty} a_n z^n. \tag{8.62}$$

   Let

$$\kappa = \lim_{n \to \infty} \sup\{|a_n|^{1/n}: 1 \le n < \infty\}, \tag{8.63}$$

so that $\rho = \kappa^{-1}$ is the radius of convergence of $X(z)$. Show that the radius of convergence for the derivative,

$$X'(z) = \frac{dX(z)}{dz} = \sum_{n=0}^{+\infty} na_n z^{n-1}, \tag{8.64}$$

is also ρ.

4. Let $Z(x(n)) = X(z)$. Show the following z-transform symmetry properties:
   (a) $Z[x^*(n)] = X^*(z^*)$, where z^* is the complex conjugate of z.
   (b) (Time Reversal) If $y(n) = x(-n)$, then $Z[y(n)] = Y(z) = X(z^{-1})$, and $ROC_Y = \{z \in \mathbb{C}: z^{-1} \in ROC_X\}$.
   (c) If $y(n) = \text{Real}[x(n)]$, then $Y(z) = [X(z) + X^*(z^*)]/2$.
   (d) If $y(n) = \text{Imag}[x(n)]$, then $Y(z) = j[X^*(z^*) - X(z)]/2$.
   (e) Find the z-transform of $x_e(n)$, the even part of $x(n)$.
   (f) Find the z-transform of $x_o(n)$, the odd part of $x(n)$.

5. Suppose $X(z) = z/(z - a)$, $a \neq 0$, with $ROC_X = \{z \in \mathbb{C}: |a| < |z|\}$. In the first example of Section 8.1.1, we found that $x(-1) = x(-2) = 0$ and claimed that $x(n) = 0$ for $n < -2$. For the last case, $n < -2$, verify that
   (a) $\text{Res}(f(z), z = 0) = -a^{-n}$.
   (b) $\text{Res}(f(z), z = a) = a^{-n}$.
   (c) $x(n) = 0$ for $n < -2$.

6. Suppose $X(z) = z/(z - a)$, $a \neq 0$, with $ROC_X = \{z \in \mathbb{C}: |z| < |a|\}$. Using the method of contour integration, find $x(n)$ for all $n \in \mathbb{Z}$.

7. Suppose $X(z) = z(z - 2)^{-1}(z - 1)^{-1}$.
   (a) Let $ROC_X = \{z \in \mathbb{C}: |z| < 1\}$. With the method of inverse z-transformation by computation of the Laurent series, find $x(n)$.
   (b) Suppose now that $ROC_X = \{z \in C: 2 > |z| > 1\}$. Is it possible to use the long division method to find the Laurent series form of $X(z)$ and thence find $x(n)$? Explain.

8. Suppose that

$$X(z) = \frac{z}{(z-1)(z+2)^2}, \tag{8.65}$$

and $ROC_X = \{z \in \mathbb{C}: 2 < |z|\}$.
   (a) Find A, B, and C to derive the expansion of $z^{-1}X(z)$ into partial fractions:

$$\frac{X(z)}{z} = \frac{1}{(z-1)(z+2)^2} = \frac{A}{(z-1)} + \frac{B}{(z+2)^2} + \frac{C}{(z+2)}. \tag{8.66}$$

   (b) Find the discrete signal whose z-transform is $z^{-1}X(z)$.
   (c) Find the discrete signal whose z-transform is $X(z)$.

9. Again suppose

$$X(z) = \frac{z}{(z-1)(z+2)^2}. \tag{8.67}$$

Find all of the discrete signals whose *z*-transforms are equal to $X(z)$. For each such signal,

(a) State the region of convergence.

(b) Sketch the region of convergence.

(c) State whether the signal is causal, anticausal, or neither.

10. Signal $x(n)$ has *z*-transform $X(z)/z = 1 / (z^2 - 3z/2 - 1)$. Find three different possibilities for $x(n)$ and give the ROC of $X(z)$ for each.

11. If $x(n)$ has *z*-transform $X(z) = z / (z^2 - 5z - 14)$, then find three different possibilities for $x(n)$ and give the ROC of $X(z)$ for each.

12. Let $X^+(z)$ be the one-sided *z*-transform for $x(n)$.

(a) Show that the one-sided *z*-transform is linear.

(b) Show that the one-sided *z*-transform is not invertible by giving examples of different signals that have the same transform.

(c) Show that if $x(n) = 0$ for $n < 0$, then $X^+(z) = X(z)$.

(d) Let $y(n) = x(n - k)$. If $k > 0$, show that the shift property becomes

$$Y^+(z) = x(-k) + x(-k+1)z^{-1} + \cdots + x(-1)z^{-m+1} + z^{-m}X^+(z). \tag{8.68}$$

13. A simple difference equation,

$$y(n) = ay(n-1) + x(n), \tag{8.69}$$

describes a signal processing system. Some signed fraction $0 < |a| < 1$ of the last filtered value is added to the current input value $x(n)$. One application of the one-sided *z*-transform is to solve the difference equation associated with this system [4, 6]. Find the unit step response of this system, given the initial condition $y(-1) = 1$, as follows.

(a) Take the one-sided *z*-transforms of both sides of (8.69):

$$Y^+(z) = a\left[Y^+(z)z^{-1} + y(-1)\right] + X^+(z). \tag{8.70}$$

(b) Use the initial condition to get

$$Y^+(z) = \frac{a}{(1 - az^{-1})} + \frac{1}{(1 - z^{-1})(1 - az^{-1})}. \tag{8.71}$$

(c) Apply the partial fractions method to get the inverse *z*-transform:

$$y(n) = \frac{(1 - a^{n+2})}{(1 - a)}u(n). \tag{8.72}$$

14. The Fibonacci[2] sequence is defined by $f(-2) = 1$, $f(-1) = 0$, and

$$f(n) = f(n-1) + f(n-2). \tag{8.73}$$

(a) Show that $f(0) = f(1) = 1$.

(b) Using the one-sided z-transform [4], show

$$y(n) = \frac{u(n)}{2^{n+1}\sqrt{5}} \left[(1+\sqrt{5})^{n+1} - (1-\sqrt{5})^{n+1} \right]. \tag{8.74}$$

15. Consider the system H given by the following difference equation:

$$y(n) = 0.25 * y(n-2) + 0.25 * y(n-1) + 0.5 * x(n). \tag{8.75}$$

(a) Find the system function $H(z)$.

(b) Assuming that H is a causal system, find $h(n)$.

(c) Give ROC_H for the causal system.

(d) What are the poles for the system function?

(e) Is the system stable? Explain.

16. Show that a discrete LTI system H is causal, $h(n) = 0$ for $n < 0$, if and only if ROC_H is $\{z: |z| > r\}$ for some $r > 0$.

17. Show that a discrete LTI system H is stable (bounded input implies bounded output signal) if and only if its z-transform ROC includes the unit circle $|z| = 1$.

18. Show that a causal LTI system H is stable if and only if all of the poles of $H(z)$ lie inside the unit circle $|z| = 1$.

19. Consider the causal system H given by the following difference equation:

$$y(n) = Ay(n-1) + Bx(n). \tag{8.76}$$

(a) Find necessary and sufficient conditions on constants A and B so that H is stable.

(b) Find the unit step response $y = Hu$, where $u(n)$ is the unit step signal.

(c) Show that if A and B satisfy the stability criteria in (a), then the unit step response in (b) is bounded.

(d) Find the poles and zeros of the system function $H(z)$.

20. Assume the notation for chirp z-transform of Section (8.31).

(a) Show that if $A = 1$, $M = N$, and $W = \exp(-2\pi j/N)$ in (8.49), then $X_{A,W}(k) = X(k)$, where $X(k)$ is the DFT of order N for the signal $x(n)$.

---

[2]Leonardo of Pisa (c. 1175–1250) is known from his father's name. The algebraist and number theorist asked a question about rabbits: If an adult pair produces a pair of offspring, which mature in one month, reproduce just as their parents, and so on, then how many adult rabbits are there after N months? The answer is F_N, the Nth Fibonacci number.

(b) Show that $W_0 > 1$ implies an inward spiral and $W_0 < 1$ produces an outward spiral path.

21. Derive the periodicity relations for the Zak transform (8.57a, 8.57b).

The next few problems are computer programming projects.

22. As a programming project, implement the CZT algorithm of Section 8.3.1.2. Compare the fast CZT algorithm performance to the brute-force convolution in (8.52). Use the algorithm to compute some DFTs for large prime orders. Compare the CZT-based algorithm to straight DFT computations.

23. Implement the z-transform for finitely supported discrete signals in a computer program. Verify the convolution property of the z-transform by calculating the z-transforms, $X(z)$ and $Y(z)$, of two nontrivial signals, $x(n)$ and $y(n)$, respectively; their convolution $z(n)$; and the z-transform $Z(z)$. Finally, confirm that $Z(z) = X(z)Y(z)$ with negligible numerical error.

24. Consider the implementation of the inverse z-transform on a digital computer. Which approach might be easiest to implement? Which is the most general? Develop an application that handles some of possible forms of $X(z)$. Explain the strengths and limitations of the application.